

# **Deciphering the role of cGAS/STING signaling *in vivo* using the short-lived turquoise killifish *Nothobranchius furzeri***

Inaugural-Dissertation

zur

Erlangung des Doktorgrades

der Mathematisch-Naturwissenschaftlichen Fakultät

der Universität zu Köln

vorgelegt von

**Eugen Ballhysa**

aus Elbasan, Albania

Köln, Dezember 2024



**UNIVERSITÄT  
ZU KÖLN**

Berichterstatter: **Prof. Dr. Adam Antebi**

(Gutachter) **Prof. Dr. Björn Schumacher**

Externer Berichterstatter: **Prof. Dr. John Michael Sedivy**

(Gutachter)

Tag der mündlichen Prüfung: 19th March, 2025

## Table of Contents

1. List of abbreviations.....	5
2. Abstract.....	9
3. Introduction .....	10
3.1 The increasing ageing population and the need for ageing research .....	10
3.2 The role of model organisms in unraveling ageing mechanisms .....	12
3.3 The biology of <i>Nothobranchius furzeri</i> .....	14
3.3.1 Evolution of naturally short-lived strains.....	14
3.3.2 Establishment as a model organism.....	16
3.3.3 Similarities and differences to human ageing .....	19
3.4 Inflammaging.....	24
3.4.1 Impact on cells and tissues .....	25
3.4.2 Sources of inflammaging.....	28
3.5 The cGAS/STING pathway.....	39
3.5.1 cGAS structure .....	40
3.5.2 STING structure.....	42
3.5.3 Canonical cGAS/STING signaling cascade.....	44
3.5.4 Non-canonical functions of cGAS and STING .....	47
3.5.5 cGAS/STING impact on pathologies .....	49
3.5.6 cGAS/STING impact on normative ageing .....	51
4. Research aims.....	55
5. Results .....	56
5.1 cGAS structure and function <i>in vitro</i> are conserved from teleosts to mammals .....	56
5.2 Killifish cGAS impacts innate immunity regulation <i>in vivo</i> .....	64
5.3 Killifish cGAS modulates the transcriptional response to DNA damage and senescence <i>in vivo</i> .....	67
5.4 Killifish cGAS modulates the aging transcriptome.....	74

5.5 The killifish cGAS/STING pathway affects age-related pathology but not life span .....	80
6. Discussion .....	86
6.1 cGAS and STING are evolutionarily conserved.....	88
6.2 cGAS preserves genomic integrity.....	90
6.3 Loss of cGAS leads to low-grade sterile inflammation and stress <i>in vivo</i> .....	91
6.4 cGAS more than STING modulates senescence <i>in vivo</i> .....	93
6.5 cGAS/STING signaling regulates metabolic processes during senescence and ageing .....	94
6.6 Loss of cGAS/STING signaling impacts late-life disease occurrence but does not extend lifespan .....	96
6.7 Scientific advancements and limitations .....	99
7. Future perspectives.....	102
7.1 Investigating the physiology of aged cGAS/STING KO killifish .....	102
7.2 Elucidating the mechanism behind cGAS-mediated genomic stability or instability .....	105
7.3 Uncoupling nuclear and cytosolic function of cGAS - finding putative balance between DNA damage and inflammaging.....	106
7.4 cGAS/STING regulation of senescence outside DNA damage.....	108
7.5 Deciphering tissue-specific effects of cGAS/STING activity .....	110
7.6 Examining time-specific effects of cGAS/STING pathway .....	112
7.7 Evaluating sex-specific effects of cGAS/STING pathway .....	113
8. Material and methods.....	114
9. Acknowledgements .....	129
10. Work contributions.....	131
11. References .....	132
12. Curriculum Vitae .....	160



## 1. List of abbreviations

Abbreviation	Definition
<b>cGAS</b>	Cyclic GMP-AMP synthase
<b>STING</b>	Stimulator of interferon genes
<b>TOR</b>	Target of Rapamycin
<b>AMPK</b>	AMP Kinase
<b>IGF1</b>	Insulin/insulin-like growth factor 1
<b>AI</b>	Artificial intelligence
<b>GWAS</b>	Genome-wide association studies
<b>SLAM</b>	Study of Longitudinal Aging in Mice
<b>DNMTs</b>	DNA methyltransferases
<b>CDKN</b>	Cyclin-dependent kinase inhibitor
<b>CDK</b>	Cyclin-dependent kinase
<b>SA-<math>\beta</math>-gal</b>	Senescence-associated $\beta$ -galactosidase activity
<b>SASP</b>	Senescence-associated secretory phenotype
<b>IGFBP1</b>	Insulin Like Growth Factor Binding Protein 1
<b>EGF</b>	Epidermal Growth Factor
<b><math>\gamma</math>H2AX</b>	S139-phosphorylated H2A histone family member X
<b>APPs</b>	Acute phase proteins
<b>TNFRSF11B</b>	Tumor necrosis factor receptor superfamily, member 11b
<b>CXCL12B</b>	C-X-C Motif Chemokine Ligand 12
<b>IL</b>	Interleukine
<b>TNF<math>\alpha</math></b>	Tumor necrosis factor-alpha
<b>HSPCs</b>	Hematopoietic stem and progenitor cells
<b>MSCs</b>	Mesenchymal stem cells
<b>ROS</b>	Reactive oxygen species
<b>AKI</b>	Acute kidney injure
<b>CKD</b>	Chronic kidney disease
<b>WT</b>	Wild-type
<b>KO</b>	Knock-out

<b>RB</b>	Retinoblastoma
<b>DDR</b>	DNA damage response
<b>DNA-SCARS</b>	DNA segments with chromatin alterations reinforcing senescence
<b>RPA</b>	Replication protein A
<b>CCFs</b>	Cytoplasmic chromatin fragments
<b>OIS</b>	Oncogene-induced senescence
<b>TCA</b>	Tricarboxylic acid
<b>MMPs</b>	Matrix metalloproteinases
<b>NOTCH1</b>	Notch Receptor 1
<b>IR</b>	Ionizing radiation
<b>UV</b>	Ultraviolet
<b>SSBs</b>	Single strand breaks
<b>PARP1</b>	Poly [ADP-ribose] polymerase 1
<b>DSBs</b>	Double strand breaks
<b>NHEJ</b>	Non-homologous end joining
<b>HR</b>	Homologous recombination
<b>ATM</b>	Ataxia-telangiectasia mutated
<b>ATR</b>	ATM- and Rad3-Related
<b>DNA-PKcs</b>	DNA-dependent protein kinase
<b>NF-κB</b>	Nuclear factor kappa B
<b>GATA4</b>	GATA Binding Protein 4
<b>TLRs</b>	Toll-like receptors
<b>CLRs</b>	C-type lectin receptors
<b>NLRs</b>	Nod-like receptors
<b>RIG-I</b>	Retinoic acid-inducible gene-I
<b>RLRs</b>	RIG-I-like receptors
<b>OAS1</b>	2'-5'-oligoadenylate synthetase 1
<b>IFN</b>	Interferon
<b>AIM2</b>	Absent in melanoma 2
<b>cGAMP</b>	cyclic GMP-AMP
<b>CD-NTase</b>	cGAS/DncV-like nucleotidyltransferase
<b>DncV</b>	<i>Vibrio cholerae</i> dinucleotide cyclase

<b>Mab21</b>	Male-abnormal 21
<b>Mab21d1</b>	cGAS
<b>Mab21L</b>	Mab21-like protein
<b>NLSs</b>	Nuclear localization signals
<b>NES</b>	Nuclear export sequence
<b>CDNs</b>	Cyclic dinucleotides
<b>CTT</b>	C'-terminal tail
<b>IRF</b>	Interferon regulatory factor
<b>TBK1</b>	TANK-binding kinase 1
<b>TRAF6</b>	Tumor necrosis factor receptor-associated factor 6
<b>ER</b>	Endoplasmic reticulum
<b>STIM1</b>	Stromal interaction molecule 1
<b>CBD</b>	CDN-binding domain
<b>DD</b>	Dimerization domain
<b>ERGIC</b>	ER-Golgi intermediate compartment
<b>ISGs</b>	Interferon-stimulated genes
<b>IKK<math>\beta</math></b>	I $\kappa$ B kinase $\beta$
<b>STAT6</b>	Signal transducer and activator of transcription 6
<b>CCL</b>	CC-chemokine ligand
<b>LC3</b>	1A/1B-light chain 3
<b>WIPI2</b>	WD repeat domain phosphoinositide-interacting protein 2
<b>ATG5</b>	Autophagy protein 5
<b>GABARAP</b>	GABA type A receptor-associated protein
<b>TFEB</b>	Transcription factor EB
<b>MOMP</b>	Mitochondrial outer membrane permeabilization
<b>RIPK3</b>	Receptor-interacting serine/threonine-protein kinase 3
<b>VRACs</b>	Volume-regulated anion channels
<b>SLC19A1</b>	Solute carrier family 19 member 1
<b>ENPP</b>	Ectonucleotide pyrophosphatase/phosphodiesterase family member
<b>SMPDL3A</b>	Sphingomyelin phosphodiesterase acid-like 3A
<b>CRM1</b>	Chromosome region maintenance 1
<b>BLK</b>	B-lymphoid tyrosine kinase

<b>AGS</b>	Aicardi-Goutières Syndrome
<b>HGPS</b>	Hutchinson-Gilford progeria syndrome
<b>SLE</b>	Systemic lupus erythematosus
<b>ALS</b>	Amyotrophic lateral sclerosis
<b>SAVI</b>	STING-associated vasculopathy with onset in infancy
<b>SIRT</b>	Sirtuin
<b>BMAL1</b>	Brain and muscle ARNT-like protein-1
<b>LINE1</b>	Long interspersed nuclear element-1
<b>DAMPs</b>	Damage-associated molecular patterns
<b>COBALT</b>	Constraint-based multiple sequence alignment tool
<b>CRISPR</b>	Clustered Regularly Interspaced Short Palindromic Repeats
<b>MA</b>	Minus-average
<b>PCA</b>	Principle component analysis
<b>GSEA</b>	Gene set enrichment analysis
<b>FDR</b>	False-discovery rate
<b>Gy</b>	Gray
<b>GOBP</b>	Gene Ontology Biological Process
<b>H&amp;E</b>	Hematoxylin & Eosin
<b>IFNAR</b>	Interferon- $\alpha/\beta$ receptor
<b>MIF</b>	Macrophage migration inhibitory factor
<b>OXPHOS</b>	Oxidative phosphorylation
<b>EdU</b>	5-Ethynyl-2'-deoxyuridine
<b>PCNA</b>	Proliferating cell nuclear antigen
<b>TUNEL</b>	Terminal deoxynucleotidyl transferase dUTP nick end labeling
<b>TdT</b>	Terminal deoxynucleotidyl transferase
<b>PI</b>	Propidium Iodide
<b>LPC1</b>	lymphocyte cytosolic protein 1

## 2. Abstract

The cGAS/STING pathway is a central innate immune signaling pathway whose chronic activation has been implicated in multiple age-related pathologies, yet its impact on life span itself is unknown. Here we engineered knockouts of pathway components in the killifish *Nothobranchius furzeri*, and assessed their impact on physiology and aging. *In vitro*, loss of killifish cGAS and STING mitigated DNA damage-induced senescence in cultured primary fibroblasts, while cGAS loss uniquely triggered low levels of basal DNA damage. *In vivo*, cGAS knockout unexpectedly led to transcriptional signatures indicative of low-grade inflammation. It also attenuated changes in gene expression in response to DNA damage in young animals and age-related changes in the transcriptome of old animals, suggesting dampening of senescence and aging. Necroscopy indicated that STING KO appeared to have less infection rates and that tissue pathology tended to be milder overall in both mutants, though some tissues showed a trend for enhanced sterile macrophage infiltration. Our observation of cGAS-specific effects related to the DNA damage response and ageing transcriptome hint towards functions separate from canonical cGAS/STING pathway. Despite the attenuated aging signatures, however, longevity of cGAS or STING mutants was not significantly different from that of wild type. Our findings reveal a potential tradeoff, where inhibiting the cGAS/STING pathway alleviates age-related signatures, but increases sterile inflammation, offsetting potential beneficial effects on lifespan.

### 3. Introduction

#### 3.1 The increasing ageing population and the need for ageing research

Over the last several decades, humanity has been facing an unprecedented phenomenon of global demographic ageing. According to data from the United Nations department of economic and social affairs, the worldwide percentage of people aged 0-19 years old has dropped by 20% since 1970, while the population aged over 60 has increased by over 10% (**Figure 1a, b**), with developed countries facing heightened effects and no change in trajectory predicted for the near future (UN 2024). In countries such as Japan the percentage of elderly above 60 is already at 35% and projected to reach 45% by 2050 (**Figure 1c, d**). These demographic shifts alone already put an increasing burden on societies. Though pharmaceutical and medical advances have substantially improved health- and life expectancy (Christensen et al. 2013; Zeng et al. 2017), healthspan and life span have not grown at the same rate (Partridge, Deelen, and Slagboom 2018). And increasingly more people spend an average of 16-20% of their lives in late-life morbidity (Jagger et al. 2008), thus compounding the problem of demographic change.

Debilitating life threatening diseases such as neurodegeneration, cardiovascular diseases and cancer share ageing as their common major risk factor (Niccoli and Partridge 2012), with incidence, prevalence and death rates exponentially increasing with old age. The elderly themselves and their families are not the only ones affected. Additional medical facilities and personnel are required to care for them, placing an untold burden on healthcare systems and services. And finally, foregone productivity due to age-related diseases, as well as medical and long-term care needs impose a major cost on the economy of countries with high rates of demographic ageing (Okamoto et al. 2023). The inherent need for self-preservation and sustainability along with the socioeconomic implications, now more than ever, highlight the need for ageing research, with the goal to improve healthy ageing and compress the time of morbidity.

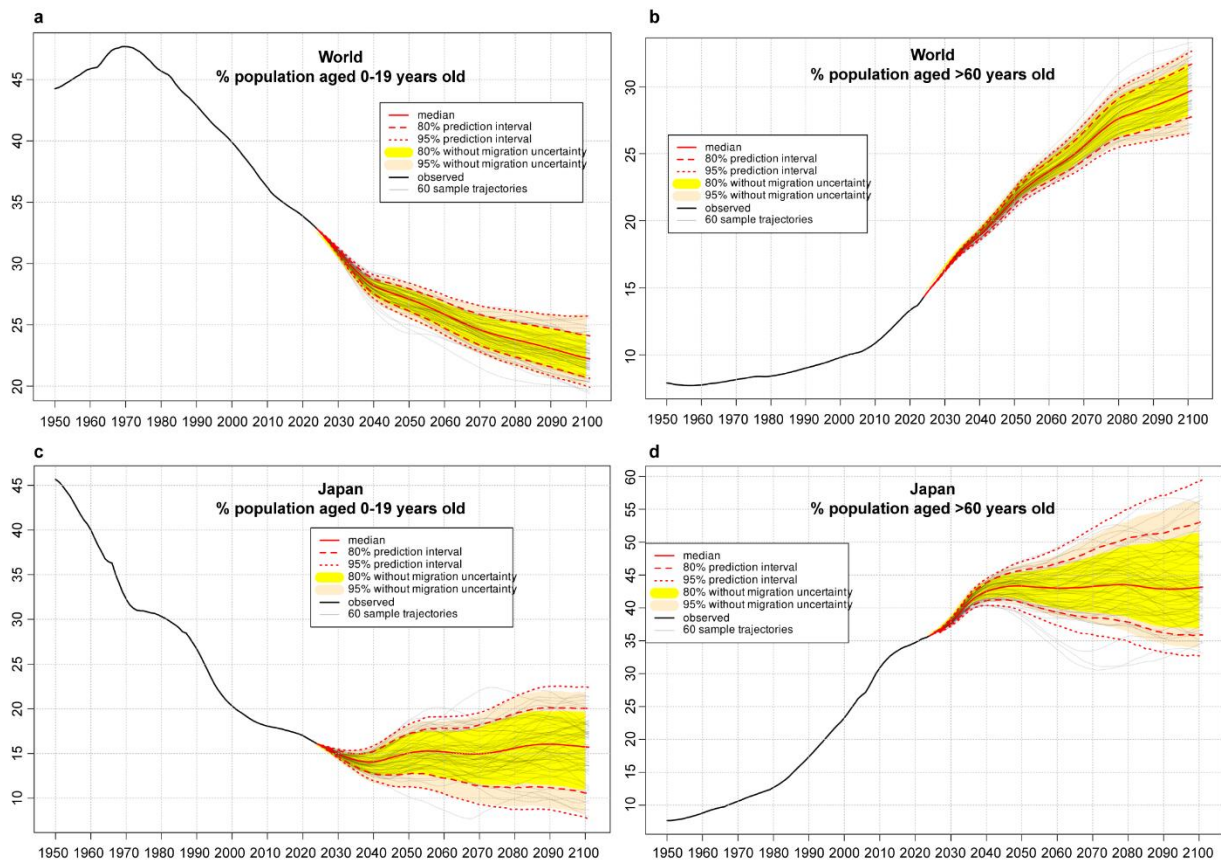


**Figure 1. Global demographic ageing population.** a, b. Worldwide percent of population aged between 0-19 and over 60 years old, respectively. c, d. Percent of population aged between 0-19 and over 60 years old, respectively, in Japan. Data represent registered population demographics from 1950 to 2024 and then followed by probabilistic data until 2100 according to World Population Prospects. Graphs were obtained from United Nations website <https://population.un.org>

The urgency for studying ageing is also apparent from our limited grasp of the fundamental mechanisms underlying the process. Ageing, as a side effect of natural selection, was considered to have a dauntingly complex genetic basis (Niccoli and Partridge 2012). However, 30 years ago it was discovered that single gene mutations can extend the lifespan of the nematode *Caenorhabditis elegans* (Johnson 1990; Kenyon et al. 1993). Also, while caloric restriction has been known to extend lifespan in diverse species for nearly a century, only in the last 20 years did scientists begin to uncover bits of the molecular mechanisms, including major metabolic regulators such as sirtuins, TOR (Target of Rapamycin), AMPK (AMP Kinase) and insulin/insulin-like growth factor 1

(IGF1) signaling (Kenyon 2010). Only 10 years ago were DNA methylation clocks discovered (Horvath 2015), enabling a quantitative measurement for biological age that researchers are still validating and refining for biologically relevant outcomes (Tomusiak et al. 2024; Oh et al. 2023). Our understanding of ageing continues to evolve and despite attempts to codify our knowledge in an increasing number of hallmarks (Lopez-Otin et al. 2023), we still have yet to reach the point where we can confidently apply this knowledge to pharmacologically improve human health span. Fortunately, with the advent of recent technological advances, such as comprehensive and sensitive -omics and artificial intelligence, progress is only accelerating. Future investment in basic ageing research will thus assist in better understanding this complex physiological process, and help make our societies more sustainable.

### 3.2 The role of model organisms in unraveling ageing mechanisms

Studying ageing in humans is crucial but involves intrinsic time constraints and ethical considerations. Despite these challenges, significant progress has been made in studying ageing directly on humans. Genome-wide association studies (GWAS), studies focused on centenarian families, as well as unusual variants associated with exceptional longevity, have helped shed light on the genetic factors that contribute to extended lifespans (Deelen et al. 2011; Rosoff et al. 2023; Deelen et al. 2021). As mentioned above, the discovery of ageing clocks in humans has revolutionized the field by allowing researchers to quantify ageing and evaluate the efficacy of interventions without waiting for individuals to succumb to old age (Horvath 2015). In parallel, the increasing prominence of health-parameter acquisition over the past decades has led to the creation of extensive datasets, such as the UK Biobank, where health metrics and genetic data can be correlated with lifespan and healthspan (Gadd et al. 2024; Oh et al. 2024). Furthermore, health scores based on relevant clinical data, such as Metabohealth (Deelen et al. 2019) and the multi-prognostic index (Pilotto et al. 2009) may eventually allow clinicians to assess the value of interventions. All of the above methodologies have limitations however. Both GWAS and dataset analysis are correlative studies and limited by the pool of pre-existing data. While the use of clocks and health indexes on humans to study interventions may ultimately be useful, they need further validation and are



currently hindered by ethical boundaries and clinical acceptance. Moreover, they are complicated by genetic heterogeneity, limiting the ability to isolate and study specific mechanisms.

Studies in model organisms can overcome such limitations. In particular, they permit causal, mechanistic studies and controlled genotypes and environments, which are not accessible in humans, while offering strengths similar to human studies, including novel biomarker approaches such as aging clocks (Meyer and Schumacher 2021; Thompson et al. 2018; Horvath et al. 2022), large datasets like the tabula muris senis (Tabula Muris 2020) and association studies in large heterogenous populations like the Study of Longitudinal Aging in Mice (SLAM)(Palliyaguru et al. 2021). The main concern, of course, is the extent of evolutionary conservation, and the limited modeling of human age-related disease, particularly cardiovascular disease and neurodegeneration. Nevertheless, it is quite remarkable that mechanisms discovered in basic organisms like yeast (Harrison et al. 2009) and nematodes (Holzenberger et al. 2003) also extend to mammalian ageing, hence their value in ageing research remains clear.

Through natural selection the tree of life has created numerous paths to solve the mystery of ageing. Organisms with vast regenerative capacity, like planaria, offer insights in the regulation of adult restoration and tissue repair (Sanchez Alvarado 2007). The exceptionally long-lived rodent, the naked mole rat, holds promise for revealing metabolic mechanisms involved in resistance against age-related systemic functional decline and cancer (Oka et al. 2023). Bats are also outliers in the mammalian body mass-lifespan correlation (Foley et al. 2018), and have evolved longevity due to their unique ecological niche. At the molecular level their longevity could stem from their uniquely adapted immune systems, low cancer occurrence and efficient DNA damage repair mechanisms (Cooper et al. 2024). Also resistant to cancer, the bowhead whale is a large mammal that has evolved mechanisms that allow it to age for up to 200 years and analysis of genome and transcriptome suggests modulation of DNA repair, cell cycle and cancer genes (Lagunas-Rangel 2021). Both short-lived and long-lived animals can provide information about ageing process. Unlike long-lived species, however, short-lived animals such as nematodes, fruit flies, killifish, and mice have the added benefit of rapid testing of genetic interventions in real time and establishing causation of life span control.

The evidence is abundantly clear that life span is under genetic control. Different species have characteristic maximal life span due to force of selection on their genetic makeup and gene regulation. Within a species, genetic variation can give rise to differences in life span. Despite this seeming genetic determinism, there is inherent stochasticity in life span and even twin studies in humans show only 25% heritability (van den Berg et al. 2017), revealing considerable plasticity. Nevertheless, there appear to be core processes whose regulation impact longevity similarly across species that model systems can reveal.

### 3.3 The biology of *Nothobranchius furzeri*

#### 3.3.1 Evolution of naturally short-lived strains

Fish belonging to the genus *Nothobranchius* have evolved to thrive in the unstable and unpredictable environments in arid regions of Africa, propagating in the temporary ponds that emerge during the rainy season (Scheel 1990). Fish of this taxon typically hatch during the rainy season, which lasts between 4-6 months. Due to this limited time frame, these annual killifish undergo rapid sexual maturation, and lay their fertilized eggs in the muddy bottom before the habitat disappears (**Figure 2**). Eggs survive the arid season encased within mud pockets in the otherwise dry earth thanks to a number of adaptations (Dolfi et al. 2019). One such adaptation is their remarkably thick and robust chorion (Hartmann and Englert 2012). Another adaptation is their slow cell cycle time during early development (2 hours), compared to that of non-annual fish embryonic cells (15-30 minutes) post-fertilization (Dolfi, Ripa, and Cellerino 2014). Their most profound adaptation, however, is their ability to enter a resilient state of developmental arrest, called diapause (Markofsky and Matias 1977).

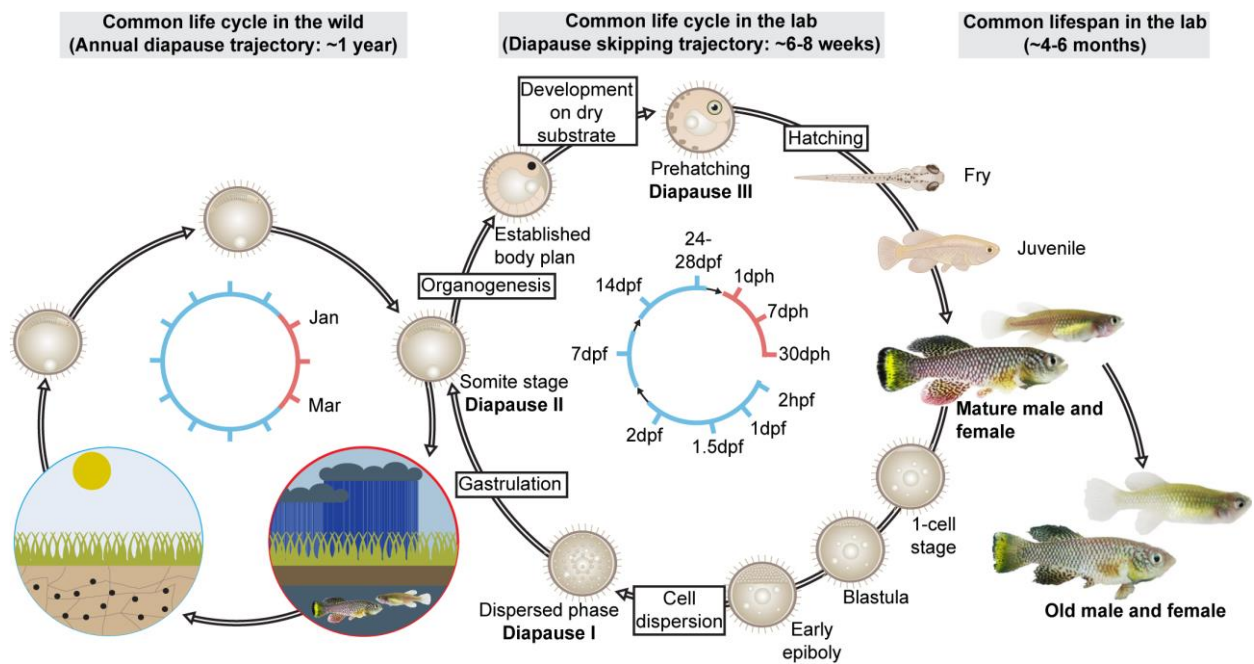


**Figure 2. The life cycle of turquoise killifish.** *Left:* In the wild, during the brief rainy season the eggs from the previous year hatch and the fish reach adulthood and lay new eggs before the end of the season. *Centre:* In laboratory conditions, diapause skipping is preferred for rapid development and hatching of the new batch. *Right:* Adult male killifish are slightly larger and more colorful than adult female killifish. Approximately 4 weeks after hatching, the fish are fertile and can breed the next cohort or grow senescent and die naturally within 4~6 months. Hpff: hours post-fertilization, pdf: days post-fertilization, dph: days post-hatching. Image adjusted from (D'Angelo, De Girolamo, and ScienceDirect 2022).

Embryonic diapause is not a unique feature of annual killifish. Many mammalian species employ diapause to uncouple mating from parturition, ensuring that both take place at the most favorable time (Fenelon, Banerjee, and Murphy 2014). However, what is unique in annual killifish is that diapause can often last longer than their entire adult life expectancy without negatively impacting subsequent growth, fertility or lifespan (Hu et al. 2020). Embryos of annual killifish can enter a state of diapause at three distinct stages of development (Wourms 1972). The first (diapause I) happens during the dispersed phase, a unique developmental stage of annual killifish where epiblast cells migrate randomly over the yolk surface. The second (diapause II) starts mid-somitogenesis when the majority of organs have developed. The third (diapause III) initiates at the final stage of embryonic growth before hatching. Diapause is not

obligatory and its duration can vary greatly. The molecular mechanisms for arresting, surviving for exceptional amounts of time and exiting diapause to initiate a healthy adult life are not well understood (Hu et al. 2020; Dolfi et al. 2019). Yet, they hold promise for unraveling long-term organismal preservation and resistance to extreme environments in vertebrates. Diapause also has practical considerations for strain maintenance, since embryos can be held in diapause for years, and then reactivated at will when returned to appropriate conditions.

One species of this genus, *Nothobranchius furzeri* (henceforth referred to simply as killifish), is considered the shortest-lived vertebrate that can be kept and bred in captivity (Valdesalici and Cellerino 2003). The short-lived strains of this killifish originate from ponds in regions of Zimbabwe and Mozambique, each region with a varying length of rainy season. Due to this extrinsic pressure, different strains appear to have evolved varying lifespans. The highly inbred GRZ strain lives 4-6 months, while the ZMZ-0403 strain can live for over a year (Kirschner et al. 2012). These fish have equivalent lifespans in captivity, despite constant immersion in a favorable environment. Thus, it appears these fish have evolved a short lifespan which makes them an advantageous model for studying rapid natural ageing. In particular, the killifish provides an opportunity to assess the impact of interventions on the life span within 4-8 months, compared to 3 years or more in mouse, bridging an important gap in studying vertebrate ageing.

### 3.3.2 Establishment as a model organism

The killifish's naturally short lifespan, along with its ability to thrive and reproduce in captivity, has established it as a valuable model for aging research. But, to effectively use it as a model, researchers have developed an extensive toolkit encompassing genetic datasets, advanced molecular techniques, and innovative husbandry systems (**Figure 3**). These resources not only facilitate studies on genetic and molecular drivers of aging but also provide a foundation for refining and expanding experimental approaches. As these tools continue to evolve, they open new avenues for in-depth, large-scale investigations using killifish as a model organism.

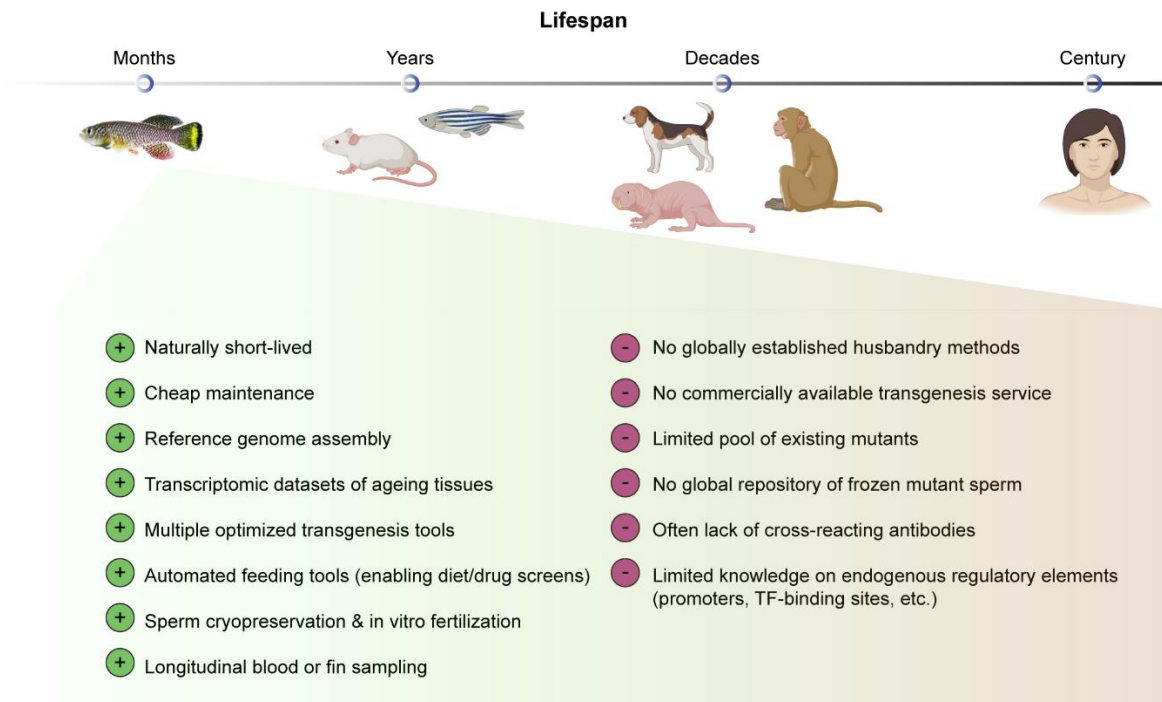


**Figure 3. Advantages and limitations of using killifish as an ageing model organism.**

The upper part indicates time-scales required for lifespan analysis in vertebrate ageing models and humans, while the lower part summarizes pros and cons of using killifish in ageing research. As a relatively new model, available resources remain limited. However, numerous genetic tools and datasets have been generated, advancing killifish aging research and establishing it as a valuable model organism in the field. Image adjusted from (Mathuru 2022).

A reference genome is typically regarded as essential for an organism to be accepted as a model system. Initial insights into the *N. furzeri* genome came from cytogenetic analysis and genome survey sequencing, revealing 19 chromosomes ( $2n = 38$ ), an estimated size of approximately 1.5 Gb, and a high abundance of repetitive elements (Reichwald et al. 2009). More recent advances in sequencing technologies allowed for two independent genome assemblies to be constructed and released in parallel (Reichwald et al. 2015; Valenzano et al. 2015). Building on the genomic references, our lab and others have generated an array of transcriptomic datasets in multiple ageing tissues (Xu et al. 2023; Bergmans et al. 2024; Ripa, Ballhysa, et al. 2023; Teefy, Lemus, et al. 2023; Benayoun et al. 2019). These datasets not only describe killifish ageing, but also enhance annotation of genes, transposable elements and small RNAs, such as miRNAs, ncRNAs (Baumgart et al. 2019) and piRNAs (Teefy, Adler, et al. 2023).

The transition from descriptive analyses of age-related pathways to direct investigation of individual gene functions requires the ability to manipulate the genome. The development of killifish egg microinjection techniques (Hartmann and Englert 2012) and the optimization of the Tol2 transposase system (Valenzano, Sharp, and Brunet 2011) marked the beginning of genome editing in this model organism. Soon afterwards, the newly developed CRISPR/Cas9 targeted mutagenesis system was established for killifish embryos (Harel et al. 2015) and then further optimized over the years (Harel, Valenzano, and Brunet 2016; Oginuma et al. 2022; Bedbrook et al. 2023). Killifish embryos develop slower than other teleosts, making transgenesis a relatively-time-consuming technique. One study demonstrated the possibility to bypass development by directly expressing a transgene in adult fish, using somatic electroporation of muscle tissue (Moses, Franek, and Harel 2023).

Turquoise killifish can tolerate a broad spectrum of water temperatures, salinity and pH and differences among laboratory aquaria often cause deviations in reported lifespans (Polacik, Blazek, and Reichard 2016). Researchers are still optimizing hatching, maintenance (Nath et al. 2023; Dodzian et al. 2018) and feeding parameters (Zak, Dykova, and Reichard 2020), but unfortunately a worldwide accepted standard method does not yet exist. Recently, one group engineered a cheap automated feeding system for adult killifish (McKay et al. 2022). This system overcomes the prohibiting costs of commercial scientific-grade automated feeding aquaria and allows for time-specific and amount-regulated feeding regimes and drug screens on killifish across their lifespan.

A number of additional tools have been developed over the years, including non-lethal blood sampling (Dolfi, Ripa, et al. 2023) for longitudinal studies, sperm cryopreservation (Dolfi, Suen, et al. 2023b) and *in vitro* fertilization (Dolfi, Suen, et al. 2023a) which combined reduce costs of maintaining multiple mutant lines and allows the generation of frozen biobanks. Many of the techniques and tools developed for killifish, including some of the ones mentioned above, are summarized in the manual recently published by Cold Spring Harbor Laboratory Press (Brunet 2023).

It is also important to note the limitations of *N. furzeri* as a model organism for ageing research. One limitation is the aforementioned lack of globally standardized husbandry. Another, involves the lack of commercially available cross-reacting antibodies, since most antibody-generating companies generally focus on mammalian

antigens. As *N. furzeri* is a relatively new model, the pool of available mutants is limited, there is no shared frozen genetic repository, and no commercial CRISPR mutagenesis services exist for killifish. As a result, any hypothesis involving genetic manipulation typically requires the in-house generation and validation of new lines from the ground up. Lastly, although time-specific and tissue-specific expression systems have been successful (Bedbrook et al. 2023; Allard, Kamei, and Duan 2013), they always involve zebrafish or medaka promoters, instead of killifish elements, and can become leaky or silenced (Valenzano, Sharp, and Brunet 2011).

### 3.3.3 Similarities and differences to human ageing

Killifish undergo significant physiological decline during adult life resembling aspects of human aging. They exhibit reduced fecundity, decreased locomotion, cognitive decline, loss of pigmentation, spinal kyphosis (Kim, Nam, and Valenzano 2016; Genade et al. 2005), sarcopenia (Ruparelia et al. 2024), neurodegeneration (Bagnoli et al. 2022), cancer (Di Cicco et al. 2011), metabolic dysfunction (Ripa, Ballhysa, et al. 2023), lipodystrophy (Ripa, Mesaros, et al. 2023) and immunosenescence (Bradshaw et al. 2022).

In addition, killifish experience several of the so-called molecular ‘hallmarks of ageing’ similar to other species (Lopez-Otin et al. 2023) (**Figure 4**). These hallmarks include: loss of proteostasis, disabled macroautophagy, dysbiosis, epigenetic alterations, mitochondrial dysfunction, deregulated nutrient-sensing, stem cell exhaustion, telomere attrition, cellular senescence, altered intercellular communication, genomic instability, and chronic inflammation. Below we outline various studies exploring these hallmarks in killifish.

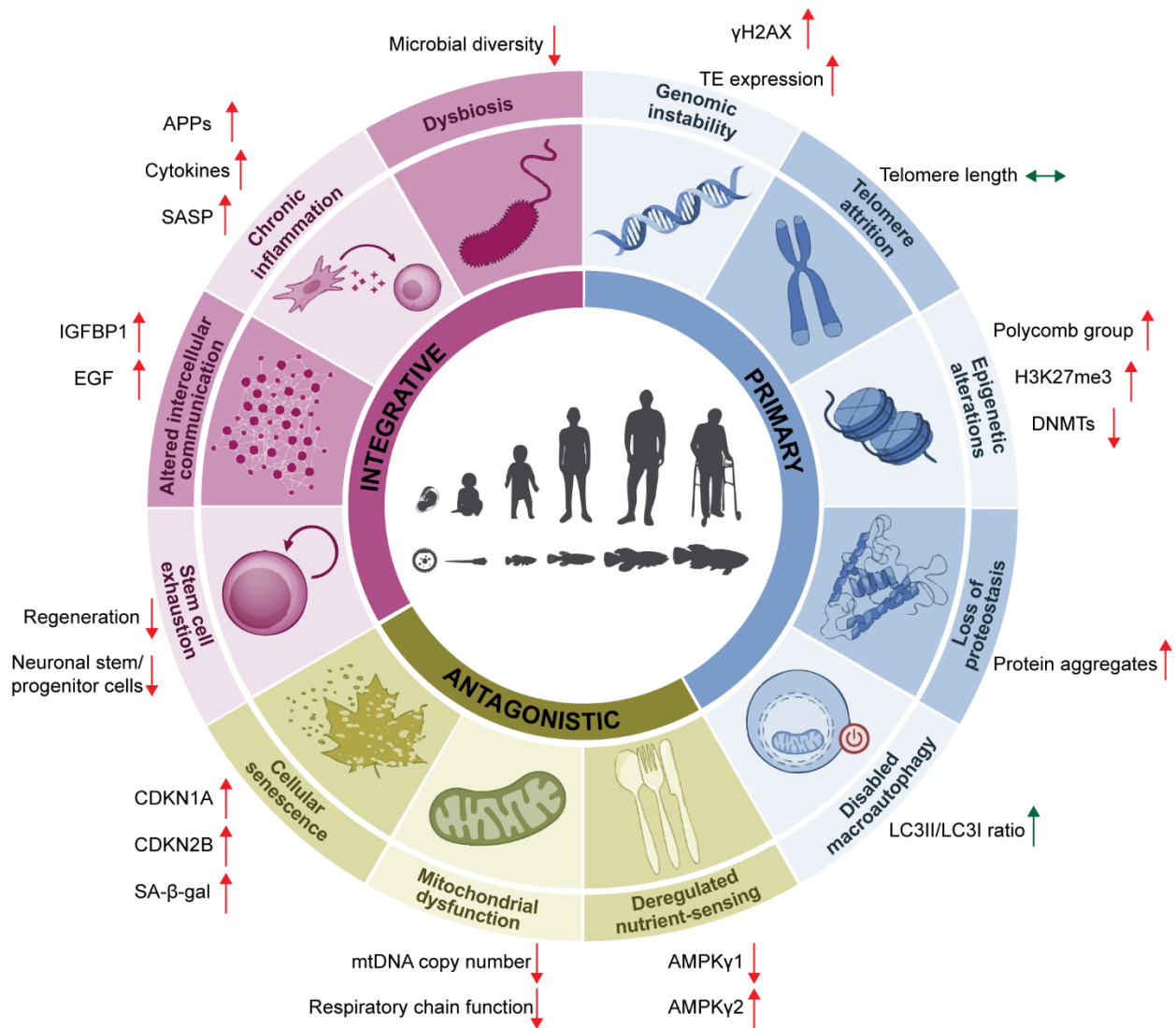


**Figure 4. Killifish ageing recapitulates human ageing hallmarks.** The figure summarizes the current knowledge on the ageing physiology of the short-lived strain of *N. furzeri*. Red arrows indicate similar regulation between human ageing and killifish ageing. Green arrows indicate the direction of regulation in killifish, but not humans. Telomere attrition has only been identified in the long-lived strain of *N. furzeri*. Apart from the opposite regulation of LC3II/LC3I ratio, there is very limited knowledge on killifish autophagy during ageing. Image adjusted from (Lopez-Otin et al. 2023).

Direct evidence for **loss of proteostasis** was recently uncovered in *Nothobranchius*. During ageing, the correlation between mRNA and protein levels in the killifish brain is progressively lost (Kelmer Sacramento et al. 2020). This leads to a disruption of stoichiometry in multiple protein complexes and accumulation of



unassembled protein aggregates. In support of this, another study showed the accumulation of aggregated proteins with prion like properties in killifish brains with age (Harel et al. 2024).

Concerning **macroautophagy** or autophagy in general, very little is known in killifish. One study has investigated autophagosome markers, such as LC3 and p62, with age in the in killifish using an immunoblot assay to assess autophagic flux. The authors found no change during ageing in muscles for either marker during most of the aging trajectory. But in very old fish, there was an increase in LC3II/LC3I ratio (marker for autophagosome formation) and reduction of p62, indicating a higher autophagic flux in animals (Ruparelia et al. 2024), possibly reflecting demographic selection for longer lived survivors undergoing caloric restriction. By contrast, humans and mice muscles exhibit decreased LC3II/LC3I ratio in muscles with old age (Carnio et al. 2014), while other tissues, such as motor neurons, appear to have either decreased LC3 or simultaneous increase of LC3 and p62, indicating reduced flux and autophagosome accumulation (Jahanian et al. 2024).

Intriguingly, humans and killifish share the same four dominant gut microbial phyla: Firmicutes, Actinobacteria, Bacteroidetes, and Proteobacteria (Smith et al. 2017). Both humans and killifish undergo age-related **dysbiosis**, manifested as reduced taxonomic diversity in intestinal microbiome with age (Biagi et al. 2016; Smith et al. 2017). Interestingly, transplantation of a young microbiota into middle-aged fish can extend their life span, providing seminal evidence for the microbiome modulating vertebrate aging.

Regarding the hallmark of **epigenetic alterations**, just like in humans (Horvath et al. 2012), killifish tissues display an increase in expression of polycomb complex members (Baumgart et al. 2014), have increased H3K27me3 histone modifications and downregulated DNMTs (DNA methyltransferases) with age (Zupkovitz et al. 2021). Killifish also undergo an erosion of DNA methylation marks with aging, but researchers have yet to develop a DNA-methylation based aging clock in this species.

**Mitochondrial dysfunction** also appears to impact killifish ageing. Similarly to humans (Filograna et al. 2021), old killifish tissues showed reduced mtDNA copy number in multiple tissues and reduced respiratory chain function in skeletal muscles with age

(Hartmann et al. 2011). Unlike humans (Samuels, Schon, and Chinnery 2004), killifish do not show increased large-scale deletions in their mtDNA with old age (Hartmann et al. 2011), suggesting that functional rather genetic disruption of mitochondria are more critical to the ageing process.

The most robust interventions that extend lifespan in mammalian models are associated with **nutrient sensing** pathways (Singh et al. 2019). Killifish males do respond to dietary restriction and live longer with fewer calories in the diet (McKay et al. 2022), but to date, there is relatively little knowledge about the effects of nutrient sensing factors, such as IGF1 or TOR, on the lifespan of killifish. On the other hand, our laboratory discovered a dynamic regulation of AMPK subunits during fasting and re-feeding in killifish (Ripa, Ballhysa, et al. 2023). We found a higher expression and usage of the  $\gamma 1$  (gamma1) subunit during feeding and  $\gamma 2$  (gamma2) during fasting. Regardless of feeding regime, with old age there is a sustained  $\gamma 2$  subunit usage. Overexpression of  $\gamma 1$  subunit improved metabolic health and prolonged lifespan in killifish, providing the first genetic evidence for AMPK regulating vertebrate life span. In humans, we found that  $\gamma 1$  expression inversely correlates with frailty score and mortality risk, suggesting this gene to be an important component of life span regulation.

Two aspects of **stem cell exhaustion** have been described in the ageing killifish; reduced limb regeneration capacity and decay of adult neurogenesis. Unlike humans, teleosts are able to regenerate the epidermis, bones, blood vessels, nerves, connective tissue and pigmentation after fin amputation. Regenerative capacity, however, has been shown to decrease in older age in the killifish (Wendler et al. 2015). Also distinct from humans, teleosts have multiple neurogenic niches and carry out adult neurogenesis in basically all regions of the brain (Ekstrom, Johnsson, and Ohlin 2001). Like humans, killifish exhibit age-dependent neurodegeneration and cognitive impairment (Tozzini et al. 2012; Valenzano et al. 2006).

**Telomere shortening** has been reported in many species, including humans, and its rate of attrition can predict lifespan (Whittemore et al. 2019). By comparing young and old skin and muscle tissues, it was found that the longer-lived MZM-0403 strain exhibited telomere shortening with age, but the shorter-lived GRZ strain did not (Hartmann et al. 2009). Apparently, the exceptional short lifespan of this strain is independent of telomere attrition. Nevertheless, similar to mammals (Pech et al. 2015),

telomere maintenance in the GRZ strain is essential, since telomerase deficiency leads to age-related degeneration of gonadal stem cells (Harel et al. 2015).

**Senescent cells accumulate** in multiple human tissues (He and Sharpless 2017) as well as killifish tissues. One study found increased expression of cyclin-dependent kinase inhibitors (CDKN1A and CDKN2B) in the skin with age in the long-lived strain, but not the short-lived (Graf et al. 2013). However, another study found increased senescence-associated  $\beta$ -galactosidase activity (SA- $\beta$ -gal) in the dermis with age in the short lived strain (Genade et al. 2005). The heart as well as the retina, optic nerve and optic tectum of the short-lived strain also exhibit strong increase in SA- $\beta$ -gal with age and increased cyclin inhibitor expression (Ahuja et al. 2019; Vanhunsel et al. 2021). In this study we also show increased cyclin-dependent kinase inhibitor expression (such as CDKN1A and CDKN2B) in both kidneys and gut of the short-lived strain. In the same tissues, we observed increased transcriptional expression of senescence-associated secretory phenotype (SASP) components, such as IGFBP1 (Insulin Like Growth Factor Binding Protein 1) and EGF (Epidermal Growth Factor), indicating conservation of the **altered intercellular communication** hallmark as well.

Human tissues undergo DNA damage and accumulate genetic mutations with age in a tissue specific manner (Yizhak et al. 2019). In killifish, skeletal muscles display a more than 3-fold increase in  $\gamma$ H2AX levels (phosphorylated H2A histone family member X, a marker of double-strand breaks) with age (Cencioni et al. 2019). Another study used flow cytometry on kidney marrow cells from young and old killifish and found increased staining intensity of  $\gamma$ H2AX and percentage of positive cells (Morabito et al. 2023). Indirect evidence of **genomic instability** in killifish ageing can also be inferred from the increase in transposable element transcripts detected in the old brain (Xu et al. 2023). Upregulation of transposable element expression is often accompanied by an increase in DNA damage due to transposition or senescence initiation (Simon et al. 2019; De Cecco et al. 2019).

All the previous hallmarks are thought to fuel **chronic inflammation** (Lopez-Otin et al. 2023). Chronic inflammation during aging has been termed ‘inflammaging’ and is characterized by low-grade sterile increase in pro-inflammatory cytokines, which are primarily identified in the blood (Ferrucci and Fabbri 2018). Plasma proteomics in killifish revealed an increase in acute phase proteins (APPs), such as complement and

coagulation factors which have been used as inflammatory markers (Morabito et al. 2023). Kidney proteomics also revealed an increase in cytokine production with age in killifish (Morabito et al. 2023). Transcriptomics in brain, heart, muscle and spleens from both male and female killifish revealed widespread upregulation in inflammatory pathways, to varying degrees, in all tissues (Xu et al. 2023). In this study we also show complement and coagulation components, as well as pro-inflammatory SASP components, such as TNFRSF11B (tumor necrosis factor receptor superfamily, member 11b) and CXCL12B (C-X-C Motif Chemokine Ligand 12) increasing with age in killifish kidneys and guts.

In sum, killifish bear many similarities to mammalian and human ageing, however, as a relatively new model system, much remains to be established and explored. Importantly, the multitude of normative ageing phenotypes at both molecular and organismal level reflect a naturally evolved short-lived vertebrate, not a progeroid or disease model. Even certain non-conserved features of killifish biology, such as enhanced regenerative capacity and diapause, can offer transformative insights into human biology, because they inform us of resilience and restoration in a living system, with important implications for regenerative medicine and ageing research.

### 3.4 Inflammaging

The term *inflammaging* was first introduced by Claudio Franceschi in 2000 (Franceschi et al. 2000) and is defined as chronic, sterile, low-grade increase in basal inflammatory levels with age (Franceschi et al. 2018). ‘Chronic’ is the key point that defines inflammaging as a negative process. Acute, transient immune responses facilitate tissue repair after injury, defend against pathogen infections, initiate turnover of damaged molecules or organelles and help clear compromised or malignant cells (Franceschi and Campisi 2014). Chronic inflammation can lead to both structural and functional decline at a cellular, tissue and eventually organismal level. Mechanistically, chronic inflammation resembles acute inflammation, but differs in intensity and duration.

An example of the distinction between acute and chronic inflammation is illustrated by IL-6 (interleukine 6) function, a key inflammatory cytokine. IL-6 levels sharply increase after exercise and enhance insulin sensitivity, stimulates anti-inflammatory cytokine production and mobilizes natural killer T cells to protect against cancer formation or progression (Orange et al. 2023). Yet prolonged IL-6 signaling can promote tumor growth and activate pro-inflammatory cytokine production, locking in a chronic low-grade inflammatory state (Orange et al. 2023).

This IL-6 example also illustrates the complex dynamic nature of inflammatory cytokines, which can paradoxically have both pro- and anti-inflammatory effects, depending on the network of interactions and feedback loops with other cytokines and receptors (Zhang and An 2007). Lack of understanding of these interactions can lead to unexpected results. For example, inhibition of TNF $\alpha$  (tumor necrosis factor-alpha), another established pro-inflammatory cytokine, can lead to uncontrolled IL-12-dependent inflammation (Zakharova and Ziegler 2005).

Markers of inflammaging include increased circulating levels of IL-1, IL-6, IL-8, IL-13, IL-18, IFN $\alpha$ , IFN $\beta$ , TGF- $\beta$  and acute phase proteins among others (Ferrucci and Fabbri 2018; Batista et al. 2020). Despite heightened inflammatory tone, the aging immune system becomes less responsive to both internal and external antigens, with a diminished ability to eliminate damaged or cancerous cells (Pawelec 2018). This decline in immune function, known as 'immunosenescence', is linked to or potentially caused by inflammaging. Apart from the immune system, these circulating inflammatory factors also have systemic effects, influencing multiple organs and ultimately reducing overall health.

### 3.4.1 Impact on cells and tissues

Circulating inflammatory cytokines like IL-1, IL-6, and TNF $\alpha$  influence hematopoietic stem and progenitor cells (HSPCs), steering their differentiation toward myeloid (neutrophils and monocytes) instead of lymphoid differentiation (natural killer cells, T-cells and B-cells) (Jahandideh et al. 2020). This creates a feedback loop, whereby innate immune cells increase at the cost of adaptive immune cells, which then in turn

increase circulating cytokines that further promote this misbalance (Pioli et al. 2019). Furthermore, these innate immune cells appear to be impaired with age. Neutrophils show increased apoptosis, decreased phagocytic capacity and dysfunctional adhesion and chemotaxis with age (Li et al. 2023). Aged macrophages downregulate both glycolysis and oxidative phosphorylation, leaving them in an energy-depleted dysfunctional state (Minhas et al. 2021). Among other deficiencies, aged macrophages also display a number of senescent hallmarks, such as increased secretion of SASP components such as IL-1 $\beta$ , IL-6, TNF $\alpha$  and the pro-fibrotic molecule TGF- $\beta$  (Yousefzadeh et al. 2021; Campbell et al. 2021). Further promoting fibrosis, aged macrophages also have decreased expression of IL-10, a crucial anti-inflammatory and anti-fibrotic cytokine (Zhang et al. 2015).

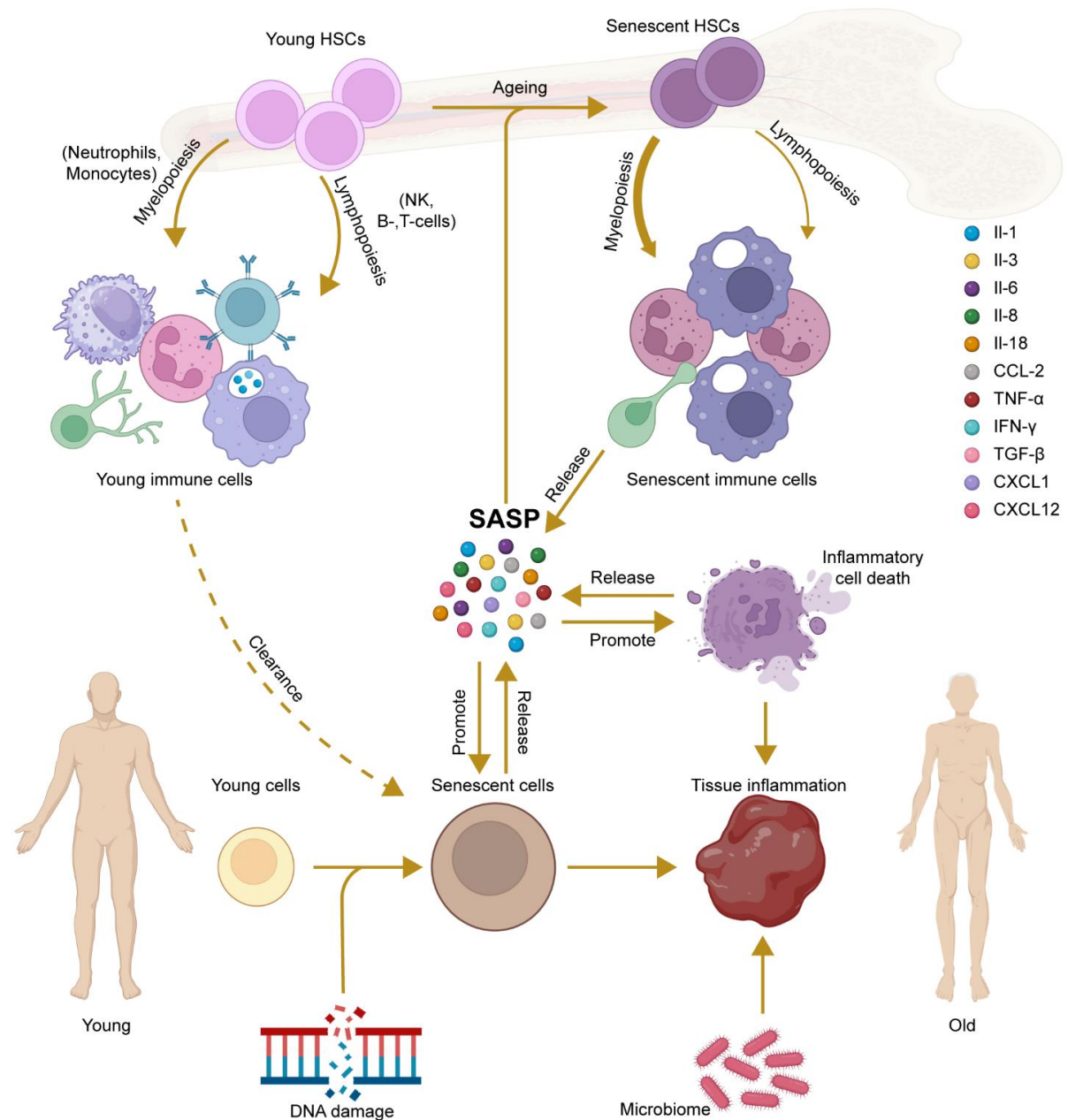


**Figure 5. Inflammageing occurs at the molecular, cellular, and organ levels during ageing.** During ageing cells within the body enter senescence, a state marked by dysfunction and release of pro-inflammatory factors known as the senescence-associated secretory phenotype (SASP). While immune cells help clear senescent cells, they are also affected by SASP, contributing to immunosenescence – a decline in immune function that reduces the body's ability to fight infections and disease. The buildup of senescent cells promotes organ inflammation, increasing susceptibility to age-related diseases. This process is amplified by feedback loops that sustain inflammation and exacerbate tissue damage, further accelerating aging and disease risk. Image adjusted from (Li et al. 2023).

The primary niche of HSPCs, the bone marrow, is also significantly affected by inflammaging; bone marrow degeneration, in turn, further exacerbates immunosenescence. Bone marrow mesenchymal stem cells (MSCs) lose stemness with age, while acquiring senescent features, such as increased DNA damage, elevated ROS levels (reactive oxygen species) and increased expression of cyclin-dependent kinase inhibitors and SASP components (Stolzing et al. 2008). This stem cell loss results in replacement of red bone marrow by fat cells and transforms into a yellow or fatty bone marrow incapable of supporting robust hematopoiesis (Gurevitch, Slavin, and Feldman 2007).

Another tissue severely impacted by chronic inflammation is the kidney. During ageing, human kidneys exhibit increased basal expression of inflammatory genes (Rodwell et al. 2004). This chronic inflammation impairs the regenerative capacity of tubular epithelial cells, which leads to a significant increase in susceptibility to acute kidney injury (AKI) with age (Sato and Yanagita 2019). Adults with chronic kidney disease (CKD) also exhibit a very similar immunosenescent phenotype (Sato and Yanagita 2019). After kidney injury, Toll-like and IL-1 receptors mediate senescence in tubular epithelial cells, connecting immune regulators and senescence in this organ (Jin et al. 2019). Though many senescent markers remain unchanged during kidney ageing, p16 expression increases (Melk et al. 2003) and clearance of these p16<sup>INK4a</sup>-expressing cells improves kidney health in ageing mice (Baker et al. 2016).

The gastrointestinal system is also strongly affected by inflammaging. The gut exhibits age-related dysbiosis, in which an imbalanced microbiome can be both the cause and effect of inflammation. The intestinal epithelium is normally coated with mucin, which prevents direct interaction between intestinal epithelial cells and microbes. It has been reported in mice (Elderman et al. 2017) and humans (Baidoo and Sanger 2024) that with aging, mucin production decreases, resulting in a thinner, more permeable and even discontinuous layer which can trigger inflammation. Microbes can also cause an age-related increase in paracellular permeability or 'gut leakiness', and infect the host (Ragonnaud and Biragyn 2021). Conversely, decreasing inflammaging appears to ameliorate dysbiosis: elderly TNF knockout (KO) mice exhibit lower levels of dysbiosis than old wild-type (WT) and anti-TNF treatment modulates the microbiome of old, but not young mice (Thevaranjan et al. 2017). Also, inflammatory cytokines can increase gut leakiness by decreasing expression of tight junction proteins (DeJong, Surette, and Bowdish 2020). Evidently, dysregulation of the gut can lead to the loss of a primary line of defense against pathogens, and propagate feedback loops that aggravate and perpetuate inflammation.

Multiple other tissues, such as brain, heart and liver, are affected by inflammaging and have a causal relationship with age-related disease (Li et al. 2023), which we don't cover here. Each tissue contributes to systemic inflammation to varying degrees and also responds differently to inflammatory stimuli. When studying such systemic physiology, it is important to compare and contrast mechanisms and responses of various tissues.

### 3.4.2 Sources of inflammaging

An important question is what are the sources of inflammaging? A number of factors that contribute to inflammatory signals can be grouped into three main categories: non-self, quasi-self and self. Non-self factors include infections such as viral and bacterial infections. These are more likely opportunistic infections that occur in the context of an already weakened immune system. Currently there is no consensus on whether early life or recurring infections strengthen or weaken the immune system later in life (Batista et al. 2020). Quasi-self triggers of inflammaging include the microbiome



and nutrients. The composition (e.g. high fat percentage) and quantity of nutrients can increase inflammation, as seen during obesity and type-2 diabetes (Frasca, Blomberg, and Paganelli 2017). But, specific categories of nutrients can also initiate inflammation, such as saturated fatty acids, which activate both TLR2 and TLR4 to trigger innate immune responses (Huang et al. 2012). Self factors include the accumulation and release of molecular debris by dying cells (dubbed 'garb-aging') (Franceschi et al. 2017) and SASP components released by senescent cells (Olivieri et al. 2015).

Cell death is also an important trigger of inflammaging. According to estimates, adult human bodies generate billions of dead cells per day (Strippoli et al. 2024). Yet, cell death *in vivo* is not always inflammatory. Under physiological conditions, apoptosis is considered to be an immunologically silent form of cell death, as apoptotic caspases (caspase-9 and caspase-3/7) block inflammatory responses (Bock and Riley 2023). On the other hand, other types of cell death can be highly inflammatory, such as necroptosis, pyroptosis and ferroptosis. Necroptosis markers increase with age in mice livers (Mohammed et al. 2021). Notably, short-term treatment of necrostatin-1s (necroptosis inhibitor) in old mice reduces M1 (pro-inflammatory) Kupffer cells (liver macrophages), senescent cells, fibrosis and pro-inflammatory cytokines (Mohammed et al. 2021). Similarly, pharmacological or genetic inhibition of pyroptosis (Zhou, Qiu, et al. 2023) or ferroptosis (Mazhar et al. 2021) can ameliorate multiple age-related diseases.

#### 3.4.2.1 Senescence

Senescent cells are considered a major source of inflammaging. Cellular senescence was first discovered by Hayflick who found unexpectedly that cultured cells do not divide indefinitely, but cease division after a certain number of rounds (Hayflick and Moorhead 1961). In this case, it turns out that telomere attrition leads to a checkpoint leading to cell cycle arrest (Harley, Futcher, and Greider 1990). It was later found that, aside from telomere attrition, there are multiple drivers of cellular senescence *in vitro*, including DNA damage (Di Leonardo et al. 1994), oncogene expression (Courtois-Cox et al. 2006), mitochondrial dysfunction (Wiley et al. 2016), infections (Reyes et al. 2023), ROS (Chen et al. 1995), nutrient imbalance (Carroll and Korolchuk 2018), mechanical

stress (Sladitschek-Martens et al. 2022), paracrine senescence mediated by SASP (Acosta et al. 2013) and other mechanisms. Depending on the stimulus, different cellular pathways can signal towards senescence establishment. But once established, senescence is typically characterized by a highly stable cell-cycle arrest with accumulation of macromolecular damage, deregulated metabolic profile and broad secretory phenotype (Gorgoulis et al. 2019; Gonzalez-Gualda et al. 2021).

Cell cycle arrest is typically mediated by two interconnected pathways involving p53/p21 and p16/Rb (Mijit et al. 2020) (**Figure 6**). p53 is a master regulator of cell cycle checkpoint control activated in response to various stressors, including DNA damage. Once expressed, p53 regulates thousands of genes and can trigger senescence under mild stress conditions and apoptosis under severe or prolonged stress (Chen, Liu, and Merrett 2000). A critical target, p21, is necessary for p53-mediated senescence (Rufini et al. 2013), and plays two roles in establishing senescence. As indicated by its alternative name CDKN1A (cyclin dependent kinase inhibitor 1A), it inhibits cyclin-dependent kinases (such as CDK2), thus preventing cell cycle progression (Dutto et al. 2015). Equally important, it serves as an apoptosis inhibitor, blocking caspase activation cascades and promoting cell survival (Yosef et al. 2017).

p53/p21 pathway activation is an early response to stress and mediates the decision to enter senescence or not. After this early phase, p53 levels drop and another pathway takes responsibility for senescence maintenance (Dolan et al. 2015). Specifically, through a complex regulatory network, p16 becomes activated during early senescence, and acts to maintain it (Rayess, Wang, and Srivatsan 2012). If p16 levels do not reach a critical threshold before p53 expression drops, senescence can be bypassed (Beausejour et al. 2003). Like p21, p16 (CDKN2A) is a cyclin-dependent kinase (CDK) inhibitor, specifically targeting CDK4 and CDK6. During cell cycle progression, cyclin-CDK complexes phosphorylate RB (retinoblastoma) family proteins. Phosphorylated RB proteins lose their ability to inhibit E2F transcription factors, which drives the expression of cell cycle genes. Cyclin-CDK inhibitors like p16 and p21 prevent CDK activity, maintaining RB in its active, unphosphorylated state, thereby suppressing E2F activity and blocking cell cycle progression (Gorgoulis et al. 2019).

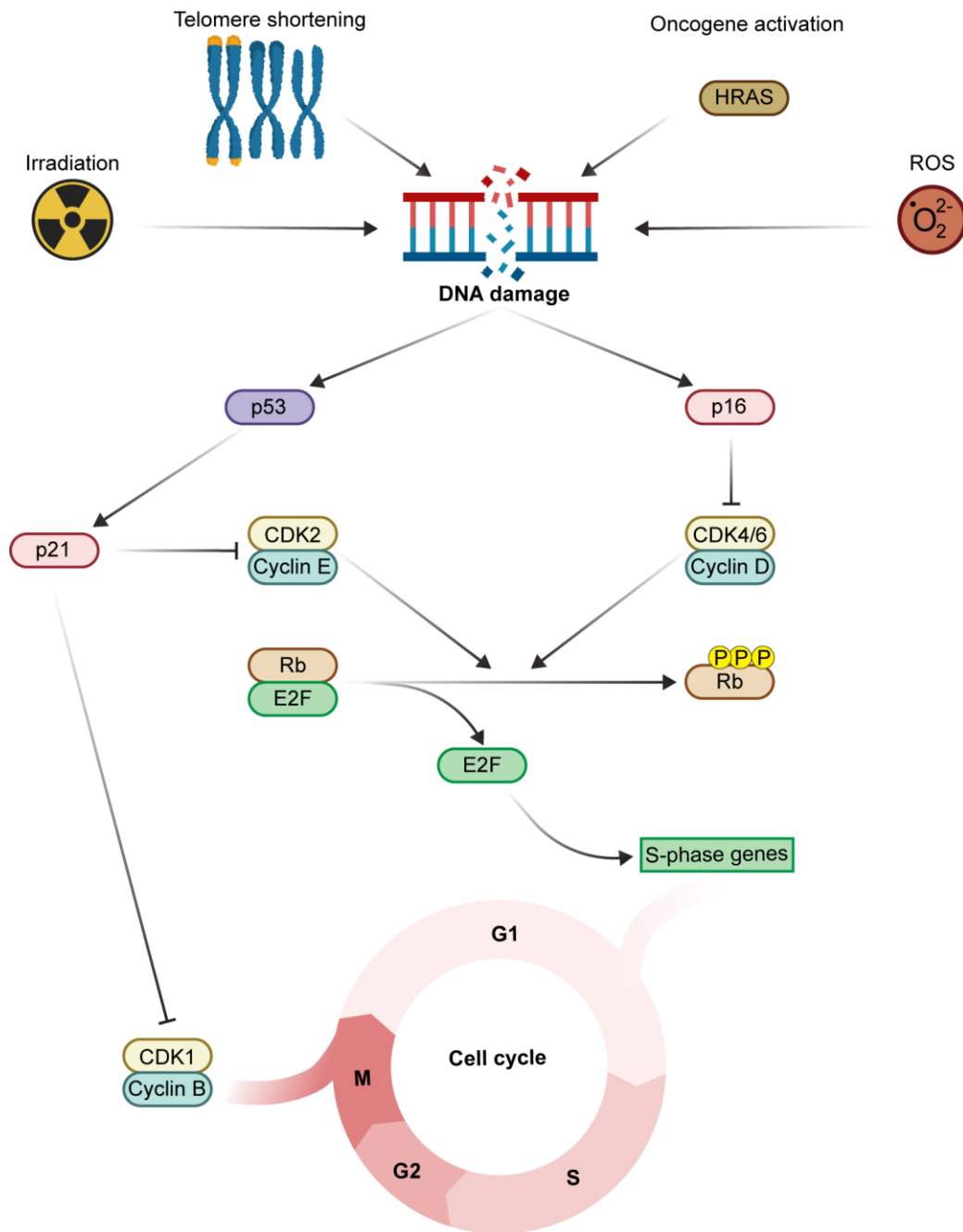


**Figure 6. Cell-cycle arrest during DNA-damaged induced senescence.** Irradiation, telomere attrition, oncogene expression and ROS lead to DNA damage which in turn activates p53/p21 and p16. These elements inhibit cyclin-dependent kinases required for Rb phosphorylation and E2F release. By inhibiting the cyclin-dependent kinases, p53/p21 and p16 cause irreversible cell cycle arrest at G1/S and M/G1 checkpoints. Image modified from (Lawrence et al. 2024).

Of note, RB and p53 activation also inhibit cycle progression outside the context of senescence (for example quiescence and differentiation) (Gorgoulis et al. 2019). Also, even though p16 is a widely used marker of senescence, it can be highly expressed in certain cancer cells (Sharpless and Sherr 2015). Additionally, lack of p16 can be compensated by activation of p15 (CDKN2B) and CDKN2C (Sharpless and Sherr 2015). Thus, defining cellular senescence often requires measuring additional features.

Macromolecular damage is a major hallmark of senescent cells. Notably, DNA damage is a well-established inducer of both senescence and inflammaging and will be discussed separately below. The DNA damage response (DDR) is also a consequence of senescence and markers of DDR, such as  $\gamma$ H2AX (S139-phosphorylated H2A histone family member X), can also be used as markers for senescence (Bernadotte, Mikhelson, and Spivak 2016). Further, DNA damage-induced senescent cells harbor persistent nuclear damaged foci termed DNA-SCARS (DNA segments with chromatin alterations reinforcing senescence) (Rodier et al. 2011). Unlike transient DNA damage lesions, DNA-SCARS can persist for a very long time (even years as mentioned by unpublished observations of Fabrizio d'Adda di Fagagna (d'Adda di Fagagna 2008)) and do not recruit the DNA repair proteins RPA (replication protein A) and RAD51 (Rodier et al. 2011). DNA-SCARS are mostly observed under DNA damage-induced senescence. Another DNA damage feature of senescence cells, cytoplasmic chromatin fragments (CCFs), can be observed even in replicative senescence (due to telomere shortening) or oncogene-induced senescence (OIS) (Ivanov et al. 2013). CCFs specifically have been characterized to induce inflammation through the cytoplasmic DNA surveillance pathway cGAS/STING.

Lysosomal and mitochondrial dysfunction are also hallmarks of senescent cells. Lysosomes of senescent cells increase in number and size (Robbins, Levine, and Eagle 1970), but this increase in lysosomal content does not typically translate to increased function, as the lysosomal degradation stage of autophagy declines, leading to accumulation of damaged organelles and molecules (Park et al. 2018). Increased lysosomal mass is linked to a common senescence marker, the senescence-associated beta-galactosidase (SA- $\beta$ -gal) activity, although it is neither required nor a determinant of senescence (Hernandez-Segura, Nehme, and Demaria 2018). Senescent cell mitochondria also exhibit increased mass, but also decreased membrane potential, higher proton leak, and increased tricarboxylic acid (TCA) cycle metabolites (Kaplon et

al. 2013). Some of these phenotypes likely reflect the inhibition of mitophagy, since mitophagy activation can suppress the SASP (Correia-Melo et al. 2016). The DNA surveillance pathway cGAS/STING has been shown to promote a senescent secretome during mitochondria dysfunction (West et al. 2015; Gulen et al. 2023). Both CCFs and mitochondrial dysfunction lead to mtDNA leak engaging the cGAS/STING pathway to activate the SASP.

A major feature of senescent cells is their secretory phenotype. This secretome is comprised of pro-inflammatory cytokines and chemokines, growth factors, angiogenic factors and matrix metalloproteinases (MMPs) (Coppe et al. 2010). SASP factors are not always physiologically detrimental. They contribute to embryonic patterning signals in the apical ectodermal ridge and neural roof plate during mice embryonic development (Storer et al. 2013). SASP growth factors are necessary for wound healing in mice (Demaria et al. 2014) and for limb regeneration in zebrafish (Da Silva-Alvarez et al. 2020). P53 and p16 deficient mice exhibit increased liver fibrosis following liver damage (Krizhanovsky et al. 2008), later attributed to decreased MMP production (Kim et al. 2013). Similarly, SASP components limit skin scarring, oral, renal and cardiac fibrosis and atherosclerosis (Munoz-Espin and Serrano 2014). Lastly, SASP components can activate senescence in a paracrine fashion and recruit immune cells to limit and clear tumors (Munoz-Espin and Serrano 2014). Like inflammation, then, transient SASP has evolved beneficial effects in development and disease, but chronic SASP leads to a number of pathologies.

Aberrant SASP can lead to recruitment of immature immune-suppressive myeloid cells in certain tumors (Atala 2015), while angiogenic factors contribute to vascularization and metastasis of such tumors (Coppe et al. 2010). Outside of tumor microenvironments, senescence can spread to neighboring healthy cells *in vitro* and *in vivo* due to paracrine senescence mediated by SASP components (Acosta et al. 2013). Whereas transient SASP release was shown to reduce fibrosis, chronic SASP promotes fibrosis, and senolytic drugs (compounds that cause senescent cell clearance) are being tested for multiple fibrotic diseases (O'Reilly, Tsou, and Varga 2024). Lastly, SASP components are effectively the main constituents of inflammaging (Li et al. 2023) and are linked to a number of age-related ailments, such as neurodegeneration (Diniz et al. 2021)

cardiovascular diseases (Boniewska-Bernacka, Panczyszyn, and Klinger 2020) and adipocyte dysfunction (Stout et al. 2017).

The composition and abundance of SASP components varies between senescent cells, influenced by the underlying cause of senescence, as well as cellular identity and time course of the process (Childs et al. 2015). This variability has complicated efforts to generate a definitive list of SASP factors (Coppe et al. 2010). Nevertheless, a recent study utilizing extensive datasets from bulk and single-cell RNA sequencing (scRNAseq) identified a signature of commonly transcriptionally regulated SASP and senescence markers, referred to as the 'SenMayo' gene set (Saul et al. 2022). Mechanistically, the change of SASP composition over time appears to depend on NOTCH1 (Notch Receptor 1) level fluctuations (**Figure 7**). In particular, early SASP is mediated by high NOTCH1-induced TGF- $\beta$ -regulated SASP, which is not considered as highly inflammatory (Hoare et al. 2016). Late SASP has low NOTCH1 immune-suppressing signaling, has increased C/EBP $\beta$  and NF-kB signaling (Ito, Hoare, and Narita 2017) and is characterized by derepression of LINE-1 retrotransposable elements, which then leads to highly inflammatory SASP through nucleic acid surveillance (De Cecco et al. 2019).

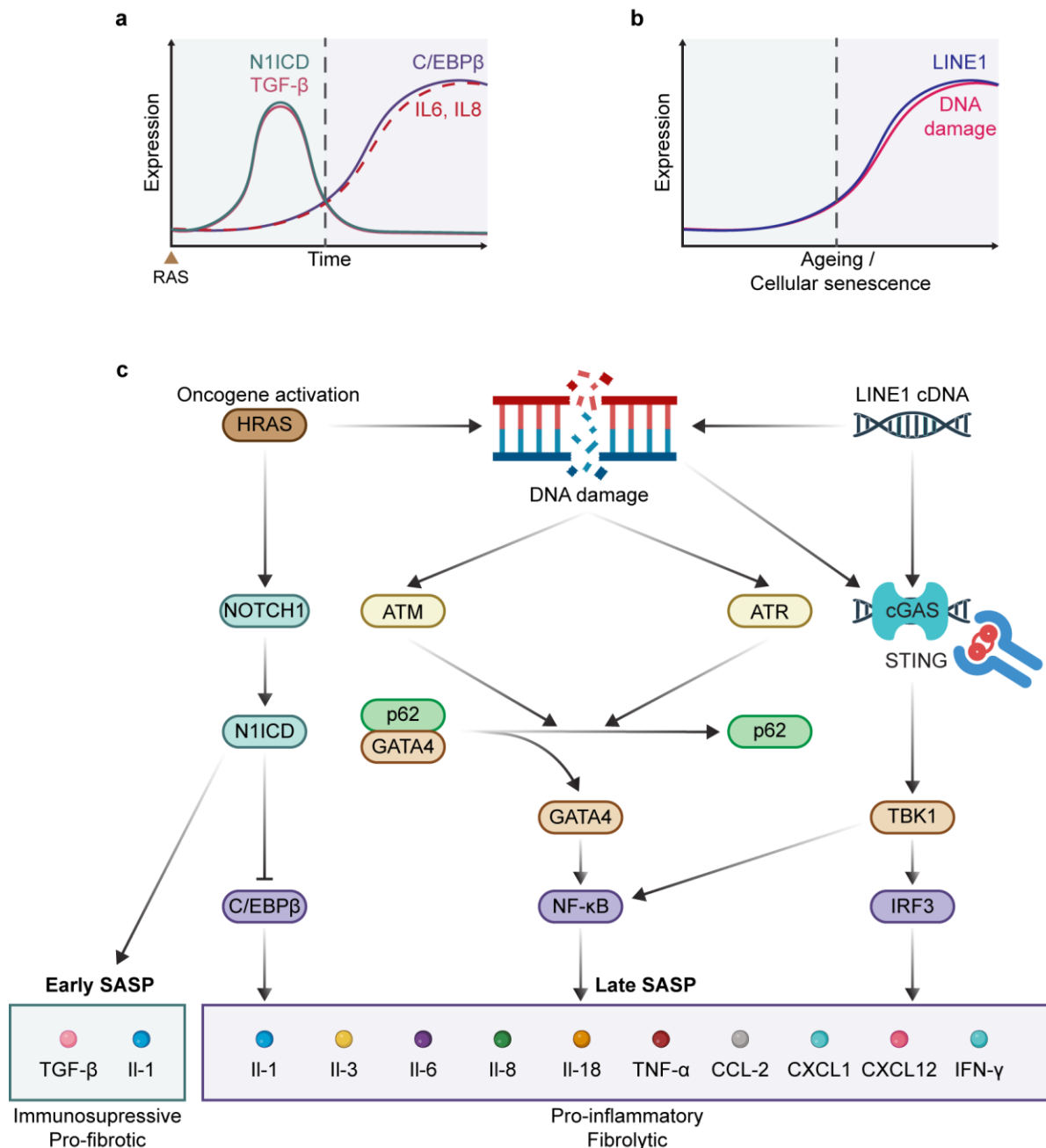


**Figure 7. Dynamic regulation and establishment of SASP components.** **a**, Modulation of early and late SASP components has been best described in oncogene induced senescence (Ito, Hoare, and Narita 2017). RAS-induced senescence leads to early upregulation of the active form of NOTCH1, the NOTCH1 intracellular domain (N1ICD) and TGF $\beta$ , which establish the early SASP. Then N1ICD and TGF $\beta$  levels drop allowing the expression of the proinflammatory transcription factor C/RBP $\beta$  and downstream late SASP. **b**, During ageing and during senescence, LINE1 retrotransposable elements are de-repressed and have been linked with late SASP expression. **c**, Regulation of early and late SASP during oncogene-, DNA damage- and retrotransposable element-induced

senescence. NOTCH1 signaling promotes early SASP and inhibits C/RBP $\beta$  expression. Late SASP is established after N1ICD drop later during senescence. DNA damage causes the activation of ATM and ATR kinases which inhibit the interaction between p62 and GATA4. Released GATA4 activates NF- $\kappa$ B-dependent SASP expression. Lastly, during ageing and late senescence, DNA damage accumulates and LINE1 elements are de-repressed. DNA fragments and LINE1 cDNA activate cGAS/STING, which then lead to a TBK1-mediated NF- $\kappa$ B and IRF3 signaling. Panel **a** is modified from (Ito, Hoare, and Narita 2017).

Although our understanding of the features of senescence has advanced significantly, confidently identifying senescent cells *in vivo* remains challenging for several reasons. In non-disease contexts, senescent cells are rare, even in old age (Idda et al. 2020). Then, the majority of cells within organisms are post-mitotic, therefore lack of cell replication on its own is not a useful marker. Also, the heterogeneity of the senescent program and inflammatory profile of different cell types further hinder senescent assessment *in vivo* (Gonzalez-Gualda et al. 2021).

Common approaches to assaying senescence *in vivo* involve staining for markers such as SA- $\beta$ -gal, p16, p21, and  $\gamma$ H2AX (Gonzalez-Gualda et al. 2021). However, each marker has limitations. SA- $\beta$ -gal staining is widely considered a reliable assay, but it requires fresh or living tissue, restricting its application with preserved samples. An alternative, Sudan Black-B (SBB) stains lipofuscin - an aggregate of oxidized proteins that accumulates in senescent cells. This method largely replicates SA- $\beta$ -gal staining in mouse tissues and can be applied to archived samples (Evangelou and Gorgoulis 2017; Georgakopoulou et al. 2013). Regarding p16, antibodies against it are considered unreliable, so it is generally preferred to use p16 promoter-regulated reporter strains instead (Omori et al. 2020; Gonzalez-Gualda et al. 2021). p21 levels usually drop after senescence is established (Stein et al. 1999), so late senescent cells are not stained. Meanwhile,  $\gamma$ H2AX is limited to DNA damage-induced induced senescence and can be confounded by cell death (Rodier et al. 2011). Finally, since all above stains can also mark cancer cells within tissues (Bojko et al. 2019), organisms are typically injected with nucleoside analogues EdU or BrdU before sacrificing and tissue harvesting. These analogues incorporate in the DNA of replicating cells and can be stained-against using click chemistry reactions (Salic and



Mitchison 2008). Ultimately, the identification of senescent cells *in vivo* requires a combination of multiple markers to overcome individual limitations and increase confidence.

Defining and characterizing senescent cells *in vivo* is important due to their profound impact on ageing physiology and even lifespan. Senolytics such as Dasatinib and Quercetin (Xu et al. 2018) or Fisetin (Yousefzadeh et al. 2018) improve health and extend lifespan in multiple model organisms (Kampkotter et al. 2008; Alugoju et al. 2018). Genetically-induced clearance of p16-positive cells leads to improved tissue function with age and lifespan in mice (Baker et al. 2011; Baker et al. 2016). Deletion of a single SASP component, IL-11, leads to delayed onset of age-related frailty and extends mouse lifespan by an average of 25% in both sexes (Widjaja et al. 2024). Thus, accurately targeting senescent cells and their inflammatory output holds great promise for prolonging healthy ageing and lifespan.

#### 3.4.2.2 DNA damage

Many features of ageing are causally and mechanistically linked with DNA damage (Schumacher et al. 2021). Endogenous DNA damage can be caused by errors in DNA replication, topoisomerase nicks and misaligned re-ligation, spontaneous deamination and hydrolysis, reactive oxygen species modifying bases and erroneous repair of methylated bases (Chatterjee and Walker 2017). It can also be triggered by exogenous factors such as ionizing (IR) and ultraviolet (UV) radiation, chemical compounds such as fungal toxins and aromatic amines (derived from smoking, fuels and industrial dyes) as well as environmental factors such as extreme heat, cold and mechanical stress (Chatterjee and Walker 2017; Gonzalo, Kreienkamp, and Askjaer 2017). Most of the above genotoxic stressors are commonly encountered throughout organismal lifespan, but under physiological conditions, most lesions are repaired.

Repair of DNA lesions depends on the type of damage. Base errors are repaired by nucleotide excision repair (mostly UV and chemotherapeutic-induced lesions), base excision repair (corrects abasic sites, oxidative, deamination and alkylation damage during G1 phase), mismatch repair, translesion synthesis (both employed by replicating

cells to ensure high replication fidelity) and interstrand cross-link repair (repairing covalently bound complementary bases) (Chatterjee and Walker 2017). Single strand breaks (SSBs) are typically generated by ROS, abasic sites and topoisomerase errors. SSBs are recognized by PARP1 (Poly [ADP-ribose] polymerase 1), which then employs a cascade of downstream factors leading to repair of the lesion (Caldecott 2022). Double strand breaks (DSBs) are highly toxic and involve two major repair pathways, homologous recombination (HR) and non-homologous end joining (NHEJ), with the former considered error free (though debated, see (Rodgers and McVey 2016)), while the latter can introduce sequence errors (Mao et al. 2008). HR requires the presence of a homologous sister chromatid as a recombination template, thus it is favored as a repair strategy at S and G2 phases, while NHEJ can happen at any point in the cell cycle (Zhao, Kim, et al. 2020).

One of the first responses to DSBs entails the activation of DNA damage response (DDR) kinases, such as ATM (ataxia-telangiectasia mutated), ATR (ATM- and Rad3-Related) and DNA-PKcs (DNA-dependent protein kinase) (Marechal and Zou 2013). These kinases phosphorylate hundreds of proteins and regulate downstream HR and NHEJ pathways (Marechal and Zou 2013) and also activate p53 to induce cell cycle arrest (Cheng and Chen 2010). H2AX (H2A. X Variant Histone) is one of their substrates, and is phosphorylated at S139 (Kuo and Yang 2008; Rogakou et al. 1998). Phosphorylated H2AX ( $\gamma$ H2AX) histones surround DSBs and staining against them with antibodies generates staining patterns known as  $\gamma$ H2AX foci. These foci are thought to represent DSBs on a 1:1 basis, making them a useful marker of DSBs (Kuo and Yang 2008). Importantly, small  $\gamma$ H2AX foci also appear in naturally replicating cells during M phase independent of DNA damage (McManus and Hendzel 2005). Therefore, it is common to employ multiple markers to identify DNA damage in cells.

DNA damage accumulates with age in all living things including mammals and teleosts (Yizhak et al. 2019; Cencioni et al. 2019). This accumulation has widespread effects at cellular and tissue levels and is considered to be one of the most upstream hallmarks of ageing, especially causing senescence and inflammaging (Schumacher et al. 2021) and can even transmit transgenerational effects (Wang, Meyer, and Schumacher 2023). This is true for several reasons. To begin with, DNA damage is considered to be a major driver of epigenetic changes with age. The above-mentioned DNA-SCARS of

senescent cells are such chromatin alterations. In addition, DDR leads to loss of H3K27me3, a histone modification whose levels alter depending on tissue in both killifish and mice (Baumgart et al. 2014), and whose loss promotes cellular senescence (Ito et al. 2018).

The most consistent and common way to induce senescence *in vitro* and *in vivo* is DNA damage. Studies will often use clastogenic compounds such as bleomycin, doxorubicin or cisplatin, all of which cause DNA-SCARS (Rodier et al. 2011). Other studies employ etoposide (which targets topoisomerase activity to induce DNA breaks), ionizing radiation, replicative senescence (uncapped telomere induced DNA damage response (Parrinello et al. 2003)) or even oncogene-induced senescence (which induces DSBs due to replication stress) (Kotsantis, Petermann, and Boulton 2018; Yang et al. 2017). All of the above genotoxic stressors activate the p53/p21 pathway to induce cell cycle arrest, and concomitant epigenetic alterations cause senescence via the p16/Rb pathway (Chen, Hales, and Ozanne 2007; Shreeya et al. 2023). Thus, DNA damage is arguably the most well-characterized cause of senescence and their accompanying secretome, the most well-characterized cause of inflammaging.

Of note, although they are critical to establish senescence, SASP expression and secretion do not depend on either p53 or p16 (Coppe et al. 2011). SASP expression is primarily regulated by NF- $\kappa$ B (Nuclear factor kappa B) activity (Salminen et al. 2008). Independently of p53 and p16, DNA damage activates ATM and ATR, which then activates GATA4 (GATA Binding Protein 4) to induce NF- $\kappa$ B-dependent SASP expression (Kang et al. 2015). However, another pathway was recently found to be equally important for both senescence and SASP; the cytosolic DNA surveillance pathway cGAS/STING (Yang et al. 2017; Gluck et al. 2017) (see chapter 3.5.3).

### 3.5 The cGAS/STING pathway

Cells have evolved multiple defense mechanisms and sensors to identify pathogens and damaged molecules in order to initiate a response. For extracellular pathogens, Toll-like receptors (TLRs, expressed primarily in immune, epithelial and endothelial cells) and C-type lectin receptors (CLRs, expressed mainly in immune cells)

are the primary sensors (Pandey, Kawai, and Akira 2014). CLRs and certain TLRs (TLR1, TLR2, and others) reside at the cell membrane and project their ligand binding domain outside the cell. Other TLRs (TLR3, TLR7, among others) reside at endosomes, but still maintain their ligand-binding domains facing away from the cytosol (Akira, Takeda, and Kaisho 2001). Within the cytosol, Nod-like receptor (NLRs) families, which include inflammasomes, can identify microbial derivatives, toxins and cellular damage to activate immunity (Almeida-da-Silva et al. 2023). For pathogen- or damage-associated RNA in the cytosol, the retinoic acid-inducible gene-I (RIG-I)-like receptors (RLRs) and OAS1 (2'-5'-oligoadenylate synthetase 1) are the main sensors, activating type-I interferon (IFN) signaling in response (Yoneyama et al. 2004). For cytosolic DNA, the main surveillance mechanisms are absent in melanoma 2 (AIM2) family members and the recently discovered cyclic GMP-AMP synthase (cGAS) (Kong et al. 2023). The cross-talk between these immune-surveillance pathways - whether synergistic, antagonistic or redundant - is a field of active study. However, the core of our study henceforth will be cGAS and its downstream pathway.

### 3.5.1 cGAS structure

cGAS was first identified by the group of Zhijian (James) Chen (Sun et al. 2013) who won the Lasker award for his groundbreaking work. In this seminal study, they purified and characterized the protein for its function as a cyclic GMP-AMP (cGAMP) synthase, which produces cGAMP as a secondary messenger to activate STING-dependent type-I IFN signaling. cGAS belongs to the cGAS/DncV-like nucleotidyltransferase (CD-NTase) family (Whiteley et al. 2019). The cyclase DncV (*Vibrio cholerae* dinucleotide cyclase) is a primordial protein found in many bacterial species that produces cyclic 3'3'-cGAMP (Whiteley et al. 2019), though it has no obvious primary sequence homology to cGAS (Sun et al. 2013). The mammalian cGAS NTase domain has remarkable structural similarity to OAS1, which polymerizes ATP into 2'-5'-linked iso-RNA (2'-5'-oligoadenylate) in response to dsRNA (Donovan, Dufner, and Korennykh 2013; Kranzusch et al. 2013). The NTase domain of cGAS is unique among other NTase family members in its ability to produce the 2'3'-cGAMP (cGAMP) conformation (Gao, Ascano, Wu, et al. 2013).

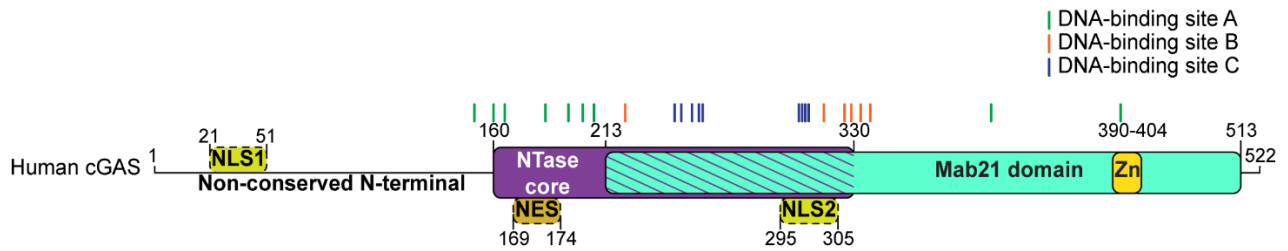


**Figure 8. Human cGAS domain structure.** Verified human cGAS protein domains include the non-conserved N-terminal tail, the enzymatic NTase core, the Mab21 domain, a zinc-finger motif critical for dsDNA binding, and three DNA binding sites (A, B and C). Residues confirmed to contribute to each binding site are marked over the human cGAS protein. Two putative NLS and one putative NES are marked with dashed circles. Numbers indicate the amino-acid residues flanking each domain.

cGAS responds to cytosolic DNA to stimulate its cGAMP-catalytic activity and harbors three DNA binding sites, all of which must be occupied to cooperatively stimulate cGAMP production (Civril et al. 2013; Xie et al. 2019). Structure analysis has revealed that when bound, cGAS and DNA form a 2:2 ratio complex (Li, Shu, et al. 2013). Binding is sequence-independent and creates a loop in the DNA moiety, which assists in subsequent oligomerization of the cGAS proteins. This facilitates rapid recruitment and accumulation of cGAS proteins, eventually leading to liquid condensation, which is important for efficient immune activation (Du and Chen 2018). Human cGAS can be activated by dsDNA that is >45bp in length, while mouse cGAS can bind to DNA as small as 17bp, indicating an evolutionary divergence in sensitivity and immune responsiveness among cGAS orthologs (Zhou et al. 2018).

Both NTase and DNA binding motifs are mostly contained within the Mab21 domain of cGAS. Mab21 (male-abnormal 21) domains were first detected in proteins involved in embryonic development of *C. elegans* (Ho, So, and Chow 2001). However, *C. elegans* lacks orthologs of cGAS and STING (Wu et al. 2014). Phylogenetic domain organization of NTase and Mab21 modules are present in cGAS homologs as early as Protozoa (Wu et al. 2014). However, only vertebrate cGAS proteins contain a zinc-ribbon domain, which was found to be crucial for dsDNA binding (Civril et al. 2013). In humans, Mab21 domain-containing genes include cGAS (Mab21d1), Mab21d2, Mab21L1 (Mab21-like protein 1), Mab21L2 and Mab21L3 (de Oliveira Mann et al. 2016). Mab21d2 cannot

catalyze cGAMP production (Liu, Yan, et al. 2023) and the other Mab21 proteins are missing key functional residues in their NTase domain (de Oliveira Mann et al. 2016). Among all cyclic dinucleotide synthases, vertebrate cGAS appears to be the only enzyme that binds to double stranded DNA to activate its cGAMP-producing activity.

cGAS also contains a poorly conserved unstructured N-terminal tail (Kranzusch et al. 2013). This N-terminal tail is not required for cGAS activity, but it has been shown to modulate its sensitivity to DNA fragments by tethering it to the plasma membrane (Barnett et al. 2019). Subsequent studies, however, localized cGAS primarily in the nucleus, where the N-terminal domain is required for its tethering to centromeres and, to a lesser degree, to LINE elements (Gentili et al. 2019).

cGAS contains two nuclear localization signals (NLSs) and one nuclear export sequence (NES). Two putative NLSs have been identified in human cGAS, one in the N-terminus (NLS1) and one within the NTase domain (NLS2) (Liu et al. 2018). Removal of NLS1 did not affect cGAS nuclear localization (Kim et al. 2023). But, mutation of NLS2 led to cytoplasmic retention, enzymatic dysfunction and enhanced protein degradation, likely due to misfolding. On the other hand, one putative NES has been identified at the N-terminal end of the NTase domain. Studies have only shown modest increases of steady-state nuclear cGAS after mutation of this NES, but after DNA stimulation this domain assists in shuttling cGAS to the cytoplasm (Wu et al. 2022; Sun et al. 2021). Nuclear cGAS was measured to be more than 200-fold less immunostimulatory than cytoplasmic cGAS. Therefore below, we focus on cytosolic cGAS as part of the canonical cGAS/STING immune signaling pathway.

### 3.5.2 STING structure

The STING (stimulator of interferon genes) protein was identified before cGAS, and was actually discovered in parallel by multiple groups, and therefore known by different names, such as MITA (Zhong et al. 2008), ERIS (Sun et al. 2009) and MPYS (Jin et al. 2008). As with cGAS, phylogenetic domain organization identifies STING homologs from protozoa to mammals, with the only exception being nematodes (Wu et al. 2014). Interestingly, STING is conserved in structure and function in metazoans. The most

divergent functional STING homolog (nvSTING) was identified in the starlet sea anemone *Nematostella vectensis* (Kranzusch et al. 2015). Despite having only 29% sequence identity with human (hSTING), nvSTING has a nearly identical crystal structure and binds to cyclic dinucleotides (CDNs). Also, in response to cyclic dinucleotides, anemone STING activates NF- $\kappa$ B-dependent immune responses, making it one of the first immune regulators to evolve in metazoan phyla (Margolis et al. 2021).

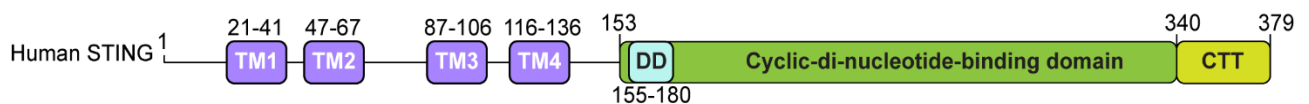


**Figure 9. Human STING domain structure.** Verified human STING protein domains include 4 transmembrane domains (TM1-4), a dimerization domain (DD), a cyclic-di-nucleotide-binding domain and the C'-terminal tail (CTT). Numbers indicate the amino-acid residues flanking each domain.

Starting from vertebrates, STING genes evolved an additional domain at the C'-terminal tail (CTT). This CTT is critical to activate IRF3 (Interferon regulatory factor 3) and its downstream type-I IFN signaling (de Oliveira Mann et al. 2019). After binding to CDNs, the CTT changes conformation to allow recruitment of the kinase TBK1 (TANK-binding kinase 1), which then phosphorylates the CTT to recruit IRF3 (Chen, Sun, and Chen 2016). Since TBK1 can activate both IRF3 and NF- $\kappa$ B pathways, it becomes clear that the CTT domain is important for regulating the activity of STING. One study investigated the differences between mammalian and teleost CTT domains and found that zebrafish CTT has an additional 18 amino acids at the C'-end that allows TRAF6 (Tumor necrosis factor receptor-associated factor 6) binding, shifting downstream signaling towards stronger NF- $\kappa$ B signaling (de Oliveira Mann et al. 2019). Lack of this structure in mammals favors IRF3-mediated IFN signaling. Sequence comparison reveals that killifish do not have these 18 amino acids at the C'-end.

Apart from the CTT, STING proteins also contain 1-4 transmembrane domains (4 for vertebrates, with the exception of birds) which tether the protein at the endoplasmic reticulum (ER) through interactions with the STIM1 (stromal interaction molecule 1) (Sun et al. 2009). Finally, STING also contains a CDN-binding domain (CBD) within which

lies a dimerization domain (DD) (Burdette and Vance 2013). The CBD is facing the cytoplasm and can bind different conformations of cGAMP and other bacterial-derived CDNs (Gao, Ascano, Zillinger, et al. 2013). Although 2'3'-cGAMP production started with vertebrates, anemone STING and mammalian STING have higher affinity for 2'3'-cGAMP rather than other bacterial CDNs (Margolis et al. 2021). Apparently the 2'3'-cGAMP conformation evolved afterwards to be a stronger inducer of the pre-existing STING protein. Additionally, STING can reportedly be activated by bacterial CDNs such as c-di-AMP, released by *Listeria monocytogenes* (Woodward, Iavarone, and Portnoy 2010). Curiously, though, multiple studies have shown that mice deficient in STING or type-I IFN signaling are actually more resistant to *L. monocytogenes* infections (Auerbuch et al. 2004; Carrero, Calderon, and Unanue 2004; O'Connell et al. 2004; Archer, Durack, and Portnoy 2014).

### 3.5.3 Canonical cGAS/STING signaling cascade

The canonical cGAS/STING pathway begins with the presence of DNA or DNA:RNA hybrids (Mankan et al. 2014) in the cytosol. In nature, cytosolic DNA can derive from viral or bacterial infections (Tan et al. 2018), mitochondrial DNA leakage during mitophagy or mtDNA packaging deficiencies (Rongvaux 2018), cellular debris in phagocytic cells (King et al. 2017) and micronuclei formed by lagging chromosomes in replicating cells after DNA damage (Mackenzie et al. 2017). DNA:RNA hybrids can originate from viruses, but also from retrotransposable elements during retrotranscription (Simon et al. 2019; De Cecco et al. 2019).

cGAS is enzymatically activated after bound to dsDNA or DNA:RNA hybrids in the cytosol. DNA-bound cGAS changes conformation and oligomerizes on DNA scaffolds creating a liquid-liquid phase separation from the rest of the cytosol (Du and Chen 2018). Enzymatically active cGAS within the liquid condensates converts GTP and ATP into a unique isomer of CDN, the 2'3'-cGAMP (Wu et al. 2013; Diner et al. 2013). Purified cGAS in combination with DNA, GTP and ATP produces cGAMP in comparable amounts to cGAS within a cell lysate (Ablasser, Goldeck, et al. 2013), hinting towards a function



independent of co-factors. Of note, this ability to function independently allows for functional analysis of cGAS in heterologous systems.

STING has high affinity for cyclic dinucleotides, especially 2'3'-cGAMP, and responds quickly to its presence (Burdette et al. 2011). Once bound to cGAMP, STING changes conformation and forms dimers, tetramers and higher-order oligomers (Shang et al. 2019). The conformational changes lead to detachment of STIM1 in the ER and loading into COPII vesicles and traffic through the ER-Golgi intermediate compartment (ERGIC) (Dobbs et al. 2015). Once it reaches the Golgi, STING is palmitoylated, which is critical for its downstream function (Mukai et al. 2016). Then STING interacts with TBK1, a kinase that phosphorylates the CTT region of STING (Liu et al. 2015). The phosphorylated CTT acts as a docking site for IRF3 which is then also phosphorylated by TBK1. Phosphorylated IRF3 dimerizes and translocates to the nucleus to activate the transcription of interferon- $\beta$  (IFN $\beta$ ) (Agalioti et al. 2000). IFN $\beta$  is a secreted type-I IFN cytokine which acts in an autocrine and paracrine manner to activate interferon receptors (such as IFN $\alpha$  receptor 1 and 2) signaling the cells to activate a broad anti-viral response through multiple interferon-stimulated genes (ISGs) (Schneider, Chevillotte, and Rice 2014).

cGAS/STING signaling also activates the NF- $\kappa$ B pathway. Although it has not been shown directly, TBK1 likely phosphorylates the NF- $\kappa$ B activator IKK $\beta$  (I $\kappa$ B kinase  $\beta$ ), which then phosphorylates and releases the NF- $\kappa$ B inhibitor (Fang et al. 2017). Released NF- $\kappa$ B enters the nucleus to activate the expression of a broad range of pro-inflammatory cytokines. In addition to IRF3 and NF- $\kappa$ B, STAT6 (Signal transducer and activator of transcription 6) is another transcription factor activated by the STING/TBK1 complex (Chen et al. 2011). Phosphorylated STAT6 also translocates to the nucleus to activate transcription of another set of chemokines, such as CCL2 (CC-chemokine ligand 2), CCL20 and CCL26.

A natural outcome of canonical cGAS/STING pathway activation is cellular senescence, since both its transcriptional mediators, IRF3 and NF- $\kappa$ B, function in this process. In particular, all of the aforementioned DNA-damage methods of inducing senescence (chapter 3.4.2.2) have been shown to stimulate the cGAS/STING pathway (Yang et al. 2017; Gluck et al. 2017). In addition, cGAS is essential for establishment of senescent markers in these DNA-damaged cells. The mechanism behind this regulation

was recently discovered to reflect the interaction between nuclear IRF3 and RB (retinoblastoma) (Wu et al. 2024). The IRF3-RB interaction prevents RB phosphorylation, leading to senescence establishment. At the same time, IRF3 and, more prominently, NF- $\kappa$ B drive the expression of SASP components (Gluck et al. 2017; Salminen et al. 2008).

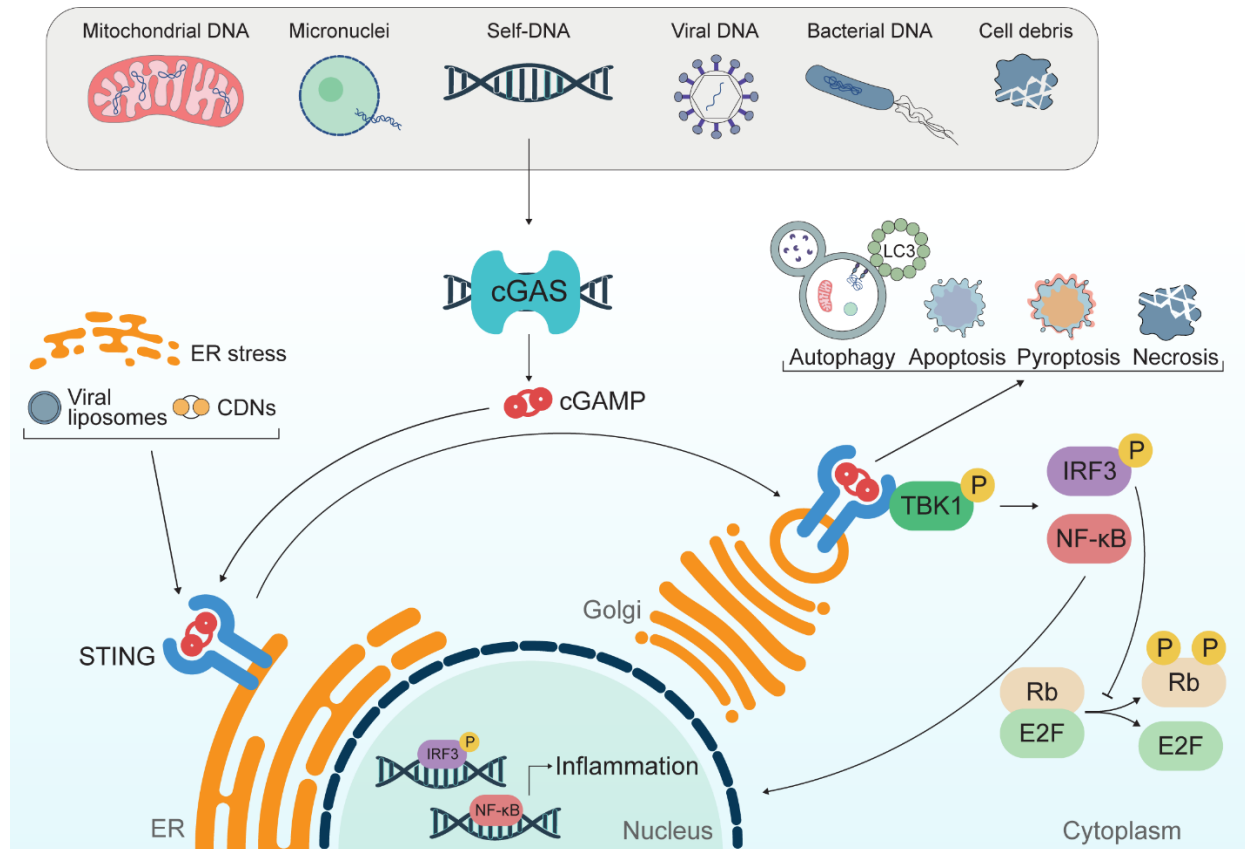


**Figure 10. Canonical and non-canonical functions of the cGAS/STING pathway.** cGAS is a cytosolic DNA surveillance protein that binds to dsDNA in a sequence-independent manner. Various endogenous and exogenous sources of DNA can stimulate cGAS activity to produce the cyclic dinucleotide cGAMP. STING responds to cyclic dinucleotides, such as cGAMP, and translocates to the Golgi to stimulate the self-phosphorylation and activation of TBK1. ER stress and empty viral liposomes have also been described to stimulate STING translocation (Moretti et al. 2017; Holm et al. 2012). Active TBK1 leads to NF- $\kappa$ B and IRF3 nuclear translocation to activate Type-I IFN signaling and other cytokines. IRF3 also prevents phosphorylation of Rb, leading to cell cycle arrest. Non-canonical functions of STING include autophagy induction and cell death. Image modified from (Motwani, Pesiridis, and Fitzgerald 2019).

### 3.5.4 Non-canonical functions of cGAS and STING

Both cGAS and STING have non-canonical functions beyond TBK1-mediated IFN and NF- $\kappa$ B signaling. Chen and co-workers discovered that STING plays a key role in inducing autophagy (Gui et al. 2019). Upon binding to cGAMP, STING traffics through the ERGIC to reach the Golgi; STING-containing ERGIC serves as a membrane source for microtubule-associated protein 1A/1B-light chain 3 (LC3) lipidation, a key step in autophagosome biogenesis. This cGAMP-induced LC3 lipidation is dependent on WD repeat domain phosphoinositide-interacting protein 2 (WIPI2) and autophagy protein 5 (ATG5). The researchers also found that STING-dependent autophagy is important for DNA and viral particle clearance. Even the evolutionarily distant sea anemone also induces STING-dependent autophagy upon stimulation with cGAMP. These findings suggest that autophagy induction is a primordial function of the cGAS/STING pathway that has been conserved through evolution.

Recent studies have further linked STING activity and autophagy. Like LC3, lipidation of GABARAP (GABA type A receptor-associated protein) is also key for autophagy (Weidberg et al. 2010). Activated STING also mediates GABARAP lipidation, impairing mTORC1-mediated phosphorylation of TFEB (transcription factor EB), and thereby triggering its nuclear translocation (Lv et al. 2024; Xu et al. 2024). TFEB itself is a master regulator of lysosomal biogenesis and autophagy (Settembre et al. 2011). The function of cGAS/STING in regulating autophagy independent of TBK1 is conserved in humans, mice and even frogs, showing an ancient origin. In contrast to nutrient sensing-mediated autophagy regulation by mTOR and TFEB, cGAS/STING-activated autophagy is required for the elimination of cytoplasmic DNA, bacteria and viruses (Xu et al. 2024).

Inflammasomes are multiprotein complexes that regulate production and maturation of pro-inflammatory cytokines (such as IL-1 family), as well as pyroptosis, a highly inflammatory form of cell death (Broz and Dixit 2016). Originally it was thought that AIM2, another cytosolic DNA sensor, activates the inflammasome (Hu et al. 2016). In myeloid cells, however, it was found that the cGAS/STING pathway is the main driver of inflammasome-mediated cell death, independent of AIM2 (Gaidt et al. 2017). Prolonged

STING activation can also induce apoptosis in lymphoid cells through mitochondrial outer membrane permeabilization (MOMP)-mediated apoptosis (Tang et al. 2016). The pivot point between inflammation or cell death was found to be the signal intensity or signal duration, but different cells can have different thresholds for this switch (Gulen et al. 2017). Finally, cGAS/STING activation can elicit necroptosis in bone marrow-derived macrophages through activation of receptor-interacting serine/threonine-protein kinase 3 (RIPK3) (Brault et al. 2018). RIPK3 activation is downstream of the IFN response, but it requires STING hyperactivation, so it is not considered a part of the canonical cGAS/STING pathway.

cGAMP is a polar water-soluble molecule that cannot readily pass through cell membranes. However, multiple studies have identified means by which cGAMP acts *in trans*, stimulating inflammation in a paracrine manner. Firstly, cGAMP was found to pass through gap-junctions between neighboring cells (Ablasser, Schmid-Burgk, et al. 2013). Then, two groups in parallel found that cGAMP molecules can be loaded into viral particles during viral assembly and released into the newly infected cells (Bridgeman et al. 2015; Gentili et al. 2015). More recent studies found channels that can export or import cGAMP, such as VRACs (volume-regulated anion channels) (Zhou et al. 2020) and SLC19A1 (solute carrier family 19 member 1) (Luteijn et al. 2020; Ritchie et al. 2019). In addition, enzymes that hydrolyze cGAMP act primarily in extracellular milieu. These include ENPP1 (ectonucleotide pyrophosphatase/phosphodiesterase family member 1), ENPP3 and SMPDL3A (Sphingomyelin phosphodiesterase acid-like 3A) (Li et al. 2015; Hou et al. 2023). The above data suggest that *trans*-activation of immunity by cGAMP might play an equal or more important role *in vivo* as *cis*-activation.

Recent studies have found non-canonical functions of cGAS as well, which primarily relate to its nuclear localization. An increasing number of studies have shown cGAS to primarily localize within the nucleus (Volkman et al. 2019; Zhao, Xu, et al. 2020). Nuclear cGAS was found to be immunologically-silenced (Gentili et al. 2019). Electron microscopy revealed that nuclear cGAS is bound to H2A-H2B histone dimers and nucleosomal DNA, has all three DNA binding sites repurposed or inaccessible and cGAS dimerization is inhibited, hence hindering its biochemical activity (Kujirai et al. 2020). In response to cytoplasmic DNA, cGAS is exported from the nucleus in a CRM1-dependent (chromosome region maintenance 1) manner, possibly facilitated by the nuclear export

signal (NES) (Sun et al. 2021). Then, cGAS retention to the cytoplasm is mediated by phosphorylation at tyrosine 215 by the BLK (B-lymphoid tyrosine kinase) (Liu et al. 2018). In the cytosol, cGAS functions through the canonical cGAS/STING pathway. In the absence of DNA stimulation, DNA damage leads to de-phosphorylation of cGAS and nuclear import. This translocation is mediated by importin- $\beta$ , potentially due to interaction with the two nuclear localization domains of cGAS (Kim et al. 2023). This nuclear shuttling during DNA damage was shown to inhibit homologous recombination due to cGAS direct binding to PARP1, which blocks subsequent recruitment of repair modulators.

Apart from the above example of genotoxic function of cGAS, nuclear cGAS can also have a protective role to genomic DNA. In replicating cells, nuclear cGAS slows replication forks leading to increased DNA replication fidelity and less accumulation of DNA damage (Chen et al. 2020). Another study showed that cGAS inhibiting double strand break repair safeguards the genome (Li et al. 2022). Specifically, lack of cGAS in mitotic cells led to the deployment of DSB repair mechanisms reacting to telomeres, which attempts to repair them by end-to-end chromosome fusion, eventually leading to genomic instability. Both DNA-damaging and DNA-protective roles of nuclear cGAS are STING-independent.

### 3.5.5 cGAS/STING impact on pathologies

cGAS/STING activity has been connected to a number of diseases in humans. The most well-studied pathology in that regard is the Aicardi-Goutières Syndrome (AGS). AGS is a monogenetic disease caused by mutations in any one of 9 genes (TREX1, RNASEH2A, RNASEH2B, RNASEH2C, SAMHD1, ADAR, IFIH1, LSM11 and RNU7-1) and is characterized by aberrant type-I IFN activation (Oleksy et al. 2022). Mutation in 7 out of 9 of the above genes leads to cGAS/STING-driven AGS interferonopathy (Dvorkin et al. 2024). Two AGS genes encode antiretroviral enzymes (TREX1 and SAMHD1) (Beck-Engeser, Eilat, and Wabl 2011; Rice et al. 2018), four genes encode enzymes that prevent formation of micronuclei or metabolize DNA within them (TREX1, RNASEH2A, RNASEH2B and RNASEH2C) (Mackenzie et al. 2017) and two genes (LSM11 and RNU7-1) contribute to accurate expression of histones and histone linkers (Uggenti et al. 2020). This disease-

context example highlights the importance of histone-tethering and inhibition of nuclear cGAS during steady state, as well as degradation of retrotransposons and micronuclei to prevent aberrant cGAS/STING signaling.

Bloom syndrome is another monogenetic disease caused by mutation in the BLM RecQ-like helicase, a gene necessary for genome integrity (Kaur, Agrawal, and Sengupta 2021). BLM-deficient cells accumulate micronuclei and drive IFN signaling in a cGAS/STING dependent manner (Gratia et al. 2019). Similarly, mutations in ATM (Ataxia-telangiectasia mutated), a central DNA-repair machinery kinase (chapter 3.4.2.2) results in Ataxia Telangiectasia (AT). ATM deficiency causes robust type I IFN signaling driven by cGAS/STING (Hartlova et al. 2015). cGAS/STING activity was implicated in neurodegeneration of AT rat models (Quek et al. 2017). Once again, cGAS appears to play an important role in monitoring DNA integrity and micronuclei formation *in vivo*.

Lamin genes stabilize the nuclear envelope and mutations in these genes cause Hutchinson-Gilford progeria syndrome (HGPS) (Plasilova et al. 2011). Lamin deficiency in cell cultures showed DNA leakage from the nucleus which co-localized and activated cGAS (Gluck et al. 2017). A truncated lamin A protein, called “progerin”, can cause HGPS in a dominant manner (Batista et al. 2023). Progerin induces genomic instability in multiple ways and activates a cGAS/STING-mediated IFN response (Coll-Bonfill et al. 2020). In another auto-immune disease, patients with systemic lupus erythematosus (SLE) were reported to have higher cGAMP levels in their sera (An et al. 2017). Patients with the neurodegenerative ALS (amyotrophic lateral sclerosis) disease have increased mtDNA release causing cGAS/STING activation (Yu et al. 2020). All of the above diseases are associated with aberrant activation of cGAS.

Another rare disease directly connected to STING activity is SAVI (STING-associated vasculopathy with onset in infancy) (Lin et al. 2020). Patients with this syndrome exhibit mutations in STING which are considered to cause constitutive ligand-independent STING polymerization and trafficking to the Golgi (Ergun et al. 2019). Patients with COPA syndrome exhibit similar pathologies to SAVI patients (Vece et al. 2016). The COP $\alpha$  protein is an important subunit of the COPI complex, which shuttles proteins from the Golgi to the ER, the return path of STING after its activity is complete (Deng et al. 2020). In this study, the researchers demonstrated that STING retention in

the Golgi of COPI-defective mice constitutively activates aberrant immunity, and that pharmacological or genetic inhibition of STING ameliorates COPA syndrome.

So far, it is clear that over-activation of cGAS or STING can lead to a number of pathologies. Although not associated with any specific syndrome, it should be noted that dysfunctional cGAS/STING leads to severe increase in viral and bacterial susceptibility and mortality (Li, Wu, et al. 2013; Wiens and Ernst 2016). In addition, cGAS/STING activity is necessary for tumor immunization and clearance. STING deficient mice failed to activate inflammation in response to oncogene induced tumor formation and STING re-expression led to immune-mediated clearance of these tumors (Dou et al. 2017). Also, bioinformatic analysis in lung adenocarcinoma patients revealed a strong correlation between low cGAS expression and decreased survival, hinting towards an important role for cGAS in tumor immunization (Yang et al. 2017). Depending on the cancer type, stage and immune cell recruitment, inflammation can also be pro-tumorigenic and indeed cGAS/STING activity can also impair tumor cell clearance, as observed in colon cancer patients after radiation therapy (Liang et al. 2017). cGAS/STING ability to induce senescence and make tumors immunogenic has made it an attractive model for cancer therapy; however, the balance between pro- and anti-tumorigenic effect is still under investigation.

### 3.5.6 cGAS/STING impact on normative ageing

There is a plethora of indirect evidence that suggest cGAS/STING is involved in the ageing process. cGAS/STING plays a critical role in initiating senescence and SASP in response to DNA damage. DNA damage, senescence and SASP are established hallmarks of aging. In addition, cells lacking cGAS or STING fail to enter senescence or express SASP components (Gluck et al. 2017; Dou et al. 2017). So far, no method of senescence induction has established SASP-secreting senescent cells in the absence of these genes. These findings support the hypothesis that all senescent and SASP-secreting cells accumulating *in vivo* during aging depend on a functional cGAS/STING pathway. This hypothesis becomes even more compelling if DNA damage is indeed the root cause of the other hallmarks of aging (Schumacher et al. 2021). Furthermore, given that the depletion

of senescent cells extends lifespan and healthspan, the indirect link between cGAS/STING and aging is further reinforced (van Deursen 2014).

Although still indirect, there is *in vivo* evidence of cGAS/STING regulating age-related pathology. During ageing, stromal and contractile cells lose YAP/TAZ nuclear localization and activity, which leads to mechano-defective extracellular matrix in these cells (Sladitschek-Martens et al. 2022). This study found that YAP/TAZ signaling also maintains nuclear integrity, whose loss leads to cGAS/STING mediated senescence. Genetic ablation of YAP/TAZ leads to premature ageing phenotypes, such as senescent cell accumulation in the dermis, heart and kidneys atrophy. Loss of STING completely rescued the above phenotypes in mice.

There is extensive research showing retrotransposable element activation with age and in age-related diseases (Gorbunova et al. 2021). One study in *Drosophila* found that retrotransposon silencing extended lifespan (Wood et al. 2016). In aged fibroblasts (Simon et al. 2019), in SIRT6- (sirtuin 6) (Van Meter et al. 2014), SIRT7- ('Correction to: SIRT7 antagonizes human stem cell aging as a heterochromatin stabilizer' 2024) or BMAL1 (Brain and muscle ARNT-like protein-1)-deficient cells (Liang et al. 2022) and also in senescent cells (De Cecco et al. 2019), LINE1 retrotransposable elements are de-repressed. In all of these studies, the researchers found that LINE1 activation is followed by cGAS/STING-mediated senescence and SASP secretion.

Another interesting clue behind a possible connection between cGAS/STING and ageing comes from bats. As mentioned above, bats are exceptionally long-lived for their size. Bats also have a unique tolerance towards viral infections that allow them to act as viral reservoirs without clinical signs of disease (Irving et al. 2021). The first mechanistic study of this immune tolerance found that STING signaling in these animals is dampened due to mutation in a serine residue (S358) of STING (Xie et al. 2018). This mutation is shared among all bats, despite its otherwise high conservation among other mammals. This mutation might have emerged to reduce immune responsiveness of the cGAS/STING pathway to DNA damage which occurs during flight. This resultant dampened STING signaling and subsequent healthy immune balance during infections and DNA damage might contribute to their exceptional lifespan.



One recent study has studied the direct effect of cGAS/STING on normative ageing (Gulen et al. 2023). The researchers found that genetic or pharmacological inhibition of STING in mice reduced innate immune and SASP markers that naturally increased with age in liver, brain and kidney. Old STING inhibited mice exhibited increased physical health and memory compared to wild type (WT) mice. STING inhibited mice also showed reduced microgliosis and increased neuronal density in the hippocampus. The researchers showed that aged microglia have misshapen mitochondria and increased cytosolic mtDNA and suggested that this mtDNA is the culprit behind cGAS activation and subsequent age-related neurodegeneration. A parallel study also suggests mtDNA release as the culprit behind inflammaging (Vitorelli et al. 2024). They found that senescence-associated mitochondrial outer membrane permeabilization (MOMP) activates cGAS/STING through mtDNA release. Inhibition of MOMP decreased inflammatory markers and increased healthspan in mice. However, unlike the previous study this is also indirect evidence of cGAS/STING involvement in ageing.

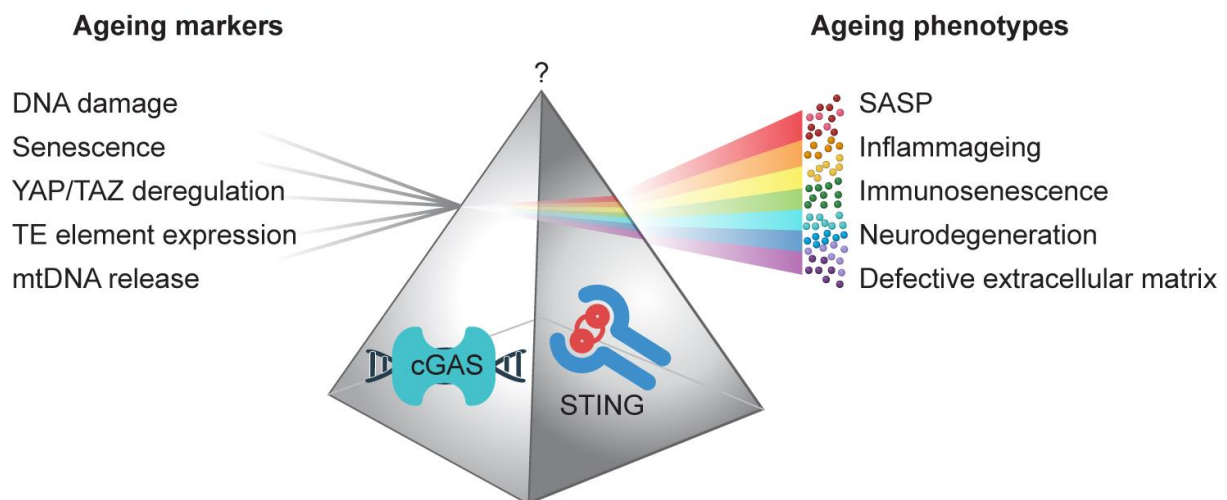


**Figure 11. cGAS/STING signaling potentially translates cellular markers of ageing into ageing physiology.** During ageing, cells accumulate DNA damage, they gain senescent features, YAP/TAZ mechanosignaling becomes dysfunctional, TE elements are derepressed and mtDNA is released into the cytosol. The cGAS/STING pathway responds to all above cellular phenotypes and drives features observed in old organisms, such as increased SASP, inflammaging, immunosenescence, neurodegeneration and extracellular matrix dysfunction. Blocking the cGAS/STING pathway could ameliorate these ageing phenotypes.

Although the connection is obvious, there is very little direct evidence on the importance of cGAS/STING pathway in the physiology of ageing itself *in vivo*. The only physiological relevance identified so far is neurodegeneration and the mechanism behind remains speculative. The pathway's direct physiological relevance in other ageing tissues is still uncertain. In addition, cGAS and STING can have independent roles outside their shared canonical pathway, yet most studies usually investigate only one of the genes.

## 4. Research aims

During aging, cells accumulate DNA damage, dysfunctional mitochondria, and reactivated retrotransposable elements, while tissues experience a buildup of senescent cells and systemic inflammation. The complexity of the damage-associated molecular patterns (DAMPs) and the breadth of downstream inflammatory cascades, amplified through autocrine and paracrine signaling, present a daunting biological landscape. However, the cGAS/STING pathway emerges as a pivotal convergence point, integrating these diverse stress signals to drive downstream inflammatory outputs. By addressing this central node, the vast network of upstream and downstream factors can be modulated more effectively. While this approach has shown promise in disease models and cell cultures, regulation of organismal ageing remains largely unexplored.

We hypothesize that the age-related accumulation of DAMPs leads to aberrant activation of cGAS/STING signaling, which in turn drives inflammaging and contributes to age-associated pathologies. In the absence of viral infections or cancer, downregulating cGAS/STING may reduce inflammatory burden, promoting organismal vitality and extending lifespan. Although the cGAS/STING pathway has ancient origins, vertebrate cGAS and STING have evolved distinct domains absent in distant homologs. Thus, the short-lived killifish *Nothobranchius furzeri* presents an ideal model to investigate this hypothesis.

Taking into account the above, we aim to address the following questions:

1. Is senescence regulation by the cGAS/STING pathway conserved in teleosts?
2. What lies downstream of cGAS/STING activity under basal levels and post DNA damage-induced senescence *in vivo*?
3. What lies downstream of cGAS/STING activity during ageing?
4. How does cGAS/STING function in different tissues in response to senescence and ageing?
5. Do cGAS and STING proteins have the same impact in senescence and ageing *in vivo*?
6. Do cGAS or STING proteins have an impact on lifespan?
7. Do cGAS or STING proteins play a role in late-life-onset diseases?

## 5. Results

### 5.1 cGAS structure and function *in vitro* are conserved from teleosts to mammals

The cGAS/STING pathway has been extensively studied in mammalian cell culture models, but relatively little is known about its function in teleosts (Ge et al. 2015; de Oliveira Mann et al. 2019; Sellaththurai et al. 2023; Liu et al. 2020). We therefore sought to investigate its function in the short-lived African killifish *N. furzeri*, an important model system for vertebrate aging (Valdesalici and Cellerino 2003; Kim, Nam, and Valenzano 2016; Boos, Chen, and Brunet 2024). BLAST analysis of the *N. furzeri* genome (UI\_Nfuz\_MZM\_1.0 reference genome) revealed one copy of the cGAS gene (XM\_015944714.2, kcGAS), showing 35% amino acid identity to its human ortholog (**Figure 12a, b**). Like other members of the family, the predicted protein contained conserved domains including the NTase core, involved in the catalytic production of cGAMP, the mab21 domain, implicated in DNA binding, as well as a non-conserved N'-terminal region (**Figure 12a**). Structural alignment of the human cGAS (PDB 5VDO) with AlphaFold 3-predicted model of kcGAS showed a root mean square deviation of 1.015 angstroms across 277 pruned atom pairs (**Figure 13a**), indicating a high degree of tertiary structural similarity.

To begin to unravel the physiologic function of kcGAS, we first generated a CRISPR/Cas9 knock-out. The sgRNA caused random mutagenesis within the NTase core, resulting in a 34bp tandem duplication that led to a frameshift and early stop codon, and hence a presumptive null allele (**Figure 12a**) (Annibal et al. 2021). Analysis of kcGAS mRNA expression levels revealed strong downregulation in multiple tissues, indicating nonsense-mediated RNA decay (**Figure 12c**). Furthermore, by LC-MS we previously observed a complete lack of cGAMP in the liver and gut of the cGAS KO fish (Annibal et al. 2021). Altogether these results confirm the efficacy of the knock-out.

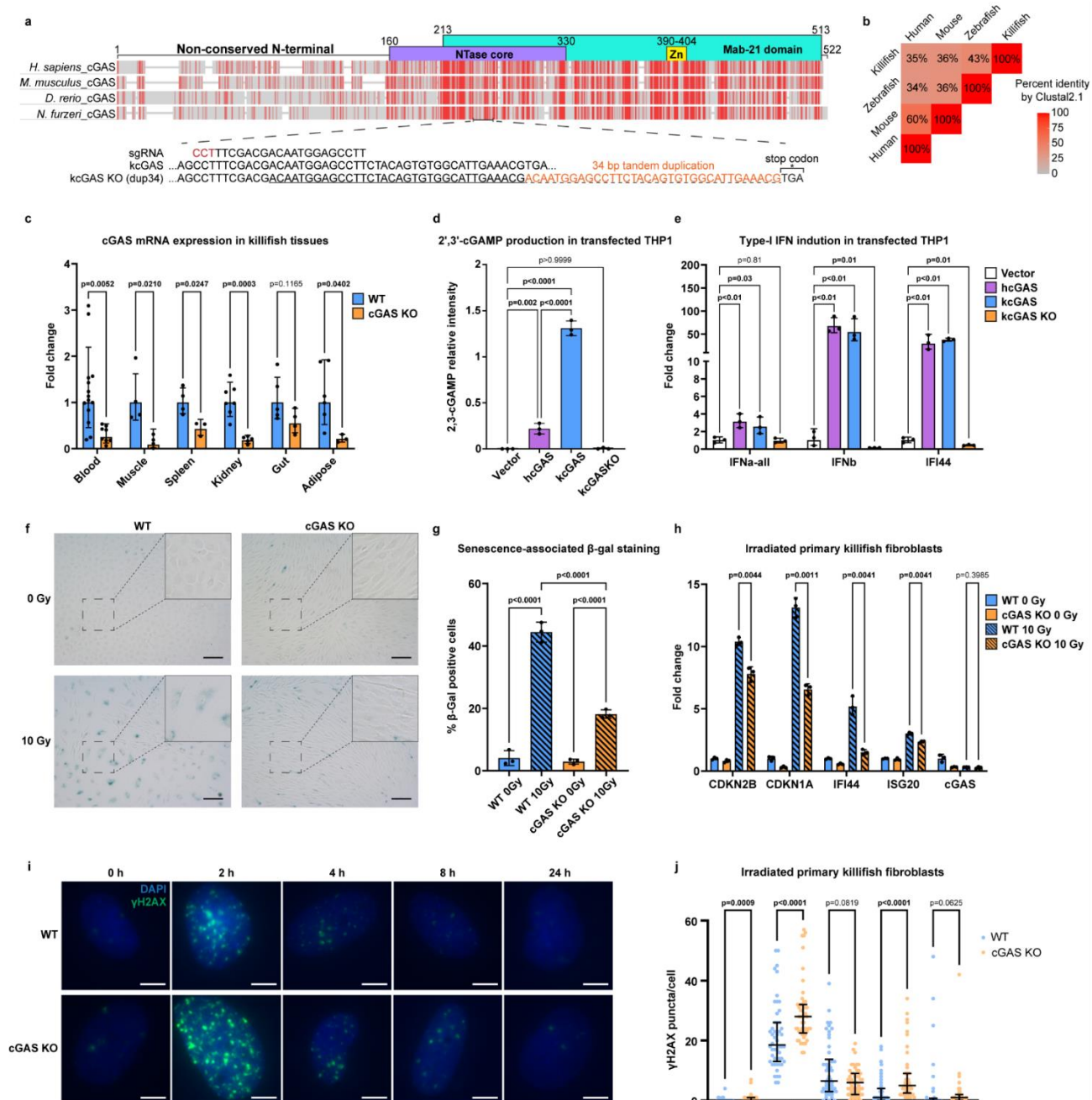


**Figure 12. cGAS structure and function are conserved from teleosts to humans.**

**a**, Multiple sequence amino acid alignment of cGAS with orthologues from other species using constraint-based multiple sequence alignment tool (COBALT). Red= identical amino acids, grey= non-identical. Above the alignment are shown the NTase and Mab21 domains and the Zn finger. Below the alignment is a schematic of the CRISPR-Cas9-generated mutated region of killifish cGAS and the used sgRNA. **b**, Triangle heatmap showing percent identity between aligned cGAS genes of different organisms using ClustalW. **c**, Expression of cGAS mRNA measured using qPCR in different tissues of WT

and cGAS KO mutant killifish. Each dot represents data from one fish.  $n \geq 3$  per tissue and genotype. Statistical analysis was done with Student's t-test using the normalized expression values of cGAS to GAPDH. **d**, LC-MS-based targeted metabolomics of 2',3'-cGAMP extracted from THP1 cells transfected with human cGAS (hcGAS), killifish cGAS (kcGAS), and mutated killifish cGAS (kcGAS KO). Statistical analysis was performed using one-way ANOVA with Dunn-Šidák correction for multiple comparisons. **e**, Expression of interferon and interferon-stimulated genes by qPCR from cell extracts of cGAS KO THP1 cells transfected with the indicated cGAS genes. Samples are identical to those used in (D). Statistical analysis was done using Student's t-test using the normalized expression values to GAPDH. **f**, Bright field images of WT and cGAS KO killifish primary fibroblasts 9 days post 10 Gy  $\gamma$ -radiation, stained for senescence associated  $\beta$ -galactosidase activity. Scale bar = 100  $\mu$ m. **g**, Quantitation of senescence associated  $\beta$ -galactosidase positive cells from images in (f). At least 100 cells were counted per replicate. Statistical analysis was performed using One-way ANOVA with Dunn-Šidák correction for multiple comparisons. **h**, qPCR measurement of senescence and interferon-stimulated genes in irradiated WT and cGAS KO primary fibroblasts. Statistical analysis was done with Student's t-test using the normalized expression values to EIF3c. **i**, Representative images of primary killifish fibroblasts stained for  $\gamma$ H2AX (Green) and DAPI (blue) of indicated genotypes. Cells were fixed at the indicated times after 10 Gy of  $\gamma$ -radiation. Non-irradiated cells were used as 0 h controls. Scale bar = 20  $\mu$ m. **j**, Quantitation of phosphorylated  $\gamma$ H2AX puncta measured from images in (i). Statistical analysis was performed using the Mann-Whitney test. Each dot represents one cell,  $n \geq 50$  cells were measured for each condition. All cell culture experiments in **d-j** were performed in 3 independent biological replicates with  $n = 3$  plates each time. Each panel shows one of three independent experiments.

Upon activation, cGAS triggers the initiation of type-I interferon signaling in mammalian systems (Ablasser, Goldeck, et al. 2013). To validate the conservation of the axis in the killifish we initially adopted a heterologous cell culture setting. We transfected wild-type killifish cGAS (kcGAS), mutated killifish cGAS (kcGAS KO) and human cGAS (hcGAS) into cGAS deficient human THP1 cells using an expression vector carrying GFP as an internal control for transfection efficiency (**Figure 13b**). We detected high levels of cGAMP in cells expressing human and killifish cGAS, while the empty vector and kcGAS

KO showed no cGAMP production (**Figure 12d**). Interestingly, kcGAS produced higher levels of cGAMP compared to hcGAS (**Figure 12d**), possibly reflecting higher intrinsic enzymatic activity of kcGAS, similar to mouse cGAS (Zhou et al. 2018). Indeed, despite higher levels of cGAMP, kcGAS had lower transfection efficiency compared to hcGAS (**Figure 13c, d**) while transgene expression load was similar within transfected cells (**Figure 13e, f**). We also observed that transfection efficiency was lower in WT kcGAS and hcGAS compared to kcGAS KO (**Figure 13c-f**), presumably because of activation of the cytosolic DNA response. In line with this, the presence of kcGAS but not kcGAS KO was sufficient to stimulate expression of type I interferon response genes (**Figure 12e**). We conclude that kcGAS contains intrinsic cGAMP producing activity that is disrupted by the kcGAS KO mutation.

Concurrently, we also investigated the role of killifish STING (kSTING). The killifish genome harbors one functional copy of kSTING, which showed 36% percent identity to human STING1 (hSTING) (**Figure 14a, b**). Alignment of the AlphaFold 3-predicted kSTING model with hSTING dimer (PDB 8FLM) showed a root mean square deviation of 1.28 angstroms from 164 pruned atom pairs (**Figure 14c**), suggesting a high degree of conservation in tertiary structure. We next generated a killifish STING KO mutant strain using CRISPR/Cas9 (**Figure 14a**), in this case using two sgRNAs simultaneously, and obtained two small deletions of 2 and 5 base pairs, both of which led to frameshift mutations. qPCR confirmed a marked reduction in STING mRNA levels in tissues of this mutant, indicating non-sense mediated decay (**Figure 14d**). Transfection of kSTING gene into STING KO THP1 monocytes, unlike kcGAS, failed to activate immune genes (**Figure 14e**), conceivably due to incompatibility with heterologous human co-factors such as TBK1 (**Figure 14f**) (Dobbs et al. 2015; Zhang et al. 2019; Zhao et al. 2019). In addition, transfection efficiency in STING KO THP1 cells was markedly lower (**Figure 14g, h**) compared to cGAS KO cells (**Figure 13c-f**), possibly because of the presence of endogenous cGAS.

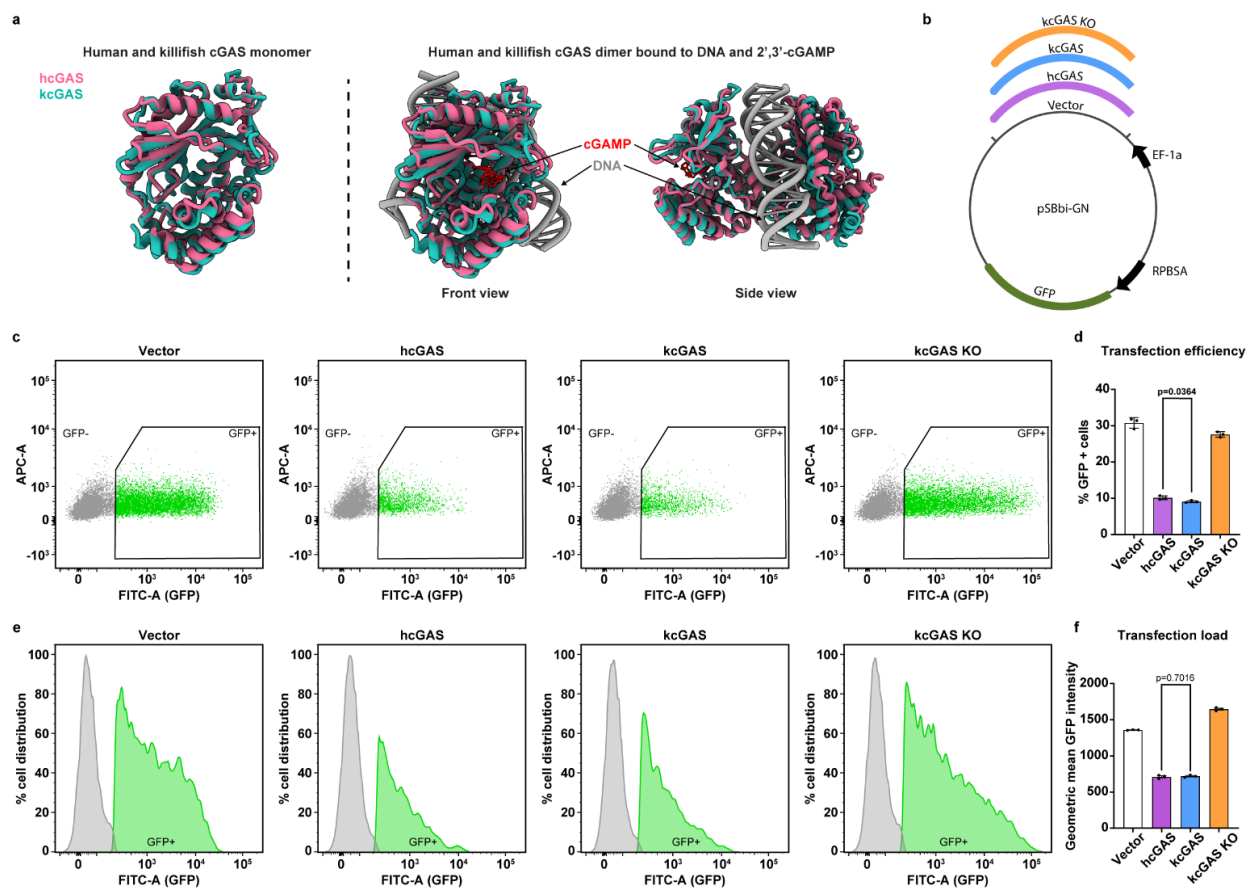


**Figure 13. Extended Data. Killifish and human cGAS have similar tertiary structures and affect THP1 cell transfection efficiency.**

**a**, Structural alignment of the human cGAS (PDB 5VDO) with the AlphaFold 3-predicted model of killifish cGAS. Left, monomers of killifish (turquoise) and human (purple) cGAS proteins are shown in superposition. Right, two strands of DNA are flanked by kcGAS and hcGAS in superposition in the dimeric conformation. Also shown bound is the enzymatic product 2',3'-cGAMP. **b**, Schematic of the expression vector used for transfecting hcGAS, kcGAS and kcGAS KO to THP1 cells. Genes of interest are constitutively expressed under the control of the EF-1a promoter, while in parallel, GFP is constitutively expressed under control of the RPBSA promoter. Plasmid maps and sequences can be found in Extended Data table 1. **c**, Representative dot plots from flow cytometry of alive THP1 cells after transfection with plasmids carrying the indicated cGAS genes. The GFP intensity on the x-axis (FITC-A) is plotted against background noise intensity of an empty gate (APC-A). Cells within the GFP+ gate are considered successfully transfected. **d**, Quantification of transfected cGAS KO THP1 cell percentages falling within GFP+ gate as shown in (c). Student's t-test was used to compare hcGAS and kcGAS means. **e**, Histograms depicting



the distribution of GFP fluorescence intensity within cell populations of transfected THP1 cells. The GFP intensity on the x-axis (FITC-A) is plotted against the percent distribution of cells at each intensity level. The grey peak represents alive GFP<sup>-</sup> cells, while the green peak represents alive GFP<sup>+</sup> cells. **f**, Geometric means of GFP intensities of the GFP<sup>+</sup> cells shown in **(e)**. Student's t-test was used to compare hcGAS and kcGAS geometric means. Flow cytometry data in **c-e** were obtained from the same samples as those used in Figure 12**d, e** and are thus representative of the transfection efficiency that comes with those data. Experiments were performed in 3 independent biological replicates with n = 3 plates each time. Each panel shows one of three independent experiments.

In mammalian cell culture, cGAS and STING are required to establish aspects of the senescent phenotype (Gluck et al. 2017; Yang et al. 2017; Dou et al. 2017; Gulen et al. 2023). Whether this function is conserved in teleosts, however, remains unknown. We therefore asked if killifish cGAS plays a similar role in cellular senescence. To test this idea, we isolated primary fibroblasts from the fins of WT and cGAS KO killifish and induced senescence with DNA damage, subjecting cell cultures to 0 Gy or 10 Gy of  $\gamma$ -radiation. Nine days post-irradiation, we observed that cGAS KO fibroblasts retained their fiber-like morphology and had significantly fewer cells staining for senescence associated  $\beta$ -galactosidase activity compared to WT fibroblasts (**Figure 12f, g**), suggesting lower levels of senescence. From these cell cultures, we extracted RNA and performed qPCR to measure the expression of senescence markers (CDKN2B, CDKN1A) and IFN signaling genes (IFI44, ISG20). While all genes showed induction post-irradiation, cGAS KO fibroblasts had significantly lower expression levels compared to WT fibroblasts (**Figure 12h**). We also established killifish STING KO primary fibroblasts and carried out the same experiment. Nine days post-irradiation, STING KO fibroblasts also exhibited blunted expression of senescence and interferon markers (**Figure 14i**). Notably, this experiment complemented the heterologous cell culture data described above and showed the ability of kSTING to fully promote the interferon response in its native cellular environment. Altogether, these data support the evidence that killifish cGAS and STING loss of function lead to mitigation of cellular senescence in an evolutionary conserved manner.

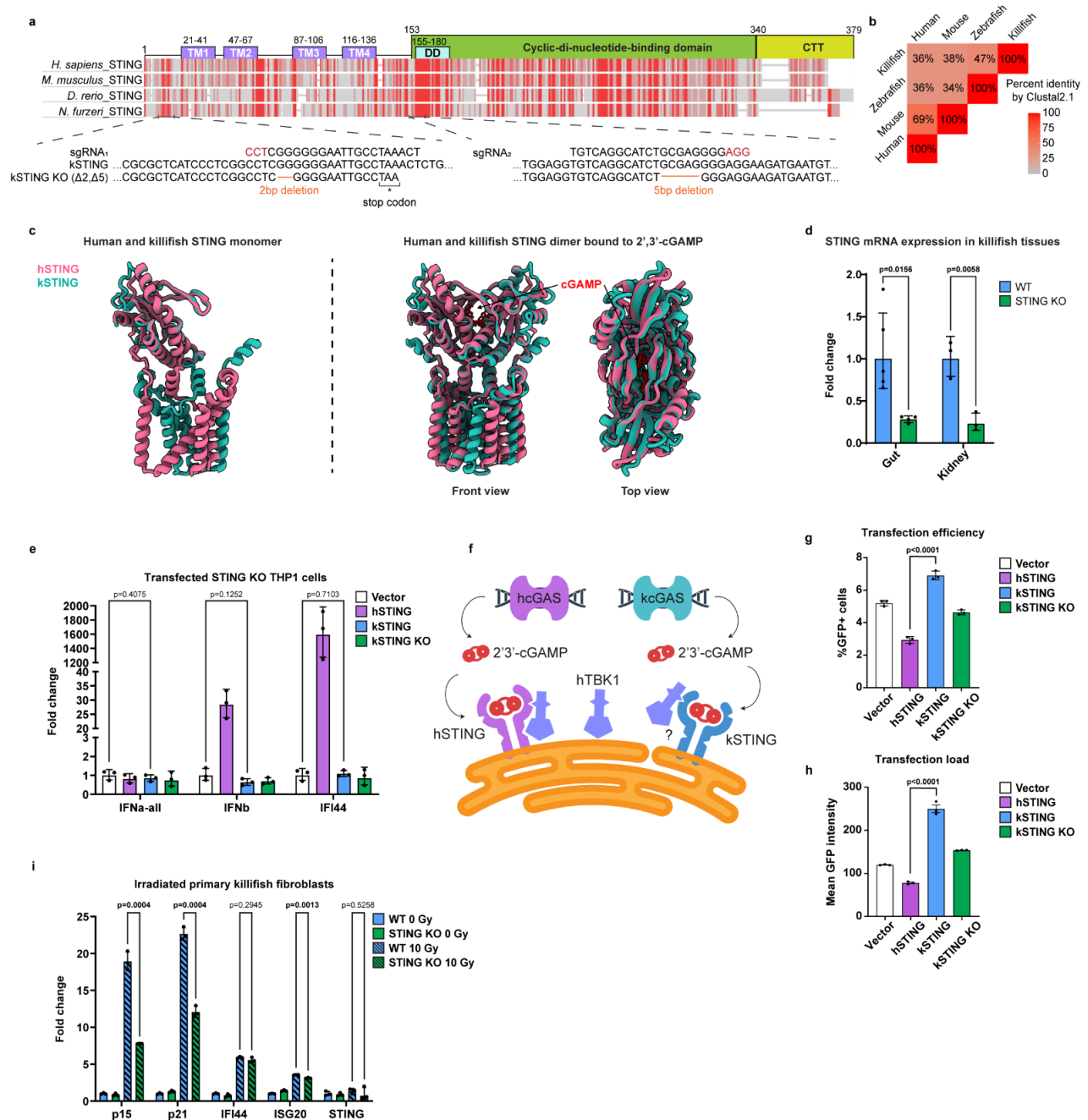


**Figure 14. Extended Data. STING structure and function are conserved from teleosts to humans.**

**a**, Multiple sequence amino acid alignment of STING1 (STING) with orthologues from other species using constraint-based multiple sequence alignment tool (COBALT). Red= identical amino acids, grey= non-identical. Above the alignment are shown the four transmembrane domains (TM1-4), the dimerization domain (DD), the cyclic-di-nucleotide-binding domain and the C-terminal tail (CTT). Below the alignment is a schematic of the CRISPR-Cas9-generated mutated region of killifish STING and the used

sgRNAs. **b**, Triangle heatmap showing percent identity between aligned STING genes of different organisms using ClustalW. **c**, Structural alignment of the human STING (PDB 8FLM) using the AlphaFold 3-predicted model of killifish STING. Left, monomers of killifish (turquoise) and human (purple) STING proteins are shown in superposition. Right, the conformation of hSTING and kSTING dimers bound to 2',3'-cGAMP is shown. **d**, Expression of STING mRNA measured using qPCR in different tissues of WT and STING KO mutant killifish. Each dot represents data from one fish.  $n \geq 3$  per tissue and genotype. Statistical analysis was done with Student's t-test using the normalized expression values of STING to GAPDH. **e**, Expression of interferon and interferon-stimulated genes by qPCR from cell extracts of STING KO THP1 cells transfected with the indicated STING genes. Statistical analysis was done with Student's t-test using the normalized expression values to GAPDH. **f**, Schematic depicting human and killifish cGAS/STING signaling. Both human and killifish cGAS produce the same secondary messenger 2',3'-cGAMP. The illustration also shows the potential lack of binding affinity of human TBK1 protein to kSTING. **g**, Quantifications of transfected STING KO THP1 cell percentages after flow cytometric analysis of cells falling within the GFP+ gate. Gating strategy was similar to the one shown in Figure 13C, but baseline adjusted to levels of the control untransfected STING KO THP1 cells. Student's t-test was used to compare hSTING and kSTING means. **h**, Geometric means of GFP intensities of the GFP+ THP1 cells from (**g**). Student's t-test was used to compare hSTING and kSTING means. **i**, qPCR measurement of senescence and interferon-stimulated genes in irradiated WT and STING KO primary fibroblasts. Statistical analysis was done with Student's t-test using the normalized expression values to EIF3c. STING KO THP1 cell transfections in **e-h** were performed in 2 independent biological replicates with  $n = 3$  plates each time. qPCR on irradiated primary STING KO fibroblasts in **i** was performed in 3 independent biological replicates with  $n = 3$  plates each time. Each panel shows one of three independent experiments.

To further understand the response to the genotoxic stress, we irradiated WT and killifish cGAS KO primary fibroblasts and stained them for  $\gamma$ H2AX at various time points (0h, 2h, 4h, 8h, and 24h). Even without irradiation (0h) cGAS KO fibroblasts showed few but significantly more  $\gamma$ H2AX puncta compared to WT cells. At 2h post-irradiation,  $\gamma$ H2AX puncta spiked higher in cGAS KO cells compared to WT cells, and persisted over the next

few hours until they dropped to basal levels 24h post-irradiation (**Figure 12i, j**). This finding suggests that, despite dampened senescence and immune marker activation, cGAS KO primary fibroblasts inherently display more DNA damage and/or take longer to repair such damage.

## 5.2 Killifish cGAS impacts innate immunity regulation *in vivo*

We next wondered how lack of cGAS affected killifish physiology *in vivo* under basal conditions. To investigate this, we first performed bulk RNAseq from the kidneys of young (7-8 week) healthy WT and cGAS KO fish. We first chose the kidney because of its central role in hematopoiesis, immune cell production and differentiation, and its function as the primary lymph node in teleosts (Bjorgen and Koppang 2021).

Principle component analysis (PCA) plots showed subtle differentiation of the genotypes (**Figure 15a**) and minus-average (MA) plot revealed only modest overall transcriptomic differences (**Figure 15b**). Among the changed transcripts were several involved in vesicular trafficking (ARF1L, SREBF1, SEC23b, SEC24c), secreted metalloproteinases (MMP19, MEP1a.1), TSC1b (mTOR signaling inhibitor) and several lncRNAs. To decipher potential differences further, we used gene set enrichment analysis (GSEA) and identified a number of significantly enriched pathways in the absence of cGAS. Notably, immune-related pathways such as Rig-I-like receptor signaling, Toll-like receptor signaling, Nod-like receptor signaling, and complement and coagulation cascades, were upregulated in the cGAS KO relative to wild type (**Figure 15c**). Closer analysis of these upregulated immune genes revealed that some act directly downstream of cGAS, such as STING and TBK1, suggesting compensation for cGAS loss (**Figure 15d**). However, the majority of these upregulated immune genes act upstream (TRAF6, RIPK1L), downstream (IL12BB) or within NF- $\kappa$ B signaling cascades (NFKB1, RELA, TNFA), even in the absence of an overt stimulus (**Figure 15d**) suggesting increased inflammation. Other gene categories upregulated in cGAS KO included lysosome function and apoptosis. Upregulation of lysosomal genes (CTSZ, CTSB, ATP6V0C and ATP6V0B) suggests an enhanced capacity for degradation and recycling of cellular components, which is a common response to cellular stress or damage, while upregulation of apoptotic

genes (CASP7, MAP3K14, BAX and BIRC2) suggests an increase in apoptotic signaling, which might indicate that mutant cells are under stress and are more prone to undergo cell death.

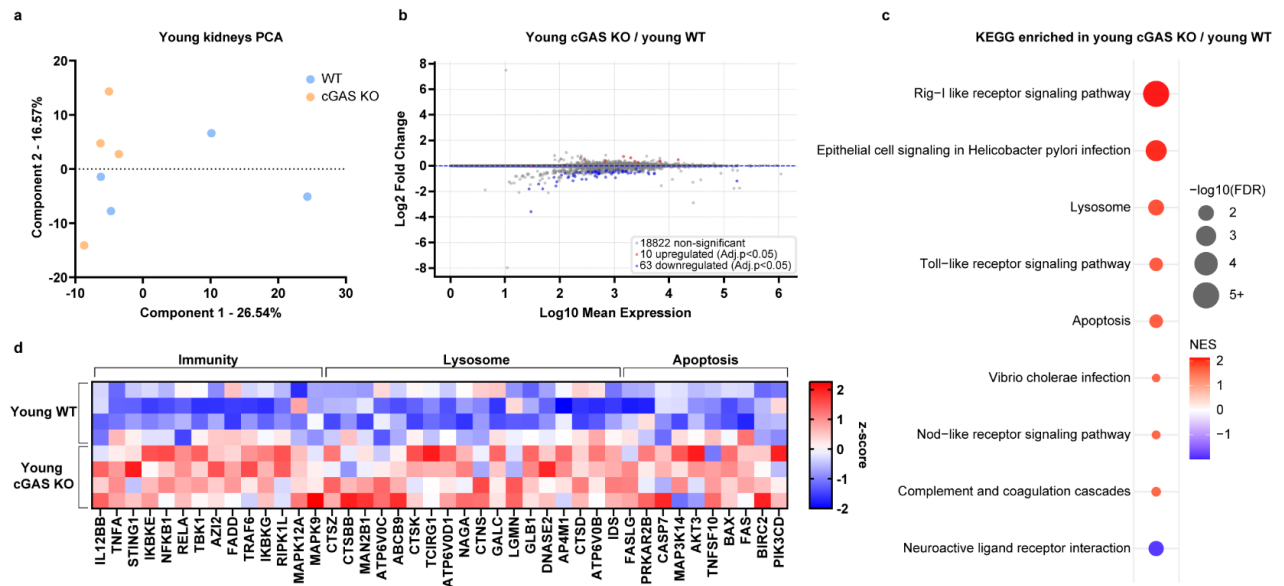


**Figure 15. Loss of cGAS stimulates upregulation of downstream innate immune signaling components in young killifish.** **a**, PCA plot of WT and cGAS KO transcriptomes from young (8 weeks) killifish kidneys. **b**, MA plot showing differential mRNA expression comparing cGAS KO to WT young kidneys. Throughout the paper, all genes with adjusted p-value < 0.05 are considered significant and marked as upregulated (red) or downregulated (blue). **c**, GSEA comparing transcriptomes of young kidneys of cGAS KO to WT. All significantly upregulated and downregulated KEGG pathways are shown (FDR < 0.05). Unless noted otherwise, gene sets throughout the paper are derived from the KEGG\_LEGACY subset of canonical pathways. **d**, Heatmap of z-score normalized expression values of the genes with the highest positive and lowest negative rank metric scores from representative GSEA pathways shown in (c). NES: Normalized enrichment score, FDR: False discovery rate. N = 4 fish per genotype.

To examine another tissue, we also performed RNAseq of gut samples from young WT and cGAS KO killifish. We chose the gut since this tissue serves as a first line of defense against various pathogens, in line with the innate immune function of cGAS/STING. As with the kidneys, we saw no clear separation of genotypes in the PCA plot, nor was there a large impact on gene regulation (**Figure 16a, b**). GSEA revealed processes that were

significantly upregulated (complement, ribosome) and downregulated (DNA replication, cell cycle, amino acyl tRNA biosynthesis) in cGAS KO guts relative to WT (**Figure 16c**), although we observed high variability between replicates in core regulatory genes within these processes (**Figure 16d**).

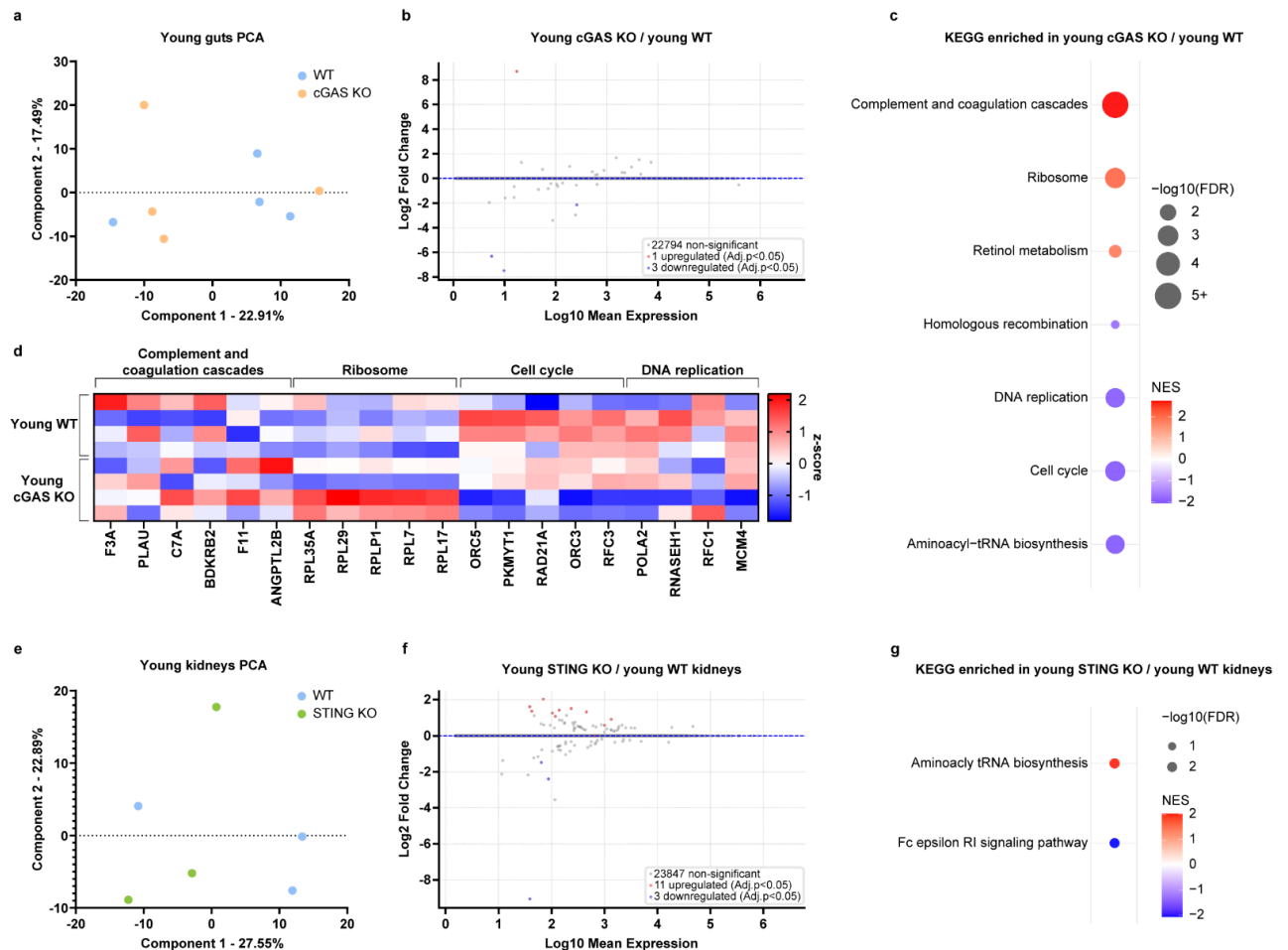


**Figure 16. Extended Data. Lack of cGAS moderately impacts the gut transcriptome, while lack of STING marginally impacts the kidney transcriptome of young fish.**

**a**, PCA plot of WT and cGAS KO transcriptomes from young (8 weeks) killifish guts. **b**, MA plot showing differential mRNA expression comparing cGAS KO to WT young guts. All genes with adjusted p-value < 0.05 are considered significant and marked as upregulated (red) or downregulated (blue). **c**, GSEA comparing transcriptomes of cGAS KO to WT young guts. All KEGG pathways significantly upregulated and downregulated in cGAS KO are shown (FDR < 0.05). **d**, Heatmap of z-score normalized expression values of the genes with the highest positive and lowest negative rank metric scores from representative GSEA pathways shown in (c). **e**, PCA plot of WT and STING KO transcriptomes from young (8 weeks) killifish kidneys. **f**, MA plot showing differential mRNA expression comparing

STING KO to WT young kidneys. All genes with adjusted p-value < 0.05 are considered, upregulated (red), downregulated (blue). **g**, GSEA comparing transcriptomes of STING KO and WT young kidneys. All KEGG pathways significantly upregulated and downregulated in STING KO are shown (FDR < 0.05). NES: Normalized enrichment score, FDR: False discovery rate. n = 4 fish per genotype.

We also carried out transcriptome analysis comparing young WT and STING KO kidneys under basal conditions. This analysis revealed only minor differences in overall transcription and little impact on cellular pathways (**Figure 16e-g**).

### 5.3 Killifish cGAS modulates the transcriptional response to DNA damage and senescence *in vivo*

Given the small differences we observed in young animals under basal conditions, we next asked how the cGAS/STING pathway responded to stress *in vivo*. In particular, since we had observed that cGAS impacts DNA damage response and senescence *in vitro*, we wished to examine these features *in vivo*. To this end, we irradiated young healthy WT and cGAS KO fish with 15Gy of  $\gamma$ -radiation and 5 days later, harvested their tissues and assessed the transcriptional response in the kidneys. We chose this time point in order to potentially capture early senescence events *in vivo* (Schoetz et al. 2021; Turnquist et al. 2019). In this case, PCA plots showed a clear separation between irradiated (15 Gy) and non-irradiated (0 Gy) samples (**Figure 17a**) with hundreds of genes responding to the stimuli (**Figure 17b**) and widespread transcriptional regulation dependent on cGAS (**Figure 17a, c**). This indicates that cGAS is important for transcriptional regulation in response to DNA damage in young healthy tissues.





to non-irradiated young WT kidneys. All genes with adjusted p-value < 0.05 are considered significant, upregulated (red), downregulated (blue). **c**, MA plot showing differential mRNA expression comparing irradiated cGAS KO to irradiated WT young kidneys. All genes with adjusted p-value < 0.05 are considered significant, upregulated (red), downregulated (blue). **d**, Linear regression analysis of the Log2 (fold change) in all genes significantly changed in expression during irradiation in WT and cGAS KO kidneys, showing a slope significantly < 1. A dashed line with slope = 1 is shown for comparison. **e**, Venn diagram depicting the overlap of significantly changed genes post-irradiation in WT and cGAS KO kidneys. **f**, GSEA comparing irradiated to non-irradiated WT kidneys. The top KEGG pathways upregulated and downregulated in irradiated WT are shown. **g**, GSEA comparing irradiated cGAS KO and WT kidneys. The top KEGG pathways upregulated and downregulated in cGAS KO are shown. **h**, Heatmap of z-score normalized expression values of the genes with the highest positive and lowest negative rank metric scores from representative GSEA pathways shown in (**f**, **g**). **i**, Heatmap of z-score normalized expression values of genes with the highest positive and lowest negative rank metric scores from GSEA when comparing irradiated to non-irradiated WT kidneys. The gene sets investigated were the SenMayo gene set and the GOBP Cellular Senescence gene set. GOBP: Gene Ontology Biological Process. N ≥ 4 fish per genotype and treatment

Interestingly, linear regression of all significantly regulated genes of WT and cGAS KO during irradiation showed high linear correlation ( $R^2 = 0.6847$ ) but with a slope significantly less than 1 ( $m = 0.6908$ ). This observation indicates that genes are generally regulated in the same direction, but with a lower response in cGAS KO kidneys during irradiation compared to WT (**Figure 17d**). Comparing transcripts up- and downregulated in WT and cGAS KO showed high overlap as well as distinct significantly changing gene sets in WT and cGAS KO kidneys, identifying gene responses completely dependent on cGAS (**Figure 17e**). Virtually no genes were oppositely regulated, further supporting the idea that cGAS modulates the magnitude rather than the directionality of the transcriptional response.

To better understand which pathways were differentially regulated in the absence of cGAS, we performed GSEA. In line with the linear regression analysis, the regulation of most pathways by irradiation was significantly dampened in the cGAS KO kidney

transcriptome (**Figure 17f, g**). These included pathways involved in innate immunity (complement components C6, C9, SERPING1), extracellular matrix, cell adhesion and focal adhesion (COL1A2, LAMA2; CDH, ITGA9; CAV1, MYLK) and cardiomyopathy (ITGB4, ACTC2) (**Figure 17g, h**). In addition, we observed that the cGAS KO kidney transcriptome showed higher basal levels of processes associated with growth and proliferation, which were less downregulated by irradiation (**Figure 17h**). With this in mind, we revisited our data on young non-irradiated cGAS KO versus WT kidneys, and noticed that a number of specific genes associated with DNA replication (e.g. MCM family), protein homeostasis (e.g. proteasome subunits PSMA2, PSME3; ribosomal subunits RPS6, RPL21) and mRNA splicing (e.g. PUF60B, SF3B2) were elevated relative to WT (**Figure 17h**), though their pathways did not emerge as significantly enriched (**Figure 15c**). Conceivably, this upregulation may reflect an attenuated stress response or relaxation of checkpoints that regulate growth and cell division.

Curiously, the expression of DNA repair pathways themselves were downregulated in both cGAS KO and WT at this 5-day timepoint consistent with previous observations that cells on a senescent trajectory downregulate DNA repair (Collin et al. 2018). Because the KEGG\_LEGACY pathways only partially represent senescence and SASP factors, we decided to specifically investigate the expression of genes under the Cellular Senescence GO Biological Process (GOBP) term as well as the SenMayo (Saul et al. 2022) gene set. Notably, we observed a blunted senescent gene expression in the cGAS KO kidneys (**Figure 17i**) especially of SASP components (MIF, CXCL12B, IGFBP3/5A, MMP2/9), corroborating our *in vitro* findings.

Altogether, despite the presence of a DNA damage and senescence responses in the absence of cGAS, the magnitude of regulation was markedly reduced, suggesting that cGAS serves to amplify the transcriptional response of these processes *in vivo*.

We also analyzed the gut transcriptome from the same irradiated fish as above. As with the kidney, PCA plots showed that the genotypes clustered separately after irradiation (**Figure 18a**). Linear regression of the significantly changed genes during irradiation comparing both genotypes again showed a decreased slope ( $m=0.4059$ ), though the linear correlation was weaker ( $R^2=0.3564$ ) (**Figure 18b**). GSEA analysis revealed widespread regulation of multiple pathways after irradiation (**Figure 18c**), while the lack of cGAS again blunted the response, especially of ribosomal protein

regulation (**Figure 18c, d**). Notably, the attenuation of gene and KEGG pathway regulations were less prominent than those observed in the kidney. However, senescence and SASP activation were blunted similarly to the kidney (**Figure 18e**), suggesting cGAS functions in multiple tissues during genotoxic stress, but the breadth of regulation appears tissue specific.



**a**, PCA plot of WT and cGAS KO transcriptomes from guts of irradiated and non-irradiated young (8 weeks) killifish. **b**, Linear regression analysis of the Log<sub>2</sub>(Fold change) of all genes significantly changed in expression after irradiation in WT and cGAS KO guts, showing a slope significantly < 1. Dashed line with slope = 1 is shown for comparison. **c**, GSEA of guts from irradiated compared to non-irradiated WT fish. The top KEGG pathways upregulated and downregulated in irradiated WT are shown. **d**, GSEA of guts from irradiated cGAS KO compared to WT killifish. The top KEGG pathways upregulated and downregulated in cGAS KO are shown. **e**, Heatmap of z-score normalized expression values of genes with the highest positive and lowest negative rank metric scores from GSEA when comparing guts from irradiated to non-irradiated WT fish. The gene sets investigated were the Sen\_Mayo gene set and the GOBP\_Cellular Senescence gene set. **f**, PCA plot of WT and STING KO transcriptomes of kidneys from irradiated and non-irradiated young (8 weeks) killifish. **g**, MA plot showing differential mRNA expression comparing kidneys from young irradiated STING KO to kidneys from irradiated WT killifish. All genes with adjusted p-value < 0.05 are considered significant, upregulated (red), downregulated (blue). **h**, GSEA of kidneys from irradiated STING KO compared to WT killifish. The top KEGG pathways upregulated and downregulated in STING KO are shown. **i**, Heatmap of z-score normalized expression values of genes with the highest positive and lowest negative rank metric scores from GSEA when comparing guts from irradiated to non-irradiated WT fish. Genes shown derive from representative pathways from (**h**) as well as Sen\_Mayo gene set and the GOBP\_Cellular Senescence gene set.

We next investigated the transcriptional response to DNA damage in the STING KO kidneys. PCA plots showed that irradiated STING KO transcriptomes separated from irradiated WT, and a number of genes were differentially regulated (**Figure 18f, g**). In this case, the attenuation of gene regulation, as seen in the cGAS KO, was not observed in the STING KO (**Figure 18h**). In fact, pathways that were most affected, namely the complement and coagulation cascades and proteasome (**Figure 17f**), were more upregulated or downregulated, respectively (**Figure 18h, i**). By comparison, proteasome subunits did not show uniform regulation across batches when relating non-irradiated to irradiated WT kidneys (**Figure 17h, Figure 18i**). Still, genes involved in inflammation (C7, C4B and SERPINA1) and cellular stress responses (SCARA3 and NTD5) showed

upregulation in the STING KO, opposite to what we observed with cGAS KO (**Figure 17h**). While many senescent genes appeared to be similarly regulated between WT and STING KO, we noticed a number of SASP genes within the SenMayo gene set (IGFBP family, CXCL12B) to have blunted regulation (**Figure 18i**), which is consistent with what has been observed in human cell cultures (Gulen et al. 2023; Gluck et al. 2017; Dou et al. 2017).

Collectively, these observations hint towards a broad STING-independent and tissue specific role of cGAS as an important modulator of the transcriptional response to DNA damage and senescence.

#### 5.4 Killifish cGAS modulates the aging transcriptome

Aging is associated with increased DNA damage, inflammation, and senescence. In addition, aged mice brains have shown higher cGAMP levels when compared to young brains, indicating higher cGAS activity or lower cGAMP turnover with age (Gulen et al. 2023). In killifish we detected increased cGAMP levels in the old kidneys, but no significant change in the gut when compared to young tissues (**Figure 20a**). Hence, we sought to understand the impact of cGAS to the normative aging transcriptome. We used the young (8 weeks) healthy WT and cGAS KO fish as reference and performed RNAseq in old (18 weeks) WT and cGAS KO kidneys. Similar to what we observed post-irradiation, PCA plots showed that the two genotypes separated better in old age than in young (**Figure 19a**). Overall, the killifish kidney transcriptome was vastly deregulated, and the aged cGAS KO transcriptional profile deviated significantly from the aged WT counterpart (**Figure 19b, c**).

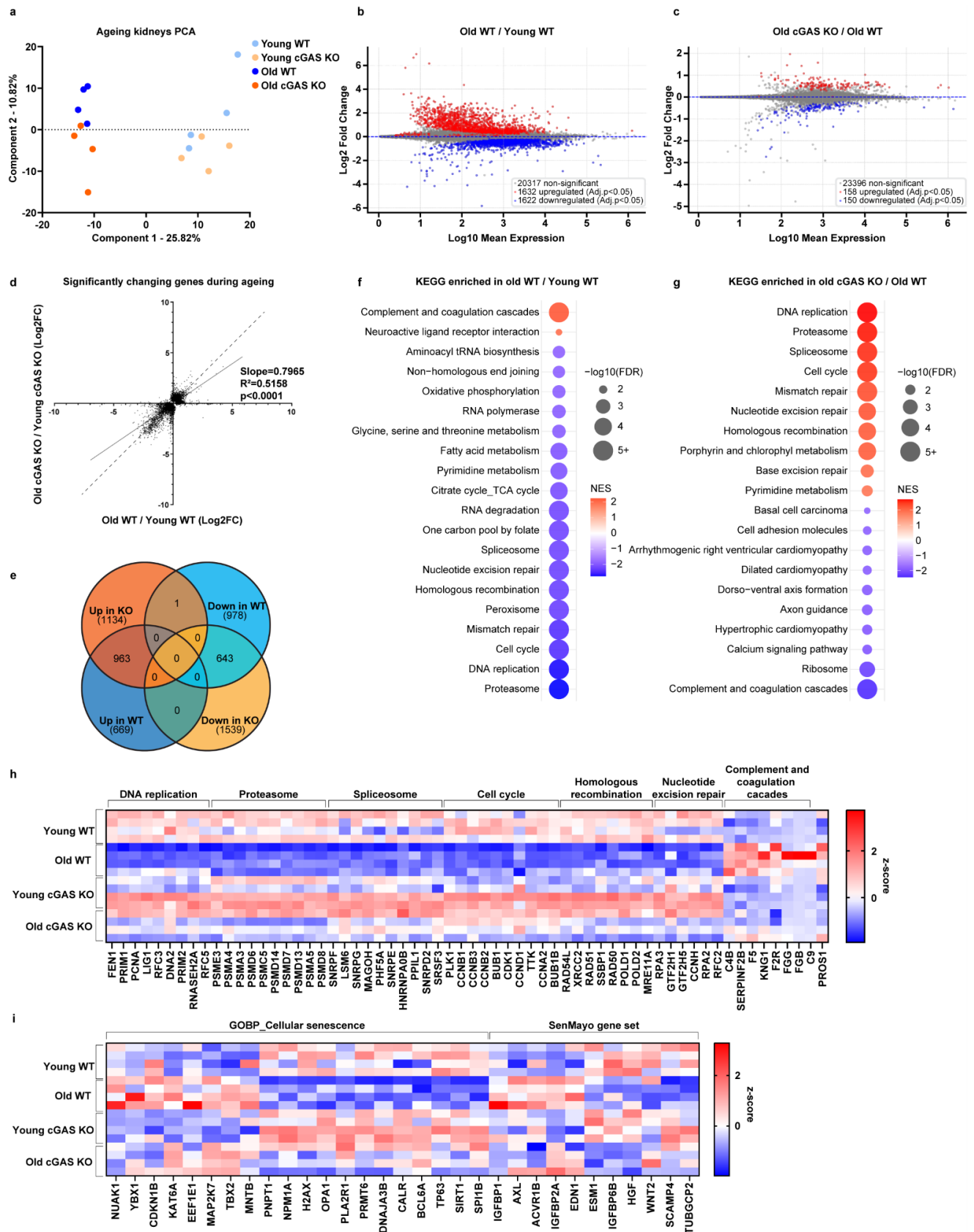


**Figure 19. cGAS modulates transcriptional changes during ageing.** a, PCA plot of WT and cGAS KO transcriptomes from young (8 weeks) and old (18 weeks) killifish kidneys.

**b**, MA plot showing differential mRNA expression comparing old to young WT kidneys. All genes with adjusted p-value < 0.05 are considered significant, upregulated (red), downregulated (blue). **c**, MA plot showing differential mRNA expression comparing old cGAS KO to old WT kidneys. All genes with adjusted p-value < 0.05 are considered significant, upregulated (red), downregulated (blue). **d**, Linear regression analysis of the Log<sub>2</sub>(Fold change) of all genes significantly changed in expression during ageing in WT and cGAS KO kidneys, showing a slope significantly < 1. Genes significantly regulated only in WT ageing or cGAS KO ageing or inversely regulated are also included. A dashed line with slope = 1 is shown for comparison. **e**, Venn diagram depicting the overlap of significantly changed genes during ageing in WT and cGAS KO kidneys. **f**, GSEA comparing old to young WT kidneys. All KEGG pathways significantly upregulated and the top downregulated in old WT kidneys are shown. **g**, GSEA comparing old cGAS KO to old WT kidneys. The top KEGG pathways upregulated and downregulated in cGAS KO are shown. **h**, Heatmap of z-score normalized expression values of the genes with the highest positive and lowest negative rank metric scores from representative GSEA pathways shown in (**f**, **g**). **i**, Heatmap of z-score normalized expression values of genes with the highest positive and lowest negative rank metric scores from GSEA when comparing old to young WT kidneys. The gene sets investigated were the SenMayo gene set and the GOBP\_Cellular Senescence gene set.

As with irradiation, cGAS clearly impacted the aging kidney transcriptome. Comparing cGAS KO to WT, linear regression of all transcripts significantly regulated with age showed a significantly reduced slope ( $m=0.7965$ ) (**Figure 19d**), with reasonable linear correlation ( $R^2=0.5158$ ), and virtually no genes inversely regulated in the two genotypes (**Figure 19e**). These findings point towards robust changes in gene regulation with age, which are blunted by cGAS KO. GSEA revealed that KEGG pathways upregulated with normative aging included complement and coagulation cascades, and neuroactive ligand receptor interaction, while KEGG pathways downregulated with aging included proteasome, DNA replication, cell cycle, DNA repair, peroxisome, spliceosome, one-carbon metabolism, TCA cycle and oxphos among others (**Figure 19f**).

Attenuation of gene expression changes by cGAS KO applied broadly to a majority of pathways dysregulated with age, revealing a widespread effect (**Figure 19f, g**). In



particular, GSEA revealed that DNA replication and repair pathways, cell cycle, spliceosome, proteasome, and pyrimidine metabolism were less downregulated (**Figure 19f, g**), while complement and coagulation and ribosome were less upregulated in old cGAS relative to old WT. For example, the aging cGAS KO kidneys lacked the strong reduction of cell proliferation markers (FEN1, PCNA, RFC3, CCNB1/2/3), suggesting less replicative arrest (**Figure 19h**). These patterns suggest that cGAS KO cells may be more proliferative and actively engaged in the cell cycle.

We also examined senescence and SASP markers. Surprisingly, in the case of the old kidney, we did not see a strong signature of senescence markers with age (**Figure 19i**), likely reflecting the small proportion of senescent cells that accumulate within a given tissue during aging (Idda et al. 2020). Senescent gene profiles from old cGAS KO kidneys were not very distinct compared to old WT (**Figure 19i**), with the exception of a handful of genes (NUAK1, CDKN1B, IGFBP1) that appeared less upregulated.

In contrast to the kidney, the aging killifish gut transcriptome showed much less dependence on cGAS (**Figure 20b, c**), which is in line with lack of increased cGAMP activity with age. Pathways significantly regulated during aging were not deregulated in the absence of cGAS, and the dampening effect was less prominent than in the kidney (**Figure 20d, e**). Surprisingly, however, the transcriptomes of old WT guts showed a clearer signature of senescent genes upregulated (CDKN1B/2B, YPEL3, PTBP1) in old age, and lack of cGAS attenuated this regulation (**Figure 20f**).

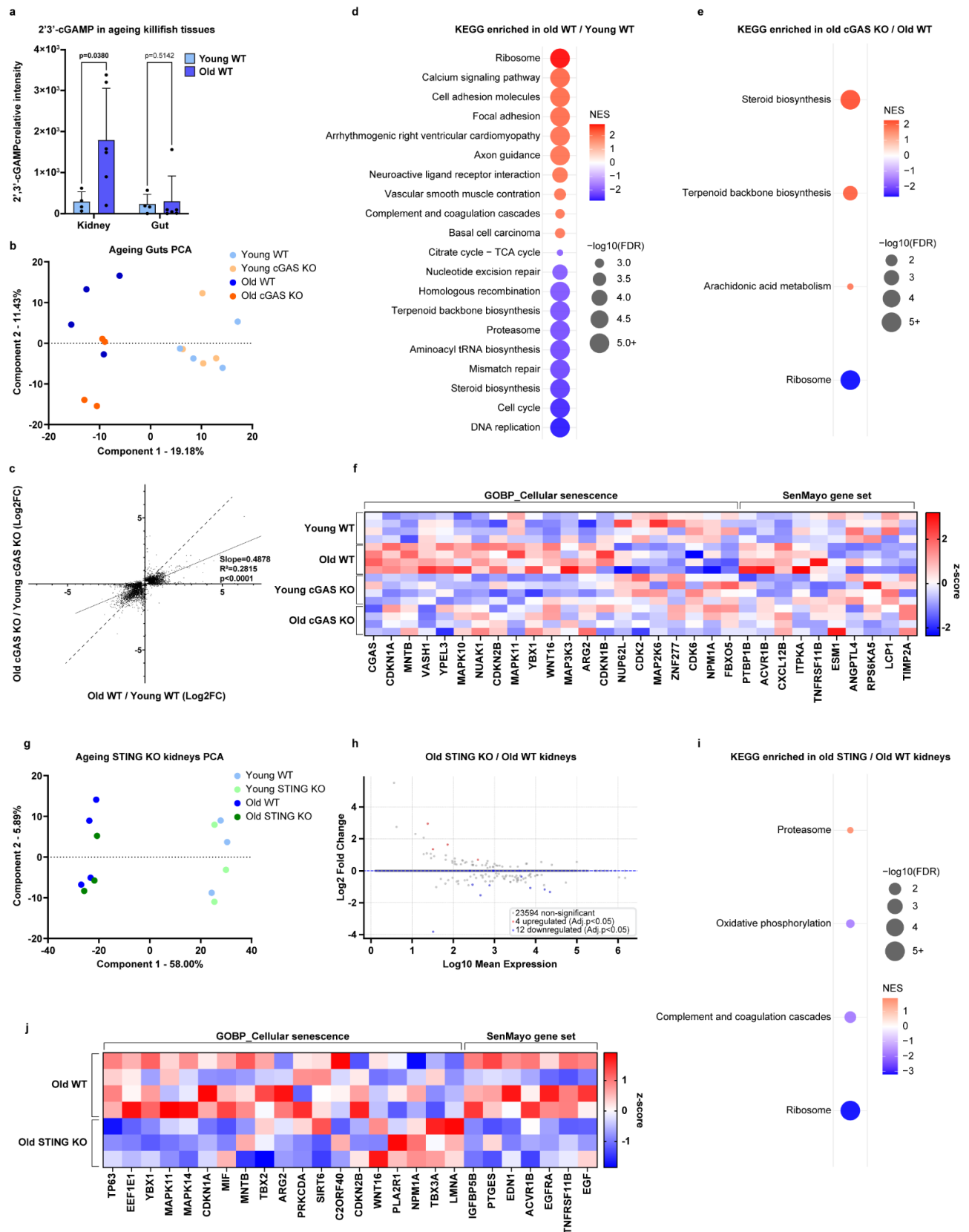


**Figure 20. Extended Data. cGAS and STING modulate senescent transcriptional signatures during ageing in killifish kidneys and guts.**

**a**, LC-MS-based targeted metabolomics of 2',3'-cGAMP extracted from young (7 weeks, n = 4) and old (18 weeks, n = 6) WT kidneys and guts. Statistical analysis was performed using Mann-Whitney U test. **b**, PCA plot of WT and cGAS KO transcriptomes from young (8 weeks) and old (18 weeks) killifish guts. For each condition n = 4. **c**, Linear regression analysis of the Log2(Fold change) of all genes significantly changed in expression during ageing in WT and cGAS KO guts, showing a slope significantly < 1. Dashed line with slope = 1 is shown for comparison. **d**, GSEA comparing old to young WT guts. The top KEGG pathways upregulated and downregulated in old WT guts are shown. **e**, GSEA comparing old cGAS KO to WT guts. All KEGG pathways upregulated and downregulated in cGAS KO are shown. **f**, Heatmap of z-score normalized expression values of genes with the highest positive and lowest negative rank metric scores from GSEA when comparing old to young WT guts. The gene sets investigated were the Sen\_Mayo gene set and the GOBP\_Cellular Senescence gene set. **g**, PCA plot of WT and STING KO transcriptomes from young (9 weeks) and old (18 weeks) killifish kidneys. For old WT n = 4, for all other conditions n = 3. **h**, MA plot showing differential mRNA expression comparing old STING KO to old WT kidneys. All genes with adjusted p-value < 0.05 are considered significant, upregulated (red), downregulated (blue). **i**, GSEA comparing old STING KO to WT kidneys. All KEGG pathways upregulated and downregulated in STING KO are shown. **j**, Heatmap of z-score normalized expression values of genes with the highest positive and lowest negative rank metric scores from GSEA when comparing old STING KO to WT kidneys. The gene sets investigated were the Sen\_Mayo gene set and the GOBP\_Cellular Senescence gene set.

Unlike cGAS, lack of STING showed hardly any separation of transcriptional profiles with old age when compared to WT in the kidneys (**Figure 20g, h**). However, GSEA showed that proteasome downregulation and complement and coagulation upregulation were blunted in the old STING KO (**Figure 19f, Figure 20i**). In addition, senescent markers (TP63, CDKN1A), SASP regulators (YBX1, MAPK11/14) and SASP components (MIF, IGFBP5, EGF) were downregulated in old STING KO when compared to old WT (**Figure 20j**).

In sum, cGAS modulates the transcriptional landscape during both DNA damage and aging, two conditions that are linked, but the scale of this effect is tissue-specific. STING does not appear to regulate the transcriptional landscape in the kidneys as

broadly. Yet, to different degrees, lack of either cGAS or STING attenuates senescent marker and SASP component expression in old age.

## 5.5 The killifish cGAS/STING pathway affects age-related pathology but not life span

Since killifish cGAS KO and STING KO mitigated senescence in cultured fibroblasts and many age-related transcriptional signatures in the kidney *in vivo*, we sought to investigate the possibility of altered lifespan in our mutants. In particular, we hypothesized that our mutants might live longer than controls due to the amelioration of these age-related phenotypes. To address this, after at least four rounds of backcrossing with WT fish, we generated, expanded, and measured the life span of cGAS and STING KO mutants along with WT fish. Males and females were singly housed, and their life span measured within the same cohort. Demographic analysis showed that cGAS KO fish had fairly similar lifespans to WT fish (**Figure 21a, Figure 22a-c**), contravening our hypothesis. Median and maximum life span of cGAS KO and wild type were comparable and Log rank statistics showed the survival curves were not significantly different ( $p=0.43$ ). Furthermore, STING KO fish showed a tendency for reduced lifespan (**Figure 21b, Figure 22a-c**), but it did not reach significance ( $p=0.10$ ).

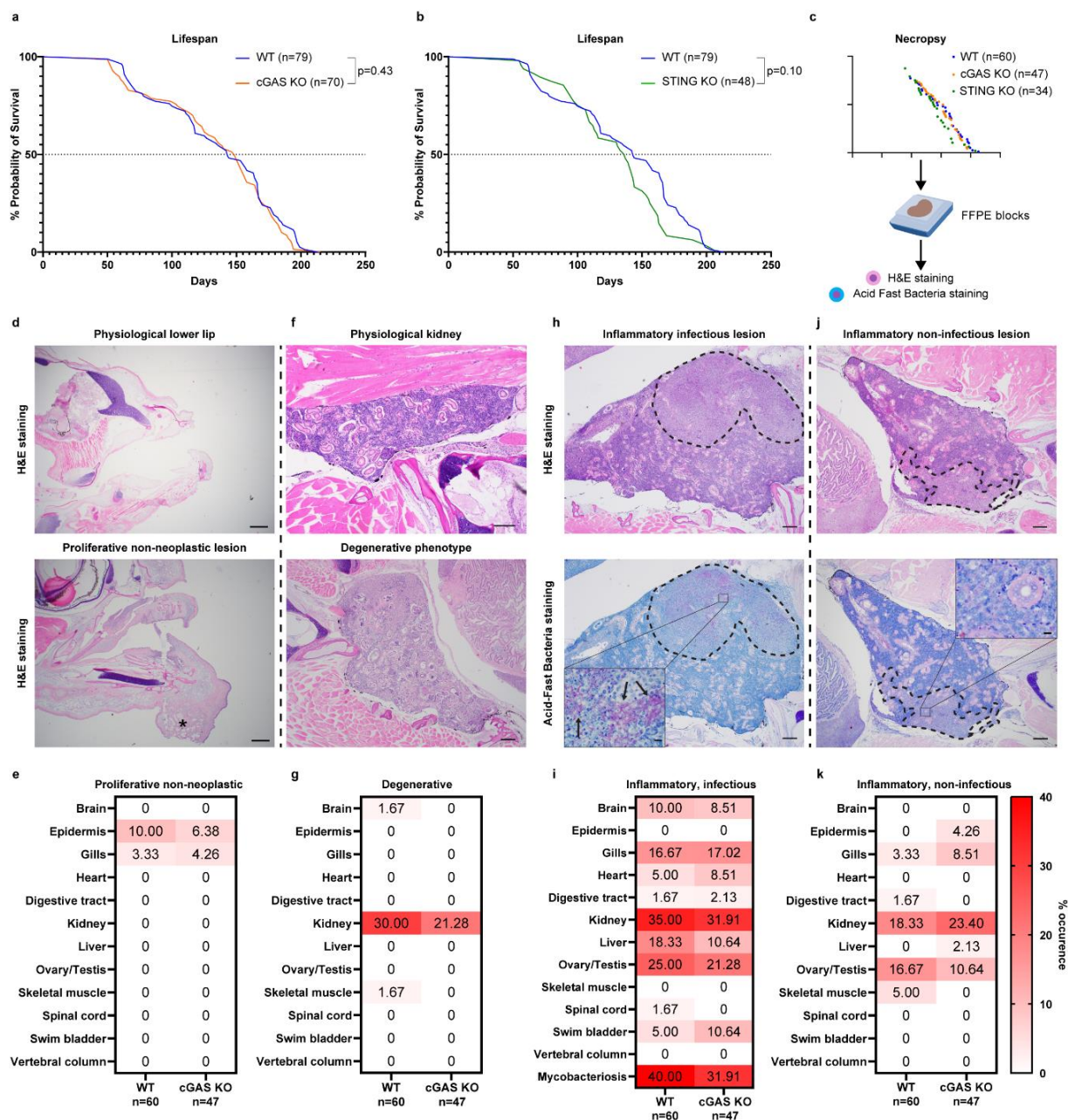


**Figure 21. Killifish cGAS/STING pathway influences degenerative and inflammatory disease occurrence but not lifespan.** **a**, Kaplan-Meier curve showing the survival of WT (n = 79) and cGAS KO (n = 70) killifish. Indicated p-value represents comparison between cGAS KO and WT using the log-rank Mantel-Cox test. **b**, Kaplan-Meier curve showing the survival of WT (n = 79) and STING KO (n = 48) killifish. Indicated p-value represents comparison between STING KO and WT using the log-rank Mantel-Cox test. **c**, Schematic of all fish samples collected from the lifespan experiments in (a) and (b) for necropsy analysis, with FFPE sections stained with Hematoxylin & Eosin (H&E) and Acid-Fast Bacteria stains. **d**, H&E histological images of the jaw region depicting a healthy and a proliferative non-neoplastic lesion in the lower lip indicated

with an asterisk (\*). **e**, Heatmap showing the percent occurrence of the proliferative non-neoplastic pathology in 12 tissues analyzed during necropsy in WT and cGAS KO tissues. **f**, H&E histological images depicting a healthy kidney and a kidney displaying degenerative tubular changes. **g**, Percent occurrence of the degenerative pathology in indicated tissues and genotypes. **h**, H&E and Acid-Fast Bacteria-stained histological images of a kidney depicting an inflammatory lesion containing mycobacteria organisms. The outlined area consists of necrosis and mononuclear inflammatory infiltrates. Within the outlined necrotic and inflamed region, arrows point to aggregates of Acid-Fast positive rod-shaped bacteria in the zoomed inset. **i**, Percent occurrence of the inflammatory infectious pathology in indicated tissues and genotypes. Separately, the percent incidence of mycobacteriosis among all tissue is shown. **j**, H&E and Acid-Fast Bacteria-stained histological images of a kidney depicting an inflammatory lesion with no apparent bacteria within it. The inflammatory cell aggregate within the kidney is outlined. Neither positive, nor negative staining acid-fast rod-shaped organisms were detected in these lesions. **k**, Percent occurrence of the inflammatory non-infectious pathology in indicated tissues and genotypes. 60 WT fish and 47 cGAS KO fish were used for necropsy. Bars in images of kidneys = 200  $\mu$ m. Bars in zoomed in images of kidneys = 10  $\mu$ m. Bars in jaw images = 500  $\mu$ m.

Hence, we decided to investigate aspects of pathology. In particular, upon death we preserved the fish from the demographic analysis in paraformaldehyde and performed histological necropsy with a certified veterinary pathologist. We categorized the observable disease phenotypes into five categories, namely neoplastic, proliferative non-neoplastic, degenerative, inflammatory infectious and inflammatory non-infectious, and analyzed 12 tissues using 60 WT and 47 cGAS KO preserved fish for necropsy (**Figure 21c**). Notably, we found no clear neoplastic lesions in any of the tissues analyzed. Non-neoplastic lesions were detected predominately at the mandibular lip, which was enlarged and contained nodular fibroplasia (**Figure 21d**), while few fish showed proliferative bronchitis with or without goblet cell hyperplasia. The occurrence of these non-neoplastic lesions was slightly reduced in cGAS KO fish compared to WT (**Figure 21e**). The most common degenerative lesions were found in the kidney in the form of minimal to mild tubular dilation with or without luminal mineralization (**Figure 21f**).

There, we again observed a tendency for less degenerative phenotype occurrence in the cGAS KO compared to WT kidneys (**Figure 21g**), consistent with the blunted deregulation that comes with old age in the kidney transcriptome.

Infectious and non-infectious inflammatory lesions were widespread across tissues but most prominent in the kidneys and gonads, specifically the ovaries (**Figure 22d, e**). Infectious lesions often had acid-fast positive rod-shaped bacteria within the lesion, interpreted to be mycobacterial infections (**Figure 21h**). These infections usually affected multiple organs at once within an individual. Surprisingly, cGAS KO tissues appeared to have a mild reduction in infection occurrence in kidneys, liver, and gonads (**Figure 21i**), despite this pathway's involvement in immune defense. Inflammatory non-infectious lesions were classified when significant macrophage infiltration was observed without detectable rod-shaped microorganisms (**Figure 21j**). These lesions were far less prevalent than infectious lesions but overall, some tissues showed more and others less frequency of occurrence in the cGAS KO (**Figure 21k**).

Like cGAS KO, STING KO appeared to show a similar reduction in proliferative and degenerative lesion occurrence (**Figure 22f, g**). The reduction of inflammatory lesion occurrence, however, was much more pronounced in the STING mutants, again supporting our observation of a divergent function of STING from cGAS. Infection rates dropped in multiple tissues, especially the gonads (**Figure 22h**), which could be attributed solely to lesions in female ovaries, not male testes. On the contrary, non-infectious inflammatory lesions in the ovary appeared elevated in the STING KO (**Figure 22i**).



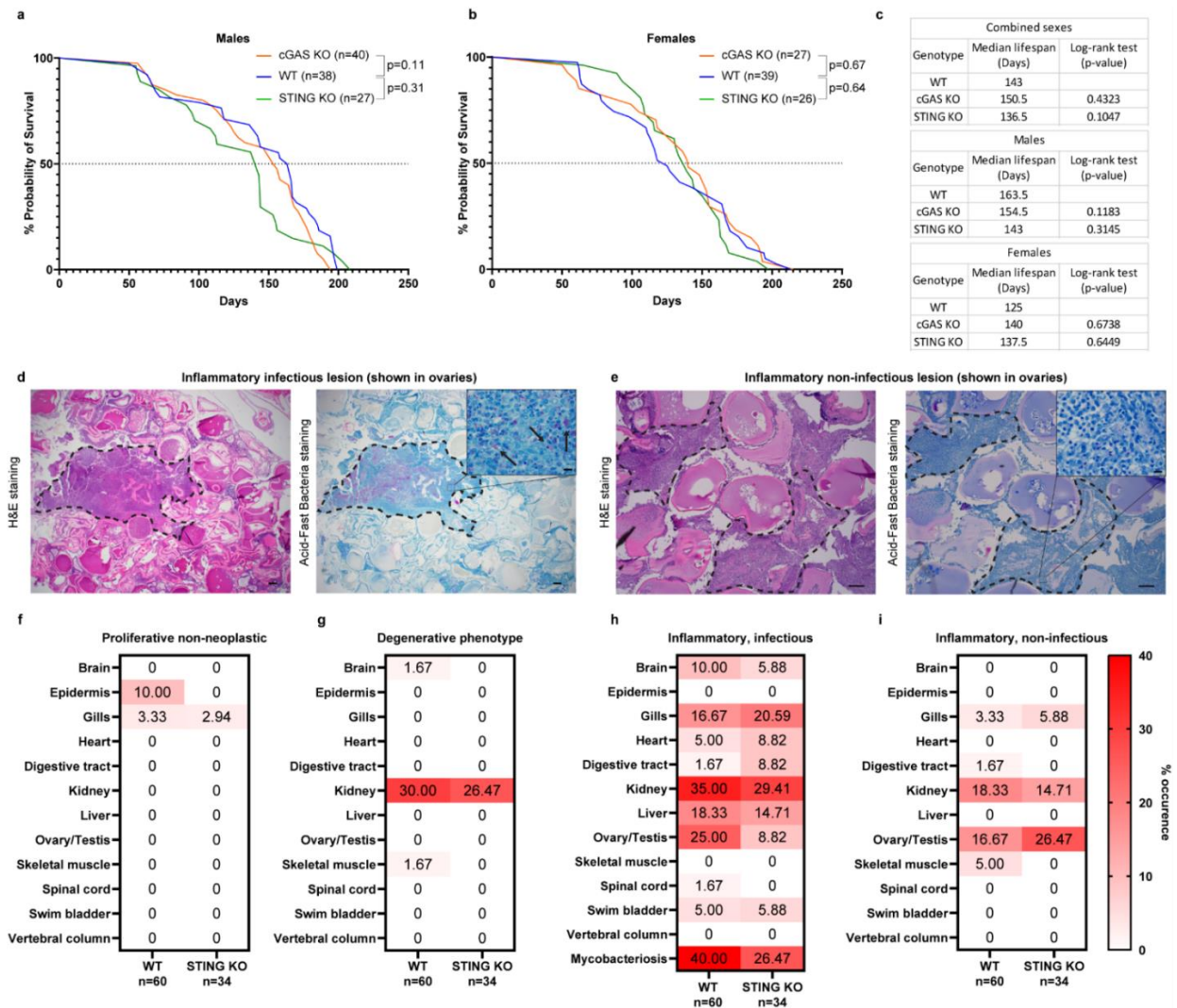


**Figure 22. Extended Data. The killifish cGAS/STING pathway contributes to degenerative and inflammatory disease occurrence but not lifespan in individual sexes.**

**a**, Kaplan-Meier curve showing the survival of WT (n = 38), cGAS KO (n = 40) and STING KO (n = 27) male killifish. Indicated p-values represent statistical comparisons between WT and cGAS KO or STING KO, respectively, using the log-rank Mantel-Cox test. **b**, Kaplan-Meier curve showing the survival of WT (n = 39), cGAS KO (n = 27) and STING KO (n = 26) female killifish. Indicated p-value represent statistical comparisons between WT and cGAS KO or STING KO, respectively, using the log-rank Mantel-Cox test. **c**, Tables summarizing the median lifespans (in days) of WT, cGAS KO and STING KO killifish. Both individual sexes and combined sexes are shown separately. Log-rank tests were performed comparing WT to cGAS or STING KO fish, respectively, and the p-values are shown for each genotype. **d**, H&E and Acid-Fast Bacteria-stained histological images of a



killifish ovary depicting an inflammatory lesion containing mycobacteria organisms. The inflammatory cell aggregate within the necrotic ovarian region is outlined. Within the necrotic and inflamed region, arrows point to clusters of Acid-Fast positive rod-shaped bacteria, shown in the zoomed inset. **e**, H&E and Acid-Fast Bacteria-stained histological images of a killifish ovary depicting an inflammatory lesion containing no apparent bacteria. The inflammatory cell aggregate within the ovary is outlined. Neither positive, nor negative Acid-Fast rod-shaped organisms were detected in these lesions. **f**, Heatmap showing the percent occurrence of proliferative non-neoplastic pathology in 12 tissues as analyzed during necropsy in WT and STING KO tissues. **g**, Percent occurrence of the degenerative pathology in indicated tissues and genotypes. **h**, Percent occurrence of the inflammatory infectious pathology in indicated tissues and genotypes. Separately, the percent incidence of mycobacteriosis among all tissues is shown. **i**, Percent occurrence of inflammatory non-infectious pathology in indicated tissues and genotypes. 60 WT fish and 34 STING KO fish were used for necropsy. Bars in images of ovaries = 200  $\mu$ m. Bars in inset images of ovaries = 10  $\mu$ m.

It is important to mention that the number of fish used for such histological analyses is not sufficient to definitively determine a protective or detrimental role for each genotype because the differences in odds ratios for most lesions and tissues were small. The only comparison where Fischer's Exact test revealed a significant change ( $p=0.034$ ) was the reduction in ovarian infectious lesions in STING KO (3/20 ovaries) compared to WT (15/32 ovaries). Yet the consistent reduction in occurrence of different morbidities across tissues, hints towards an effect of the cGAS/STING pathway beyond ovarian infectious lesions. Most curiously, both cGAS and STING KO appear more susceptible to sterile macrophage infiltration than mycobacterial infections in some tissues.

## 6. Discussion

Inflammaging and immune dysfunction significantly contribute to age-related pathology and disease, and interventions that rebalance these processes can have a profound impact on health and life span (Widjaja et al. 2024; Moiseeva et al. 2013; Moiseeva et al. 2023). The cGAS/STING pathway is a central innate immune signaling pathway that detects cytosolic DNA (Decout et al. 2021), and has been implicated in senescence cascades induced by DNA damage (Yang et al. 2017; Dou et al. 2017) or mitochondrial dysfunction (West et al. 2015; Victorelli et al. 2024), eventually leading to SASP secretion (Coppe et al. 2010). It has been postulated that low grade activation of cGAS/STING over the life course could be a source of chronic inflammation, and in the long term, contribute to aging pathology and organismal demise (Decout et al. 2021; Franceschi et al. 2018; Benayoun et al. 2019; Gulen et al. 2023).

In this work, we sought to elucidate the function of the cGAS/STING pathway during ageing using the naturally short-lived killifish *N. furzeri*. We found cGAS and STING regulation of senescence to be conserved in teleosts *in vitro* and *in vivo*. We then showed that cGAS, more than STING, impacts aging-related signatures; however, neither gene significantly regulates lifespan on its own.

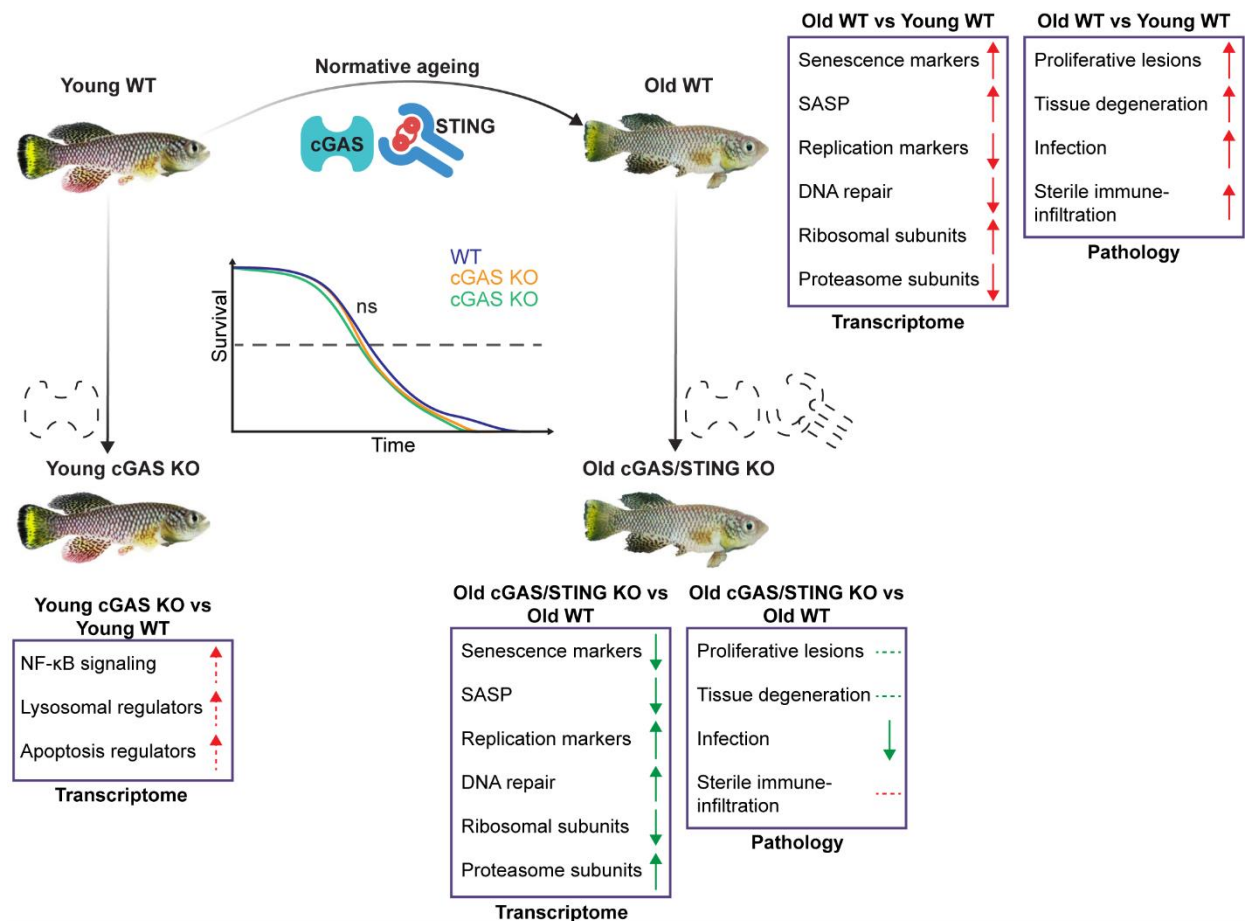


**Figure 23. Summary of cGAS/STING impact on killifish tissue transcriptome and pathology during normative ageing.** Knock out of cGAS, but not STING causes low-grade upregulation of NF-κB signaling and lysosomal and apoptotic regulators in the kidney. Compared to old WT tissues, cGAS or STING KO fish exhibit reduced expression of senescent and SASP markers, cellular replication modulators, DNA repair components and ribosomal and proteasomal subunits. Collectively, knock out of cGAS or STING significantly dampens the age-related transcriptional landscape. In accord, proliferative lesions and tissue degeneration tend to appear with less frequency, while infection rates are significantly lower. However, sterile immune-infiltration in old tissues also tends to increase. Despite mitigation of multiple age-related signatures, cGAS and STING KO killifish do not exhibit increased lifespan. Solid red arrows indicate regulation during ageing, dashed red arrows represent low-grade regulation associated with stress and solid green arrows represent dampening of age-related changes.

## 6.1 cGAS and STING are evolutionarily conserved

The cGAS protein is evolutionarily conserved across distant taxa. The invertebrate sea anemone cGAS has been functionally verified to be able to produce 3'3'-cGAMP (Kranzusch et al. 2015). Yet, phylogenetic analysis of cGAS proteins showed that vertebrates evolved key functional domains and residues for DNA binding and 2'3'-cGAMP production (Wu et al. 2014). Our previously published work was the first to demonstrate that killifish cGAS is indeed capable of biochemically producing 2'3'-cGAMP (Annibal et al. 2021), making it the most distant verified ortholog.

Despite this general conservation, cGAS sequence and structure is not as well conserved. Human and mouse cGAS exhibit only 60% sequence identity, are sensitive to varying DNA lengths, and have great differences in enzymatic activity, with mouse cGAS 20 times more active in cGAMP production (Zhou et al. 2018). Their different structures render small molecule inhibitors unable to function in both organisms (Liu, Zhang, et al. 2023). Even comparing two teleost sequences, such as killifish and zebrafish, yields only a 43% sequence identity, indicating a strong positive selection for evolution to optimize functions. Multiple sequence alignment showed that killifish cGAS has 35% and 36% sequence identity with human and mouse proteins, respectively. Conserved residues cluster within functional domains, indicating that core functions are preserved, but signal intensity or sensitivity may vary.

Our transfection experiments show that killifish cGAS indeed has cyclic GMP-AMP activity and can complement the gene knockout in a heterologous system. In fact, when we introduced cGAS into human cGAS KO THP1 cells, we found that kcGAS produced over 4-times more cGAMP than the human homolog and had lower transfection efficiency presumably due activation of the antiviral response. This finding is consistent with other studies that show cGAS/STING activity reduces transfection efficiency and knock out of either cGAS or STING enhances both transfection and transgene expression (Fu et al. 2020; Langereis et al. 2015). Downstream activation of interferon signaling was similar between the killifish and human proteins, however, this is probably due to signal saturation during transient transfection. Overall, our findings suggest that kcGAS has higher enzymatic activity than hcGAS, but precise determination requires an equimolar, purified *in vitro* comparison.

In both human and mouse cells cGAS plays an important role in cellular senescence (Yang et al. 2017). During replicative senescence or DNA damage-induced senescence both mouse embryonic fibroblasts and neonatal human fibroblasts SA- $\beta$ -gal staining and SASP markers were greatly reduced (Yang et al. 2017; Gluck et al. 2017). Similarly, irradiated cGAS KO killifish fibroblasts showed reduced SA- $\beta$ -gal staining, cyclin inhibitor expression and IFN-signaling, markedly less than WT control fibroblasts. Notably, in all three species senescence induction was down but not completely abolished, suggesting other pathways may be at work. It is also possible that our results would differ at different irradiation intensities or time points since these parameters can lead to differences in senescence induction of cGAS KO human and mouse fibroblasts (Yang et al. 2017). Importantly, our data shows that loss of kcGAS attenuates senescence similar to mammalian species and establishes that cGAS-dependent senescence activation is conserved in teleosts. Hence, killifish present a valuable model to study age-related functions of this pathway.

STING is also conserved but has a few noteworthy differences. Mouse and human STING proteins are slightly more related, facilitating the discovery of small molecule inhibitors that block both proteins, such as H-151 (Haag et al. 2018). Still, overall amino-acid sequence identity between human, mouse, zebrafish and killifish STING is still below 50%, with the most conserved residues lying within functional domains among all proteins. Conceivably the non-conserved regions could reflect genetic drift or species-specific positive selection/interactions. On a functional level, transfection of kSTING did not activate IFN signaling in heterologous cells potentially due to ineffective interaction between kSTING and human TBK1, which is necessary for downstream signaling.

Compared to cGAS, STING has been reported to have a weaker role in modulating cellular senescence. While cGAS KO mouse fibroblasts spontaneously immortalize after ~10 passages, STING KO cells do so after ~18 passages (Yang et al. 2017). Further, while STING inhibition ameliorated SASP and age-related neurodegeneration, it did not reduce SA- $\beta$ -gal staining and p21 expression in cell cultures (Gulen et al. 2023). In contrast, genetic or pharmacological inhibition of STING reduces cyclin inhibitors and SA- $\beta$ -gal staining in diabetes-induced senescence (Liu, Ghosh, et al. 2023), bleomycin-induced DNA damage in lung fibroblasts (Rosas et al. 2023) and IL-1 $\beta$ -induced senescence in chondrocytes (Guo et al. 2021). However, in cases of etoposide- or oxidative stress-

induced senescence, neither cGAS nor STING inhibition reduced cyclin inhibitors (Dou et al. 2017; Gluck et al. 2017), but in both cases there was a reduction of downstream inflammatory markers and SASP. A number of other studies have also shown the role of STING in YAP/TAZ-deficiency (Sladitschek-Martens et al. 2022) and retrotransposon-induced senescence (Simon et al. 2019; De Cecco et al. 2019). Taken together, cGAS appears to regulate various aspects of senescence by both STING-dependent and STING-independent mechanisms.

In accord with published literature, we observed that STING inhibition significantly reduced cyclin inhibitor activation after irradiation-induced senescence, along with a modest decrease in downstream IFN signaling. Therefore, STING-dependent senescence regulation is conserved from teleosts to mammals, highlighting again the value of killifish as a model organism of *in vivo* studies of the pathway.

## 6.2 cGAS preserves genomic integrity

Our work suggests that cGAS plays a role in protecting genome integrity. We observed that primary killifish cGAS KO fibroblasts had higher levels of  $\gamma$ H2AX with or without irradiation, suggesting that cGAS normally prevents intrinsic DNA damage or facilitates repair in vitro. Relatedly, cGAS KO kidney transcriptomes from old fish showed elevated levels of genes involved in DNA repair, such as mismatch repair, nucleotide excision repair, base excision repair and homologous recombination. This increase of DNA repair pathways in old cGAS mutants could be due to WT cGAS tempering all of these pathways or these pathways are upregulated in response to increased DNA damage in these mutants. In any case, our data support that cGAS plays an important role in DNA damage regulation, possibly guarding DNA against spontaneous and genotoxicity-induced lesions.

Findings from different groups have also demonstrated genoprotective roles of cGAS. For example, cGAS inhibits transposable elements both at both basal levels and post DNA damage (Zhen et al. 2023; Martinez et al. 2024), slows replication forks (Chen et al. 2020) and prevents chromosome end-joining (Li et al. 2022), guarding against DNA fragmentation. Interestingly, the studies related to cGAS-mediated role in genomic

stability are shown to be STING-independent. Consistently, STING KO killifish transcriptomes did not show altered regulation of DNA repair mechanisms in either young, old or irradiated tissues. Cumulatively, we demonstrate a conserved role for cGAS in maintaining genomic stability and provide evidence that cGAS, independent of STING, safeguards the genome both *in vitro* and *in vivo*.

On the other hand, some studies suggest that cGAS may exert genotoxic effects. For instance, one study reported that cGAS overexpression in cGAS KO cancer cells leads to DNA fragmentation (Liu et al. 2018). Another study showed that WT bone marrow-differentiated monocytes exhibited increased micronuclei formation after irradiation when compared to cGAS-deficient cells (Jiang et al. 2019). Both studies demonstrated that cGAS, independently of STING, inhibits homologous recombination (HR). This inhibition appears to be conserved in killifish since we observed upregulation of HR components in old cGAS KO kidneys. Curiously, we did not see any impact on HR in young fish neither at steady state nor post-irradiation. What the above studies observed in cell cultures and tumors might only apply in old age, but not in young tissues. Future investigations may unravel the molecular interplay that allows cGAS to cause or prevent DNA damage in different biological contexts.

### 6.3 Loss of cGAS leads to low-grade sterile inflammation and stress *in vivo*

The cGAS/STING pathway stimulates the production of IFN-I and other cytokines that activate immune cells and establish a pro-inflammatory state. The killifish kidneys contain HSPCs, which generate all hematopoietic cell lineages and acts as a primary lymph node responding to any overt stimulus by increasing inflammation. Given the conserved role of cGAS/STING signaling in promoting senescence, downregulation of this pathway would be predicted to lower basal inflammation. Yet, by comparing the transcriptomes of WT and cGAS KO killifish kidneys, we observed a low-grade upregulation of inflammatory markers.

These markers were primarily pathway mediators downstream of cGAS (STING and TBK1) and cytokines downstream of NF- $\kappa$ B (e.g. TNF $\alpha$  and IL-12). Two recent studies showed that post-activation, STING is suppressed by lysosomal degradation (Kuchitsu et

al. 2023; Gentili et al. 2023), ensuring homeostatic regulation of STING signaling. Another study discovered a unique role of TBK1 as an E3 ubiquitin ligase, which can catalyze self-degradation after activation (Li et al. 2019). Presumably, lack of basal cGAS signaling leads to low-grade increase of STING and TBK1 proteins due to lack of negative self-regulation. Alternately, cells compensate for lack of cGAS by increasing downstream immunity, in order to respond to DAMPs by less efficient cGAS-independent means.

The concurrent upregulation of NF- $\kappa$ B-regulated cytokines, however, may also reflect a response to stress. Given increased basal levels of DNA damage in primary cGAS KO cell cultures, this could, by inference, arise from basal DNA damage *in vivo*, though this has not been directly measured. Consistently, lysosomal and apoptotic genes are also upregulated, hinting that the kidney cells are under stress. It should be noted that these responses appear quite mild, however. Without irradiation, the increased amount of  $\gamma$ H2AX in cGAS KO fibroblasts was significant, but modest. Consistently, the increase in all above pathways is significant, but small. STING deficiency did not show a similar upregulation of these components at steady-state, in agreement with the STING-independent role of cGAS in genome stability, Future investigations of DNA lesions *in vivo* would distinguish if stress derives from genomic instability or other DAMPs. Collectively, our data imply that lack of cGAS in young age causes destabilization of cellular components – likely DNA - leading to activation of stress response pathways.

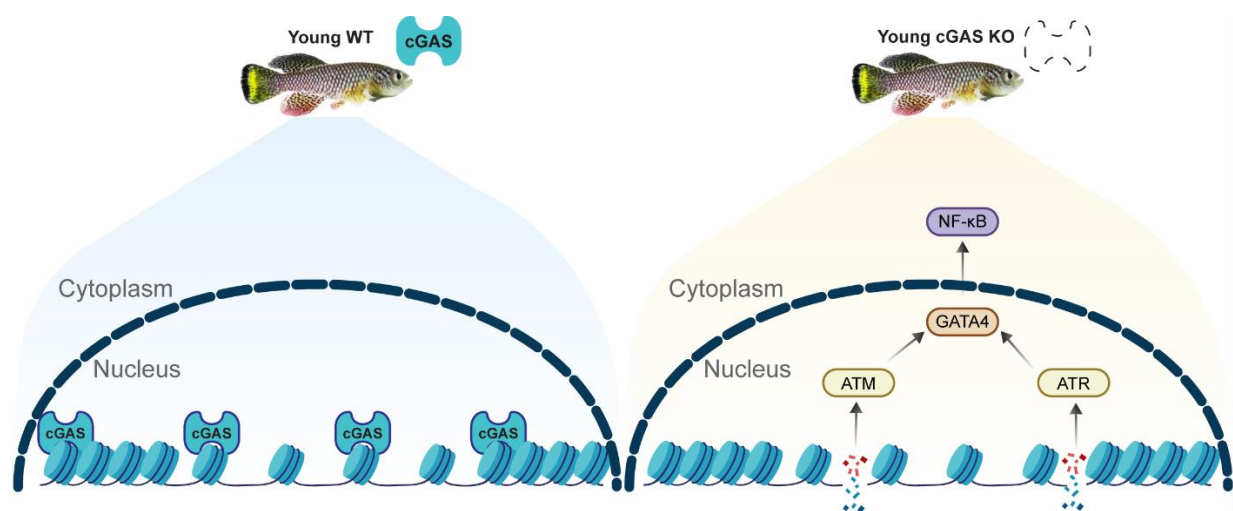


**Figure 24. cGAS safeguards the genome against DNA damage.** The illustration depicts a hypothetical model where chromatin-bound cGAS protects against spontaneous and induced double-strand breaks *in vivo*. In young cGAS KO organisms, this increase in DNA damage would lead to activation of NF- $\kappa$ B activity.



## 6.4 cGAS more than STING modulates senescence *in vivo*

Although extensively studied in cell cultures, the impact of cGAS/STING in senescence *in vivo* is largely unknown. One study that directly investigated senescence *in vivo* observed that YAP/TAZ/STING triple knock out mice had less senescent cells in aorta, kidney and dermis compared to YAP/TAZ-deficient mice (Sladitschek-Martens et al. 2022). Another study examined the effect of cGAS on irradiation- and oncogene-induced senescence in lung and liver *in vivo* (Gluck et al. 2017). To my knowledge, all other findings are either *in vitro* or only show SASP regulation but not other senescence markers. Consistent with our *in vitro* data, irradiated killifish cGAS KO kidneys and guts displayed greatly attenuated senescent marker regulation after DNA damage-induced senescence. Age-associated modulation by cGAS of senescent markers was much more modest, with a handful of markers regulated in the kidney (e.g. CDKN1B and NUA1). We observed a stronger cGAS-dependent regulation of senescent markers during aging in the gut (e.g. CDKN1A/2B, IGF1R, MIF). Interestingly we found certain senescent markers, such as CDKN1A (p21), that were tissue specifically expressed (e.g. CDKN1A was only regulated in the gut both during irradiation and ageing). Thus, our study provide a framework to decipher cGAS/STING-regulated senescence and SASP components across tissues *in vivo*.

Senescence consistently appears to be regulated by cGAS, but not always by STING (Yang et al. 2017; Gulen et al. 2023). Relatedly, the downregulation of senescence markers in irradiated STING KO fish was not as strong as cGAS KO. How might STING impact senescence less than cGAS? Conceivably, loss of STING, but not cGAS, could lead to activation of compensatory senescence-activating pathways. Of note, we observed in our transcriptome data that young irradiated STING KO, but not cGAS KO, fish upregulated JAK/STAT signaling. JAK/STAT pathway is known to stabilize IRF3 in the nucleus (Czerkies et al. 2018) and the interaction between IRF3 and Rb in the nucleus prevents Rb phosphorylation, leading to cycle arrest and cellular senescence (Wu et al. 2024). It is still unknown why lack of STING can be compensated, but lack of cGAS largely cannot and a potential interaction with JAK/STAT signaling is only one such possibility (**Figure 25**). Therefore, although only hinted in other studies, our work underscores the

necessity to investigate the interaction between individual cGAS/STING pathway components and senescence mediators.

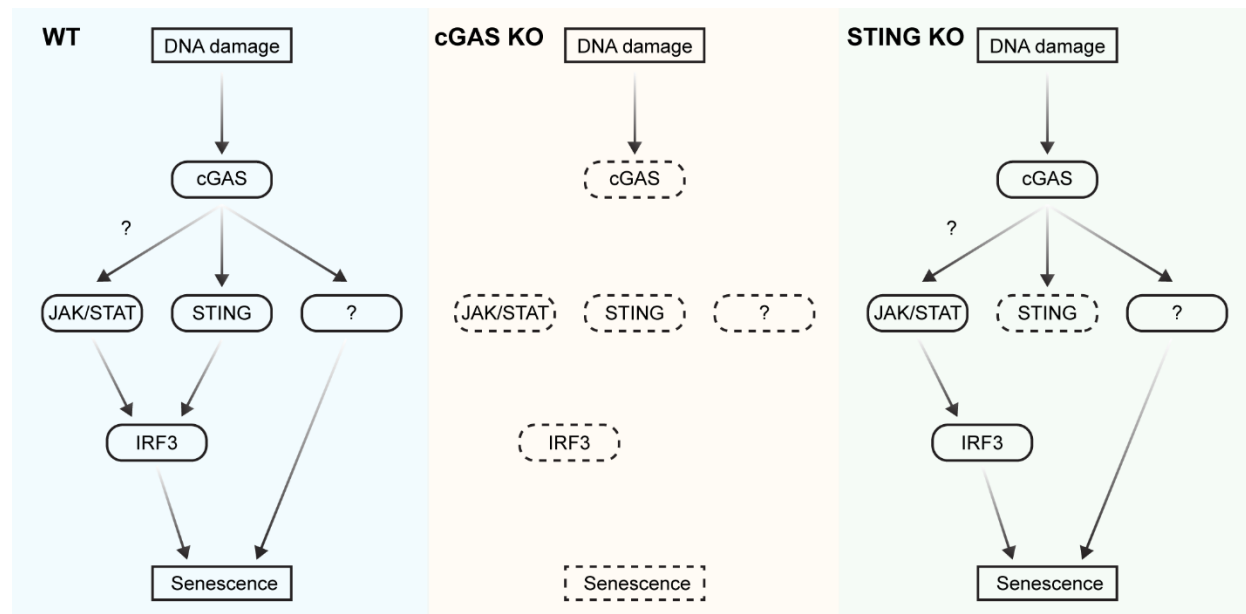


**Figure 25. cGAS can induce DNA damage-induced senescence STING-independently.** Although cGAS has always been recognized as a critical step for DNA damage-induced senescence, STING can sometimes be bypassed. STING-independent mechanisms have not been described, but could involve an interaction between cGAS and JAK/STAT signaling or other pathways.

## 6.5 cGAS/STING signaling regulates metabolic processes during senescence and ageing

Senescence and SASP transcriptional markers are defined by a number of pathways and cellular components. Central nodes within this transcriptional signature include growth hormones, extracellular components and protease inhibitors, among others (Saul et al. 2022). Our data shown that all the above biological processes are transcriptionally impacted by cGAS and STING in killifish. IGBP growth factor family members that increase during irradiation and old age in WT tissues are decreased in both cGAS and STING KO counterparts. During irradiation and ageing, cGAS more than STING appears to potentiate the regulation of a broad range of collagens, laminins, and other cell

adhesion molecules. Finally, in the kidney, proteasomal subunits are downregulated in irradiated and old fish, but significantly less so in the absence of cGAS or STING.

cGAS and STING appear to regulate a number of pathways and cellular components *in vivo*, which are not directly encompassed by senescent signatures. Ribosomal subunits are among the most regulated genes during irradiation and ageing. Ribosomal subunits are significantly decreased in the kidneys during irradiation. Counteracting this decrease, cGAS-deficiency led to higher levels of ribosomal subunits when compared to irradiated WT kidneys. The gut showed the opposite phenotype, where ribosomal subunits are significantly increased both during irradiation and ageing. Interestingly, countering the increase of these subunits, irradiated cGAS-deficient and old cGAS/STING-deficient guts exhibited significantly lower levels of these proteins when compared to WT guts. It appears that regardless of the direction of transcriptional change in senescent and aged tissues, the cGAS/STING pathway is an important modulator of ribosomal subunit expression.

Other pathways not directly related to senescence, yet still modulated by cGAS included and pyrimidine metabolism and aminoacyl-tRNA biosynthesis. These pathways coordinate transcription and translation. The increase in all of these pathways in cGAS KO kidneys and concurrent increase in ribosomal functions, DNA replication, and cell cycle regulators would indicate that these kidney cells are generally more anabolic than their WT counterparts (Biffo, Ruggero, and Santoro 2024). Similarly, STING KO fish exhibited reduced oxidative phosphorylation (OXPHOS), hinting towards decreased catabolism. However, these metabolic modulations could still be an indirect consequence of altered senescence *in vivo*. Senescent cells exhibit a deregulated metabolic profile characterized by concurrently increased anabolic (mTOR) and catabolic (AMPK and GSK3) signaling cascades (Kwon et al. 2019). Hence, cGAS/STING might impact metabolism by modulating senescence both during DNA damage and ageing *in vivo*.

However, the cGAS/STING pathway plays a key role in regulating catabolism beyond its well-known function in TBK1-mediated IFN signaling. STING trafficking can promote LC3 (Gui et al. 2019) and GABARAP (Lv et al. 2024) lipidation, leading to TFEB-driven lysosomal biogenesis (Xu et al. 2024). This suggests that even in the absence of senescence, a deficiency in cGAS/STING could impair autophagy and reduce catabolic activity. As a result, it is tempting to speculate that cGAS/STING signaling sits at the

intersection of DNA damage, senescence, inflammation, but also metabolic changes during aging. Exploring whether cGAS/STING directly influences cellular metabolic state—independently of senescence—could reveal new insights into its broader role in cellular homeostasis and ageing.

## 6.6 Loss of cGAS/STING signaling impacts late-life disease occurrence but does not extend lifespan

In this study, we sought to elucidate the impact of cGAS/STING signaling in organismal ageing. We found that killifish lacking cGAS or STING have diminished expression of senescence-associated genes during DNA damage-induced senescence and natural ageing and have an overall more youthful-like transcriptional profile than age-matched WT counterparts. The reduction of senescence and SASP components is associated with reduced tissue degeneration (Diniz et al. 2021; Boniewska-Bernacka, Panczyszyn, and Klinger 2020), tumor progression (Atala 2015; Coppe et al. 2010), immunosenescence (Stolzing et al. 2008), and increased lifespan (Baker et al. 2011; Baker et al. 2016). Hence, we sought to investigate all above phenotypes in our WT and cGAS/STING mutant killifish by performing demographic and pathophysiological post-mortem analysis.

Our work is the first to perform such a large-scale multi-tissue pathophysiological analysis in killifish providing valuable insight into the ageing physiology of this model organism. We observed that both cGAS KO and STING KO fish showed overall milder tissue pathology related to proliferative non-neoplastic, degenerative, and infectious lesions, consistent with an amelioration of age-related pathology seen in mouse models (Gulen et al. 2023). Our findings are thus in accord with the hypothesis that inhibition of this conserved pathway could temper senescence and inflammaging and extend life span.

Yet surprisingly, neither cGAS KO nor STING KO strains are longer lived than wild type.

This unexpected result suggests that if there are benefits to these age-related changes, they are offset by other factors that limit lifespan and could arise for various

speculative reasons. For example, we found that kidneys from cGAS KO fish showed upregulation of components of the cGAS/STING regulatory cascade, including STING itself and low-grade sterile NF- $\kappa$ B immune signaling, whose chronic activity can be detrimental to tissue physiology (Salminen et al. 2008) and lifespan (Zhang et al. 2013; Kounatidis et al. 2017). It is also possible that absence of cGAS/STING renders fish more susceptible to viral and bacterial infection. This would certainly be true in the wild (Li, Wu, et al. 2013). However, laboratory fish aquaria are largely void of fish-infecting viruses (Matthews 2004). Instead, we generally observed less pathology in the various tissues with decreased cGAS/STING, and somewhat surprisingly, trends to lower levels of infectious pathology rather than non-infectious macrophage infiltration. Perhaps the upregulation of NF- $\kappa$ B signaling or other immune pathways we observed helps ward off such infections. Preprint studies parallel to our own further support that lack of cGAS/STING can increase macrophage infiltration of tissues and even decrease lifespan in mice (Hopkins et al. 2024; Martinez 2024, under review).

Of note, mice have exceptionally high rates for cancer occurrence (>90% at 18-months old) (Zhou, Xia, et al. 2023) and lack of cGAS/STING can be fatal during tumor progression (Hu et al. 2023). In our hands, killifish had very low rates of proliferative lesions, without detectable neoplasias in any tissue under investigation, which could explain the lack of severe drop in lifespan that was observed in the above preprints in cGAS/STING mutant mice.

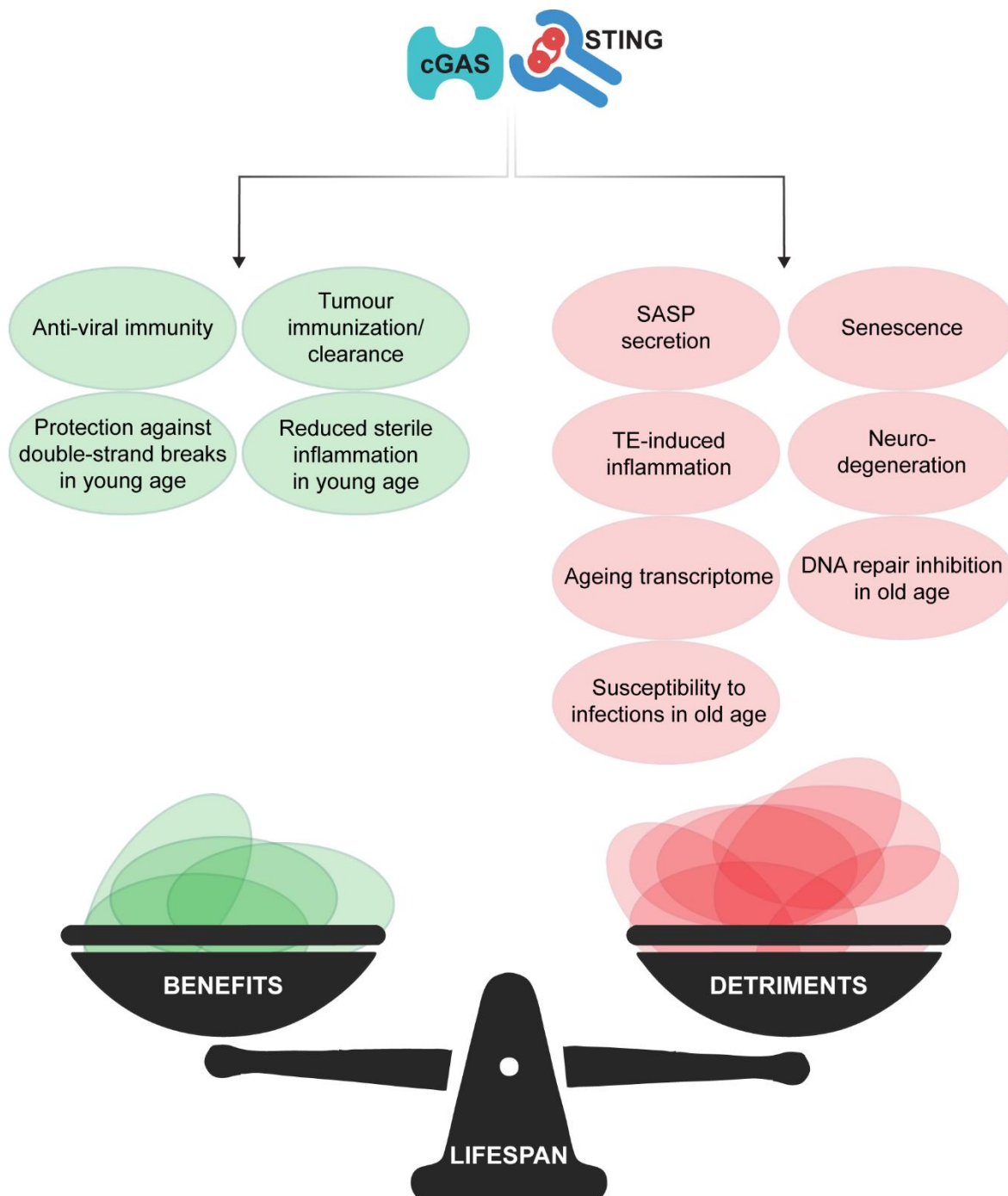


**Figure 26. The cGAS/STING pathway leads to a number of beneficial and detrimental effects balancing out any effects on lifespan.** Other studies have demonstrated that cGAS/STING is important for anti-viral immunity and tumour immunization and clearance and we showed that cGAS also has genoprotective role in young primary fibroblasts and reduced inflammation in young kidneys. On the other hand, cGAS/STING has been reported to drive neurodegeneration and TE-element induced inflammation and we observed more senescence and SASP markers in old tissues with functional cGAS. In addition, abrogation of cGAS/STING dampened age-related

transcriptional signatures, increased DNA repair genes and fish had less infections, hinting towards improved immune function. In killifish, these effects appear to counter each other and lifespan remains unchanged.

It is also possible that the beneficial effects of cGAS/STING inhibition are limited only to specific tissues, which might not have an overall impact on organismal life span. For example, we observed that amelioration of most age-related transcriptional events in the cGAS KO was more pronounced in the kidney, and not as prominent in the intestine. On the other hand, cGAS KO appeared to more greatly attenuate the regulation of senescent genes in the aged intestine. In addition, cGAS and STING KO mostly effected disease occurrence in the kidneys and gonads, with a smaller effect on other tissues. Different tissues develop varying degrees of DNA damage (Wang et al. 2012), senescent load (Yousefzadeh et al. 2020) and immune activation (Tabula Muris 2020) with age, potentially deploying the cGAS/STING pathway to varying degrees. At the same time, senescence and SASP can also offer protective roles (Gorgoulis et al. 2019; Huang et al. 2022) and even stimulate proliferation (Coppe et al. 2010). Hence their deregulation might also carry adverse effects. Along similar lines, timing may also be important; lifelong attenuation of such a core signaling cascade might lead to deficient transcriptional responses to stress that counteract the ameliorated ageing transcriptome. Further study of the physiological impact of cGAS/STING across tissues may address these questions in the future.

## 6.7 Scientific advancements and limitations

The discovery of cGAS and the characterization of the cGAS/STING pathway took place just a decade ago. Over this period, numerous studies have highlighted the critical role of this pathway in regulating various hallmarks of aging. cGAS/STING signaling is important for the establishment of senescence, influences and responds to genomic instability, drives the expression of inflammaging markers, and contributes to age-related neurodegeneration. In this work, we aimed to directly assess the impact of cGAS and STING on different aging tissues and organismal lifespan. Towards that aim, we

concomitantly generated an array of datasets that provide a valuable resource for studies even beyond the scope of the cGAS/STING pathway.

We are the first to perform deep RNA sequencing analysis of young and old killifish kidneys and guts. These data provide valuable insights for studies in areas such as age-related kidney diseases and gut dysbiosis, using the killifish as a model organism. In parallel, we conducted transcriptomic analysis of these tissues following DNA damage-induced senescence, creating an essential resource for examining tissue-specific nuances in senescent expression profiles *in vivo*. Additionally, we are the first to characterize multiple late-life-onset morbidities across a broad range of solid tissues in killifish, further advancing our understanding of their rapid aging physiology.

Regarding the cGAS/STING pathway, we found that its role in regulating senescence is conserved in killifish both *in vitro* and *in vivo*. cGAS deficiency led to increased DNA damage in primary fibroblasts and elevated levels of NF- $\kappa$ B signaling, as well as lysosomal and apoptotic regulators in young kidneys. During aging, the absence of cGAS more than STING attenuated the age-related transcriptional regulation. The impact of this pathway was more pronounced in the kidney compared to the gut, with cGAS deficiency exerting a stronger effect than STING deficiency, suggesting cGAS-specific functions. Consistent with the improved age-related transcriptome, late-life-onset diseases were less frequent in cGAS/STING mutants, with STING KO fish showing significantly lower infection rates in the gonads. However, despite these benefits, neither cGAS nor STING KO killifish exhibited increased lifespan, with STING KO fish tending to have shorter lifespans. Our findings suggest a potential tradeoff, where inhibition of the cGAS/STING pathway mitigates age-related molecular signatures but promotes genomic instability and sterile inflammation, ultimately offsetting any positive effects on lifespan.

Our study also has several limitations. RNA-seq data were obtained exclusively from male killifish. Given the well-documented differences in physiology, immunity, and metabolism between sexes, and the broad influence of cGAS, sex-specific effects cannot be ruled out. Additionally, the killifish model was invaluable for studying the pathway in the context of normative aging physiology, due to being largely void of tumors and viral infections. However, in humans, aging is often accompanied by these factors, albeit less frequently than in mice. For a more translational approach, it would be valuable to investigate whether the beneficial effects we observed can be replicated through partial



reduction of cGAS/STING activity, rather than complete knockout to prevent cancer and virus-induced mortality.

Given the broad influence of cGAS/STING on the aging transcriptome, we anticipated that the effect on late-life-onset diseases would be stronger. Yet, apart from infectious diseases, our numbers generally lacked the power to conclusively demonstrate the impact of cGAS/STING signaling on their occurrence. Notably, the killifish in our hands exhibited low rates of degenerative, proliferative or non-infectious diseases but importantly, cGAS/STING did not drastically affect their occurrence. Collectively, our data provide a valuable foundation for the pathophysiological analysis of naturally aged killifish, guiding future cGAS/STING-dependent or -independent studies toward more targeted, data-driven power analysis and investigations.

Lastly, given the limited information on the *in vivo* role of cGAS/STING in aging physiology, our study prioritized deep transcriptomic analysis to provide a comprehensive overview of tissue biology. Future histological analysis will help determine whether the observed changes stem from altered DNA damage, senescent load or modifications in pathway wiring.

## 7. Future perspectives

### 7.1 Investigating the physiology of aged cGAS/STING KO killifish

Our results deliver an in-depth summary of the transcriptome of two tissues in aged WT and cGAS/STING mutant killifish. We observed a widespread attenuation of transcriptional signatures of ageing, involving pathways related to cell replication/senescence, SASP/inflammaging components, ribosomal subunits and DNA damage repair among others. Necropsy analysis revealed a trend for increased sterile macrophage infiltration, but decreased tissue-degenerative and infection rates. To understand how the transcriptome relates to the observed pathophysiologies it is important to understand the physiology of the tissues in old animals.

To that end, we plan to make use of the transcriptome as our basis to design data-driven histological analyses. Since a number of senescent markers are affected, we will begin by performing SA- $\beta$ -gal staining on young and old WT and cGAS/STING mutants. Killifish senescence studies have found increased SA- $\beta$ -gal staining in the old dermis (Genade et al. 2005), heart (Ahuja et al. 2019), optic nerve and retina (Vanhunsel et al. 2021). Our data suggest that the gut, more than the kidneys, may exhibit increased senescence in old age and that this senescence is reduced in the cGAS KO tissues more than in STING KO. This experiment adds to the transcriptional data and to our understanding the cGAS/STING pathway plays in senescence, allowing us to pinpoint specific cell types and regions affected most.

Irreversible cell cycle arrest is a hallmark of cellular senescence (Hernandez-Segura, Nehme, and Demaria 2018) and our RNAseq analyses revealed a strong positive regulation of cell proliferation markers increasing in old cGAS mutants. Therefore, complementing the identification of senescent cells, we will also stain for cell proliferation markers. A common way to investigate cell proliferation involves injection of EdU (5-Ethynyl-2'-deoxyuridine), a thymidine analog that incorporates into DNA during active replication. After injection, dividing cells take up EdU. Staining uses a click chemistry reaction with fluorescent azide, allowing visualization and quantification of proliferating cells under a microscope. Subsequently, killifish studies also employ staining against PCNA (Proliferating cell nuclear antigen) (Tozzini et al. 2012), a protein

involved in DNA replication and repair. It marks cells in the S-phase, highlighting proliferating cells.

Senescence and the secreted extracellular matrix components within the SASP significantly impact fibrosis within tissues (Yousefzadeh et al. 2021; Campbell et al. 2021; Zhang et al. 2015). Consistently, a wide array of collagens, laminins, and other cell adhesion molecules had largely muted age-dependent regulation in irradiated and old cGAS KO fish. Increased fibrosis negatively impacts function and mechanobiology of ageing tissues (Selman and Pardo 2021) and reduced cGAS/STING signaling could ameliorate this phenotype. To investigate fibrosis, we will employ Sirius Red/Fast Green staining. Sirius Red/Fast Green staining differentiates collagen and non-collagenous proteins in tissue samples. Sirius Red binds to collagen fibers, appearing red, while Fast Green stains other proteins, appearing green. This dual staining allows for the quantification of collagen relative to total protein content, commonly used in fibrosis and extracellular matrix studies (Segnani et al. 2015).

Our data suggest that lack of cGAS leads to increased DNA damage, but decreased senescence. Decreased senescence could be due to fewer cells entering senescence or due to increased apoptosis of pre-senescent cells. DNA damage leads to activation of p53 and persistent p53 signaling can shift the balance from senescence-initiation to apoptosis (Chen, Liu, and Merrett 2000). This is especially true in cells with lower expression of the apoptotic-inhibitor p21 (Yosef et al. 2017), which is exactly what we observe in cGAS KO fish. We observed a reduction in tissue degeneration but an increase in macrophage infiltration in tissues of cGAS KO animals. This could be explained by concurrent increases of cell death and proliferation leading to an enhanced cellular turnover within tissues, which maintains tissue homeostasis but triggers macrophage infiltration to remove cell debris. Thus, we aim to investigate cell death in cGAS/STING KO animals. To investigate for cell death, we will perform TUNEL (terminal deoxynucleotidyl transferase dUTP nick end labeling). TUNEL staining works by labeling free 3'-OH ends of fragmented DNA, which manifest during cell death, with fluorescent or chromogenic tags using terminal deoxynucleotidyl transferase (TdT), allowing visualization under a microscope. To differentiate between apoptosis and necroptosis, we will also employ the combined staining for Annexin V and Propidium Iodide (PI). This staining works primarily for flow cytometric analyses. Briefly, we will harvest the kidneys and guts from old WT and

cGAS/STING mutants and then dissociate the tissues into single cell suspensions using the tissue dissociation method described by Bresciani et al. (Bresciani, Broadbridge, and Liu 2018). The single cell suspension will then be incubated with Annexin V and PI. Annexin V binds phosphatidylserine on the outer membrane of apoptotic cells, while PI intercalates with DNA in late apoptotic and necrotic cells with compromised membranes. Then, we will run these cells in a flow cytometric device to retrieve the alive : apoptotic : late-apoptotic/necrotic cell ratio.

Another key feature in need of further investigation is inflammaging. Senescent cell accumulation and SASP are largely attributed to cause inflammaging (Franceschi et al. 2018; Li et al. 2023). However, inflammaging is primarily characterized by the increase of circulating immune markers in the blood (Ferrucci and Fabbri 2018). Since we observe a reduction in senescent markers in old cGAS/STING mutants, circulating pro-inflammatory molecules might also decrease. We aim to employ two independent methods to explore the above. In both cases, we aim to purify the protein content from old WT and cGAS/STING plasma. Then we will perform plasma proteomics in an attempt to identify immune markers as well as tissue-specific secreted proteins that define ageing in different organs (Oh et al. 2023). Due to the inherently low abundance of the immune markers in plasma proteomics however, we also will perform Western Blot and ELISA techniques to identify common circulating inflammaging markers (IL-1, IL-6, IL-8, IL-13, IL-18, IFN $\alpha$ , IFN $\beta$ , TGF- $\beta$ ) (Ferrucci and Fabbri 2018).

Lastly, although we observed a trend for increased immune infiltration in our histopathology of naturally deceased fish, we do not know if this is an old-age feature or a late-life disease feature. Supporting the former, two independent pre-prints show that cGAS (Martinez et al. 2024) and STING KO (Hopkins et al. 2024) mice have increased numbers of infiltrating cells in old tissues compared to WT counterparts. It would be interesting to see if these observations are conserved in teleosts. To stain for inflammatory cell infiltration in fish, researchers have made use of antibodies against the conserved LPC1 (lymphocyte cytosolic protein 1); a hematopoietic-lineage marker (Kell et al. 2018). By staining against LCP1 in old WT and cGAS/STING KO tissues, we will discern if this phenotype is indeed a feature of aged cGAS/STING-deficient killifish. Also, since we observe an increase in inflammatory markers in the young kidney

transcriptome, we will also stain young WT and cGAS/STING KO tissues to investigate if there is an early-life onset immune-infiltration in cGAS/STING mutants.

The above histological and flow cytometry analyses will provide us a wide array of physiological parameters in the tissues from aged mutant fish that will either complement our transcriptomic analyses or raise new questions. Collectively, we will observe senescence, proliferation, fibrosis, cell death (and the type of cell death employed), inflammaging and immune infiltration in the old mutant tissues.

## 7.2 Elucidating the mechanism behind cGAS-mediated genomic stability or instability

In the current study, we showed that cGAS-deficiency leads to increased  $\gamma$ H2AX signaling at both basal levels and after genotoxic stress in primary fibroblasts. Different studies have claimed either genoprotective (Zhen et al. 2023; Martinez et al. 2024; Chen et al. 2020; Li et al. 2022) or genotoxic (Liu et al. 2018; Jiang et al. 2019) effects of cGAS. The genotoxic effects are demonstrated as reduced homologous recombination after DNA damage or during overexpression of cGAS. Genoprotective effects include cGAS impact on retrotransposable element expression, retarding of replication forks and prevention of chromosome end-joining. All studies showed that these effects were STING-independent and were performed on cell cultures or primary cell lines.

Our data have shown that lack of cGAS increases the expression of a number of DNA repair pathways in old age, including homologous recombination (HR). But in primary fibroblasts cGAS-deficiency also caused increased  $\gamma$ H2AX signaling both at basal level and post-irradiation. The observed increase in HR along with other DNA repair pathways might be due to loss of cGAS-mediated inhibition or it could be a compensatory increase due to increased DNA damage. To investigate these possibilities, we now want to study DNA damage *in vivo*. Firstly, we plan to investigate the tissues of WT and cGAS KO fish by staining for  $\gamma$ H2AX (double strand breaks) and RAD51 (DNA repair). We will also dissociate the tissues into single-cell suspension and perform comet assay to investigate DNA fragmentation. We aim to do this experiment both under basal

conditions and within minutes post-irradiation to see whether cGAS confers stability to the genome *in vivo*.

The above experiments, combined with existing knowledge, will help elucidate the mechanism underlying cGAS-mediated genomic stability. If cGAS is genotoxic *in vivo* and we observe decreased fragmentation of genomic DNA in cGAS KO tissues, then this indeed could be caused by cGAS impairing homologous recombination systems, and the upregulation of its components might reflect a compensatory mechanism. If cGAS is genoprotective *in vivo* and we continue to see increased DNA damage in cGAS KO tissues at both basal level and within minutes after irradiation, then this is likely not due to retrotransposable elements, chromosome end-joining or replication forks. In that case, we suspect that the effect of cGAS on chromatin organization itself might confer its protective role. Indeed, one of the above studies observed increased chromatin accessibility in cGAS KO cells (Martinez et al. 2024). Heterochromatin might prevent certain DNA repair mechanisms (Wu, Qu, and Liu 2024), but it also confers genomic stability (Schumacher et al. 2021; Fortuny et al. 2021).

### 7.3 Uncoupling nuclear and cytosolic function of cGAS - finding putative balance between DNA damage and inflammaging

All above studies related to cGAS and genomic stability attribute their findings to nuclear, rather than cytoplasmic, cGAS. Nuclear cGAS is enzymatically inactive due to the repurposing or inaccessibility of its DNA-binding regions and blocked dimerization (Kujirai et al. 2020), and thus does not initiate downstream inflammatory signaling (Gentili et al. 2019). Our work demonstrated that in young fish, the absence of basal cGAS expression results in constitutive low-grade inflammation and a slight increase in double-strand breaks in primary fibroblasts. This suggests a detrimental impact of cGAS deficiency on cellular physiology in early life. Conversely, in aged fish, cGAS deficiency is associated with reduced senescence, SASP, and other aging markers, along with lower rates of infection and tissue pathology. These findings highlight the dual nature of cGAS: nuclear cGAS may provide a protective role in maintaining genomic stability, while

cytoplasmic cGAS appears to promote senescence, SASP, and contribute to inflammaging and immunosenescence.

No study to date has investigated cGAS localization in tissues during normative ageing. DNA damage generally accumulates with age (Schumacher et al. 2021) and cGAS translocates to the nucleus during DNA damage (Liu et al. 2018), therefore cGAS is suspected to show increased nuclear localization with age. However, nuclear cGAS is not immunostimulatory (Gentili et al. 2019) and during ageing we observed reduced pro-inflammatory SASP marker expression in cGAS KO tissues. We speculate there might be an imbalance in cGAS shuttling with age. Therefore, we plan to perform immunohistochemistry or -fluorescence against endogenous cGAS in different tissues in young and old WT organisms. This would be straightforward using mouse tissues. But, in killifish we will first need to generate antibodies against killifish cGAS or CRISPR knock-in a tag in the endogenous cGAS protein. The former being the safest option with regards to cGAS folding and localization.

Whether cGAS localization shifts during ageing or not, it would still be interesting to investigate the physiological impact of these different modes. We first plan to generate nuclear-localized and cytoplasmic-localized mutants of the cGAS protein and investigate the impact on genomic stability in each case. Due to lack of cross-reacting antibodies for killifish cGAS, we will first investigate this effect in human cells. A valuable model for the initial *in vitro* investigation is the HEK293T cell line which is a non-cancer immortalized cell line that is naturally cGAS-muted (Sun et al. 2013). We mentioned that cGAS has two putative nuclear localization signals (NLSs) and one nuclear export sequence (NES). However, mutating NLS1 did not affect cGAS localization and mutating NLS2 causes degradation of cGAS (Kim et al. 2023), while mutated NES only affects cGAS localization after DNA damage (Wu et al. 2022; Sun et al. 2021). One strategy we can employ, is to add an additional NLS or NES signal to shift the balance in cGAS localization in the desired direction (Lu et al. 2021).

Since overexpression of cGAS has been shown to increase DNA fragmentation, it would be more informative to use CRISPR knock-in of above cGAS mutants. Using lentiviral delivery systems, we can CRISPR knock-in expression cassettes of all above cGAS variants and investigate DNA damage by  $\gamma$ H2AX, RAD51 and comet assay, as well as senescence and SASP expression at basal levels and post-irradiation. Through these

experiments, we will get a first glimpse of the impact of nuclear and cytoplasmic cGAS, but also verify whether our system works well, by immunofluorescence using antibodies against cGAS. By including a tag, along with the NLS or NES signals, we can also perform this experiment in killifish cGAS KO fibroblasts. Using antibodies against the tag, we can investigate whether cGAS shows the desired localization. Collectively, we can more accurately define whether nuclear-bound or cytoplasmic-bound cGAS impact genomic stability as well as senescence and inflammatory SASP expression.

The last step would be to CRISPR the endogenous cGAS gene in killifish in the same manner we generated and verified in our cell culture systems. By investigating the ageing physiology and lifespan of WT, nuclear- and cytoplasmic-cGAS mutant fish, we will further expand our understanding of cGAS function *in vivo*. We also stand to shed more light on the mechanism behind the beneficial and detrimental effects of cGAS. Finally, if indeed one mode of cGAS action is more beneficial than the other during ageing, we can reshape and improve our efforts in developing cGAS targeting drugs, a number of which are already under clinical trials (Li et al. 2021). Such drugs could potentially mask cGAS NLS or NES motifs to shift the balance in the desired direction.

#### 7.4 cGAS/STING regulation of senescence outside DNA damage

In accord with published work, we show that cGAS and STING KO fibroblasts and tissues have decreased DNA damage-induced senescent marker expression when compared to WT fibroblasts. During ageing, we also observe reduced senescent marker expression, which could also derive from DNA damage accumulating during ageing. Senescence, however, can also be initiated by natural factors beyond DNA damage, such as during development (Storer et al. 2013) and wound healing in mice (Demaria et al. 2014). In line with wound healing in mammals, fin amputation in zebrafish leads to increased senescence in the regenerating region and senolytic treatment results in severely impaired regeneration (Da Silva-Alvarez et al. 2020). Since killifish are also able to regenerate amputated fins, it would be interesting to investigate senescence initiation and fin regeneration in cGAS/STING KO organisms.



Towards that aim, we already investigated the regeneration of fins in young male killifish. Briefly, we clipped the fins of young (65 days old) male fish and 5 days later, we sacrificed the fish and obtained their entire fins for  $\beta$ -gal staining and regeneration measurement. Since male GRZ killifish fins are heavily pigmented, we first bleached the fins using 3%  $H_2O_2$  at 55 degrees for 1h. Then proceeded to stain for  $\beta$ -gal staining according to the kit's instructions (Cell Signaling #9860). Surprisingly, the cGAS KO regenerating fins had equal  $\beta$ -gal staining as WT fins (Figure XXa, b). This is the first time any study has observed the same or even a trend for increased  $\beta$ -gal staining in cGAS KO cells. The study in zebrafish noted that different regions of the fin regenerate at different rates (Da Silva-Alvarez et al. 2020), so we separated the regenerating regions into 3 equal parts for each fin and measured regeneration in each part separately. cGAS KO fins appeared to regenerate as well as WT fins and in the inner part of the fin, they actually tended to regenerate faster (Figure XXc).

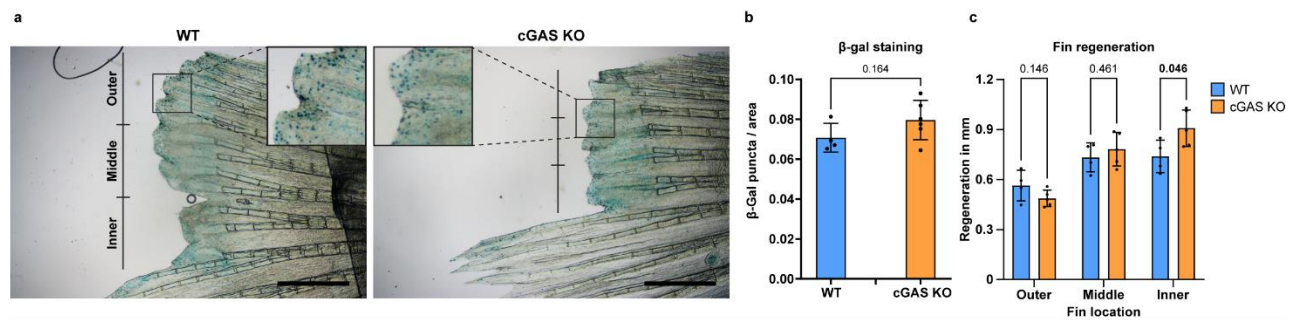


**Figure XX. Loss of cGAS does not decrease senescence during wound healing-induced senescence.** **a**,  $\beta$ -gal staining of WT and cGAS KO regenerating fins 5 days after amputation. The length of the regenerating fin is divided into 3 equal parts, namely inner, middle and outer regenerating region. Scale bar = 1mm. **b**,  $\beta$ -gal staining puncta normalized to regenerating area in WT and cGAS KO fins. Student's t-test was performed for statistical analysis. **c**, Regeneration measured in the center of each region (inner, middle and outer) of regenerating fin in WT and cGAS KO fish. Student's t-test was performed for statistical analysis. WT fins n = 4, cGAS KO fins n = 5.

In mammals (Gao et al. 2024) and teleosts (Nguyen-Chi et al. 2015), during wound healing, monocytes migrate to the wounded area where they initially differentiate into M1 (pro-inflammatory) macrophages. M1 macrophages are essential in the initial phase after wounding, since they fight off infections and promote angiogenesis and fibroplasia.

After the initial phase, however, macrophages need to transition to their M2 (anti-inflammatory) type, where they stimulate proliferation of keratinocytes and fibroblasts. If the transition between M1 and M2 happens too early or too late, human injuries have poorly healing outcomes (Alhamdi et al. 2019). cGAS activity has been shown to polarize macrophages towards the pro-inflammatory M1 state and cGAS-deficiency alleviated sepsis-induced acute lung injury in mice (Shen et al. 2023). Therefore, it is tempting to speculate that cGAS not only does not impair wound healing-induced senescence, but it might also reduce the regenerative capacity in favor of increased immunity.

The above hypothesis has significant translational potential, but it must be carefully investigated. Teleosts have an exceptional regenerative capacity that goes beyond fin regeneration. Killifish can also regenerate heart (Wang et al. 2020) and brain (Van Houcke et al. 2021) after injury. By inducing different types of injuries, we intend to investigate whether cGAS KO positively or negatively impacts regeneration in different tissues. However, due to the enhanced regeneration in teleosts, the impact of cGAS on wound healing might lack conservation in mammals. Thus, it would be important to test skin wound healing in cGAS KO mice as well. If the phenotype is conserved, cGAS or cGAMP modulators might hold promise for skin and tissue regeneration in human injuries. If the features are not conserved, then differences in cGAS activity or mode of action could be one of the evolutionary diversions that led to reduced mammalian regenerative capacity in favor of other immune responses.

If the above data are replicable and there is an impact on tissue regeneration, it would be important to get a deeper understanding of the mechanism behind this. One approach would be to dissociate the regenerating fin and perform scRNAseq. This way, we will be able to investigate the population dynamics of monocytes as well as senescent and proliferating mesenchymal cells within the blastema (apical epithelial cap of regenerating region).

## 7.5 Deciphering tissue-specific effects of cGAS/STING activity

In the current work, we demonstrated that lack of cGAS leads to a higher degree of transcriptional regulation in the kidney compared to the gut, even though the gut

displayed a clearer age-related senescence signature. In addition, our pathophysiology only showed a significant impact of STING in ovarian infections. We also know that there is a large discrepancy between tissues on age-related senescence accumulation in mammals, with the intestine exhibiting the highest increase (Yousefzadeh et al. 2020). Different tissues also vary in senescent and immune responsiveness to DNA damage. Five days after 10Gy  $\gamma$ -radiation in killifish, the tissues exhibiting the highest increase in senescent and immune marker expression were the skin and spleen (Figure XX).

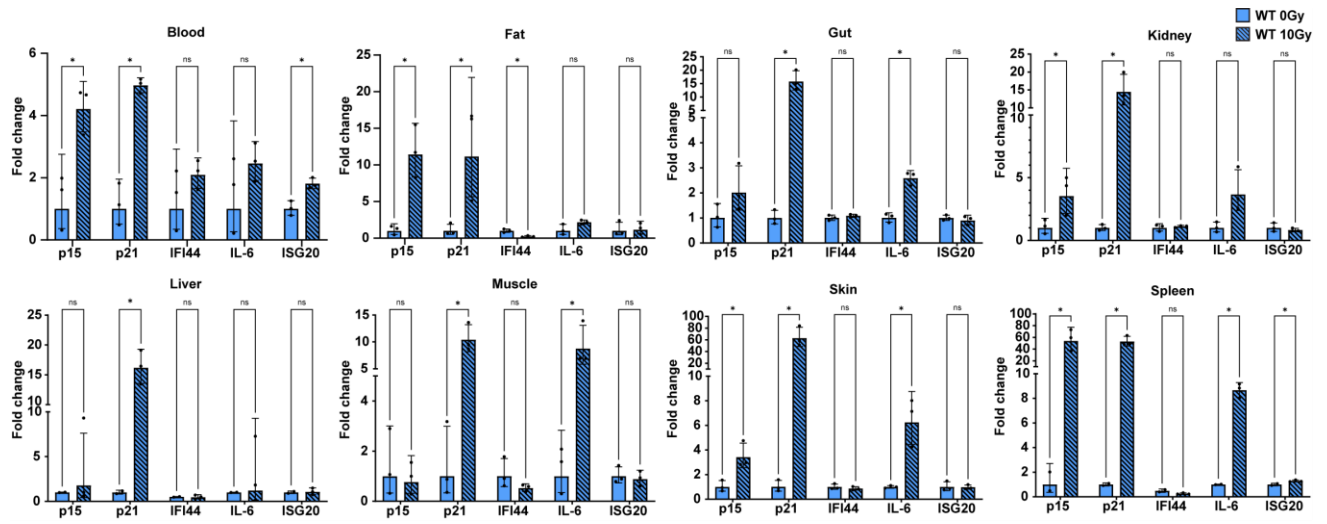


**Figure 28. Senescence and immunity markers vary in expression across different tissues after irradiation.** a, 60 days old WT male killifish were irradiated with 10Gy of  $\gamma$ -radiation and 5 days later their tissues were harvested for RNA extraction and subsequent qPCR. Data represent fold-change expression in non-irradiated and irradiated tissues. In both conditions  $n = 3$  and all tissues derive from the same fish. Student's t-test was performed for statistical analysis with Holm-Šidák correction for multiple comparisons. ns = not significant, \* indicates  $p < 0.05$ .

For a more comprehensive analysis of the impact of cGAS/STING in the ageing physiology, it is important to investigate additional tissues apart from the ones presented in this work. Especially considering that this pathway also causes both beneficial (genoprotection and ageing transcriptome attenuation) and adverse effects (increased basal inflammation in young age, reduced DNA repair with old age and increased infection rates). By understanding the impact on different tissues, we can then address the mechanisms more directly through tissue-specific knock outs of cGAS and STING.

Such an approach presents the opportunity to preserve cGAS function in some tissues and allow anti-viral and anti-tumor effects of cGAS, while reducing deleterious effects where present in other tissues.

## 7.6 Examining time-specific effects of cGAS/STING pathway

Along the same lines as tissue-specificity, the balance between positive and negative effects of cGAS/STING can be time-dependent as well. In young immune systems of cGAS KO fish, we observe increased basal pro-inflammatory levels, as well as lysosomal and apoptotic regulators. On the other hand, in old cGAS-deficient tissues, SASP components and other age-dependent transcriptional signatures are dampened. It is conceivable, that late-life knock-out or inhibition of the cGAS/STING pathway might impact organismal physiology, and potentially lifespan, in a different manner than the one we observed from whole-life deletion.

Lifespan-extending modalities often exhibit a degree of time-dependent efficacy. For example, the longest extension of lifespan from dietary restriction comes from early-life-initiated regimes (Hahn et al. 2019). On the other hand, senolytics such as Dasatinib and Quercetin (Xu et al. 2018) or Fisetin (Yousefzadeh et al. 2018) have only been shown to extend lifespan when administered later in life. Also, while removal of p16 (p16INK4a)-positive cells in adult mice extends lifespan (Baker et al. 2016), p16 knockout mice die prematurely from tumors (Sharpless et al. 2004). Since cGAS/STING also impacts senescence, we hypothesize late-life inhibition might prove more beneficial in organismal physiology and potentially lifespan.

Both tissue-specificity and time-specificity can be achieved by using a Cre-ERT<sup>2</sup> system (Indra et al. 1999). In short, LoxP sites are knocked in within the gene of interest in such a way that they flank the sequence to be deleted. Then a second construct is knocked in, which involves the Cre recombinase fused to ERT<sup>2</sup> downstream of a tissue-specific gene promoter. The ERT<sup>2</sup> fragment keeps Cre inactive in the cytoplasm until recombination is desired. The gene of interest can be irreversibly knocked out of the tissue of interest by administering tamoxifen at any point in the organism's lifespan.

## 7.7 Evaluating sex-specific effects of cGAS/STING pathway

Lifespan and lifespan-extending regimes are frequently divergent between sexes (Austad and Fischer 2016). As noted earlier, a key limitation of our study is that we have only examined the impact of the cGAS/STING pathway in male transcriptomes. While our lifespan data suggest a potential reduction in lifespan in male STING KO fish, the sample size is insufficient to detect subtle, sex-specific differences with statistical confidence. To gain a holistic understanding of the pathway's role in organismal and aging physiology, both our transcriptomic analyses and all above-mentioned future experimental directions need to encompass both sexes.

## 8. Material and methods

### Fish husbandry

All experiments were performed on adult (young, aged 7-8 weeks; and old, aged 18-19 weeks) African turquoise killifish *N. furzeri* laboratory strain GRZ-AD. Adult fish were housed singularly in 2.8 L tanks from the second week of life. Water parameters were pH 7–8, kH 3–5 and temperature of 27.5°C. The system was automatically replenished with 10% fresh water daily. Fish were raised in 12 h of light and 12 h of darkness and fed with 10 mg of dry pellet (BioMar INICIO Plus G) and Premium Artemia Coppins twice a day, with total amount of daily food delivered equivalent to 2 – 3% of fish body weight. The first feeding occurred at 8:30, the second at 13:30. For breeding, 3 female fish and one male fish were housed in a 9.5 L breeder tank and a plastic container with autoclaved sand was placed at 8:00am. At 12:00 noon, the sand box was collected, the sand is rinsed through a mesh and the eggs are collected into a petri dish with 100 µL/L methylene blue (Sigma-Aldrich, # M9140) in sterilized aquarium system water. Eggs are kept at 28 °C dry incubator for 3 weeks until eggs reach diapause III. Water is replaced and dead eggs are removed daily while eggs remain within methylene blue tank water. After this period, eggs are transferred on top of Whatman paper, soaked with autoclaved 1 g/L Humic acid (Roth, #7821.1) in system water. When the eye of the fish has completely developed (~1 week later), eggs are placed in a 1 L plastic container connected with a bubbling system (pressurized air released by needle-size holes from otherwise closed plastic tubes). The hatching medium is 20°C autoclaved 1 g/L Humic acid in system water for hatching. The next day after hatching, and every following day, half of the water is replaced by autoclaved system water without Humic acid. Seven days after hatching, fries are transferred to the system housed as 4 fries per 0.8 L tank equipped with 400 µm fry screen. Finally, seven days afterwards the fish are housed singularly in 2.8 L tanks as described above.

For tissue collection, fish were euthanized by rapid chilling using the setting described in **Figure 29**. When the water temperature reaches 1-2°C fish are quickly transferred from normal system temperature water into the tank containing chilled water, ensuring complete immersion. After 10 seconds, signs of life cease due to the

abrupt decrease in temperature and resulting reduction of blood flow to the brain. After opercular movements stop, fish remain in the cold water for an additional 10 minutes (for adults) or 20 minutes (for hatchlings 5-6 days post hatching). Temperature is monitored throughout the procedure and more ice is added if necessary to keep temperature at 1-2°C.

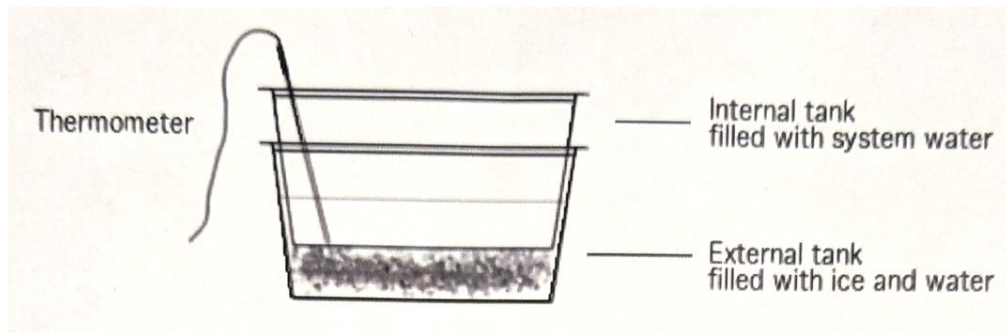


**Figure 29. Setting required for rapid chilling euthanasia.** A tank containing aquarium systems water is placed inside another tank containing 5:1 (v/v) ice : water. Alternatively, a perforated container or mesh sieve may be placed directly into a tank containing ice and system water. A thermometer is placed inside the top tank containing systems water only.

Tissues were quickly dissected, snap-frozen in liquid nitrogen and stored at  $-80^{\circ}\text{C}$ . For irradiation experiments, fish from each genotype were taken out of the system at 15:00 (after both feeding times are complete) and pooled together in a 5 L tank, irradiated with 15 Gy of  $\gamma$ -radiation in a Biobeam 8000 device ( $\sim 4\text{-}5$  min for 15Gy), and then returned to single housed tanks. Five days post irradiation, fish were sacrificed at 15:00 for tissue collection. Animal experiments were conducted in accordance with relevant guidelines and approved by 'Landesamt für Natur, Umwelt und Verbraucherschutz Nordrhein-Westfalen' under license number 2023.A109.

### Generation of cGAS KO and STING KO lines

CRISPR/Cas9 genome editing was performed as described previously (Harel, Valenzano, and Brunet 2016). All the single guide RNAs (sgRNAs) were designed based on the CHOP-CHOP web-based tool (<https://chopchop.cbu.uib.no>). Alt-R S.p. HiFi Cas9 Nuclease and the Alt-R sgRNA were purchased from IDT (see **Table 1** for sgRNA sequences).

**Table 1. sgRNAs used for CRISPR/Cas9 in killifish.**

Name	Sequence 5' -> 3'
sgRNA targeting cGAS	AAGGCTCCATTGTCGTCGAAAGG
sgRNA targeting upstream STING	AGTTTAGGCAATTCCCCCGAGG
sgRNA targeting downstream STING	TGTCAGGCATCTGCGAGGGGAGG

One-cell-stage embryos were injected with 1 – 2 nl of injection solution containing Cas9 enzyme (200 ng  $\mu\text{l}^{-1}$ ), sgRNA (20 ng  $\mu\text{l}^{-1}$ ), KCl (0.2 M) and 1% phenol red. Injection solution can be used directly or stored at  $-80^{\circ}\text{C}$  for future injections. The F0 generation was genotyped by fin-clipping to identify potential founders, which were then backcrossed with the GRZ-AD strain for at least four generations to remove potential off-target mutations induced by CRISPR editing.

For fin clipping, fish are removed from the system and anaesthetized in a container with 0.15 g/l MS222 (tricaine dissolved in aquarium water) (Sigma-Aldrich, # E10521). In about 5-10 minutes, the fish stops swimming, the muscle movements are significantly reduced and it no longer shows any motor reflexes. Then the fish is completely anaesthetized. The fish is then gently placed on a tray and a small section (approx. 2 mm<sup>2</sup>) of the caudal or anal fin is quickly cut off with a blade. This procedure needs to take place quickly and in no more than 30 seconds. The fish are then immediately returned to the fish holding system, where they are observed until they have fully recovered from the anesthetic. The fish are inspected every day for 2 days after fin clipping. If an animal reaches a termination criterion, the fish is euthanized immediately. The fin is placed in a 1.5 mL Eppendorf and quickly placed in ice. Within 1h DNA extraction takes place.

For DNA extraction the fin biopsy is submersed in 20  $\mu\text{L}$  of 25mM NaOH, 0.2mM EDTA (stored at room temperature). The Eppendorf is placed in a  $90^{\circ}\text{C}$  heatblock for 20 min. Then, the Eppendorf is returned in ice and 20  $\mu\text{L}$  of 1 M Tris-HCL pH 5.5 are added and then the tube is spined at 10.000 g for 1 min to pellet tissue debris. The aqueous phase can be used directly as template for genotyping PCR reactions.



**Table 2. Genotyping PCR solutions and reactions.**

PCR reagents		PCR cycles		
DreamTaq PCR Master Mix (2X) (Thermo Scientific, #K1081)	25 uL	95°C	3 min	1 cycle
Forward primer	1 uM	95°C	30 s	30 cycles
Reverse primer	1 uM	57°C (all genotyping primer sets)	30 s	
Template	2 uL	72°C	40 s (all genotyping primer sets)	
Nuclease free water	21 uL	72°C	5 min	1 cycle
		4°C	Hold	Hold

**Table 3. Genotyping PCR primer sets.**

Name	Forward	Reverse	Notes
cGAS KO genotyping	GTTAAGGAACCCCTTCG CACT	TTGCCGTCATCTCCCATTCT G	Used for genotyping cGAS mutant fish
STING KO 1 genotyping	TTTCTGCGTAACCACAT CCCC	GAGGGGAAGTCCAGAAACCA C	Used for genotyping STING upstream mutation
STING KO 2 genotyping	GCAGCAGAGACATGGG GATG	AAACTCAGACCTAAAGCAGA ACCTC	Used for genotyping STING downstream mutation

**Establishment of killifish fin fibroblast primary cell cultures**

Killifish primary fibroblasts were established as described by Astre et al. (Astre et al. 2023) with modifications. Specifically, 10-week-old male WT, cGAS KO and STING KO killifish were sacrificed by rapid chilling and their caudal fin excised, washed twice with Dulbecco's PBS (DPBS, Gibco), and then transferred under a sterile laminar flow hood for subsequent procedures. The fins were washed another two times with sterile DPBS, and then disinfected for 10 min with 25 ppm iodine solution (PVP-I, Sigma-Aldrich) in DPBS. The fins were then washed once with DPBS and the samples further sterilized for 2 h in antibiotic solution with Gentamicin (50ug/ml Gibco) and Primocin® (50ug/ml InvivoGen) in DPBS at room temperature. The fins were then washed again with DPBS and then digested for 20 min in Collagenase P solution (1mg/ml, Merck Millipore) in Leibovitz's L-15 medium, 2 mM L-glutamine (Gibco). Without washing, the fins were transferred to cell culture plates where they were cut into small pieces using sterile scalpels. The tissues were left on the plate with covers open under the hood for 10 minutes, allowing the digestion solution to evaporate and tissues to adhere to the plate. Plates were then filled with 10 ml L-15 medium supplemented with 15% FBS, Gentamycin (50 ug/ml) and Primocin® (50 ug/ml). The plates were carefully washed with DPBS so that the tissues did not detach, and media was refreshed every 4 days. When egress of cells from the tissues became visible, the tissues were removed while the cells were then detached with Trypsin-EDTA 0.05% (Gibco) and passaged onto a new plate. For the first 5 passages, cells were grown in media containing Gentamycin and Primocin (50 ug/ml each), and thereafter grown without antibiotics.

### **Cell culture maintenance**

cGAS KO and STING KO human THP1 monocytes were purchased from Invivogen (THP1-Dual™ KO-cGAS Cells and THP1-Dual™ KO-STING Cells). THP1 cells were cultured under 5% CO<sub>2</sub> at 37°C in RPMI 1640 (Gibco), 4.5 g/L D-Glucose, 2.383 g/L HEPES, 2 mM L-glutamine, 1.5 g/L Sodium Bicarbonate, 110 mg/L Sodium Pyruvate, 50 µM 2-Mercaptoethanol (Gibco), 20% (v/v) heat-inactivated fetal bovine serum (FBS; 30 min at 56°C for heat inactivation). Killifish fin fibroblasts were cultured in a humidified 28°C incubator with no addition of CO<sub>2</sub> in Leibovitz's L-15 medium (Gibco), 2 mM L-glutamine, 15% (v/v) fetal bovine serum.

Both human and killifish cells were repeatedly tested for mycoplasma infection using Eurofins Genomics Mycoplasmacheck Service testing for all mycoplasma species listed in the European Pharmacopoeia 2.6.7.

### **Primary cell culture irradiation and senescence-associated $\beta$ -galactosidase staining**

Killifish primary cells were irradiated with 10 Gy of  $\gamma$ -radiation in a Biobeam 8000 device 24h after the last passage, while still in the medium-filled plate. The time the cells are kept outside the 28°C incubator in total should not exceed 20 min (irradiation of 10Gy requires ~3-4 min). For senescence-associated  $\beta$ -galactosidase staining, cells were fixed and stained nine days post-irradiation using the Senescence  $\beta$ -Galactosidase Staining Kit (Cell Signaling #9860) according to the manufacturer's instructions. Images of the cells were taken using an EVOS FL Auto 2 microscope and analyzed with the EVOS FL Auto 2 Cell Imaging System software. Imaging took place using true color camera under bright field (Trans mode) at 4X magnification. Since after 9-days within the same well, cells reach homogeneity within the wells, so one image was taken at the center of all wells within the plates used (3 wells per genotype per condition per biological replicate). Stained and non-stained cells were counted manually using the EVOS FL Auto 2 image analysis tool, which allows marking each cell positive or negative. Percentage of SA- $\beta$ -gal positive to total cells were then calculated for each image. Samples were always blinded to prevent bias.

### **Plasmids**

All plasmids were generated using the pSBbi-GN backbone, designed by Eric Kowarz (Kowarz, Loscher, and Marschalek 2015) (Addgene ID #60517). The kcGAS and kSTING genes were amplified from cDNA (reaction described in **table 4** and primers in **table 5**) obtained from the killifish primary cell cultures using primers with overhangs matching the Gibson Assembly regions on pSBbi-GN. Similarly, the hcGAS and hSTING genes were amplified from WT THP1 (InvivoGen) cDNA (reaction described in **table 4** and primers in **table 5**). The pSBbi-GN vector was linearized with SfiI (NEB), run in 1% agarose gel (TEA buffer with 5 uL Roti® -GelStain) at 60V for 60 min, gel extracted using kit (QIAquick Gel Extraction Kit, Qiagen, #28704) and the linear plasmid backbone was combined with the amplified cDNAs for Gibson Assembly (NEBuilder® HiFi DNA

Assembly, NEB) (reaction described in **table 6**). Gibson Assembly is accomplished by incubation at 50°C for 60 min and then hold-stage at 4°C. All cloning products used in the experiments have been submitted to Addgene (kcGAS: #225274, hcGAS #225275, kcGAS KO #225276, kSTING #225277, hSTING #225278, kSTING KO #225279).

**Table 4. kcGAS, hcGAS, kSTING and hSTING gene amplification PCR solutions and reactions.**

PCR reagents		PCR cycles		
Phusion™ DNA Polymerase (Thermo scientific (#F530))	0.5 uL	98°C	30 s	1 cycle
Forward primer	1 uM	98°C	10 s	30 cycles
Reverse primer	1 uM	57°C (all primer sets)	30 s	
cDNA	20 ng (1uL from 20 ng/uL cDNA)	72°C	50 s (all primer sets)	
5X Phusion™ HF Buffer	10 uL	72°C	5 min	1 cycle
10 mM dNTPs	1 uL	4°C	Hold	Hold
DMSO	1.5 uL			
Nuclease free water	34 uL			

**Table 5. kcGAS, hcGAS, kSTING and hSTING gene amplification primers.**

Name	Forward	Reverse	Notes
kcGAS Gi-As	ctacccaagctggcctctgCG CGTAGCAGTTTCAGCC AA	atccccaagctggcctgacCC CCAGTTTCTACCTGGGA TTCA	Used to clone kcGAS into pSBbi-GN using Gibson Assembly

kSTIN G Gi- As	ctacccaagctggcctctgAC GACACACCGAGATTCTG TC	atccccaagcttggcctgacCT CATCGGTTTCAGGTCGAG G	Used to clone kSTING into pSBbi-GN using Gibson Assembly
hcGAS Gi-As	CTACCCCAAGCTGGCCT CTGCCGCCAGTAGTGCT TGGTTT	atccccaagcttggcctgacTG TATTCTCCAGGATTTAG GGTGAC	Used to clone hcGAS into pSBbi-GN using Gibson Assembly
hSTIN G Gi- As	ctacccaagctggcctctgTC GTCATCATCCAGAGCA GC	atccccaagcttggcctgacCT GCTGGACATTCAGCCAC T	Used to clone hSTING into pSBbi-GN using Gibson Assembly

**Table 6. Gibson assembly reaction volumes.**

Reagent	Amount
Vector	100 ng
Insert	3:1 inster:vector molar count
NEBuilder HiFi DNA Assembly Master Mix	10 uL
Nuclease free water	10 uL – volume of vector and instert

## Cell culture transfections

THP1 cells were transfected using GeneXPlus (ATCC) according to the manufacturer's instructions. Detailed protocol:

### *A. Preparation of the cells for transfection*

The day of transfection:

1. Count and measure cells for density and viability.
2. Plate  $1.0 \times 10^6$  cells per well in 2.0 mL of complete growth medium (RPMI-1640 + 10% FBS + 0.05 mM 2-mercaptoethanol).
3. Incubate cells at 37°C with 5% CO<sub>2</sub>.

### *B. Preparation of the DNA:TransfeX transfection complexes*

1. Warm GeneXPlus, plasmid DNA, and Opti-MEM I Reduced-Serum Medium to room temperature and vortex gently to mix.
2. Pipette 200  $\mu\text{L}$  Opti-MEM I Reduced-Serum Medium into a sterile microcentrifuge tube.
3. Add 1.0  $\mu\text{L}$  (1.0  $\mu\text{g}/\mu\text{L}$ ) plasmid DNA.
4. Mix thoroughly with gently pipetting.
5. Add 3.0  $\mu\text{L}$  GeneXPlus Reagent to the diluted DNA mixture. Note: Do not let the pipette tip or the reagent come into contact with the sides of the plastic tube.
6. Mix GeneXPlus complexes thoroughly using either a vortex or by pipetting briefly.
7. Collect contents at bottom of the tube using a mini-centrifuge.
8. Incubate GeneXPlus:DNA complexes at room temperature for 15 minutes.

#### *C. Addition of DNA:GeneXPlus transfection complexes to the cells*

1. Distribute the complexes to the cells by adding the complexes drop-wise to different areas of the wells.
2. Gently rock the culture vessel back and forth and from side to side to evenly distribute the GeneXPlus:DNA complexes.

#### *D. Post-Transfection Handling*

1. Incubate for 48 hours. Replace transfection medium with fresh complete growth medium every 24 hours post transfection.
2. 48 h after transfection, the cells were split in three equal parts. One part was used for 2',3'-cGAMP measurement, one part was used for RNA extraction and qPCRs and one part was used for flow cytometry to determine transfection efficiency.

### **LC-MS-based targeted metabolomic measurements of cyclic nucleotides**

The method was adapted from our previous work (Annibal et al. 2021). Briefly, cells were extracted using a two-phase extraction method with a mixture of DW:MeOH:CHCl<sub>3</sub> (1:2:2). After centrifugation, the separated upper and lower layers were dried under a vacuum evaporator and stored at  $-80\text{ }^{\circ}\text{C}$  until further analysis. The protein content in the cell pellet was then used for normalization, determined by the Pierce<sup>TM</sup> BCA protein assay kit (Thermo Fisher Scientific).

Compounds were separated using a reversed-phase column (HSS T3 column 1.8  $\mu$ m, 100 mm  $\times$  2.1 mm, Waters) at 40 °C by the Vanquish UHPLC system (ThermoFisher Scientific GmbH, Bremen, Germany) coupled to a triple quadrupole mass spectrometer (TSQ Altis, ThermoFisher Scientific GmbH, Bremen, Germany).

The mobile phases consisted of 1% formic acid in H<sub>2</sub>O (A) and 1% formic acid in ACN (B) with a flow rate of 0.3 mL/min. The gradient was set as follows: 1% B was maintained for 1 min, then ramped up to 15% B over 3 min and reached 50% in an additional 1 min. At min 7, it reached 70% B and was maintained for 1.5 min. The gradient then quickly decreased to 1% B and re-equilibrated for 3 min.

2'3'-cGAMP (m/z 675.67) was quantified using a fragment ion at m/z 476.01 and validated by an ion at m/z 505.9. The signal was calculated by dividing the peak area by an internal standard peak area (adenosine-13C10,15N5-5'-monophosphate, m/z 363.12  $\rightarrow$  m/z 146.08) and further normalized to protein concentration. Data were analyzed using Skyline Version 22.2.0.527.

### **RNA extraction and qPCR analysis**

Killifish tissues were ground in a liquid nitrogen filled mortar using a pestle until completely pulverized. The powder was then thawed in 200  $\mu$ L RLT buffer (QIAGEN) with 1%  $\beta$ -ME v/v on ice. Samples were then centrifuged at 10.000 g for 10 min at 4°C. The supernatant was collected for subsequent RNA extraction.

As non-adherent cells, THP1 cells were collected by centrifugation at 500 g for 4 min at room temperature. The pellet was washed once with DPBS and then snap frozen in liquid nitrogen. The frozen pellets were thawed in 30  $\mu$ L/million cells ( $\sim$ 300  $\mu$ L per confluent flask) RLT buffer (QIAGEN) with 1%  $\beta$ -ME v/v on ice for subsequent RNA extraction.

Nine days post irradiation, killifish fibroblasts on culture dishes were washed with PBS, then 400  $\mu$ L RLT buffer (QIAGEN) with 1%  $\beta$ -ME v/v was added for each 6-well and the plate was kept on ice for 5 min, before the cells were scraped and used for subsequent RNA extraction. 400  $\mu$ L RLT buffer is added to each 6-well

For all above samples in RLT, RNA extraction was performed using the RNeasy Mini kit (QIAGEN) according to the manufacturer's instructions. The optional DNase step

was always performed using the RNase-Free DNase Set kit (QIAGEN) according to the manufacturer's instructions. The concentration and purity of the RNA were measured by NanoDrop. 1 ug of RNA was always used for cDNA synthesis which was generated using iScript (Bio-Rad). qPCR with reverse transcription was performed with Power SYBR Green (Applied Biosystems) on a ViiA 7 Real-Time PCR System (Applied Biosystems) (reaction described in **table 7**, reaction volumes in **table 8** and qPCR primers in **table 9**). Four technical replicates were averaged for each sample per primer reaction. GAPDH for cell cultures and EIF3C for killifish tissues were used as internal controls for killifish samples, GAPDH was used for human THP1 cells. Results were analyzed using Livak  $\Delta\Delta C_t$  after normalizing to internal control.

**Table 7. qPCR reaction**

Stage	Step	Temperature (°C)	Duration	Ramp Rate (°C/s)	Cycles
<b>Hold Stage</b>	Initial Denaturation	50	2:00	1.6	1
<b>PCR Stage</b>	Denaturation	95	10:00	1.6	40
	Annealing	95	0:15	1.6	
	Extension	60	1:00	1.6	
<b>Melt Curve Stage</b>	Denaturation	95	0:15	1.6	1
	Annealing	60	1:00	1.6	
	Melting Curve	95	0:15	0.05	

**Table 8. qPCR reaction volumes in a single well of the 384-well plate.**

cDNA template (1 uL template from 1 ng of RNA)	0.7 ul
Forward primer (10 uM stock)	0.5 ul
Reverse primer (10 uM stock)	0.5 ul



2x Power SYBR Green Master Mix (ABI)	5 ul
ddH2O	3.3 ul
total volume	10 ul

**Table 9. Primers used for qPCR.**

<i>Killifish primer list</i>			
<b>Name</b>	<b>Forward</b>	<b>Reverse</b>	<b>Notes</b>
Eif3c	ggttaccagcagaagcagtc	tgttgaggaatgaagacgacg	Used for qPCR
GAPDH	CGACGATATCAAGAAG GTTGTG	CAAAGATGGAGGAGTGG CAGTC	Used for qPCR
cGAS	GTTTGGCGGGTTTCCTT TTCT	TCTTGACGTGGTAGGAG CAG	Used for qPCR
STING	CCGAACCCTAACCACCA CTT	ACAATGAGCTCAGTAGC CTCC	Used for qPCR
p15 (CDKN 2B)	AGCTGCGGTGAACGGG GTG	GTCGTGCAACGGGGTGG TC	Used for qPCR
p21 (CDKN 1A)	TGCCCTACAGATCCAGC GTC	TTCCGTCTCTGATGTTGT CTC	Used for qPCR
IFI44	CCAGAGATGTGAGTGA GGTC	TGGAACGATGTAGGAGG TGG	Used for qPCR
ISG20	TTACAACACGTCTTCTG AGTCG	ACCTTTCCTCCCAGCCTG TATC	Used for qPCR

<i>Human primer list</i>			
<b>Name</b>	<b>Forward</b>	<b>Reverse</b>	<b>Notes</b>
GAPDH	GAGTCAACGGATTTGG TCGT	GACAAGCTTCCCGTTCTC AG	Used for qPCR
IFNa-all	AATCTCTCCTTTCTCCT G	TCTGACAACCTCCCAGGC ACA	Used for qPCR. Binds to a region common to all IFNa isoforms.

IFNb	CTTCTCCACTACAGCTC TTTCC	GCCAGGAGGTTCTCAAC AAT	Used for qPCR. Binds to IFNb1 cDNA
IFI44	GTGAGCCTGTGAGGTC CAAG	CCTCCCTTAGATTCCCTA TTTGCT	Used for qPCR

## Flow cytometry

THP1 cells were pelleted by centrifugation at 500 g for 4 min, then washed once with DPBS (Gibco) and pelleted again the same way. Cell pellets were resuspended in cold 2% (v/v) FBS in DPBS and passed through a 35 µm nylon mesh cell strainer to obtain single cells. 0.1 µg/mL DAPI was added to each sample and at least 10.000 cells were then immediately recorded using a BD FACSCanto II flow cytometer. THP1 cells were gated by FSC-A/SSC-A followed by gating on singlets by FSC-A/FSC-W and SSC-A/SSC-W. Live singlets were determined by FSC-A/DAPI-A and GFP positive by GFP-A/APC-A. Gates for viability and GFP positive cells were defined based on the expression profiles of unstained/untransfected and FMO controls. Data were analyzed using FloJo software. Briefly, cells were gated based on forward and side scatter and doublets were excluded. Gates for GFP positive cells were adjusted by comparison to untransfected THP1 cells. Gates for DAPI positive cells were adjusted by comparison to samples without DAPI. Compensation between DAPI and GFP was made using samples without DAPI and/or GFP.

## Immunofluorescence

Killifish cells were plated on glass slide chambers (Nunc™ Lab-Tek™ II) where they were allowed to attach for 24 h. Then starting with the 24 h timepoint, the chambers were irradiated with 10 Gy of γ-radiation in a Biobeam 8000 device and then placed back in a humidified 28°C incubator without CO<sub>2</sub> supplementation. The time the cells are kept outside the 28 °C incubator in total should not exceed 20 min (irradiation of 10Gy requires ~3-4 min). After all timepoints were completed (8 h, 4 h, 2 h and non-irradiated 0 h), the slides were processed together at room temperature unless otherwise specified. They were washed with DPBS (Gibco) once and then fixed in freshly prepared 4% (w/v) paraformaldehyde (Sigma-Aldrich) in PBS with adjusted pH 7.2 for 15 min. They were then washed three times with DPBS and permeabilized with 0.5% (v/v) Triton-X100

(Sigma-Aldrich) in DPBS for 10 min. They were washed again 3 times with DPBS and then blocked for 1 h in 8% (v/v) FBS, 0.3% (v/v) Triton-X100 in DPBS. After blocking, primary antibody for  $\gamma$ H2AX (#9718 Cell Signaling) was used at 1:200 dilution in 5% (v/v) FBS, 0.1% (v/v) Triton-X100 in DPBS and incubated at 4°C overnight. The slides were washed three times with DPBS and then incubated for 1 h with Alexa Fluor™ 488-conjugated secondary antibody (#A21206, Invitrogen) diluted 1:1000 in 5% (v/v) FBS, 0.1% (v/v) Triton-X100 in DPBS. The secondary antibody solution was washed off the slides 3 times and the slides were mounted using Fluoromount-G™ with DAPI (Invitrogen). Images were taken under a Leica DMI6000 B microscope at 63X oil-immersion objective, using 360/4 (UV) for DAPI and 480/40 excitation filter with 470/40 and 527/30 suppression filter, respectively. Exposure (~50ms – 500ms for both DAPI and Alexa Fluor™ 488) varied between biological replicates but kept consistent within each replicate. Images were analyzed with FIJI. Specifically, a stringent intensity threshold was set such that only intense and separate puncta were counted. Due to blinding, images with distinct puncta were chosen randomly to set the threshold, which was then applied across all images. After thresholding, only objects with size 1-50 pixels were counted per cell in order to avoid clumps. At least 50 cells per slide were imaged.

### **RNAseq analysis**

Kidneys and guts (stomach and intestine) from cGAS KO as well as kidneys from STING KO fish were collected for RNAseq analysis. The young irradiated and non-irradiated kidneys from STING KO fish were processed in one batch, while all other samples were processed in another. Both WT and KO mutants derived from offspring of heterozygous parents to ensure similar genetic backgrounds. To reduce circadian variability, fish in each batch were killed all at once within 2 h in the early afternoon. Collected tissues were snap-frozen in liquid nitrogen and stored at -80°C. RNA extraction of all samples in each batch was performed at the same time.

Libraries were prepared from 500 ng total RNA. ERCC RNA Spike-In Mix 1 (Thermo Fischer) was added to the samples before library preparation. Enzymatic depletion of ribosomal RNA with the Ribo-Zero Gold rRNA Depletion kit (Illumina) was followed by library preparation with the TruSeq Stranded Total RNA sample preparation kit (Illumina). The depleted RNA was fragmented and reverse transcribed with random hexamer primers, second strand synthesis with dUTPs was followed by A-tailing, adapter

ligation and library amplification (15 cycles). Next, library validation and quantification (Agilent Tape Station) were performed, followed by pooling of equimolar amounts of libraries. The library pools were then quantified using the Peqlab KAPA Library Quantification Kit and the Applied Biosystems 7900HT Sequence Detection System and sequenced on an Illumina NovaSeq6000 sequencing instrument with a PE100 protocol aiming for 50 million clusters per sample.

After removal of residual rRNA and tRNA reads, remaining reads were pseudo aligned to the reference genome (Nfu\_20140520) using Kallisto (v.0.45.0) (Bray et al. 2016) and RSeQC/4.0.0 was used to identify mapping strand (Wang, Wang, and Li 2012). A strand was identified by having more than 60% of reads mapped to it. Cases with less than 60% of reads in each strand were defined as unstranded. Genes with fewer than ten overall reads were removed. After normalization of read counts making use of the standard median ratio for estimation of size factors, pairwise differential gene expression analysis was performed using DESeq2 (v.1.24.0) (Love, Huber, and Anders 2014). The log<sub>2</sub> fold changes were shrunk using approximate posterior estimation for GLM coefficients. Gene Set Enrichment Analysis (GSEA) (Subramanian et al. 2005; Mootha et al. 2003) and Principal Component Analysis (PCA) were performed for all comparisons using Flaski (<https://flaski.age.mpg.de/>).

### **Tissue fixation, H&E staining, and Acid-Fast Bacteria staining**

Fish within the lifespan cohorts were monitored 4 times a day to check for viability. Dead fish were collected, their visceral cavity was opened, and then they were placed in 10% Formalin solution at room temperature. Fish with severe post-mortem autolysis typically due to 16-24 hr between death and detection, were not included in the study. The fish were kept in Formalin until the completion of the lifespan experiment. 141 samples were then submitted for processing and histopathologic evaluation by IDEXX BioAnalytics. Briefly, all fish were paraffin embedded and 4 sections were taken from each fish. After deparaffinization the sections were stained for either H&E or Acid-Fast Bacteria (AFB) staining. The presence or absence of neoplastic, proliferative but non-neoplastic, degenerative, non-infectious inflammatory, and infectious inflammatory lesions were recorded for a routine tissue list including the brain, epidermis, gills, heart, digestive tract (headgut, foregut, midgut, hindgut), kidney, liver, gonads (ovary or testes), skeletal muscle, spinal cord, swim bladder, and vertebral column.

## **Lifespan analysis**

For both cGAS and STING mutants, P0 heterozygous fish were bred to produce the F1 KO fish that were the parents of all F2 fish used in the lifespan. All fish used in the lifespan derived from eggs collected within the span of 10 days. After hatching, larvae were housed together (seven larvae per 1.1 L tank), until they reached 2 weeks of age. Then they were single-housed in 2.8 L tanks for the remaining lifespan. Fish mortality was scored starting at the sixth week, when full sexual maturation was reached. By that time, no fish had detectable abnormalities in body size or swimming and as such no fish were censored from the study. Senescent fish (> 28 weeks) that showed visible signs of stress, lethargy, anorexia, and abnormal swimming behaviors were sacrificed for humane reasons. The age of fish sacrificed for such reasons was recorded as the estimate time of natural death. Survival curves were calculated using the Kaplan–Meier estimator. Statistical significance was calculated by the Mantel Cox log-rank test.

## **9. Acknowledgements**

One sees further by standing on the shoulders of giants. If my research has contributed to advancing our knowledge of biology, it is because of the giants who supported and guided me throughout this endeavor:

First of all, my professor Dr. Adam Antebi has been instrumental in shaping my project and fostering my scientific thinking. He provided a supportive and collaborative environment that allowed me to develop the above project, standing by me through both challenges and successes.

Huge thanks also go to Dr. Roberto Ripa, who also mentored me throughout the entire endeavor. Roberto's daily supervision and insightful scientific discussions were pivotal in both shaping and progressing the project. He has not only been a great teacher but also a close friend.

Special thanks also to my thesis advisory committee members; Dr. Thomas Langer and Dr. Dario Riccardo Valenzano, for their continued support and crucial feedback. It has been a true privilege to have you by my side throughout this journey.

I cannot imagine the past five years of my life without all of my old and new friends: Dr. Raymond Laboy Morales, Dr. Tim Nonninger, Dr. Victoria Eugenia Martinez Miguel, (soon to be Dr.) Klara Schilling, Dr. Alex Zaufel, Dr. Charilaos Giannitsis, Dr. Asterios Arampatzis, (soon to be Dr.) Elissavet Sandaltzopoulou, Athanasios Theocharis, Konstantinos Samaras-Tsakiris, (soon to be Dr.) Konstantinos Tsaridis and, of course, my partner Celina Knippertz. You were all there for me (even though COVID regulations said you should not) and I will always be grateful for it.

I would like to thank the entire A-Team for providing an incredibly pleasant environment to learn and perform science. Special thanks to Dr. Tin Tin Manh Nguyen and Dr. Joachim David Steiner for their contributions to my project. It is important to mention how incredibly grateful I am to the technicians of our lab, especially my dear friend Nadine Hochhard, who provided extensive technical support. Also, many thanks to the former and current administrative members of the lab Dr. Birgit Gerisch, Dr. Orsolya Symmons, and especially Dr. Sarah Kreuz who also helped review my thesis and manuscripts.

My two students Baptiste Ferreri and Elena Hoffmann I had the pleasure and honour to supervise.

The Cologne Graduate School of Ageing Research for their generous funding and especially the coordinators Dr. Daniela Morick and Dr. Julia Zielinski for all their support.

The Core Facilities of the Max Planck Institute for Biology of Ageing, especially the Killifish caretakers, Bioinformatics and FACS & Imaging facilities.

## 10. Work contributions

This study is a product of collaborative efforts. Dr. Adam Antebi and Dr. Roberto Ripa supported the conceptualization and experimental design. Nadine Hochhard provided technical assistance in multiple experiments presented here. LC-MS analysis for cGAMP measurement was performed by Dr. Tin Tin Manh Nguyen. Histopathology was performed by Dr. Jennifer L. Brazzell from IDEXX BioAnalytics. Baptiste Ferreri and Elena Hoffmann assisted with cloning transfection cassettes and establishing primary killifish fibroblasts. The FACS & Imaging facility and Dr. Joachim David Steiner assisted in generating and analyzing the flow cytometry data. The MPI-AGE FACS & Imaging Facility assisted with microscopy training. The RNAseq was conducted by the Max Planck Genome-Center Cologne and the MPI-AGE Bioinformatics facility assisted with downstream analysis and statistical accuracy of data.

## 11. References



- Ablasser, A., M. Goldeck, T. Cavlar, T. Deimling, G. Witte, I. Rohl, K. P. Hopfner, J. Ludwig, and V. Hornung. 2013. 'cGAS produces a 2'-5'-linked cyclic dinucleotide second messenger that activates STING', *Nature*, 498: 380-4.
- Ablasser, A., J. L. Schmid-Burgk, I. Hemmerling, G. L. Horvath, T. Schmidt, E. Latz, and V. Hornung. 2013. 'Cell intrinsic immunity spreads to bystander cells via the intercellular transfer of cGAMP', *Nature*, 503: 530-4.
- Acosta, J. C., A. Banito, T. Wuestefeld, A. Georgilis, P. Janich, J. P. Morton, D. Athineos, T. W. Kang, F. Lasitschka, M. Andrulis, G. Pascual, K. J. Morris, S. Khan, H. Jin, G. Dharmalingam, A. P. Snijders, T. Carroll, D. Capper, C. Pritchard, G. J. Inman, T. Longerich, O. J. Sansom, S. A. Benitah, L. Zender, and J. Gil. 2013. 'A complex secretory program orchestrated by the inflammasome controls paracrine senescence', *Nat Cell Biol*, 15: 978-90.
- Agalioti, T., S. Lomvardas, B. Parekh, J. Yie, T. Maniatis, and D. Thanos. 2000. 'Ordered recruitment of chromatin modifying and general transcription factors to the IFN-beta promoter', *Cell*, 103: 667-78.
- Ahuja, G., D. Bartsch, W. Yao, S. Geissen, S. Frank, A. Aguirre, N. Russ, J. E. Messling, J. Dodzian, K. A. Lagerborg, N. E. Vargas, J. S. Muck, S. Brodesser, S. Baldus, A. Sachinidis, J. Hescheler, C. Dieterich, A. Trifunovic, A. Papantonis, M. Petrascheck, A. Klinke, M. Jain, D. R. Valenzano, and L. Kurian. 2019. 'Loss of genomic integrity induced by lysosphingolipid imbalance drives ageing in the heart', *EMBO Rep*, 20.
- Akira, S., K. Takeda, and T. Kaisho. 2001. 'Toll-like receptors: critical proteins linking innate and acquired immunity', *Nat Immunol*, 2: 675-80.
- Alhamdi, J. R., T. Peng, I. M. Al-Naggar, K. L. Hawley, K. L. Spiller, and L. T. Kuhn. 2019. 'Controlled M1-to-M2 transition of aged macrophages by calcium phosphate coatings', *Biomaterials*, 196: 90-99.
- Allard, J. B., H. Kamei, and C. Duan. 2013. 'Inducible transgenic expression in the short-lived fish *Nothobranchius furzeri*', *J Fish Biol*, 82: 1733-8.
- Almeida-da-Silva, C. L. C., L. E. B. Savio, R. Coutinho-Silva, and D. M. Ojcius. 2023. 'The role of NOD-like receptors in innate immunity', *Front Immunol*, 14: 1122586.
- Alujoju, P., S. S. Janardhanshetty, S. Subaramanian, L. Periyasamy, and M. Dyavaiah. 2018. 'Quercetin Protects Yeast *Saccharomyces cerevisiae* pep4 Mutant from Oxidative and Apoptotic Stress and Extends Chronological Lifespan', *Curr Microbiol*, 75: 519-30.
- An, J., L. Durcan, R. M. Karr, T. A. Briggs, G. I. Rice, T. H. Teal, J. J. Woodward, and K. B. Elkon. 2017. 'Expression of Cyclic GMP-AMP Synthase in Patients With Systemic Lupus Erythematosus', *Arthritis Rheumatol*, 69: 800-07.
- Annibal, A., R. Ripa, E. Ballhysa, C. Latza, N. Hochhard, and A. Antebi. 2021. 'Mass spectrometric characterization of cyclic dinucleotides (CDNs) in vivo', *Anal Bioanal Chem*, 413: 6457-68.
- Archer, K. A., J. Durack, and D. A. Portnoy. 2014. 'STING-dependent type I IFN production inhibits cell-mediated immunity to *Listeria monocytogenes*', *PLoS Pathog*, 10: e1003861.
- Astre, G., T. Atlan, U. Goshtchevsky, A. Oron-Gottesman, M. Smirnov, K. Shapira, A. Velan, J. Deelen, T. Levy, E. Y. Levanon, and I. Harel. 2023. 'Genetic perturbation of AMP biosynthesis extends lifespan and restores metabolic health in a naturally short-lived vertebrate', *Dev Cell*, 58: 1350-64 e10.
- Atala, A. 2015. 'Re: Tumour-infiltrating Gr-1+ myeloid cells antagonize senescence in cancer', *J Urol*, 193: 2146.

- Auerbuch, V., D. G. Brockstedt, N. Meyer-Morse, M. O'Riordan, and D. A. Portnoy. 2004. 'Mice lacking the type I interferon receptor are resistant to *Listeria monocytogenes*', *J Exp Med*, 200: 527-33.
- Austad, S. N., and K. E. Fischer. 2016. 'Sex Differences in Lifespan', *Cell Metab*, 23: 1022-33.
- Bagnoli, S., B. Fronte, C. Bibbiani, E. Terzibasi Tozzini, and A. Cellerino. 2022. 'Quantification of noradrenergic-, dopaminergic-, and tectal-neurons during aging in the short-lived killifish *Nothobranchius furzeri*', *Aging Cell*, 21: e13689.
- Baidoo, N., and G. J. Sanger. 2024. 'Age-related decline in goblet cell numbers and mucin content of the human colon: Implications for lower bowel functions in the elderly', *Exp Mol Pathol*, 139: 104923.
- Baker, D. J., B. G. Childs, M. Durik, M. E. Wijers, C. J. Sieben, J. Zhong, R. A. Saltness, K. B. Jeganathan, G. C. Verzosa, A. Pezeshki, K. Khazaie, J. D. Miller, and J. M. van Deursen. 2016. 'Naturally occurring p16(Ink4a)-positive cells shorten healthy lifespan', *Nature*, 530: 184-9.
- Baker, D. J., T. Wijshake, T. Tchkonja, N. K. LeBrasseur, B. G. Childs, B. van de Sluis, J. L. Kirkland, and J. M. van Deursen. 2011. 'Clearance of p16Ink4a-positive senescent cells delays ageing-associated disorders', *Nature*, 479: 232-6.
- Barnett, K. C., J. M. Coronas-Serna, W. Zhou, M. J. Ernandes, A. Cao, P. J. Kranzusch, and J. C. Kagan. 2019. 'Phosphoinositide Interactions Position cGAS at the Plasma Membrane to Ensure Efficient Distinction between Self- and Viral DNA', *Cell*, 176: 1432-46 e11.
- Batista, M. A., F. Calvo-Fortes, G. Silveira-Nunes, G. C. Camatta, E. Speziali, S. Turroni, A. Teixeira-Carvalho, O. A. Martins, N. Neretti, T. U. Maioli, R. R. Santos, P. Brigidi, C. Franceschi, and A. M. C. Faria. 2020. 'Inflammaging in Endemic Areas for Infectious Diseases', *Frontiers in Immunology*, 11.
- Batista, N. J., S. G. Desai, A. M. Perez, A. Finkelstein, R. Radigan, M. Singh, A. Landman, B. Drittell, D. Abramov, M. Ahsan, S. Cornwell, and D. Zhang. 2023. 'The Molecular and Cellular Basis of Hutchinson-Gilford Progeria Syndrome and Potential Treatments', *Genes (Basel)*, 14.
- Baumgart, M., E. Barth, A. Savino, M. Groth, P. Koch, A. Petzold, I. Arisi, M. Platzer, M. Marz, and A. Cellerino. 2019. 'Correction to: A miRNA catalogue and ncRNA annotation of the short-living fish *Nothobranchius furzeri*', *BMC Genomics*, 20: 898.
- Baumgart, M., M. Groth, S. Priebe, A. Savino, G. Testa, A. Dix, R. Ripa, F. Spallotta, C. Gaetano, M. Ori, E. Terzibasi Tozzini, R. Guthke, M. Platzer, and A. Cellerino. 2014. 'RNA-seq of the aging brain in the short-lived fish *N. furzeri* - conserved pathways and novel genes associated with neurogenesis', *Aging Cell*, 13: 965-74.
- Beausejour, C. M., A. Krtolica, F. Galimi, M. Narita, S. W. Lowe, P. Yaswen, and J. Campisi. 2003. 'Reversal of human cellular senescence: roles of the p53 and p16 pathways', *EMBO J*, 22: 4212-22.
- Beck-Engeser, G. B., D. Eilat, and M. Wabl. 2011. 'An autoimmune disease prevented by anti-retroviral drugs', *Retrovirology*, 8: 91.
- Bedbrook, C. N., R. D. Nath, R. Nagvekar, K. Deisseroth, and A. Brunet. 2023. 'Rapid and precise genome engineering in a naturally short-lived vertebrate', *Elife*, 12.
- Benayoun, B. A., E. A. Pollina, P. P. Singh, S. Mahmoudi, I. Harel, K. M. Casey, B. W. Dulken, A. Kundaje, and A. Brunet. 2019. 'Remodeling of epigenome and transcriptome landscapes with aging in mice reveals widespread induction of inflammatory responses', *Genome Res*, 29: 697-709.

- Bergmans, S., N. C. L. Noel, L. Masin, E. G. Harding, A. M. Krzywanska, J. D. De Schutter, R. Ayana, C. K. Hu, L. Arckens, P. A. Ruzycski, R. B. MacDonald, B. S. Clark, and L. Moons. 2024. 'Age-related dysregulation of the retinal transcriptome in African turquoise killifish', *Aging Cell*: e14192.
- Bernadotte, A., V. M. Mikhelson, and I. M. Spivak. 2016. 'Markers of cellular senescence. Telomere shortening as a marker of cellular senescence', *Aging (Albany NY)*, 8: 3-11.
- Biagi, E., C. Franceschi, S. Rampelli, M. Severgnini, R. Ostan, S. Turrone, C. Consolandi, S. Quercia, M. Scurti, D. Monti, M. Capri, P. Brigidi, and M. Candela. 2016. 'Gut Microbiota and Extreme Longevity', *Curr Biol*, 26: 1480-5.
- Biffo, S., D. Ruggero, and M. M. Santoro. 2024. 'The crosstalk between metabolism and translation', *Cell Metab*, 36: 1945-62.
- Bjorgen, H., and E. O. Koppang. 2021. 'Anatomy of teleost fish immune structures and organs', *Immunogenetics*, 73: 53-63.
- Bock, F. J., and J. S. Riley. 2023. 'When cell death goes wrong: inflammatory outcomes of failed apoptosis and mitotic cell death', *Cell Death Differ*, 30: 293-303.
- Bojko, A., J. Czarnecka-Herok, A. Charzynska, M. Dabrowski, and E. Sikora. 2019. 'Diversity of the Senescence Phenotype of Cancer Cells Treated with Chemotherapeutic Agents', *Cells*, 8.
- Boniewska-Bernacka, E., A. Panczyszyn, and M. Klinger. 2020. 'Telomeres and telomerase in risk assessment of cardiovascular diseases', *Exp Cell Res*, 397: 112361.
- Boos, F., J. Chen, and A. Brunet. 2024. 'The African Turquoise Killifish: A Scalable Vertebrate Model for Aging and Other Complex Phenotypes', *Cold Spring Harb Protoc*, 2024: 107737.
- Bradshaw, W. J., M. Poeschla, A. Placzek, S. Kean, and D. R. Valenzano. 2022. 'Extensive age-dependent loss of antibody diversity in naturally short-lived turquoise killifish', *Elife*, 11.
- Brault, M., T. M. Olsen, J. Martinez, D. B. Stetson, and A. Oberst. 2018. 'Intracellular Nucleic Acid Sensing Triggers Necroptosis through Synergistic Type I IFN and TNF Signaling', *J Immunol*, 200: 2748-56.
- Bray, N. L., H. Pimentel, P. Melsted, and L. Pachter. 2016. 'Erratum: Near-optimal probabilistic RNA-seq quantification', *Nat Biotechnol*, 34: 888.
- Bresciani, E., E. Broadbridge, and P. P. Liu. 2018. 'An efficient dissociation protocol for generation of single cell suspension from zebrafish embryos and larvae', *MethodsX*, 5: 1287-90.
- Bridgeman, A., J. Maelfait, T. Davenne, T. Partridge, Y. Peng, A. Mayer, T. Dong, V. Kaefer, P. Borrow, and J. Rehwinkel. 2015. 'Viruses transfer the antiviral second messenger cGAMP between cells', *Science*, 349: 1228-32.
- Broz, P., and V. M. Dixit. 2016. 'Inflammasomes: mechanism of assembly, regulation and signalling', *Nat Rev Immunol*, 16: 407-20.
- Brunet, A. 2023. *African Turquoise Killifish (Nothobranchius Furzeri): A Laboratory Manual* (Cold Spring Harbor Laboratory Press).
- Burdette, D. L., K. M. Monroe, K. Sotelo-Troha, J. S. Iwig, B. Eckert, M. Hyodo, Y. Hayakawa, and R. E. Vance. 2011. 'STING is a direct innate immune sensor of cyclic di-GMP', *Nature*, 478: 515-8.
- Burdette, D. L., and R. E. Vance. 2013. 'STING and the innate immune response to nucleic acids in the cytosol', *Nat Immunol*, 14: 19-26.
- Caldecott, K. W. 2022. 'DNA single-strand break repair and human genetic disease', *Trends Cell Biol*, 32: 733-45.

- Campbell, R. A., M. H. Docherty, D. A. Ferenbach, and K. J. Mylonas. 2021. 'The Role of Ageing and Parenchymal Senescence on Macrophage Function and Fibrosis', *Front Immunol*, 12: 700790.
- Carnio, S., F. LoVerso, M. A. Baraibar, E. Longa, M. M. Khan, M. Maffei, M. Reischl, M. Canepari, S. Loeffler, H. Kern, B. Blaauw, B. Friguet, R. Bottinelli, R. Rudolf, and M. Sandri. 2014. 'Autophagy impairment in muscle induces neuromuscular junction degeneration and precocious aging', *Cell Rep*, 8: 1509-21.
- Carrero, J. A., B. Calderon, and E. R. Unanue. 2004. 'Type I interferon sensitizes lymphocytes to apoptosis and reduces resistance to *Listeria* infection', *J Exp Med*, 200: 535-40.
- Carroll, B., and V. I. Korolchuk. 2018. 'Nutrient sensing, growth and senescence', *FEBS J*, 285: 1948-58.
- Cencioni, C., J. Heid, A. Krepelova, S. M. M. Rasa, C. Kuenne, S. Guenther, M. Baumgart, A. Cellerino, F. Neri, F. Spallotta, and C. Gaetano. 2019. 'Aging Triggers H3K27 Trimethylation Hoarding in the Chromatin of *Nothobranchius furzeri* Skeletal Muscle', *Cells*, 8.
- Chatterjee, N., and G. C. Walker. 2017. 'Mechanisms of DNA damage, repair, and mutagenesis', *Environ Mol Mutagen*, 58: 235-63.
- Chen, H., H. Chen, J. Zhang, Y. Wang, A. Simoneau, H. Yang, A. S. Levine, L. Zou, Z. Chen, and L. Lan. 2020. 'cGAS suppresses genomic instability as a decelerator of replication forks', *Sci Adv*, 6.
- Chen, H., H. Sun, F. You, W. Sun, X. Zhou, L. Chen, J. Yang, Y. Wang, H. Tang, Y. Guan, W. Xia, J. Gu, H. Ishikawa, D. Gutman, G. Barber, Z. Qin, and Z. Jiang. 2011. 'Activation of STAT6 by STING is critical for antiviral innate immunity', *Cell*, 147: 436-46.
- Chen, J. H., C. N. Hales, and S. E. Ozanne. 2007. 'DNA damage, cellular senescence and organismal ageing: causal or correlative?', *Nucleic Acids Res*, 35: 7417-28.
- Chen, Q., A. Fischer, J. D. Reagan, L. J. Yan, and B. N. Ames. 1995. 'Oxidative DNA damage and senescence of human diploid fibroblast cells', *Proc Natl Acad Sci U S A*, 92: 4337-41.
- Chen, Q. M., J. Liu, and J. B. Merrett. 2000. 'Apoptosis or senescence-like growth arrest: influence of cell-cycle position, p53, p21 and bax in H<sub>2</sub>O<sub>2</sub> response of normal human fibroblasts', *Biochem J*, 347: 543-51.
- Chen, Q., L. Sun, and Z. J. Chen. 2016. 'Regulation and function of the cGAS-STING pathway of cytosolic DNA sensing', *Nat Immunol*, 17: 1142-9.
- Cheng, Q., and J. Chen. 2010. 'Mechanism of p53 stabilization by ATM after DNA damage', *Cell Cycle*, 9: 472-8.
- Childs, B. G., M. Durik, D. J. Baker, and J. M. van Deursen. 2015. 'Cellular senescence in aging and age-related disease: from mechanisms to therapy', *Nat Med*, 21: 1424-35.
- Christensen, K., M. Thinggaard, A. Oksuzyan, T. Steenstrup, K. Andersen-Ranberg, B. Jeune, M. McGue, and J. W. Vaupel. 2013. 'Physical and cognitive functioning of people older than 90 years: a comparison of two Danish cohorts born 10 years apart', *Lancet*, 382: 1507-13.
- Civril, F., T. Deimling, C. C. de Oliveira Mann, A. Ablasser, M. Moldt, G. Witte, V. Hornung, and K. P. Hopfner. 2013. 'Structural mechanism of cytosolic DNA sensing by cGAS', *Nature*, 498: 332-7.
- Coll-Bonfill, N., R. Cancado de Faria, S. Bhoopatiraju, and S. Gonzalo. 2020. 'Calcitriol Prevents RAD51 Loss and cGAS-STING-IFN Response Triggered by Progerin', *Proteomics*, 20: e1800406.

- Collin, G., A. Huna, M. Warnier, J. M. Flaman, and D. Bernard. 2018. 'Transcriptional repression of DNA repair genes is a hallmark and a cause of cellular senescence', *Cell Death Dis*, 9: 259.
- Cooper, L. N., M. Y. Ansari, G. Capshaw, A. Galazyuk, A. M. Lauer, C. F. Moss, K. E. Sears, M. Stewart, E. C. Teeling, G. S. Wilkinson, R. C. Wilson, T. P. Zwaka, and R. Orman. 2024. 'Bats as instructive animal models for studying longevity and aging', *Ann N Y Acad Sci*, 1541: 10-23.
- Coppe, J. P., P. Y. Desprez, A. Krtolica, and J. Campisi. 2010. 'The senescence-associated secretory phenotype: the dark side of tumor suppression', *Annu Rev Pathol*, 5: 99-118.
- Coppe, J. P., F. Rodier, C. K. Patil, A. Freund, P. Y. Desprez, and J. Campisi. 2011. 'Tumor suppressor and aging biomarker p16(INK4a) induces cellular senescence without the associated inflammatory secretory phenotype', *J Biol Chem*, 286: 36396-403.
- 'Correction to: SIRT7 antagonizes human stem cell aging as a heterochromatin stabilizer'. 2024. *Protein Cell*, 15: 76-77.
- Correia-Melo, C., F. D. Marques, R. Anderson, G. Hewitt, R. Hewitt, J. Cole, B. M. Carroll, S. Miwa, J. Birch, A. Merz, M. D. Rushton, M. Charles, D. Jurk, S. W. Tait, R. Czapiewski, L. Greaves, G. Nelson, Y. M. Bohlooly, S. Rodriguez-Cuenca, A. Vidal-Puig, D. Mann, G. Saretzki, G. Quarato, D. R. Green, P. D. Adams, T. von Zglinicki, V. I. Korolchuk, and J. F. Passos. 2016. 'Mitochondria are required for pro-ageing features of the senescent phenotype', *EMBO J*, 35: 724-42.
- Courtois-Cox, S., S. M. Genther Williams, E. E. Reczek, B. W. Johnson, L. T. McGillicuddy, C. M. Johannessen, P. E. Hollstein, M. MacCollin, and K. Cichowski. 2006. 'A negative feedback signaling network underlies oncogene-induced senescence', *Cancer Cell*, 10: 459-72.
- Czerkies, M., Z. Korwek, W. Prus, M. Kochanczyk, J. Jaruszewicz-Blonska, K. Tudelska, S. Blonski, M. Kimmel, A. R. Brasier, and T. Lipniacki. 2018. 'Cell fate in antiviral response arises in the crosstalk of IRF, NF-kappaB and JAK/STAT pathways', *Nat Commun*, 9: 493.
- d'Adda di Fagagna, F. 2008. 'Living on a break: cellular senescence as a DNA-damage response', *Nat Rev Cancer*, 8: 512-22.
- D'Angelo, Livia, Paolo De Girolamo, and ScienceDirect. 2022. *Laboratory fish in biomedical research : biology, husbandry and research applications for zebrafish, medaka, killifish, swordtail fish, cavefish, stickleback, goldfish and Danionella translucida* (Academic Press, an imprint of Elsevier: London, UK).
- Da Silva-Alvarez, S., J. Guerra-Varela, D. Sobrido-Camean, A. Quelle, A. Barreiro-Iglesias, L. Sanchez, and M. Collado. 2020. 'Cell senescence contributes to tissue regeneration in zebrafish', *Aging Cell*, 19: e13052.
- De Cecco, M., T. Ito, A. P. Petrashen, A. E. Elias, N. J. Skvir, S. W. Criscione, A. Caligiana, G. Broccoli, E. M. Adney, J. D. Boeke, O. Le, C. Beausejour, J. Ambati, K. Ambati, M. Simon, A. Seluanov, V. Gorbunova, P. E. Slagboom, S. L. Helfand, N. Neretti, and J. M. Sedivy. 2019. 'Author Correction: L1 drives IFN in senescent cells and promotes age-associated inflammation', *Nature*, 572: E5.
- de Oliveira Mann, C. C., R. Kiefersauer, G. Witte, and K. P. Hopfner. 2016. 'Structural and biochemical characterization of the cell fate determining nucleotidyltransferase fold protein MAB21L1', *Sci Rep*, 6: 27498.
- de Oliveira Mann, C. C., M. H. Orzalli, D. S. King, J. C. Kagan, A. S. Y. Lee, and P. J. Kranzusch. 2019. 'Modular Architecture of the STING C-Terminal Tail Allows Interferon and NF-kappaB Signaling Adaptation', *Cell Rep*, 27: 1165-75 e5.

- Decout, A., J. D. Katz, S. Venkatraman, and A. Ablasser. 2021. 'The cGAS-STING pathway as a therapeutic target in inflammatory diseases', *Nat Rev Immunol*, 21: 548-69.
- Deelen, J., M. Beekman, H. W. Uh, Q. Helmer, M. Kuningas, L. Christiansen, D. Kremer, R. van der Breggen, H. E. Suchiman, N. Lakenberg, E. B. van den Akker, W. M. Passtoors, H. Tiemeier, D. van Heemst, A. J. de Craen, F. Rivadeneira, E. J. de Geus, M. Perola, F. J. van der Ouderaa, D. A. Gunn, D. I. Boomsma, A. G. Uitterlinden, K. Christensen, C. M. van Duijn, B. T. Heijmans, J. J. Houwing-Duistermaat, R. G. Westendorp, and P. E. Slagboom. 2011. 'Genome-wide association study identifies a single major locus contributing to survival into old age; the APOE locus revisited', *Aging Cell*, 10: 686-98.
- Deelen, J., D. S. Evans, D. E. Arking, N. Tesi, M. Nygaard, X. Liu, M. K. Wojczynski, M. L. Biggs, A. van der Spek, G. Atzmon, E. B. Ware, C. Sarnowski, A. V. Smith, I. Seppala, H. J. Cordell, J. Dose, N. Amin, A. M. Arnold, K. L. Ayers, N. Barzilai, E. J. Becker, M. Beekman, H. Blanche, K. Christensen, L. Christiansen, J. C. Collerton, S. Cubaynes, S. R. Cummings, K. Davies, B. Debrabant, J. F. Deleuze, R. Duncan, J. D. Faul, C. Franceschi, P. Galan, V. Gudnason, T. B. Harris, M. Huisman, M. A. Hurme, C. Jagger, I. Jansen, M. Jylha, M. Kahonen, D. Karasik, S. L. R. Kardia, A. Kingston, T. B. L. Kirkwood, L. J. Launer, T. Lehtimäki, W. Lieb, L. P. Lyytikäinen, C. Martin-Ruiz, J. Min, A. Nebel, A. B. Newman, C. Nie, E. A. Nohr, E. S. Orwoll, T. T. Perls, M. A. Province, B. M. Psaty, O. T. Raitakari, M. J. T. Reinders, J. M. Robine, J. I. Rotter, P. Sebastiani, J. Smith, T. I. A. Sorensen, K. D. Taylor, A. G. Uitterlinden, W. van der Flier, S. J. van der Lee, C. M. van Duijn, D. van Heemst, J. W. Vaupel, D. Weir, K. Ye, Y. Zeng, W. Zheng, H. Holstege, D. P. Kiel, K. L. Lunetta, P. E. Slagboom, and J. M. Murabito. 2021. 'Publisher Correction: A meta-analysis of genome-wide association studies identifies multiple longevity genes', *Nat Commun*, 12: 2463.
- Deelen, J., J. Kettunen, K. Fischer, A. van der Spek, S. Trompet, G. Kastenmuller, A. Boyd, J. Zierer, E. B. van den Akker, M. Ala-Korpela, N. Amin, A. Demirkan, M. Ghanbari, D. van Heemst, M. A. Ikram, J. B. van Klinken, S. P. Mooijaart, A. Peters, V. Salomaa, N. Sattar, T. D. Spector, H. Tiemeier, A. Verhoeven, M. Waldenberger, P. Wurtz, G. Davey Smith, A. Metspalu, M. Perola, C. Menni, J. M. Geleijnse, F. Drenos, M. Beekman, J. W. Jukema, C. M. van Duijn, and P. E. Slagboom. 2019. 'A metabolic profile of all-cause mortality risk identified in an observational study of 44,168 individuals', *Nat Commun*, 10: 3346.
- DeJong, E. N., M. G. Surette, and D. M. E. Bowdish. 2020. 'The Gut Microbiota and Unhealthy Aging: Disentangling Cause from Consequence', *Cell Host Microbe*, 28: 180-89.
- Demaria, M., N. Ohtani, S. A. Youssef, F. Rodier, W. Toussaint, J. R. Mitchell, R. M. Laberge, J. Vijg, H. Van Steeg, M. E. Dolle, J. H. Hoeijmakers, A. de Bruin, E. Hara, and J. Campisi. 2014. 'An essential role for senescent cells in optimal wound healing through secretion of PDGF-AA', *Dev Cell*, 31: 722-33.
- Deng, Z., Z. Chong, C. S. Law, K. Mukai, F. O. Ho, T. Martinu, B. J. Backes, W. L. Eckalbar, T. Taguchi, and A. K. Shum. 2020. 'A defect in COPI-mediated transport of STING causes immune dysregulation in COPA syndrome', *J Exp Med*, 217.
- Di Cicco, E., E. T. Tozzini, G. Rossi, and A. Cellerino. 2011. 'The short-lived annual fish *Nothobranchius furzeri* shows a typical teleost aging process reinforced by high incidence of age-dependent neoplasias', *Exp Gerontol*, 46: 249-56.
- Di Leonardo, A., S. P. Linke, K. Clarkin, and G. M. Wahl. 1994. 'DNA damage triggers a prolonged p53-dependent G1 arrest and long-term induction of Cip1 in normal human fibroblasts', *Genes Dev*, 8: 2540-51.

- Diner, E. J., D. L. Burdette, S. C. Wilson, K. M. Monroe, C. A. Kellenberger, M. Hyodo, Y. Hayakawa, M. C. Hammond, and R. E. Vance. 2013. 'The innate immune DNA sensor cGAS produces a noncanonical cyclic dinucleotide that activates human STING', *Cell Rep*, 3: 1355-61.
- Diniz, B. S., E. M. Vieira, A. P. Mendes-Silva, C. R. Bowie, M. A. Butters, C. E. Fischer, A. Flint, N. Herrmann, J. Kennedy, K. L. Lanctot, L. Mah, B. G. Pollock, B. H. Mulsant, T. K. Rajji, and PACt- M. D. Study Group on behalf of the. 2021. 'Mild cognitive impairment and major depressive disorder are associated with molecular senescence abnormalities in older adults', *Alzheimers Dement (N Y)*, 7: e12129.
- Dobbs, N., N. Burnaevskiy, D. Chen, V. K. Gonugunta, N. M. Alto, and N. Yan. 2015. 'STING Activation by Translocation from the ER Is Associated with Infection and Autoinflammatory Disease', *Cell Host Microbe*, 18: 157-68.
- Dodzian, J., S. Kean, J. Seidel, and D. R. Valenzano. 2018. 'A Protocol for Laboratory Housing of Turquoise Killifish (*Nothobranchius furzeri*)', *J Vis Exp*.
- Dolan, D. W., A. Zupanic, G. Nelson, P. Hall, S. Miwa, T. B. Kirkwood, and D. P. Shanley. 2015. 'Integrated Stochastic Model of DNA Damage Repair by Non-homologous End Joining and p53/p21-Mediated Early Senescence Signalling', *PLoS Comput Biol*, 11: e1004246.
- Dolfi, L., R. Ripa, A. Antebi, D. R. Valenzano, and A. Cellerino. 2019. 'Cell cycle dynamics during diapause entry and exit in an annual killifish revealed by FUCCI technology', *Evodevo*, 10: 29.
- Dolfi, L., R. Ripa, and A. Cellerino. 2014. 'Transition to annual life history coincides with reduction in cell cycle speed during early cleavage in three independent clades of annual killifish', *Evodevo*, 5: 32.
- Dolfi, L., R. Ripa, D. Medelbekova, E. Ballhysa, O. Symmons, and A. Antebi. 2023. 'Nonlethal Blood Sampling from the Killifish *Nothobranchius furzeri*', *Cold Spring Harb Protoc*, 2023: 107745.
- Dolfi, L., T. K. Suen, D. Medelbekova, R. Ripa, O. Symmons, and A. Antebi. 2023a. 'In Vitro Fertilization of the African Turquoise Killifish *Nothobranchius furzeri*', *Cold Spring Harb Protoc*, 2023: 107886.
- . 2023b. 'Sperm Cryopreservation of the African Turquoise Killifish *Nothobranchius furzeri*', *Cold Spring Harb Protoc*, 2023: 107885.
- Donovan, J., M. Dufner, and A. Korennykh. 2013. 'Structural basis for cytosolic double-stranded RNA surveillance by human oligoadenylate synthetase 1', *Proc Natl Acad Sci U S A*, 110: 1652-7.
- Dou, Z. X., K. Ghosh, M. G. Vizioli, J. J. Zhu, P. Sen, K. J. Wangenstein, J. Simithy, Y. M. Lan, Y. P. Lin, Z. Zhou, B. C. Capell, C. Y. Xu, M. G. Xu, J. E. Kieckhaefer, T. Y. Jiang, M. Shoshkes-Carmel, K. M. A. Al Tanim, G. N. Barber, J. T. Seykora, S. E. Millar, K. H. Kaestner, B. A. Garcia, P. D. Adams, and S. L. Berger. 2017. 'Cytoplasmic chromatin triggers inflammation in senescence and cancer', *Nature*, 550: 402-06.
- Du, M., and Z. J. Chen. 2018. 'DNA-induced liquid phase condensation of cGAS activates innate immune signaling', *Science*, 361: 704-09.
- Dutto, I., M. Tillhon, O. Cazzalini, L. A. Stivala, and E. Prosperi. 2015. 'Biology of the cell cycle inhibitor p21(CDKN1A): molecular mechanisms and relevance in chemical toxicology', *Arch Toxicol*, 89: 155-78.
- Dvorkin, S., S. Cambier, H. E. Volkman, and D. B. Stetson. 2024. 'New frontiers in the cGAS-STING intracellular DNA-sensing pathway', *Immunity*, 57: 718-30.

- Ekstrom, P., C. M. Johnsson, and L. M. Ohlin. 2001. 'Ventricular proliferation zones in the brain of an adult teleost fish and their relation to neuromeres and migration (secondary matrix) zones', *J Comp Neurol*, 436: 92-110.
- Elderman, M., B. Sovran, F. Hugenholtz, K. Graversen, M. Huijskes, E. Houtsma, C. Belzer, M. Boekschoten, P. de Vos, J. Dekker, J. Wells, and M. Faas. 2017. 'The effect of age on the intestinal mucus thickness, microbiota composition and immunity in relation to sex in mice', *PLoS One*, 12: e0184274.
- Ergun, S. L., D. Fernandez, T. M. Weiss, and L. Li. 2019. 'STING Polymer Structure Reveals Mechanisms for Activation, Hyperactivation, and Inhibition', *Cell*, 178: 290-301 e10.
- Evangelou, K., and V. G. Gorgoulis. 2017. 'Sudan Black B, The Specific Histochemical Stain for Lipofuscin: A Novel Method to Detect Senescent Cells', *Methods Mol Biol*, 1534: 111-19.
- Fang, R., C. Wang, Q. Jiang, M. Lv, P. Gao, X. Yu, P. Mu, R. Zhang, S. Bi, J. M. Feng, and Z. Jiang. 2017. 'NEMO-IKKbeta Are Essential for IRF3 and NF-kappaB Activation in the cGAS-STING Pathway', *J Immunol*, 199: 3222-33.
- Fenelon, J. C., A. Banerjee, and B. D. Murphy. 2014. 'Embryonic diapause: development on hold', *Int J Dev Biol*, 58: 163-74.
- Ferrucci, L., and E. Fabbri. 2018. 'Inflammageing: chronic inflammation in ageing, cardiovascular disease, and frailty', *Nat Rev Cardiol*, 15: 505-22.
- Filograna, R., M. Mennuni, D. Alsina, and N. G. Larsson. 2021. 'Mitochondrial DNA copy number in human disease: the more the better?', *FEBS Lett*, 595: 976-1002.
- Foley, N. M., G. M. Hughes, Z. Huang, M. Clarke, D. Jebb, C. V. Whelan, E. J. Petit, F. Touzalin, O. Farcy, G. Jones, R. D. Ransome, J. Kacprzyk, M. J. O'Connell, G. Kerth, H. Rebelo, L. Rodrigues, S. J. Puechmaille, and E. C. Teeling. 2018. 'Growing old, yet staying young: The role of telomeres in bats' exceptional longevity', *Sci Adv*, 4: eaao0926.
- Fortuny, A., A. Chansard, P. Caron, O. Chevallier, O. Leroy, O. Renaud, and S. E. Polo. 2021. 'Imaging the response to DNA damage in heterochromatin domains reveals core principles of heterochromatin maintenance', *Nat Commun*, 12: 2428.
- Franceschi, C., M. Bonafe, S. Valensin, F. Olivieri, M. De Luca, E. Ottaviani, and G. De Benedictis. 2000. 'Inflamm-aging. An evolutionary perspective on immunosenescence', *Ann N Y Acad Sci*, 908: 244-54.
- Franceschi, C., and J. Campisi. 2014. 'Chronic inflammation (inflammaging) and its potential contribution to age-associated diseases', *J Gerontol A Biol Sci Med Sci*, 69 Suppl 1: S4-9.
- Franceschi, C., P. Garagnani, P. Parini, C. Giuliani, and A. Santoro. 2018. 'Inflammaging: a new immune-metabolic viewpoint for age-related diseases', *Nat Rev Endocrinol*, 14: 576-90.
- Franceschi, C., P. Garagnani, G. Vitale, M. Capri, and S. Salvioli. 2017. 'Inflammaging and 'Garb-aging'', *Trends Endocrinol Metab*, 28: 199-212.
- Frasca, D., B. B. Blomberg, and R. Paganelli. 2017. 'Aging, Obesity, and Inflammatory Age-Related Diseases', *Front Immunol*, 8: 1745.
- Fu, Y., Y. Fang, Z. Lin, L. Yang, L. Zheng, H. Hu, T. Yu, B. Huang, S. Chen, H. Wang, S. Xu, W. Bao, Q. Chen, and L. Sun. 2020. 'Inhibition of cGAS-Mediated Interferon Response Facilitates Transgene Expression', *iScience*, 23: 101026.
- Gadd, D. A., R. F. Hillary, Z. Kuncheva, T. Mangelis, Y. Cheng, M. Dissanayake, R. Admanit, J. Gagnon, T. Lin, K. L. Ferber, H. Runz, Team Biogen Biobank, C. N. Foley, R. E. Marioni, and B. B. Sun. 2024. 'Blood protein assessment of leading incident diseases and mortality in the UK Biobank', *Nat Aging*, 4: 939-48.



- Gaidt, M. M., T. S. Ebert, D. Chauhan, K. Ramshorn, F. Pinci, S. Zuber, F. O'Duill, J. L. Schmid-Burgk, F. Hoss, R. Buhmann, G. Wittmann, E. Latz, M. Subklewe, and V. Hornung. 2017. 'The DNA Inflammasome in Human Myeloid Cells Is Initiated by a STING-Cell Death Program Upstream of NLRP3', *Cell*, 171: 1110-24 e18.
- Gao, M., H. Guo, X. Dong, Z. Wang, Z. Yang, Q. Shang, and Q. Wang. 2024. 'Regulation of inflammation during wound healing: the function of mesenchymal stem cells and strategies for therapeutic enhancement', *Front Pharmacol*, 15: 1345779.
- Gao, P., M. Ascano, Y. Wu, W. Barchet, B. L. Gaffney, T. Zillinger, A. A. Serganov, Y. Liu, R. A. Jones, G. Hartmann, T. Tuschl, and D. J. Patel. 2013. 'Cyclic [G(2',5')pA(3',5')p] is the metazoan second messenger produced by DNA-activated cyclic GMP-AMP synthase', *Cell*, 153: 1094-107.
- Gao, P., M. Ascano, T. Zillinger, W. Wang, P. Dai, A. A. Serganov, B. L. Gaffney, S. Shuman, R. A. Jones, L. Deng, G. Hartmann, W. Barchet, T. Tuschl, and D. J. Patel. 2013. 'Structure-function analysis of STING activation by c[G(2',5')pA(3',5')p] and targeting by antiviral DMXAA', *Cell*, 154: 748-62.
- Ge, R., Y. Zhou, R. Peng, R. Wang, M. Li, Y. Zhang, C. Zheng, and C. Wang. 2015. 'Conservation of the STING-Mediated Cytosolic DNA Sensing Pathway in Zebrafish', *J Virol*, 89: 7696-706.
- Genade, T., M. Benedetti, E. Terzibasi, P. Roncaglia, D. R. Valenzano, A. Cattaneo, and A. Cellerino. 2005. 'Annual fishes of the genus *Nothobranchius* as a model system for aging research', *Aging Cell*, 4: 223-33.
- Gentili, M., J. Kowal, M. Tkach, T. Satoh, X. Lahaye, C. Conrad, M. Boyron, B. Lombard, S. Durand, G. Kroemer, D. Loew, M. Dalod, C. Thery, and N. Manel. 2015. 'Transmission of innate immune signaling by packaging of cGAMP in viral particles', *Science*, 349: 1232-6.
- Gentili, M., X. Lahaye, F. Nadalin, G. P. F. Nader, E. Puig Lombardi, S. Herve, N. S. De Silva, D. C. Rookhuizen, E. Zueva, C. Goudot, M. Maurin, A. Bochnakian, S. Amigorena, M. Piel, D. Fachinetti, A. Londono-Vallejo, and N. Manel. 2019. 'The N-Terminal Domain of cGAS Determines Preferential Association with Centromeric DNA and Innate Immune Activation in the Nucleus', *Cell Rep*, 26: 2377-93 e13.
- Gentili, M., B. Liu, M. Papanastasiou, D. Dele-Oni, M. A. Schwartz, R. J. Carlson, A. M. Al'Khafaji, K. Krug, A. Brown, J. G. Doench, S. A. Carr, and N. Hacohen. 2023. 'ESCRT-dependent STING degradation inhibits steady-state and cGAMP-induced signalling', *Nat Commun*, 14: 611.
- Georgakopoulou, E. A., K. Tsimaratou, K. Evangelou, P. J. Fernandez Marcos, V. Zoumpourlis, I. P. Trougakos, D. Kletsas, J. Bartek, M. Serrano, and V. G. Gorgoulis. 2013. 'Specific lipofuscin staining as a novel biomarker to detect replicative and stress-induced senescence. A method applicable in cryo-preserved and archival tissues', *Aging (Albany NY)*, 5: 37-50.
- Gluck, S., B. Guey, M. F. Gulen, K. Wolter, T. W. Kang, N. A. Schmacke, A. Bridgeman, J. Rehwinkel, L. Zender, and A. Ablasser. 2017. 'Innate immune sensing of cytosolic chromatin fragments through cGAS promotes senescence', *Nat Cell Biol*, 19: 1061-70.
- Gonzalez-Gualda, E., A. G. Baker, L. Fruk, and D. Munoz-Espin. 2021. 'A guide to assessing cellular senescence in vitro and in vivo', *FEBS J*, 288: 56-80.
- Gonzalo, S., R. Kreienkamp, and P. Askjaer. 2017. 'Hutchinson-Gilford Progeria Syndrome: A premature aging disease caused by LMNA gene mutations', *Ageing Res Rev*, 33: 18-29.

- Gorbunova, V., A. Seluanov, P. Mita, W. McKerrow, D. Fenyo, J. D. Boeke, S. B. Linker, F. H. Gage, J. A. Kreiling, A. P. Petrashen, T. A. Woodham, J. R. Taylor, S. L. Helfand, and J. M. Sedivy. 2021. 'The role of retrotransposable elements in ageing and age-associated diseases', *Nature*, 596: 43-53.
- Gorgoulis, V., P. D. Adams, A. Alimonti, D. C. Bennett, O. Bischof, C. Bishop, J. Campisi, M. Collado, K. Evangelou, G. Ferbeyre, J. Gil, E. Hara, V. Krizhanovsky, D. Jurk, A. B. Maier, M. Narita, L. Niedernhofer, J. F. Passos, P. D. Robbins, C. A. Schmitt, J. Sedivy, K. Vougas, T. von Zglinicki, D. Zhou, M. Serrano, and M. Demaria. 2019. 'Cellular Senescence: Defining a Path Forward', *Cell*, 179: 813-27.
- Graf, M., N. Hartmann, K. Reichwald, and C. Englert. 2013. 'Absence of replicative senescence in cultured cells from the short-lived killifish *Nothobranchius furzeri*', *Exp Gerontol*, 48: 17-28.
- Gratia, M., M. P. Rodero, C. Conrad, E. Bou Samra, M. Maurin, G. I. Rice, D. Duffy, P. Revy, F. Petit, R. C. Dale, Y. J. Crow, M. Amor-Gueret, and N. Manel. 2019. 'Bloom syndrome protein restrains innate immune sensing of micronuclei by cGAS', *J Exp Med*, 216: 1199-213.
- Gui, X., H. Yang, T. Li, X. Tan, P. Shi, M. Li, F. Du, and Z. J. Chen. 2019. 'Autophagy induction via STING trafficking is a primordial function of the cGAS pathway', *Nature*, 567: 262-66.
- Gulen, M. F., U. Koch, S. M. Haag, F. Schuler, L. Apetoh, A. Villunger, F. Radtke, and A. Ablasser. 2017. 'Signalling strength determines proapoptotic functions of STING', *Nat Commun*, 8: 427.
- Gulen, M. F., N. Samson, A. Keller, M. Schwabenland, C. Liu, S. Gluck, V. V. Thacker, L. Favre, B. Mangeat, L. J. Kroese, P. Krimpenfort, M. Prinz, and A. Ablasser. 2023. 'cGAS-STING drives ageing-related inflammation and neurodegeneration', *Nature*, 620: 374-80.
- Guo, Q., X. Chen, J. Chen, G. Zheng, C. Xie, H. Wu, Z. Miao, Y. Lin, X. Wang, W. Gao, X. Zheng, Z. Pan, Y. Zhou, Y. Wu, and X. Zhang. 2021. 'STING promotes senescence, apoptosis, and extracellular matrix degradation in osteoarthritis via the NF-kappaB signaling pathway', *Cell Death Dis*, 12: 13.
- Gurevitch, O., S. Slavin, and A. G. Feldman. 2007. 'Conversion of red bone marrow into yellow - Cause and mechanisms', *Med Hypotheses*, 69: 531-6.
- Haag, S. M., M. F. Gulen, L. Reymond, A. Gibelin, L. Abrami, A. Decout, M. Heymann, F. G. van der Goot, G. Turcatti, R. Behrendt, and A. Ablasser. 2018. 'Targeting STING with covalent small-molecule inhibitors', *Nature*, 559: 269-73.
- Hahn, O., L. F. Drews, A. Nguyen, T. Tatsuta, L. Gkioni, O. Hendrich, Q. Zhang, T. Langer, S. Pletcher, M. J. O. Wakelam, A. Beyer, S. Gronke, and L. Partridge. 2019. 'A nutritional memory effect counteracts benefits of dietary restriction in old mice', *Nat Metab*, 1: 1059-73.
- Harel, I., B. A. Benayoun, B. Machado, P. P. Singh, C. K. Hu, M. F. Pech, D. R. Valenzano, E. Zhang, S. C. Sharp, S. E. Artandi, and A. Brunet. 2015. 'A platform for rapid exploration of aging and diseases in a naturally short-lived vertebrate', *Cell*, 160: 1013-26.
- Harel, I., Y. R. Chen, I. Ziv, P. P. Singh, D. Heinzer, P. Navarro Negredo, U. Goshtchevsky, W. Wang, G. Astre, E. Moses, A. McKay, B. E. Machado, K. Hebestreit, S. Yin, A. Sanchez Alvarado, D. F. Jarosz, and A. Brunet. 2024. 'Identification of protein aggregates in the aging vertebrate brain with prion-like and phase-separation properties', *Cell Rep*, 43: 112787.

- Harel, I., D. R. Valenzano, and A. Brunet. 2016. 'Efficient genome engineering approaches for the short-lived African turquoise killifish', *Nat Protoc*, 11: 2010-28.
- Harley, C. B., A. B. Futcher, and C. W. Greider. 1990. 'Telomeres shorten during ageing of human fibroblasts', *Nature*, 345: 458-60.
- Harrison, D. E., R. Strong, Z. D. Sharp, J. F. Nelson, C. M. Astle, K. Flurkey, N. L. Nadon, J. E. Wilkinson, K. Frenkel, C. S. Carter, M. Pahor, M. A. Javors, E. Fernandez, and R. A. Miller. 2009. 'Rapamycin fed late in life extends lifespan in genetically heterogeneous mice', *Nature*, 460: 392-5.
- Hartlova, A., S. F. Erttmann, F. A. Raffi, A. M. Schmalz, U. Resch, S. Anugula, S. Lienenklaus, L. M. Nilsson, A. Kroger, J. A. Nilsson, T. Ek, S. Weiss, and N. O. Gekara. 2015. 'DNA damage primes the type I interferon system via the cytosolic DNA sensor STING to promote anti-microbial innate immunity', *Immunity*, 42: 332-43.
- Hartmann, N., and C. Englert. 2012. 'A microinjection protocol for the generation of transgenic killifish (Species: *Nothobranchius furzeri*)', *Dev Dyn*, 241: 1133-41.
- Hartmann, N., K. Reichwald, A. Lechel, M. Graf, J. Kirschner, A. Dorn, E. Terzibasi, J. Wellner, M. Platzer, K. L. Rudolph, A. Cellerino, and C. Englert. 2009. 'Telomeres shorten while Tert expression increases during ageing of the short-lived fish *Nothobranchius furzeri*', *Mech Ageing Dev*, 130: 290-6.
- Hartmann, N., K. Reichwald, I. Wittig, S. Droese, S. Schmeisser, C. Luck, C. Hahn, M. Graf, U. Gausmann, E. Terzibasi, A. Cellerino, M. Ristow, U. Brandt, M. Platzer, and C. Englert. 2011. 'Mitochondrial DNA copy number and function decrease with age in the short-lived fish *Nothobranchius furzeri*', *Aging Cell*, 10: 824-31.
- Hayflick, L., and P. S. Moorhead. 1961. 'The serial cultivation of human diploid cell strains', *Exp Cell Res*, 25: 585-621.
- He, S. H., and N. E. Sharpless. 2017. 'Senescence in Health and Disease', *Cell*, 169: 1000-11.
- Hernandez-Segura, A., J. Nehme, and M. Demaria. 2018. 'Hallmarks of Cellular Senescence', *Trends Cell Biol*, 28: 436-53.
- Ho, S. H., G. M. So, and K. L. Chow. 2001. 'Postembryonic expression of *Caenorhabditis elegans* mab-21 and its requirement in sensory ray differentiation', *Dev Dyn*, 221: 422-30.
- Hoare, M., Y. Ito, T. W. Kang, M. P. Weekes, N. J. Matheson, D. A. Patten, S. Shetty, A. J. Parry, S. Menon, R. Salama, R. Antrobus, K. Tomimatsu, W. Howat, P. J. Lehner, L. Zender, and M. Narita. 2016. 'NOTCH1 mediates a switch between two distinct secretomes during senescence', *Nat Cell Biol*, 18: 979-92.
- Holm, C. K., S. B. Jensen, M. R. Jakobsen, N. Cheshenko, K. A. Horan, H. B. Moeller, R. Gonzalez-Dosal, S. B. Rasmussen, M. H. Christensen, T. O. Yarovinsky, F. J. Rixon, B. C. Herold, K. A. Fitzgerald, and S. R. Paludan. 2012. 'Virus-cell fusion as a trigger of innate immunity dependent on the adaptor STING', *Nat Immunol*, 13: 737-43.
- Holzenberger, M., J. Dupont, B. Ducos, P. Leneuve, A. Geloën, P. C. Even, P. Cervera, and Y. Le Bouc. 2003. 'IGF-1 receptor regulates lifespan and resistance to oxidative stress in mice', *Nature*, 421: 182-7.
- Hopkins, J. W., K. B. Sulka, M. Sawden, K. A. Carroll, R. D. Brown, S. C. Bunnell, A. Poltorak, A. Tai, E. R. Reed, and S. Sharma. 2024. 'STING promotes homeostatic maintenance of tissues and confers longevity with aging', *bioRxiv*.
- Horvath, S. 2015. 'Erratum to: DNA methylation age of human tissues and cell types', *Genome Biol*, 16: 96.
- Horvath, S., A. Haghani, N. Macoretti, J. Abulaeva, J. A. Zoller, C. Z. Li, J. Zhang, M. Takasugi, Y. Zhao, E. Rydkina, Z. Zhang, S. Emmrich, K. Raj, A. Seluanov, C. G. Faulkes, and V.

- Gorbunova. 2022. 'DNA methylation clocks tick in naked mole rats but queens age more slowly than nonbreeders', *Nat Aging*, 2: 46-59.
- Horvath, S., Y. Zhang, P. Langfelder, R. S. Kahn, M. P. Boks, K. van Eijk, L. H. van den Berg, and R. A. Ophoff. 2012. 'Aging effects on DNA methylation modules in human brain and blood tissue', *Genome Biol*, 13: R97.
- Hou, Y., Z. Wang, P. Liu, X. Wei, Z. Zhang, S. Fan, L. Zhang, F. Han, Y. Song, L. Chu, and C. Zhang. 2023. 'SMPDL3A is a cGAMP-degrading enzyme induced by LXR-mediated lipid metabolism to restrict cGAS-STING DNA sensing', *Immunity*, 56: 2492-507 e10.
- Hu, B., C. Jin, H. B. Li, J. Tong, X. Ouyang, N. M. Cetinbas, S. Zhu, T. Strowig, F. C. Lam, C. Zhao, J. Henao-Mejia, O. Yilmaz, K. A. Fitzgerald, S. C. Eisenbarth, E. Elinav, and R. A. Flavell. 2016. 'The DNA-sensing AIM2 inflammasome controls radiation-induced cell death and tissue injury', *Science*, 354: 765-68.
- Hu, C. K., W. Wang, J. Brind'Amour, P. P. Singh, G. A. Reeves, M. C. Lorincz, A. S. Alvarado, and A. Brunet. 2020. 'Vertebrate diapause preserves organisms long term through Polycomb complex members', *Science*, 367: 870-74.
- Hu, J., F. J. Sanchez-Rivera, Z. Wang, G. N. Johnson, Y. J. Ho, K. Ganesh, S. Umeda, S. Gan, A. M. Mujal, R. B. Delconte, J. P. Hampton, H. Zhao, S. Kottapalli, E. de Stanchina, C. A. Iacobuzio-Donahue, D. Pe'er, S. W. Lowe, J. C. Sun, and J. Massague. 2023. 'STING inhibits the reactivation of dormant metastasis in lung adenocarcinoma', *Nature*, 616: 806-13.
- Huang, S., J. M. Rutkowski, R. G. Snodgrass, K. D. Ono-Moore, D. A. Schneider, J. W. Newman, S. H. Adams, and D. H. Hwang. 2012. 'Saturated fatty acids activate TLR-mediated proinflammatory signaling pathways', *J Lipid Res*, 53: 2002-13.
- Huang, W., L. J. Hickson, A. Eirin, J. L. Kirkland, and L. O. Lerman. 2022. 'Cellular senescence: the good, the bad and the unknown', *Nat Rev Nephrol*, 18: 611-27.
- Idda, M. L., W. G. McClusky, V. Lodde, R. Munk, K. Abdelmohsen, M. Rossi, and M. Gorospe. 2020. 'Survey of senescent cell markers with age in human tissues', *Aging (Albany NY)*, 12: 4052-66.
- Indra, A. K., X. Warot, J. Brocard, J. M. Bornert, J. H. Xiao, P. Chambon, and D. Metzger. 1999. 'Temporally-controlled site-specific mutagenesis in the basal layer of the epidermis: comparison of the recombinase activity of the tamoxifen-inducible Cre-ER(T) and Cre-ER(T2) recombinases', *Nucleic Acids Res*, 27: 4324-7.
- Irving, A. T., M. Ahn, G. Goh, D. E. Anderson, and L. F. Wang. 2021. 'Lessons from the host defences of bats, a unique viral reservoir', *Nature*, 589: 363-70.
- Ito, T., Y. V. Teo, S. A. Evans, N. Neretti, and J. M. Sedivy. 2018. 'Regulation of Cellular Senescence by Polycomb Chromatin Modifiers through Distinct DNA Damage- and Histone Methylation-Dependent Pathways', *Cell Rep*, 22: 3480-92.
- Ito, Y., M. Hoare, and M. Narita. 2017. 'Spatial and Temporal Control of Senescence', *Trends Cell Biol*, 27: 820-32.
- Ivanov, A., J. Pawlikowski, I. Manoharan, J. van Tuyn, D. M. Nelson, T. S. Rai, P. P. Shah, G. Hewitt, V. I. Korolchuk, J. F. Passos, H. Wu, S. L. Berger, and P. D. Adams. 2013. 'Lysosome-mediated processing of chromatin in senescence', *J Cell Biol*, 202: 129-43.
- Jagger, C., C. Gillies, F. Moscone, E. Cambois, H. Van Oyen, W. Nusselder, J. M. Robine, and Ehleis team. 2008. 'Inequalities in healthy life years in the 25 countries of the European Union in 2005: a cross-national meta-regression analysis', *Lancet*, 372: 2124-31.

- Jahandideh, B., M. Derakhshani, H. Abbaszadeh, A. Akbar Movassaghpour, A. Mehdizadeh, M. Talebi, and M. Yousefi. 2020. 'The pro-Inflammatory cytokines effects on mobilization, self-renewal and differentiation of hematopoietic stem cells', *Hum Immunol*, 81: 206-17.
- Jahanian, S., M. Pareja-Cajiao, H. M. Gransee, G. C. Sieck, and C. B. Mantilla. 2024. 'Autophagy markers LC3 and p62 in aging lumbar motor neurons', *Exp Gerontol*, 194: 112483.
- Jiang, H., X. Xue, S. Panda, A. Kawale, R. M. Hooy, F. Liang, J. Sohn, P. Sung, and N. O. Gekara. 2019. 'Chromatin-bound cGAS is an inhibitor of DNA repair and hence accelerates genome destabilization and cell death', *EMBO J*, 38: e102718.
- Jin, H., Y. Zhang, Q. Ding, S. S. Wang, P. Rastogi, D. F. Dai, D. Lu, M. Purvis, C. Cao, A. Wang, D. Liu, C. Ren, S. Elhadi, M. C. Hu, Y. Chai, D. Zepeda-Orozco, J. Campisi, and M. Attanasio. 2019. 'Epithelial innate immunity mediates tubular cell senescence after kidney injury', *JCI Insight*, 4.
- Jin, L., P. M. Waterman, K. R. Jonscher, C. M. Short, N. A. Reisdorph, and J. C. Cambier. 2008. 'MPYS, a novel membrane tetraspanner, is associated with major histocompatibility complex class II and mediates transduction of apoptotic signals', *Mol Cell Biol*, 28: 5014-26.
- Johnson, T. E. 1990. 'Increased life-span of age-1 mutants in *Caenorhabditis elegans* and lower Gompertz rate of aging', *Science*, 249: 908-12.
- Kampkotter, A., C. Timpel, R. F. Zurawski, S. Ruhl, Y. Chovolou, P. Proksch, and W. Watjen. 2008. 'Increase of stress resistance and lifespan of *Caenorhabditis elegans* by quercetin', *Comp Biochem Physiol B Biochem Mol Biol*, 149: 314-23.
- Kang, C., Q. Xu, T. D. Martin, M. Z. Li, M. Demaria, L. Aron, T. Lu, B. A. Yankner, J. Campisi, and S. J. Elledge. 2015. 'The DNA damage response induces inflammation and senescence by inhibiting autophagy of GATA4', *Science*, 349: aaa5612.
- Kaplon, J., L. Zheng, K. Meissl, B. Chaneton, V. A. Selivanov, G. Mackay, S. H. van der Burg, E. M. Verdegaal, M. Cascante, T. Shlomi, E. Gottlieb, and D. S. Peeper. 2013. 'A key role for mitochondrial gatekeeper pyruvate dehydrogenase in oncogene-induced senescence', *Nature*, 498: 109-12.
- Kaur, E., R. Agrawal, and S. Sengupta. 2021. 'Functions of BLM Helicase in Cells: Is It Acting Like a Double-Edged Sword?', *Front Genet*, 12: 634789.
- Kell, M. J., R. E. Riccio, E. A. Baumgartner, Z. J. Compton, P. J. Pecorin, T. A. Mitchell, J. Topczewski, and E. E. LeClair. 2018. 'Targeted deletion of the zebrafish actin-bundling protein L-plastin (*lcp1*)', *PLoS One*, 13: e0190353.
- Kelmer Sacramento, E., J. M. Kirkpatrick, M. Mazzetto, M. Baumgart, A. Bartolome, S. Di Sanzo, C. Caterino, M. Sanguanini, N. Papaevgeniou, M. Lefaki, D. Childs, S. Bagnoli, E. Terzibasi Tozzini, D. Di Fraia, N. Romanov, P. H. Sudmant, W. Huber, N. Chondrogianni, M. Vendruscolo, A. Cellerino, and A. Ori. 2020. 'Reduced proteasome activity in the aging brain results in ribosome stoichiometry loss and aggregation', *Mol Syst Biol*, 16: e9596.
- Kenyon, C., J. Chang, E. Gensch, A. Rudner, and R. Tabtiang. 1993. 'A *C. elegans* mutant that lives twice as long as wild type', *Nature*, 366: 461-4.
- Kenyon, C. J. 2010. 'The genetics of ageing', *Nature*, 464: 504-12.
- Kim, E. Y., A. Basit, W. J. Kim, E. B. Ko, and J. H. Lee. 2023. 'Multi-functional regulation of cGAS by the nuclear localization signal2 (NLS2) motif: Nuclear localization, enzyme activity and protein degradation', *Biochem Biophys Res Commun*, 673: 1-8.

- Kim, K. H., C. C. Chen, R. I. Monzon, and L. F. Lau. 2013. 'Matricellular protein CCN1 promotes regression of liver fibrosis through induction of cellular senescence in hepatic myofibroblasts', *Mol Cell Biol*, 33: 2078-90.
- Kim, Y., H. G. Nam, and D. R. Valenzano. 2016. 'The short-lived African turquoise killifish: an emerging experimental model for ageing', *Dis Model Mech*, 9: 115-29.
- King, K. R., A. D. Aguirre, Y. X. Ye, Y. Sun, J. D. Roh, R. P. Ng, Jr., R. H. Kohler, S. P. Arlauckas, Y. Iwamoto, A. Savol, R. I. Sadreyev, M. Kelly, T. P. Fitzgibbons, K. A. Fitzgerald, T. Mitchison, P. Libby, M. Nahrendorf, and R. Weissleder. 2017. 'IRF3 and type I interferons fuel a fatal response to myocardial infarction', *Nat Med*, 23: 1481-87.
- Kirschner, J., D. Weber, C. Neuschl, A. Franke, M. Bottger, L. Zielke, E. Powalsky, M. Groth, D. Shagin, A. Petzold, N. Hartmann, C. Englert, G. A. Brockmann, M. Platzner, A. Cellerino, and K. Reichwald. 2012. 'Mapping of quantitative trait loci controlling lifespan in the short-lived fish *Nothobranchius furzeri*--a new vertebrate model for age research', *Aging Cell*, 11: 252-61.
- Kong, L. Z., S. M. Kim, C. Wang, S. Y. Lee, S. C. Oh, S. Lee, S. Jo, and T. D. Kim. 2023. 'Understanding nucleic acid sensing and its therapeutic applications', *Exp Mol Med*, 55: 2320-31.
- Kotsantis, P., E. Petermann, and S. J. Boulton. 2018. 'Mechanisms of Oncogene-Induced Replication Stress: Jigsaw Falling into Place', *Cancer Discov*, 8: 537-55.
- Kounatidis, I., S. Chtarbanova, Y. Cao, M. Hayne, D. Jayanth, B. Ganetzky, and P. Ligoxygakis. 2017. 'NF-kappaB Immunity in the Brain Determines Fly Lifespan in Healthy Aging and Age-Related Neurodegeneration', *Cell Rep*, 19: 836-48.
- Kowarz, E., D. Loscher, and R. Marschalek. 2015. 'Optimized Sleeping Beauty transposons rapidly generate stable transgenic cell lines', *Biotechnol J*, 10: 647-53.
- Kranzusch, P. J., A. S. Lee, J. M. Berger, and J. A. Doudna. 2013. 'Structure of human cGAS reveals a conserved family of second-messenger enzymes in innate immunity', *Cell Rep*, 3: 1362-8.
- Kranzusch, P. J., S. C. Wilson, A. S. Lee, J. M. Berger, J. A. Doudna, and R. E. Vance. 2015. 'Ancient Origin of cGAS-STING Reveals Mechanism of Universal 2',3' cGAMP Signaling', *Mol Cell*, 59: 891-903.
- Krizhanovsky, V., M. Yon, R. A. Dickins, S. Hearn, J. Simon, C. Miething, H. Yee, L. Zender, and S. W. Lowe. 2008. 'Senescence of activated stellate cells limits liver fibrosis', *Cell*, 134: 657-67.
- Kuchitsu, Y., K. Mukai, R. Uematsu, Y. Takaada, A. Shinojima, R. Shindo, T. Shoji, S. Hamano, E. Ogawa, R. Sato, K. Miyake, A. Kato, Y. Kawaguchi, M. Nishitani-Isa, K. Izawa, R. Nishikomori, T. Yasumi, T. Suzuki, N. Dohmae, T. Uemura, G. N. Barber, H. Arai, S. Waguri, and T. Taguchi. 2023. 'STING signalling is terminated through ESCRT-dependent microautophagy of vesicles originating from recycling endosomes', *Nat Cell Biol*, 25: 453-66.
- Kujirai, T., C. Zierhut, Y. Takizawa, R. Kim, L. Negishi, N. Uruma, S. Hirai, H. Funabiki, and H. Kurumizaka. 2020. 'Structural basis for the inhibition of cGAS by nucleosomes', *Science*, 370: 455-58.
- Kuo, L. J., and L. X. Yang. 2008. 'Gamma-H2AX - a novel biomarker for DNA double-strand breaks', *In Vivo*, 22: 305-9.
- Kwon, S. M., S. M. Hong, Y. K. Lee, S. Min, and G. Yoon. 2019. 'Metabolic features and regulation in cell senescence', *BMB Rep*, 52: 5-12.
- Lagunas-Rangel, F. A. 2021. 'Deciphering the whale's secrets to have a long life', *Exp Gerontol*, 151: 111425.

- Langereis, M. A., H. H. Rabouw, M. Holwerda, L. J. Visser, and F. J. van Kuppeveld. 2015. 'Knockout of cGAS and STING Rescues Virus Infection of Plasmid DNA-Transfected Cells', *J Virol*, 89: 11169-73.
- Lawrence, M., A. Goyal, S. Pathak, and P. Ganguly. 2024. 'Cellular Senescence and Inflammaging in the Bone: Pathways, Genetics, Anti-Aging Strategies and Interventions', *Int J Mol Sci*, 25.
- Li, D., W. Yang, J. Ren, Y. Ru, K. Zhang, S. Fu, X. Liu, and H. Zheng. 2019. 'The E3 Ubiquitin Ligase TBK1 Mediates the Degradation of Multiple Picornavirus VP3 Proteins by Phosphorylation and Ubiquitination', *J Virol*, 93.
- Li, L., Q. Yin, P. Kuss, Z. Maliga, J. L. Millan, H. Wu, and T. J. Mitchison. 2015. 'Erratum: Hydrolysis of 2'3'-cGAMP by ENPP1 and design of nonhydrolyzable analogs', *Nat Chem Biol*, 11: 741.
- Li, Q., S. Tian, J. Liang, J. Fan, J. Lai, and Q. Chen. 2021. 'Therapeutic Development by Targeting the cGAS-STING Pathway in Autoimmune Disease and Cancer', *Front Pharmacol*, 12: 779425.
- Li, X. D., J. Wu, D. Gao, H. Wang, L. Sun, and Z. J. Chen. 2013. 'Pivotal roles of cGAS-cGAMP signaling in antiviral defense and immune adjuvant effects', *Science*, 341: 1390-4.
- Li, X., C. Li, W. Zhang, Y. Wang, P. Qian, and H. Huang. 2023. 'Inflammation and aging: signaling pathways and intervention therapies', *Signal Transduct Target Ther*, 8: 239.
- Li, X., X. Li, C. Xie, S. Cai, M. Li, H. Jin, S. Wu, J. Cui, H. Liu, and Y. Zhao. 2022. 'cGAS guards against chromosome end-to-end fusions during mitosis and facilitates replicative senescence', *Protein Cell*, 13: 47-64.
- Li, X., C. Shu, G. Yi, C. T. Chaton, C. L. Shelton, J. Diao, X. Zuo, C. C. Kao, A. B. Herr, and P. Li. 2013. 'Cyclic GMP-AMP synthase is activated by double-stranded DNA-induced oligomerization', *Immunity*, 39: 1019-31.
- Liang, C., Q. Ke, Z. Liu, J. Ren, W. Zhang, J. Hu, Z. Wang, H. Chen, K. Xia, X. Lai, Q. Wang, K. Yang, W. Li, Z. Wu, C. Wang, H. Yan, X. Jiang, Z. Ji, M. Ma, X. Long, S. Wang, H. Wang, H. Sun, J. C. I. Belmonte, J. Qu, A. P. Xiang, and G. H. Liu. 2022. 'BMAL1 moonlighting as a gatekeeper for LINE1 repression and cellular senescence in primates', *Nucleic Acids Res*, 50: 3323-47.
- Liang, H., L. Deng, Y. Hou, X. Meng, X. Huang, E. Rao, W. Zheng, H. Mauceri, M. Mack, M. Xu, Y. X. Fu, and R. R. Weichselbaum. 2017. 'Host STING-dependent MDSC mobilization drives extrinsic radiation resistance', *Nat Commun*, 8: 1736.
- Lin, B., R. Berard, A. Al Rasheed, B. Aladba, P. J. Kranzusch, M. Henderlight, A. Grom, D. Kahle, S. Torreggiani, A. G. Aue, J. Mitchell, A. A. de Jesus, G. S. Schulert, and R. Goldbach-Mansky. 2020. 'A novel STING1 variant causes a recessive form of STING-associated vasculopathy with onset in infancy (SAVI)', *J Allergy Clin Immunol*, 146: 1204-08 e6.
- Liu, D., H. Zhang, Y. P. Huang, and Y. Q. Gao. 2023. 'Investigating the Activation Mechanism Differences between Human and Mouse cGAS by Molecular Dynamics Simulations', *J Phys Chem B*, 127: 5034-45.
- Liu, H., S. Ghosh, T. Vaidya, S. Bammidi, C. Huang, P. Shang, A. P. Nair, O. Chowdhury, N. A. Stepicheva, A. Strizhakova, S. Hose, N. Mitrousis, S. G. Gadde, T. Mb, P. Strassburger, G. Widmer, E. M. Lad, P. E. Fort, J. A. Sahel, J. S. Zigler, Jr., S. Sethu, P. D. Westenskow, A. D. Proia, A. Sodhi, A. Ghosh, D. Feenstra, and D. Sinha. 2023. 'Activated cGAS/STING signaling elicits endothelial cell senescence in early diabetic retinopathy', *JCI Insight*, 8.

- Liu, H., Z. Yan, D. Zhu, H. Xu, F. Liu, T. Chen, H. Zhang, Y. Zheng, B. Liu, L. Zhang, W. Zhao, and C. Gao. 2023. 'CD-NTase family member MB21D2 promotes cGAS-mediated antiviral and antitumor immunity', *Cell Death Differ*, 30: 992-1004.
- Liu, H., H. Zhang, X. Wu, D. Ma, J. Wu, L. Wang, Y. Jiang, Y. Fei, C. Zhu, R. Tan, P. Jungblut, G. Pei, A. Dorhoi, Q. Yan, F. Zhang, R. Zheng, S. Liu, H. Liang, Z. Liu, H. Yang, J. Chen, P. Wang, T. Tang, W. Peng, Z. Hu, Z. Xu, X. Huang, J. Wang, H. Li, Y. Zhou, F. Liu, D. Yan, S. H. E. Kaufmann, C. Chen, Z. Mao, and B. Ge. 2018. 'Nuclear cGAS suppresses DNA repair and promotes tumorigenesis', *Nature*, 563: 131-36.
- Liu, S., X. Cai, J. Wu, Q. Cong, X. Chen, T. Li, F. Du, J. Ren, Y. T. Wu, N. V. Grishin, and Z. J. Chen. 2015. 'Phosphorylation of innate immune adaptor proteins MAVS, STING, and TRIF induces IRF3 activation', *Science*, 347: aaa2630.
- Liu, Z. F., J. F. Ji, X. F. Jiang, T. Shao, D. D. Fan, X. H. Jiang, A. F. Lin, L. X. Xiang, and J. Z. Shao. 2020. 'Characterization of cGAS homologs in innate and adaptive mucosal immunities in zebrafish gives evolutionary insights into cGAS-STING pathway', *FASEB J*, 34: 7786-809.
- Lopez-Otin, C., M. A. Blasco, L. Partridge, M. Serrano, and G. Kroemer. 2023. 'Hallmarks of aging: An expanding universe', *Cell*, 186: 243-78.
- Love, M. I., W. Huber, and S. Anders. 2014. 'Moderated estimation of fold change and dispersion for RNA-seq data with DESeq2', *Genome Biol*, 15: 550.
- Lu, J., T. Wu, B. Zhang, S. Liu, W. Song, J. Qiao, and H. Ruan. 2021. 'Types of nuclear localization signals and mechanisms of protein import into the nucleus', *Cell Commun Signal*, 19: 60.
- Luteijn, R. D., S. A. Zaver, B. G. Gowen, S. K. Wyman, N. E. Garelis, L. Onia, S. M. McWhirter, G. E. Katibah, J. E. Corn, J. J. Woodward, and D. H. Raulet. 2020. 'Author Correction: SLC19A1 transports immunoreactive cyclic dinucleotides', *Nature*, 579: E12.
- Lv, B., W. A. Dion, H. Yang, J. Xun, D. H. Kim, B. Zhu, and J. X. Tan. 2024. 'A TBK1-independent primordial function of STING in lysosomal biogenesis', *Mol Cell*, 84: 3979-96 e9.
- Mackenzie, K. J., P. Carroll, C. A. Martin, O. Murina, A. Fluteau, D. J. Simpson, N. Olova, H. Sutcliffe, J. K. Rainger, A. Leitch, R. T. Osborn, A. P. Wheeler, M. Nowotny, N. Gilbert, T. Chandra, M. A. M. Reijns, and A. P. Jackson. 2017. 'cGAS surveillance of micronuclei links genome instability to innate immunity', *Nature*, 548: 461-65.
- Mankan, A. K., T. Schmidt, D. Chauhan, M. Goldeck, K. Honing, M. Gaidt, A. V. Kubarenko, L. Andreeva, K. P. Hopfner, and V. Hornung. 2014. 'Cytosolic RNA:DNA hybrids activate the cGAS-STING axis', *EMBO J*, 33: 2937-46.
- Mao, Z., M. Bozzella, A. Seluanov, and V. Gorbunova. 2008. 'Comparison of nonhomologous end joining and homologous recombination in human cells', *DNA Repair (Amst)*, 7: 1765-71.
- Marechal, A., and L. Zou. 2013. 'DNA damage sensing by the ATM and ATR kinases', *Cold Spring Harb Perspect Biol*, 5.
- Margolis, S. R., P. A. Dietzen, B. M. Hayes, S. C. Wilson, B. C. Remick, S. Chou, and R. E. Vance. 2021. 'The cyclic dinucleotide 2'3'-cGAMP induces a broad antibacterial and antiviral response in the sea anemone *Nematostella vectensis*', *Proc Natl Acad Sci USA*, 118.
- Markofsky, J., and J. R. Matias. 1977. 'The effects of temperature and season of collection on the onset and duration of diapause in embryos of the annual fish *Nothobranchius guentheri*', *J Exp Zool*, 202: 49-56.
- Martinez, J. C., F. Morandini, L. Fitzgibbons, N. Sieczkiewicz, S. J. Bae, M. E. Meadow, E. Hillpot, J. Cutting, V. Paige, S. A. Biashad, M. Simon, J. Sedivy, A. Seluanov, and V.



- Gorbunova. 2024. 'cGAS deficient mice display premature aging associated with de-repression of LINE1 elements and inflammation', *bioRxiv*.
- Martinez, John C. 2024, under review. 'cGAS deficient mice display premature aging associated with loss of chromatin organization, derepression of LINE1 elements and induction of inflammation', *Nat Aging*.
- Mathuru, A. S. 2022. 'The holy grail of longevity research', *Elife*, 11.
- Matthews, J. L. 2004. 'Common diseases of laboratory zebrafish', *Methods Cell Biol*, 77: 617-43.
- Mazhar, M., A. U. Din, H. Ali, G. Yang, W. Ren, L. Wang, X. Fan, and S. Yang. 2021. 'Implication of ferroptosis in aging', *Cell Death Discov*, 7: 149.
- McKay, A., E. K. Costa, J. Chen, C. K. Hu, X. Chen, C. N. Bedbrook, R. C. Khondker, M. Thielvoldt, P. Priya Singh, T. Wyss-Coray, and A. Brunet. 2022. 'An automated feeding system for the African killifish reveals the impact of diet on lifespan and allows scalable assessment of associative learning', *Elife*, 11.
- McManus, K. J., and M. J. Hendzel. 2005. 'ATM-dependent DNA damage-independent mitotic phosphorylation of H2AX in normally growing mammalian cells', *Mol Biol Cell*, 16: 5013-25.
- Melk, A., W. Kittikowit, I. Sandhu, K. M. Halloran, P. Grimm, B. M. Schmidt, and P. F. Halloran. 2003. 'Cell senescence in rat kidneys in vivo increases with growth and age despite lack of telomere shortening', *Kidney Int*, 63: 2134-43.
- Meyer, D. H., and B. Schumacher. 2021. 'BiT age: A transcriptome-based aging clock near the theoretical limit of accuracy', *Aging Cell*, 20: e13320.
- Mijit, M., V. Caracciolo, A. Melillo, F. Amicarelli, and A. Giordano. 2020. 'Role of p53 in the Regulation of Cellular Senescence', *Biomolecules*, 10.
- Minhas, P. S., A. Latif-Hernandez, M. R. McReynolds, A. S. Durairaj, Q. Wang, A. Rubin, A. U. Joshi, J. Q. He, E. Gauba, L. Liu, C. Wang, M. Linde, Y. Sugiura, P. K. Moon, R. Majeti, M. Suematsu, D. Mochly-Rosen, I. L. Weissman, F. M. Longo, J. D. Rabinowitz, and K. I. Andreasson. 2021. 'Restoring metabolism of myeloid cells reverses cognitive decline in ageing', *Nature*, 590: 122-28.
- Mohammed, S., N. Thadathil, R. Selvarani, E. H. Nicklas, D. Wang, B. F. Miller, A. Richardson, and S. S. Deepa. 2021. 'Necroptosis contributes to chronic inflammation and fibrosis in aging liver', *Aging Cell*, 20: e13512.
- Moiseeva, O., X. Deschenes-Simard, E. St-Germain, S. Igelmann, G. Huot, A. E. Cadar, V. Bourdeau, M. N. Pollak, and G. Ferbeyre. 2013. 'Metformin inhibits the senescence-associated secretory phenotype by interfering with IKK/NF-kappaB activation', *Aging Cell*, 12: 489-98.
- Moiseeva, V., A. Cisneros, V. Sica, O. Deryagin, Y. Lai, S. Jung, E. Andres, J. An, J. Segales, L. Ortet, V. Lukesova, G. Volpe, A. Benguria, A. Dopazo, S. A. Benitah, Y. Urano, A. Del Sol, M. A. Esteban, Y. Ohkawa, A. L. Serrano, E. Perdiguero, and P. Munoz-Canoves. 2023. 'Author Correction: Senescence atlas reveals an aged-like inflamed niche that blunts muscle regeneration', *Nature*, 614: E45.
- Mootha, V. K., C. M. Lindgren, K. F. Eriksson, A. Subramanian, S. Sihag, J. Lehar, P. Puigserver, E. Carlsson, M. Ridderstrale, E. Laurila, N. Houstis, M. J. Daly, N. Patterson, J. P. Mesirov, T. R. Golub, P. Tamayo, B. Spiegelman, E. S. Lander, J. N. Hirschhorn, D. Altshuler, and L. C. Groop. 2003. 'PGC-1alpha-responsive genes involved in oxidative phosphorylation are coordinately downregulated in human diabetes', *Nat Genet*, 34: 267-73.
- Morabito, Gabriele, Handan Melike Dönertas, Luca Sperti, Jens Seidel, Aysan Poursadegh, Michael Poeschla, and Dario Riccardo Valenzano. 2023. 'Spontaneous onset of

- cellular markers of inflammation and genome instability during aging in the immune niche of the naturally short-lived turquoise killifish (*Nothobranchius furzeri*), *bioRxiv*: 2023.02.06.527346.
- Moretti, J., S. Roy, D. Bozec, J. Martinez, J. R. Chapman, B. Ueberheide, D. W. Lamming, Z. J. Chen, T. Horng, G. Yeretssian, D. R. Green, and J. M. Blander. 2017. 'STING Senses Microbial Viability to Orchestrate Stress-Mediated Autophagy of the Endoplasmic Reticulum', *Cell*, 171: 809-23 e13.
- Moses, E., R. Franek, and I. Harel. 2023. 'A scalable and tunable platform for functional interrogation of peptide hormones in fish', *Elife*, 12.
- Motwani, M., S. Pesiridis, and K. A. Fitzgerald. 2019. 'DNA sensing by the cGAS-STING pathway in health and disease', *Nat Rev Genet*, 20: 657-74.
- Mukai, K., H. Konno, T. Akiba, T. Uemura, S. Waguri, T. Kobayashi, G. N. Barber, H. Arai, and T. Taguchi. 2016. 'Activation of STING requires palmitoylation at the Golgi', *Nat Commun*, 7: 11932.
- Munoz-Espin, D., and M. Serrano. 2014. 'Cellular senescence: from physiology to pathology', *Nat Rev Mol Cell Biol*, 15: 482-96.
- Nath, R. D., C. N. Bedbrook, R. Nagvekar, and A. Brunet. 2023. 'Husbandry of the African Turquoise Killifish *Nothobranchius furzeri*', *Cold Spring Harb Protoc*, 2023: pdb prot107738.
- Nguyen-Chi, M., B. Laplace-Builhe, J. Travnickova, P. Luz-Crawford, G. Tejedor, Q. T. Phan, I. Duroux-Richard, J. P. Levrard, K. Kissa, G. Lutfalla, C. Jorgensen, and F. Djouad. 2015. 'Identification of polarized macrophage subsets in zebrafish', *Elife*, 4: e07288.
- Niccoli, T., and L. Partridge. 2012. 'Ageing as a risk factor for disease', *Curr Biol*, 22: R741-52.
- O'Connell, R. M., S. K. Saha, S. A. Vaidya, K. W. Bruhn, G. A. Miranda, B. Zarnegar, A. K. Perry, B. O. Nguyen, T. F. Lane, T. Taniguchi, J. F. Miller, and G. Cheng. 2004. 'Type I interferon production enhances susceptibility to *Listeria monocytogenes* infection', *J Exp Med*, 200: 437-45.
- O'Reilly, S., P. S. Tsou, and J. Varga. 2024. 'Senescence and tissue fibrosis: opportunities for therapeutic targeting', *Trends Mol Med*, 30: 1113-25.
- Oginuma, M., M. Nishida, T. Ohmura-Adachi, K. Abe, S. Ogamino, C. Mogi, H. Matsui, and T. Ishitani. 2022. 'Rapid reverse genetics systems for *Nothobranchius furzeri*, a suitable model organism to study vertebrate aging', *Sci Rep*, 12: 11628.
- Oh, H. S., Y. Le Guen, N. Rappoport, D. Y. Urey, J. Rutledge, A. Brunet, M. D. Greicius, and T. Wyss-Coray. 2024. 'Plasma proteomics in the UK Biobank reveals youthful brains and immune systems promote healthspan and longevity', *bioRxiv*.
- Oh, H. S., J. Rutledge, D. Nachun, R. Palovics, O. Abiose, P. Moran-Losada, D. Channappa, D. Y. Urey, K. Kim, Y. J. Sung, L. Wang, J. Timsina, D. Western, M. Liu, P. Kohlfeld, J. Budde, E. N. Wilson, Y. Guen, T. M. Maurer, M. Haney, A. C. Yang, Z. He, M. D. Greicius, K. I. Andreasson, S. Sathyan, E. F. Weiss, S. Milman, N. Barzilai, C. Cruchaga, A. D. Wagner, E. Mormino, B. Lehallier, V. W. Henderson, F. M. Longo, S. B. Montgomery, and T. Wyss-Coray. 2023. 'Organ aging signatures in the plasma proteome track health and disease', *Nature*, 624: 164-72.
- Oka, K., M. Yamakawa, Y. Kawamura, N. Kutsukake, and K. Miura. 2023. 'The Naked Mole-Rat as a Model for Healthy Aging', *Annu Rev Anim Biosci*, 11: 207-26.
- Okamoto, S., H. Sakamoto, K. Kamimura, K. Komamura, E. Kobayashi, and J. Liang. 2023. 'Economic effects of healthy ageing: functional limitation, forgone wages, and medical and long-term care costs', *Health Econ Rev*, 13: 28.

- Oleksy, B., H. Mierzevska, J. Tryfon, M. Wypchlo, K. Wasilewska, Z. Zalewska-Miszkurka, R. Ploski, M. Rydzanicz, and E. Szczepanik. 2022. 'Aicardi-Goutieres Syndrome due to a SAMHD1 Mutation Presenting with Deep White Matter Cysts', *Mol Syndromol*, 13: 132-38.
- Olivieri, F., M. C. Albertini, M. Orciani, A. Ceka, M. Cricca, A. D. Procopio, and M. Bonafe. 2015. 'DNA damage response (DDR) and senescence: shuttled inflamma-miRNAs on the stage of inflamm-aging', *Oncotarget*, 6: 35509-21.
- Omori, S., T. W. Wang, Y. Johmura, T. Kanai, Y. Nakano, T. Kido, E. A. Susaki, T. Nakajima, S. Shichino, S. Ueha, M. Ozawa, K. Yokote, S. Kumamoto, A. Nishiyama, T. Sakamoto, K. Yamaguchi, S. Hatakeyama, E. Shimizu, K. Katayama, Y. Yamada, S. Yamazaki, K. Iwasaki, C. Miyoshi, H. Funato, M. Yanagisawa, H. Ueno, S. Imoto, Y. Furukawa, N. Yoshida, K. Matsushima, H. R. Ueda, A. Miyajima, and M. Nakanishi. 2020. 'Generation of a p16 Reporter Mouse and Its Use to Characterize and Target p16(high) Cells In Vivo', *Cell Metab*, 32: 814-28 e6.
- Orange, S. T., J. Leslie, M. Ross, D. A. Mann, and H. Wackerhage. 2023. 'The exercise IL-6 enigma in cancer', *Trends Endocrinol Metab*, 34: 749-63.
- Palliyaguru, D. L., C. Vieira Ligo Teixeira, E. Duregon, C. di Germanio, I. Alfaras, S. J. Mitchell, I. Navas-Enamorado, E. J. Shiroma, S. Studenski, M. Bernier, S. Camandola, N. L. Price, L. Ferrucci, and R. de Cabo. 2021. 'Study of Longitudinal Aging in Mice: Presentation of Experimental Techniques', *J Gerontol A Biol Sci Med Sci*, 76: 552-60.
- Pandey, S., T. Kawai, and S. Akira. 2014. 'Microbial sensing by Toll-like receptors and intracellular nucleic acid sensors', *Cold Spring Harb Perspect Biol*, 7: a016246.
- Park, J. T., Y. S. Lee, K. A. Cho, and S. C. Park. 2018. 'Adjustment of the lysosomal-mitochondrial axis for control of cellular senescence', *Ageing Res Rev*, 47: 176-82.
- Parrinello, S., E. Samper, A. Krtolica, J. Goldstein, S. Melov, and J. Campisi. 2003. 'Oxygen sensitivity severely limits the replicative lifespan of murine fibroblasts', *Nat Cell Biol*, 5: 741-7.
- Partridge, L., J. Deelen, and P. E. Slagboom. 2018. 'Facing up to the global challenges of ageing', *Nature*, 561: 45-56.
- Pawelec, G. 2018. 'Age and immunity: What is "immunosenescence"?', *Exp Gerontol*, 105: 4-9.
- Pech, M. F., A. Garbuzov, K. Hasegawa, M. Sukhwani, R. J. Zhang, B. A. Benayoun, S. A. Brockman, S. Lin, A. Brunet, K. E. Orwig, and S. E. Artandi. 2015. 'High telomerase is a hallmark of undifferentiated spermatogonia and is required for maintenance of male germline stem cells', *Genes Dev*, 29: 2420-34.
- Pilotto, A., D. Sancarolo, F. Panza, F. Paris, G. D'Onofrio, L. Cascavilla, F. Addante, D. Seripa, V. Solfrizzi, B. Dallapiccola, M. Franceschi, and L. Ferrucci. 2009. 'The Multidimensional Prognostic Index (MPI), based on a comprehensive geriatric assessment predicts short- and long-term mortality in hospitalized older patients with dementia', *J Alzheimers Dis*, 18: 191-9.
- Pioli, P. D., D. Casero, E. Montecino-Rodriguez, S. L. Morrison, and K. Dorshkind. 2019. 'Plasma Cells Are Obligate Effectors of Enhanced Myelopoiesis in Aging Bone Marrow', *Immunity*, 51: 351-66 e6.
- Plasilova, M., C. Chattopadhyay, A. Ghosh, F. Wenzel, P. Demougin, C. Noppen, N. Schaub, G. Szinnai, L. Terracciano, and K. Heinemann. 2011. 'Discordant gene expression signatures and related phenotypic differences in lamin A- and A/C-related Hutchinson-Gilford progeria syndrome (HGPS)', *PLoS One*, 6: e21433.

- Polacik, M., R. Blazek, and M. Reichard. 2016. 'Laboratory breeding of the short-lived annual killifish *Nothobranchius furzeri*', *Nat Protoc*, 11: 1396-413.
- Quek, H., J. Luff, K. Cheung, S. Kozlov, M. Gatei, C. S. Lee, M. C. Bellingham, P. G. Noakes, Y. C. Lim, N. L. Barnett, S. Dingwall, E. Wolvetang, T. Mashimo, T. L. Roberts, and M. F. Lavin. 2017. 'A rat model of ataxia-telangiectasia: evidence for a neurodegenerative phenotype', *Hum Mol Genet*, 26: 109-23.
- Ragonnaud, E., and A. Biragyn. 2021. 'Gut microbiota as the key controllers of "healthy" aging of elderly people', *Immun Ageing*, 18: 2.
- Rayess, H., M. B. Wang, and E. S. Srivatsan. 2012. 'Cellular senescence and tumor suppressor gene p16', *Int J Cancer*, 130: 1715-25.
- Reichwald, K., C. Lauber, I. Nanda, J. Kirschner, N. Hartmann, S. Schories, U. Gausmann, S. Taudien, M. B. Schilhabel, K. Szafranski, G. Glockner, M. Schmid, A. Cellerino, M. Scharl, C. Englert, and M. Platzer. 2009. 'High tandem repeat content in the genome of the short-lived annual fish *Nothobranchius furzeri*: a new vertebrate model for aging research', *Genome Biol*, 10: R16.
- Reichwald, K., A. Petzold, P. Koch, B. R. Downie, N. Hartmann, S. Pietsch, M. Baumgart, D. Chalopin, M. Felder, M. Bens, A. Sahm, K. Szafranski, S. Taudien, M. Groth, I. Arisi, A. Weise, S. S. Bhatt, V. Sharma, J. M. Kraus, F. Schmid, S. Priebe, T. Liehr, M. Gorlach, M. E. Than, M. Hiller, H. A. Kestler, J. N. Volff, M. Scharl, A. Cellerino, C. Englert, and M. Platzer. 2015. 'Insights into Sex Chromosome Evolution and Aging from the Genome of a Short-Lived Fish', *Cell*, 163: 1527-38.
- Reyes, A., G. Ortiz, L. F. Duarte, C. Fernandez, R. Hernandez-Armengol, P. A. Palacios, Y. Prado, C. A. Andrade, L. Rodriguez-Guilarte, A. M. Kalergis, F. Simon, L. J. Carreno, C. A. Riedel, M. Caceres, and P. A. Gonzalez. 2023. 'Contribution of viral and bacterial infections to senescence and immunosenescence', *Front Cell Infect Microbiol*, 13: 1229098.
- Rice, G. I., C. Meyzer, N. Bouazza, M. Hully, N. Boddaert, M. Semeraro, L. A. H. Zeef, F. Rozenberg, V. Bondet, D. Duffy, A. Llibre, J. Baek, M. N. Sambe, E. Henry, V. Jolaine, C. Barnerias, M. Barth, A. Belot, C. Cances, F. G. Debray, D. Doummar, M. L. Fremond, N. Kitabayashi, A. Lepelley, V. Levrat, I. Melki, P. Meyer, M. C. Nougues, F. Renaldo, M. P. Rodero, D. Rodriguez, A. Roubertie, L. Seabra, C. Ugenti, H. Abdoul, J. M. Treluyer, I. Desguerre, S. Blanche, and Y. J. Crow. 2018. 'Reverse-Transcriptase Inhibitors in the Aicardi-Goutieres Syndrome', *N Engl J Med*, 379: 2275-7.
- Ripa, R., E. Ballhysa, J. D. Steiner, R. Laboy, A. Annibal, N. Hochhard, C. Latza, L. Dolfi, C. Calabrese, A. M. Meyer, M. C. Polidori, R. U. Muller, and A. Antebi. 2023. 'Refeeding-associated AMPK(gamma1) complex activity is a hallmark of health and longevity', *Nat Aging*, 3: 1544-60.
- Ripa, R., A. Mesaros, O. Symmons, E. Ballhysa, L. Dolfi, and A. Antebi. 2023. 'Micro-CT Analysis of Fat in the Killifish *Nothobranchius furzeri*', *Cold Spring Harb Protoc*, 2023: 107884.
- Ritchie, C., A. F. Cordova, G. T. Hess, M. C. Bassik, and L. Li. 2019. 'SLC19A1 Is an Importer of the Immunotransmitter cGAMP', *Mol Cell*, 75: 372-81 e5.
- Robbins, E., E. M. Levine, and H. Eagle. 1970. 'Morphologic changes accompanying senescence of cultured human diploid cells', *J Exp Med*, 131: 1211-22.
- Rodgers, K., and M. McVey. 2016. 'Error-Prone Repair of DNA Double-Strand Breaks', *J Cell Physiol*, 231: 15-24.
- Rodier, F., D. P. Munoz, R. Teachenor, V. Chu, O. Le, D. Bhaumik, J. P. Coppe, E. Campeau, C. M. Beausejour, S. H. Kim, A. R. Davalos, and J. Campisi. 2011. 'DNA-SCARS: distinct

- nuclear structures that sustain damage-induced senescence growth arrest and inflammatory cytokine secretion', *J Cell Sci*, 124: 68-81.
- Rodwell, G. E., R. Sonu, J. M. Zahn, J. Lund, J. Wilhelmy, L. Wang, W. Xiao, M. Mindrinos, E. Crane, E. Segal, B. D. Myers, J. D. Brooks, R. W. Davis, J. Higgins, A. B. Owen, and S. K. Kim. 2004. 'A transcriptional profile of aging in the human kidney', *PLoS Biol*, 2: e427.
- Rogakou, E. P., D. R. Pilch, A. H. Orr, V. S. Ivanova, and W. M. Bonner. 1998. 'DNA double-stranded breaks induce histone H2AX phosphorylation on serine 139', *J Biol Chem*, 273: 5858-68.
- Rongvaux, A. 2018. 'Innate immunity and tolerance toward mitochondria', *Mitochondrion*, 41: 14-20.
- Rosas, L., N. D. P. Vanegas, M. Riley, E. L. Dale, V. Peters, S. D. Stacey, M. Kaestle, P. Seither, A. L. Mora, and M. Rojas. 2023. 'STING inhibitor ameliorates senescence via inhibiting cGAS-STING pathway in Idiopathic Pulmonary Fibrosis', *European Respiratory Journal*, 62.
- Rosoff, D. B., L. A. Mavromatis, A. S. Bell, J. Wagner, J. Jung, R. E. Marioni, G. Davey Smith, S. Horvath, and F. W. Lohoff. 2023. 'Multivariate genome-wide analysis of aging-related traits identifies novel loci and new drug targets for healthy aging', *Nat Aging*, 3: 1020-35.
- Rufini, A., P. Tucci, I. Celardo, and G. Melino. 2013. 'Senescence and aging: the critical roles of p53', *Oncogene*, 32: 5129-43.
- Ruparelia, A. A., A. Salavaty, C. K. Barlow, Y. Lu, C. Sonntag, L. Hersey, M. J. Eramo, J. Krug, H. Reuter, R. B. Schittenhelm, M. Ramialison, A. Cox, M. T. Ryan, D. J. Creek, C. Englert, and P. D. Currie. 2024. 'The African killifish: A short-lived vertebrate model to study the biology of sarcopenia and longevity', *Aging Cell*, 23: e13862.
- Salic, A., and T. J. Mitchison. 2008. 'A chemical method for fast and sensitive detection of DNA synthesis in vivo', *Proc Natl Acad Sci U S A*, 105: 2415-20.
- Salminen, A., J. Huuskonen, J. Ojala, A. Kauppinen, K. Kaarniranta, and T. Suuronen. 2008. 'Activation of innate immunity system during aging: NF-kB signaling is the molecular culprit of inflamm-aging', *Ageing Res Rev*, 7: 83-105.
- Samuels, D. C., E. A. Schon, and P. F. Chinnery. 2004. 'Two direct repeats cause most human mtDNA deletions', *Trends Genet*, 20: 393-8.
- Sanchez Alvarado, A. 2007. 'Stem cells and the Planarian *Schmidtea mediterranea*', *C R Biol*, 330: 498-503.
- Sato, Y., and M. Yanagita. 2019. 'Immunology of the ageing kidney', *Nat Rev Nephrol*, 15: 625-40.
- Saul, D., R. L. Kosinsky, E. J. Atkinson, M. L. Doolittle, X. Zhang, N. K. LeBrasseur, R. J. Pignolo, P. D. Robbins, L. J. Niedernhofer, Y. Ikeno, D. Jurk, J. F. Passos, L. J. Hickson, A. Xue, D. G. Monroe, T. Tchkonja, J. L. Kirkland, J. N. Farr, and S. Khosla. 2022. 'A new gene set identifies senescent cells and predicts senescence-associated pathways across tissues', *Nat Commun*, 13: 4827.
- Scheel, Jorgen J. 1990. *Atlas of Killifishes of the Old World* (TFH Publications).
- Schneider, W. M., M. D. Chevillotte, and C. M. Rice. 2014. 'Interferon-stimulated genes: a complex web of host defenses', *Annu Rev Immunol*, 32: 513-45.
- Schoetz, U., D. Klein, J. Hess, S. Shnayien, S. Spoerl, M. Orth, S. Mutlu, R. Hennel, A. Sieber, U. Ganswindt, B. Luka, A. R. Thomsen, K. Unger, V. Jendrosseck, H. Zitzelsberger, N. Bluthgen, C. Belka, S. Unkel, B. Klinger, and K. Lauber. 2021. 'Early senescence and production of senescence-associated cytokines are major determinants of

- radioresistance in head-and-neck squamous cell carcinoma', *Cell Death Dis*, 12: 1162.
- Schumacher, B., J. Pothof, J. Vijg, and J. H. J. Hoeijmakers. 2021. 'The central role of DNA damage in the ageing process', *Nature*, 592: 695-703.
- Segnani, C., C. Ippolito, L. Antonioli, C. Pellegrini, C. Blandizzi, A. Dolfi, and N. Bernardini. 2015. 'Histochemical Detection of Collagen Fibers by Sirius Red/Fast Green Is More Sensitive than van Gieson or Sirius Red Alone in Normal and Inflamed Rat Colon', *PLoS One*, 10: e0144630.
- Sellathurai, S., S. Jung, M. J. Kim, K. Nadarajapillai, S. Ganeshalingam, J. B. Jeong, and J. Lee. 2023. 'CRISPR/Cas9-Induced Knockout of Sting Increases Susceptibility of Zebrafish to Bacterial Infection', *Biomolecules*, 13.
- Selman, M., and A. Pardo. 2021. 'Fibroageing: An ageing pathological feature driven by dysregulated extracellular matrix-cell mechanobiology', *Ageing Res Rev*, 70: 101393.
- Settembre, C., C. Di Malta, V. A. Polito, M. Garcia Arencibia, F. Vetrini, S. Erdin, S. U. Erdin, T. Huynh, D. Medina, P. Colella, M. Sardiello, D. C. Rubinsztein, and A. Ballabio. 2011. 'TFEB links autophagy to lysosomal biogenesis', *Science*, 332: 1429-33.
- Shang, G., C. Zhang, Z. J. Chen, X. C. Bai, and X. Zhang. 2019. 'Cryo-EM structures of STING reveal its mechanism of activation by cyclic GMP-AMP', *Nature*, 567: 389-93.
- Sharpless, N. E., M. R. Ramsey, P. Balasubramanian, D. H. Castrillon, and R. A. DePinho. 2004. 'The differential impact of p16(INK4a) or p19(ARF) deficiency on cell growth and tumorigenesis', *Oncogene*, 23: 379-85.
- Sharpless, N. E., and C. J. Sherr. 2015. 'Forging a signature of in vivo senescence', *Nat Rev Cancer*, 15: 397-408.
- Shen, X., C. Sun, Y. Cheng, D. Ma, Y. Sun, Y. Lin, Y. Zhao, M. Yang, W. Jing, X. Cui, and L. Han. 2023. 'cGAS Mediates Inflammation by Polarizing Macrophages to M1 Phenotype via the mTORC1 Pathway', *J Immunol*, 210: 1098-107.
- Shreeya, T., M. S. Ansari, P. Kumar, M. Saifi, A. A. Shati, M. Y. Alfaifi, and S. E. I. Elbehairi. 2023. 'Senescence: A DNA damage response and its role in aging and Neurodegenerative Diseases', *Front Aging*, 4: 1292053.
- Simon, M., M. Van Meter, J. Abulaeva, Z. Ke, R. S. Gonzalez, T. Taguchi, M. De Cecco, K. I. Leonova, V. Kogan, S. L. Helfand, N. Neretti, A. Roichman, H. Y. Cohen, M. V. Meer, V. N. Gladyshev, M. P. Antoch, A. V. Gudkov, J. M. Sedivy, A. Seluanov, and V. Gorbunova. 2019. 'LINE1 Derepression in Aged Wild-Type and SIRT6-Deficient Mice Drives Inflammation', *Cell Metab*, 29: 871-85 e5.
- Singh, P. P., B. A. Demmitt, R. D. Nath, and A. Brunet. 2019. 'The Genetics of Aging: A Vertebrate Perspective', *Cell*, 177: 200-20.
- Sladitschek-Martens, H. L., A. Guarnieri, G. Brumana, F. Zanconato, G. Battilana, R. L. Xiccato, T. Panciera, M. Forcato, S. Bicciato, V. Guzzardo, M. Fassan, L. Ulliana, A. Gandin, C. Tripodo, M. Foiani, G. Brusatin, M. Cordenonsi, and S. Piccolo. 2022. 'YAP/TAZ activity in stromal cells prevents ageing by controlling cGAS-STING', *Nature*, 607: 790-98.
- Smith, P., D. Willemsen, M. Popkes, F. Metge, E. Gandiwa, M. Reichard, and D. R. Valenzano. 2017. 'Regulation of life span by the gut microbiota in the short-lived African turquoise killifish', *Elife*, 6.
- Stein, G. H., L. F. Drullinger, A. Soulard, and V. Dulic. 1999. 'Differential roles for cyclin-dependent kinase inhibitors p21 and p16 in the mechanisms of senescence and differentiation in human fibroblasts', *Mol Cell Biol*, 19: 2109-17.

- Stolzing, A., E. Jones, D. McGonagle, and A. Scutt. 2008. 'Age-related changes in human bone marrow-derived mesenchymal stem cells: consequences for cell therapies', *Mech Ageing Dev*, 129: 163-73.
- Storer, M., A. Mas, A. Robert-Moreno, M. Pecoraro, M. C. Ortells, V. Di Giacomo, R. Yosef, N. Pilpel, V. Krizhanovsky, J. Sharpe, and W. M. Keyes. 2013. 'Senescence is a developmental mechanism that contributes to embryonic growth and patterning', *Cell*, 155: 1119-30.
- Stout, M. B., J. N. Justice, B. J. Nicklas, and J. L. Kirkland. 2017. 'Physiological Aging: Links Among Adipose Tissue Dysfunction, Diabetes, and Frailty', *Physiology (Bethesda)*, 32: 9-19.
- Strippoli, P., R. Casadei, F. Frabetti, L. Vitale, and S. Canaider. 2024. 'Commentary to the article: an estimation of the number of cells in the human body', *Ann Hum Biol*, 51: 2407587.
- Subramanian, A., P. Tamayo, V. K. Mootha, S. Mukherjee, B. L. Ebert, M. A. Gillette, A. Paulovich, S. L. Pomeroy, T. R. Golub, E. S. Lander, and J. P. Mesirov. 2005. 'Gene set enrichment analysis: a knowledge-based approach for interpreting genome-wide expression profiles', *Proc Natl Acad Sci U S A*, 102: 15545-50.
- Sun, H., Y. Huang, S. Mei, F. Xu, X. Liu, F. Zhao, L. Yin, D. Zhang, L. Wei, C. Wu, S. Ma, J. Wang, S. Cen, C. Liang, S. Hu, and F. Guo. 2021. 'A Nuclear Export Signal Is Required for cGAS to Sense Cytosolic DNA', *Cell Rep*, 34: 108586.
- Sun, L., J. Wu, F. Du, X. Chen, and Z. J. Chen. 2013. 'Cyclic GMP-AMP synthase is a cytosolic DNA sensor that activates the type I interferon pathway', *Science*, 339: 786-91.
- Sun, W., Y. Li, L. Chen, H. Chen, F. You, X. Zhou, Y. Zhou, Z. Zhai, D. Chen, and Z. Jiang. 2009. 'ERIS, an endoplasmic reticulum IFN stimulator, activates innate immune signaling through dimerization', *Proc Natl Acad Sci U S A*, 106: 8653-8.
- Tabula Muris Consortium. 2020. 'A single-cell transcriptomic atlas characterizes ageing tissues in the mouse', *Nature*, 583: 590-95.
- Tan, X., L. Sun, J. Chen, and Z. J. Chen. 2018. 'Detection of Microbial Infections Through Innate Immune Sensing of Nucleic Acids', *Annu Rev Microbiol*, 72: 447-78.
- Tang, C. H., J. A. Zundell, S. Ranatunga, C. Lin, Y. Nefedova, J. R. Del Valle, and C. C. Hu. 2016. 'Agonist-Mediated Activation of STING Induces Apoptosis in Malignant B Cells', *Cancer Res*, 76: 2137-52.
- Teefy, B. B., A. Adler, A. Xu, K. Hsu, P. P. Singh, and B. A. Benayoun. 2023. 'Dynamic regulation of gonadal transposon control across the lifespan of the naturally short-lived African turquoise killifish', *Genome Res*, 33: 141-53.
- Teefy, B. B., A. J. J. Lemus, A. Adler, A. Xu, R. Bhala, K. Hsu, and B. A. Benayoun. 2023. 'Widespread sex dimorphism across single-cell transcriptomes of adult African turquoise killifish tissues', *Cell Rep*, 42: 113237.
- Thevaranjan, N., A. Puchta, C. Schulz, A. Naidoo, J. C. Szamosi, C. P. Verschoor, D. Loukov, L. P. Schenck, J. Jury, K. P. Foley, J. D. Schertzer, M. J. Larche, D. J. Davidson, E. F. Verdu, M. G. Surette, and D. M. E. Bowdish. 2017. 'Age-Associated Microbial Dysbiosis Promotes Intestinal Permeability, Systemic Inflammation, and Macrophage Dysfunction', *Cell Host Microbe*, 21: 455-66 e4.
- Thompson, M. J., K. Chwialkowska, L. Rubbi, A. J. Lusis, R. C. Davis, A. Srivastava, R. Korstanje, G. A. Churchill, S. Horvath, and M. Pellegrini. 2018. 'A multi-tissue full lifespan epigenetic clock for mice', *Aging (Albany NY)*, 10: 2832-54.
- Tomusiak, A., A. Floro, R. Tiwari, R. Riley, H. Matsui, N. Andrews, H. G. Kasler, and E. Verdin. 2024. 'Development of an epigenetic clock resistant to changes in immune cell composition', *Commun Biol*, 7: 934.

- Tozzini, E. T., M. Baumgart, G. Battistoni, and A. Cellerino. 2012. 'Adult neurogenesis in the short-lived teleost *Nothobranchius furzeri*: localization of neurogenic niches, molecular characterization and effects of aging', *Aging Cell*, 11: 241-51.
- Turnquist, C., J. A. Beck, I. Horikawa, I. E. Obiorah, N. Von Muhlinen, B. Vojtesek, D. P. Lane, C. Grunseich, J. J. Chahine, H. M. Ames, D. D. Smart, B. T. Harris, and C. C. Harris. 2019. 'Radiation-induced astrocyte senescence is rescued by Delta133p53', *Neuro Oncol*, 21: 474-85.
- Ugenti, C., A. Lepelley, M. Depp, A. P. Badrock, M. P. Rodero, M. T. El-Daher, G. I. Rice, S. Dhir, A. P. Wheeler, A. Dhir, W. Albawardi, M. L. Fremond, L. Seabra, J. Doig, N. Blair, M. J. Martin-Niclos, E. Della Mina, A. Rubio-Roldan, J. L. Garcia-Perez, D. Sproul, J. Rehwinkel, J. Hertzog, A. Boland-Auge, R. Olaso, J. F. Deleuze, J. Baruteau, K. Brochard, J. Buckley, V. Cavallera, C. Cereda, L. M. H. De Waele, A. Dobbie, D. Doummar, F. Elmslie, M. Koch-Hogrebe, R. Kumar, K. Lamb, J. H. Livingston, A. Majumdar, C. M. Lorenzo, S. Orcesi, S. Peudenier, K. Rostasy, C. A. Salmon, C. Scott, D. Tonduti, G. Touati, M. Valente, H. van der Linden, Jr., H. Van Esch, M. Vermelle, K. Webb, A. P. Jackson, M. A. M. Reijns, N. Gilbert, and Y. J. Crow. 2020. 'cGAS-mediated induction of type I interferon due to inborn errors of histone pre-mRNA processing', *Nat Genet*, 52: 1364-72.
- UN. 2024. "World Population Prospects." In, edited by Population Division. United Nations Department of Economic and Social Affairs. <https://population.un.org/>.
- Valdesalici, S., and A. Cellerino. 2003. 'Extremely short lifespan in the annual fish *Nothobranchius furzeri*', *Proc Biol Sci*, 270 Suppl 2: S189-91.
- Valenzano, D. R., B. A. Benayoun, P. P. Singh, E. Zhang, P. D. Etter, C. K. Hu, M. Clement-Ziza, D. Willemsen, R. Cui, I. Harel, B. E. Machado, M. C. Yee, S. C. Sharp, C. D. Bustamante, A. Beyer, E. A. Johnson, and A. Brunet. 2015. 'The African Turquoise Killifish Genome Provides Insights into Evolution and Genetic Architecture of Lifespan', *Cell*, 163: 1539-54.
- Valenzano, D. R., S. Sharp, and A. Brunet. 2011. 'Transposon-Mediated Transgenesis in the Short-Lived African Killifish *Nothobranchius furzeri*, a Vertebrate Model for Aging', *G3 (Bethesda)*, 1: 531-8.
- Valenzano, D. R., E. Terzibasi, A. Cattaneo, L. Domenici, and A. Cellerino. 2006. 'Temperature affects longevity and age-related locomotor and cognitive decay in the short-lived fish *Nothobranchius furzeri*', *Aging Cell*, 5: 275-8.
- van den Berg, N., M. Beekman, K. R. Smith, A. Janssens, and P. E. Slagboom. 2017. 'Historical demography and longevity genetics: Back to the future', *Ageing Res Rev*, 38: 28-39.
- van Deursen, J. M. 2014. 'The role of senescent cells in ageing', *Nature*, 509: 439-46.
- Van Houcke, J., V. Marien, C. Zandecki, S. Vanhunsel, L. Moons, R. Ayana, E. Seuntjens, and L. Arckens. 2021. 'Aging impairs the essential contributions of non-glial progenitors to neurorepair in the dorsal telencephalon of the Killifish *Nothobranchius furzeri*', *Aging Cell*, 20: e13464.
- Van Meter, M., M. Kashyap, S. Rezazadeh, A. J. Geneva, T. D. Morello, A. Seluanov, and V. Gorbunova. 2014. 'SIRT6 represses LINE1 retrotransposons by ribosylating KAP1 but this repression fails with stress and age', *Nat Commun*, 5: 5011.
- Vanhunsel, S., S. Bergmans, A. Beckers, I. Etienne, J. Van Houcke, E. Seuntjens, L. Arckens, L. De Groef, and L. Moons. 2021. 'The killifish visual system as an in vivo model to study brain aging and rejuvenation', *NPJ Aging Mech Dis*, 7: 22.
- Vece, T. J., L. B. Watkin, S. Nicholas, D. Canter, M. C. Braun, R. P. Guillerman, K. W. Eldin, G. Bertolet, S. McKinley, M. de Guzman, L. Forbes, I. Chinn, and J. S. Orange. 2016.



- 'Copa Syndrome: a Novel Autosomal Dominant Immune Dysregulatory Disease', *J Clin Immunol*, 36: 377-87.
- Victorelli, S., H. Salmonowicz, J. Chapman, H. Martini, M. G. Vizioli, J. S. Riley, C. Cloix, E. Hall-Younger, J. Machado Espindola-Netto, D. Jurk, A. B. Lagnado, L. Sales Gomez, J. N. Farr, D. Saul, R. Reed, G. Kelly, M. Eppard, L. C. Greaves, Z. Dou, N. Pirius, K. Szczepanowska, R. A. Porritt, H. Huang, T. Y. Huang, D. A. Mann, C. A. Masuda, S. Khosla, H. Dai, S. H. Kaufmann, E. Zacharioudakis, E. Gavathiotis, N. K. LeBrasseur, X. Lei, A. G. Sainz, V. I. Korolchuk, P. D. Adams, G. S. Shadel, S. W. G. Tait, and J. F. Passos. 2024. 'Author Correction: Apoptotic stress causes mtDNA release during senescence and drives the SASP', *Nature*, 625: E15.
- Volkman, H. E., S. Cambier, E. E. Gray, and D. B. Stetson. 2019. 'Tight nuclear tethering of cGAS is essential for preventing autoreactivity', *Elife*, 8.
- Wang, J., C. L. Clauson, P. D. Robbins, L. J. Niedernhofer, and Y. Wang. 2012. 'The oxidative DNA lesions 8,5'-cyclopurines accumulate with aging in a tissue-specific manner', *Aging Cell*, 11: 714-6.
- Wang, L., S. Wang, and W. Li. 2012. 'RSeQC: quality control of RNA-seq experiments', *Bioinformatics*, 28: 2184-5.
- Wang, S., D. H. Meyer, and B. Schumacher. 2023. 'Inheritance of paternal DNA damage by histone-mediated repair restriction', *Nature*, 613: 365-74.
- Wang, W., C. K. Hu, A. Zeng, D. Alegre, D. Hu, K. Gotting, A. Ortega Granillo, Y. Wang, S. Robb, R. Schnittker, S. Zhang, D. Alegre, H. Li, E. Ross, N. Zhang, A. Brunet, and A. Sanchez Alvarado. 2020. 'Changes in regeneration-responsive enhancers shape regenerative capacities in vertebrates', *Science*, 369.
- Weidberg, H., E. Shvets, T. Shpilka, F. Shimron, V. Shinder, and Z. Elazar. 2010. 'LC3 and GATE-16/GABARAP subfamilies are both essential yet act differently in autophagosome biogenesis', *EMBO J*, 29: 1792-802.
- Wendler, S., N. Hartmann, B. Hoppe, and C. Englert. 2015. 'Age-dependent decline in fin regenerative capacity in the short-lived fish *Nothobranchius furzeri*', *Aging Cell*, 14: 857-66.
- West, A. P., W. Khoury-Hanold, M. Staron, M. C. Tal, C. M. Pineda, S. M. Lang, M. Bestwick, B. A. Duguay, N. Raimundo, D. A. MacDuff, S. M. Kaech, J. R. Smiley, R. E. Means, A. Iwasaki, and G. S. Shadel. 2015. 'Mitochondrial DNA stress primes the antiviral innate immune response', *Nature*, 520: 553-7.
- Whiteley, A. T., J. B. Eaglesham, C. C. de Oliveira Mann, B. R. Morehouse, B. Lowey, E. A. Nieminen, O. Danilchanka, D. S. King, A. S. Y. Lee, J. J. Mekalanos, and P. J. Kranzusch. 2019. 'Bacterial cGAS-like enzymes synthesize diverse nucleotide signals', *Nature*, 567: 194-99.
- Whittemore, K., E. Vera, E. Martinez-Nevado, C. Sanpera, and M. A. Blasco. 2019. 'Telomere shortening rate predicts species life span', *Proc Natl Acad Sci U S A*, 116: 15122-27.
- Widjaja, A. A., W. W. Lim, S. Viswanathan, S. Chothani, B. Corden, C. M. Dasan, J. W. T. Goh, R. Lim, B. K. Singh, J. Tan, C. J. Pua, S. Y. Lim, E. Adami, S. Schafer, B. L. George, M. Sweeney, C. Xie, M. Tripathi, N. A. Sims, N. Hubner, E. Petretto, D. J. Withers, L. Ho, J. Gil, D. Carling, and S. A. Cook. 2024. 'Inhibition of IL-11 signalling extends mammalian healthspan and lifespan', *Nature*, 632: 157-65.
- Wiens, K. E., and J. D. Ernst. 2016. 'The Mechanism for Type I Interferon Induction by Mycobacterium tuberculosis is Bacterial Strain-Dependent', *PLoS Pathog*, 12: e1005809.

- Wiley, C. D., M. C. Velarde, P. Lecot, S. Liu, E. A. Sarnoski, A. Freund, K. Shirakawa, H. W. Lim, S. S. Davis, A. Ramanathan, A. A. Gerencser, E. Verdin, and J. Campisi. 2016. 'Mitochondrial Dysfunction Induces Senescence with a Distinct Secretory Phenotype', *Cell Metab*, 23: 303-14.
- Wood, J. G., B. C. Jones, N. Jiang, C. Chang, S. Hosier, P. Wickremesinghe, M. Garcia, D. A. Hartnett, L. Burhenn, N. Neretti, and S. L. Helfand. 2016. 'Chromatin-modifying genetic interventions suppress age-associated transposable element activation and extend life span in *Drosophila*', *Proc Natl Acad Sci U S A*, 113: 11277-82.
- Woodward, J. J., A. T. Iavarone, and D. A. Portnoy. 2010. 'c-di-AMP secreted by intracellular *Listeria monocytogenes* activates a host type I interferon response', *Science*, 328: 1703-5.
- Wourms, J. P. 1972. 'Developmental biology of annual fishes. I. Stages in the normal development of *Austrofundulus myersi* Dahl', *J Exp Zool*, 182: 143-67.
- Wu, J., L. Sun, X. Chen, F. Du, H. Shi, C. Chen, and Z. J. Chen. 2013. 'Cyclic GMP-AMP is an endogenous second messenger in innate immune signaling by cytosolic DNA', *Science*, 339: 826-30.
- Wu, Q., X. Leng, Q. Zhang, Y. Z. Zhu, R. Zhou, Y. Liu, C. Mei, D. Zhang, S. Liu, S. Chen, X. Wang, A. Lin, X. Lin, T. Liang, L. Shen, X. H. Feng, B. Xia, and P. Xu. 2024. 'IRF3 activates RB to authorize cGAS-STING-induced senescence and mitigate liver fibrosis', *Sci Adv*, 10: eadj2102.
- Wu, X., F. H. Wu, X. Wang, L. Wang, J. N. Siedow, W. Zhang, and Z. M. Pei. 2014. 'Molecular evolutionary and structural analysis of the cytosolic DNA sensor cGAS and STING', *Nucleic Acids Res*, 42: 8243-57.
- Wu, Y., K. Song, W. Hao, J. Li, L. Wang, and S. Li. 2022. 'Nuclear soluble cGAS senses double-stranded DNA virus infection', *Commun Biol*, 5: 433.
- Wu, Z., J. Qu, and G. H. Liu. 2024. 'Roles of chromatin and genome instability in cellular senescence and their relevance to ageing and related diseases', *Nat Rev Mol Cell Biol*, 25: 979-1000.
- Xie, J., Y. Li, X. Shen, G. Goh, Y. Zhu, J. Cui, L. F. Wang, Z. L. Shi, and P. Zhou. 2018. 'Dampened STING-Dependent Interferon Activation in Bats', *Cell Host Microbe*, 23: 297-301 e4.
- Xie, W., L. Lama, C. Adura, D. Tomita, J. F. Glickman, T. Tuschl, and D. J. Patel. 2019. 'Human cGAS catalytic domain has an additional DNA-binding interface that enhances enzymatic activity and liquid-phase condensation', *Proc Natl Acad Sci U S A*, 116: 11946-55.
- Xu, A., B. B. Teefy, R. J. Lu, S. Nozownik, A. M. Tyers, D. R. Valenzano, and B. A. Benayoun. 2023. 'Transcriptomes of aging brain, heart, muscle, and spleen from female and male African turquoise killifish', *Sci Data*, 10: 695.
- Xu, M., T. Pirtskhalava, J. N. Farr, B. M. Weigand, A. K. Palmer, M. M. Weivoda, C. L. Inman, M. B. Ogrodnik, C. M. Hachfeld, D. G. Fraser, J. L. Onken, K. O. Johnson, G. C. Verzosa, L. G. P. Langhi, M. Weigl, N. Giorgadze, N. K. LeBrasseur, J. D. Miller, D. Jurk, R. J. Singh, D. B. Allison, K. Ejima, G. B. Hubbard, Y. Ikeno, H. Cubro, V. D. Garovic, X. Hou, S. J. Weroha, P. D. Robbins, L. J. Niedernhofer, S. Khosla, T. Tchkonja, and J. L. Kirkland. 2018. 'Senolytics improve physical function and increase lifespan in old age', *Nat Med*, 24: 1246-56.
- Xu, Y., Q. Wang, J. Wang, C. Qian, Y. Wang, S. Lu, L. Song, Z. He, W. Liu, and W. Wan. 2024. 'The cGAS-STING pathway activates transcription factor TFEB to stimulate lysosome biogenesis and pathogen clearance', *Immunity*.

- Yang, H., H. Z. Wang, J. Y. Ren, Q. Chen, and Z. J. J. Chen. 2017. 'cGAS is essential for cellular senescence', *Proceedings of the National Academy of Sciences of the United States of America*, 114: E4612-E20.
- Yizhak, K., F. Aguet, J. Kim, J. M. Hess, K. Kubler, J. Grimsby, R. Frazer, H. Zhang, N. J. Haradhvala, D. Rosebrock, D. Livitz, X. Li, E. Arich-Landkof, N. Shores, C. Stewart, A. V. Segre, P. A. Branton, P. Polak, K. G. Ardlie, and G. Getz. 2019. 'RNA sequence analysis reveals macroscopic somatic clonal expansion across normal tissues', *Science*, 364.
- Yoneyama, M., M. Kikuchi, T. Natsukawa, N. Shinobu, T. Imaizumi, M. Miyagishi, K. Taira, S. Akira, and T. Fujita. 2004. 'The RNA helicase RIG-I has an essential function in double-stranded RNA-induced innate antiviral responses', *Nat Immunol*, 5: 730-7.
- Yosef, R., N. Pilpel, N. Papismadov, H. Gal, Y. Ovadya, E. Vadai, S. Miller, Z. Porat, S. Ben-Dor, and V. Krizhanovsky. 2017. 'p21 maintains senescent cell viability under persistent DNA damage response by restraining JNK and caspase signaling', *EMBO J*, 36: 2280-95.
- Yousefzadeh, M. J., R. R. Flores, Y. Zhu, Z. C. Schmiechen, R. W. Brooks, C. E. Trussoni, Y. Cui, L. Angelini, K. A. Lee, S. J. McGowan, A. L. Burrack, D. Wang, Q. Dong, A. Lu, T. Sano, R. D. O'Kelly, C. A. McGuckian, J. I. Kato, M. P. Bank, E. A. Wade, S. P. S. Pillai, J. Klug, W. C. Ladiges, C. E. Burd, S. E. Lewis, N. F. LaRusso, N. V. Vo, Y. Wang, E. E. Kelley, J. Huard, I. M. Stromnes, P. D. Robbins, and L. J. Niedernhofer. 2021. 'An aged immune system drives senescence and ageing of solid organs', *Nature*, 594: 100-05.
- Yousefzadeh, M. J., J. Zhao, C. Bukata, E. A. Wade, S. J. McGowan, L. A. Angelini, M. P. Bank, A. U. Gurkar, C. A. McGuckian, M. F. Calubag, J. I. Kato, C. E. Burd, P. D. Robbins, and L. J. Niedernhofer. 2020. 'Tissue specificity of senescent cell accumulation during physiologic and accelerated aging of mice', *Aging Cell*, 19: e13094.
- Yousefzadeh, M. J., Y. Zhu, S. J. McGowan, L. Angelini, H. Fuhrmann-Stroissnigg, M. Xu, Y. Y. Ling, K. I. Melos, T. Pirtskhalava, C. L. Inman, C. McGuckian, E. A. Wade, J. I. Kato, D. Grassi, M. Wentworth, C. E. Burd, E. A. Arriaga, W. L. Ladiges, T. Tchkonja, J. L. Kirkland, P. D. Robbins, and L. J. Niedernhofer. 2018. 'Fisetin is a senotherapeutic that extends health and lifespan', *EBioMedicine*, 36: 18-28.
- Yu, C. H., S. Davidson, C. R. Harapas, J. B. Hilton, M. J. Mlodzikowski, P. Laohamonthonkul, C. Louis, R. R. J. Low, J. Moecking, D. De Nardo, K. R. Balka, D. J. Calleja, F. Moghaddas, E. Ni, C. A. McLean, A. L. Samson, S. Tyebji, C. J. Tonkin, C. R. Bye, B. J. Turner, G. Pepin, M. P. Gantier, K. L. Rogers, K. McArthur, P. J. Crouch, and S. L. Masters. 2020. 'TDP-43 Triggers Mitochondrial DNA Release via mPTP to Activate cGAS/STING in ALS', *Cell*, 183: 636-49 e18.
- Zak, J., I. Dykova, and M. Reichard. 2020. 'Good performance of turquoise killifish (*Nothobranchius furzeri*) on pelleted diet as a step towards husbandry standardization', *Sci Rep*, 10: 8986.
- Zakharova, M., and H. K. Ziegler. 2005. 'Paradoxical anti-inflammatory actions of TNF- $\alpha$ : inhibition of IL-12 and IL-23 via TNF receptor 1 in macrophages and dendritic cells', *J Immunol*, 175: 5024-33.
- Zeng, Y., Q. Feng, T. Hesketh, K. Christensen, and J. W. Vaupel. 2017. 'Survival, disabilities in activities of daily living, and physical and cognitive functioning among the oldest-old in China: a cohort study', *Lancet*, 389: 1619-29.
- Zhang, B., W. M. Bailey, K. J. Braun, and J. C. Gensel. 2015. 'Age decreases macrophage IL-10 expression: Implications for functional recovery and tissue repair in spinal cord injury', *Exp Neurol*, 273: 83-91.

- Zhang, C., G. Shang, X. Gui, X. Zhang, X. C. Bai, and Z. J. Chen. 2019. 'Structural basis of STING binding with and phosphorylation by TBK1', *Nature*, 567: 394-98.
- Zhang, G., J. Li, S. Purkayastha, Y. Tang, H. Zhang, Y. Yin, B. Li, G. Liu, and D. Cai. 2013. 'Hypothalamic programming of systemic ageing involving IKK-beta, NF-kappaB and GnRH', *Nature*, 497: 211-6.
- Zhang, J. M., and J. An. 2007. 'Cytokines, inflammation, and pain', *Int Anesthesiol Clin*, 45: 27-37.
- Zhao, B., F. Du, P. Xu, C. Shu, B. Sankaran, S. L. Bell, M. Liu, Y. Lei, X. Gao, X. Fu, F. Zhu, Y. Liu, A. Laganowsky, X. Zheng, J. Y. Ji, A. P. West, R. O. Watson, and P. Li. 2019. 'A conserved PLPLRT/SD motif of STING mediates the recruitment and activation of TBK1', *Nature*, 569: 718-22.
- Zhao, B., P. Xu, C. M. Rowlett, T. Jing, O. Shinde, Y. Lei, A. P. West, W. R. Liu, and P. Li. 2020. 'The molecular basis of tight nuclear tethering and inactivation of cGAS', *Nature*, 587: 673-77.
- Zhao, F., W. Kim, J. A. Kloeber, and Z. Lou. 2020. 'DNA end resection and its role in DNA replication and DSB repair choice in mammalian cells', *Exp Mol Med*, 52: 1705-14.
- Zhen, Z., Y. Chen, H. Wang, H. Tang, H. Zhang, H. Liu, Y. Jiang, and Z. Mao. 2023. 'Nuclear cGAS restricts L1 retrotransposition by promoting TRIM41-mediated ORF2p ubiquitination and degradation', *Nat Commun*, 14: 8217.
- Zhong, B., Y. Yang, S. Li, Y. Y. Wang, Y. Li, F. Diao, C. Lei, X. He, L. Zhang, P. Tien, and H. B. Shu. 2008. 'The adaptor protein MITA links virus-sensing receptors to IRF3 transcription factor activation', *Immunity*, 29: 538-50.
- Zhou, C., X. Chen, R. Planells-Cases, J. Chu, L. Wang, L. Cao, Z. Li, K. I. Lopez-Cayuqueo, Y. Xie, S. Ye, X. Wang, F. Ullrich, S. Ma, Y. Fang, X. Zhang, Z. Qian, X. Liang, S. Q. Cai, Z. Jiang, D. Zhou, Q. Leng, T. S. Xiao, K. Lan, J. Yang, H. Li, C. Peng, Z. Qiu, T. J. Jentsch, and H. Xiao. 2020. 'Transfer of cGAMP into Bystander Cells via LRRC8 Volume-Regulated Anion Channels Augments STING-Mediated Interferon Responses and Anti-viral Immunity', *Immunity*, 52: 767-81 e6.
- Zhou, J., J. Qiu, Y. Song, T. Liang, S. Liu, C. Ren, X. Song, L. Cui, and Y. Sun. 2023. 'Pyroptosis and degenerative diseases of the elderly', *Cell Death Dis*, 14: 94.
- Zhou, W., A. T. Whiteley, C. C. de Oliveira Mann, B. R. Morehouse, R. P. Nowak, E. S. Fischer, N. S. Gray, J. J. Mekalanos, and P. J. Kranzusch. 2018. 'Structure of the Human cGAS-DNA Complex Reveals Enhanced Control of Immune Surveillance', *Cell*, 174: 300-11 e11.
- Zhou, Y., J. Xia, S. Xu, T. She, Y. Zhang, Y. Sun, M. Wen, T. Jiang, Y. Xiong, and J. Lei. 2023. 'Experimental mouse models for translational human cancer research', *Front Immunol*, 14: 1095388.
- Zupkovitz, G., J. Kabiljo, M. Kothmayer, K. Schlick, C. Schofer, S. Lagger, and O. Pusch. 2021. 'Analysis of Methylation Dynamics Reveals a Tissue-Specific, Age-Dependent Decline in 5-Methylcytosine Within the Genome of the Vertebrate Aging Model *Nothobranchius furzeri*', *Front Mol Biosci*, 8: 627143.

## 12. Curriculum Vitae



# Eugen Ballhysa

E-mail: [eugen.ballhysa@age.mpg.de](mailto:eugen.ballhysa@age.mpg.de)

Date of birth: 6<sup>th</sup> April  
1995

## Academic education

### **Doctorate of Philosophy in Molecular Genetics of Ageing (Ph.D.)**

**Nov 2019 - present**

Max Planck Institute for Biology of Ageing, University of Cologne

-Grade: N/a

### **Master of Science in Molecular Biology (MSc)**

**Oct 2018 – Nov 2019**

Department of Molecular Biology & Genetics, School of Health Sciences,  
Democritus University of Thrace

-Grade: 8,93/10 “1<sup>st</sup> Class Honours”

### **Bachelor of Science in Biology (BSc)**

**Sep 2013 – Jul 2018**

School of Biology, Faculty of Sciences, Aristotle University of Thessaloniki

-Grade: 8,5/10 “1<sup>st</sup> Class Honours”

## Academic research experience

### **Ph.D. thesis**

**Nov 2019 - present**

Max Planck Institute for Biology of Ageing, University of Cologne

- *Principal Investigator:* Prof. Dr. Adam Antebi  
*Project:* Deciphering the role of cGAS/STING signaling in senescent and ageing signatures *in vivo* using the short-lived vertebrate *Nothobranchius furzeri*.
- *Evaluation:* N/a

### **International Genetically Engineered Machine competition**

**Nov 2016 - Nov 2017**

Member of the first collegiate Greek team to participate in the iGEM competition

- *Principal Investigators:* Prof. Dr. George Koliakos, Prof. Dr. George Mosialos, Asst. Prof. Dimitra Dafou, Assoc. Prof. Dimosthenis Sarigiannis
- *Project:* Development of a genetic circuit able to identify and eliminate colorectal cancer cells and a targeted delivery system for its application.  
In-depth information regarding our work can be found [here](#).
- *Evaluation:* Gold Medal Award and nominated for the “Best Therapeutics Project” Award

**Bachelor's Research Dissertation  
2017**

**Sep 2016 - Dec**

School of Medicine, Faculty of Health Sciences, Aristotle University of Thessaloniki

- *Supervisors:* Prof. George Koliakos, Prof. Martha Kaloyanni
- *Project:* Analysis of magnetic nanoparticles' cytotoxicity to human stem cells.
- *Evaluation:* 10/10 (18 ECTS awarded)

**Erasmus+ Internship  
2016**

**Oct 2015 – Mar**

Department of Life Sciences, University of Warwick

- *Supervisors:* Prof. Lorenzo Frigerio, Dr. Emily Breeze
- *Project:* Analysis of the morphological alterations of the endoplasmic reticulum during biotic and abiotic stress in *Arabidopsis thaliana* leaves.
- *Evaluation:* High 1<sup>st</sup> Class (30 ECTS awarded)

**Industrial working and research experience**

**Research associate and Master's thesis  
2019**

**Apr 2019 – Oct**

Research Genetic Cancer Centre Group

- *Chief research officers:* Prof. Raphael Sandaltzopoulos and Dr. Ioannis Papatotiriou
- *Main Project:* Engineering of RNAi-based cellular classifier circuits that can identify Cancer Stem Cells in patient-derived samples.

**Summer internship**

**Jul 2017 – Aug 2017**

Stem Cell Bank and Biotechnology Company "Biohellenica SA"

- *Chief research officer:* Prof. George Koliakos
- *Activity:* Analysis of clinical specimens for the diagnosis of viral infections and measurements of viral load.
- *Evaluation:* 10/10 (12 ECTS awarded)

**Transferable skills**

**Communication skills:**

- Co-organized along with student-run organizations an interactive workshop on "Designing a scientific project; from brainstorming and fundraising to implementation and patenting", at the University of Thessaloniki.
- Collaborated with engineers on computational models of cellular interactions and the design of logic genetic circuits.
- Established collaborations with leading industries for both my PhD and the iGEM projects

- Co-organizer of the iGEM Alumni network to provide guidance to future teams in brainstorming, project designing and fundraising (iGEM Thessaloniki 2018, iGEM Athens 2018).

#### **Fundraising skills:**

- Independently raised **51.486€** for the implementation of our project during the iGEM competition of 2017.
- Independently raised over **40.000€** as laboratory funds for the implementation of my Master's project.

#### **Computer skills:**

- Certified courses attended: R, Vensim, Python, MODELLER, AutoDock Vina and ImageJ
- Self-taught: SPSS, Illustrator, SnapGene and Vector NTI
- Diploma in IT Skills Proficiency Certificate (Microsoft Word, Excel, Power Point and Access)

#### **Language skills:**

- Native speaker of Greek and Albanian
- Certificate of Proficiency in English (level C2)

TOEFL    IELTS

Listening	28	8.5
Speaking	27	7.5
Reading	30	7.5
Writing	27	7
<b>Overall</b>	<b>112</b>	<b>7.5</b>

- Hanyu Shuiping Kaoshi 2 Certificate, Chinese Language Test (level A2)

### **Awards**

**Gold Medal** awarded at the iGEM competition on 2017 for demonstrating our project's translational potential and our model's efficiency for designing optimal RNAi-based circuit topologies.

Nominated for the **Best Therapeutics Award** at the iGEM competition on 2017 for the innovative design and thorough implementation of a holistic therapeutic approach against colorectal cancer.

Earned **two Awards of Excellence** from the Rector of the Aristotle University of Thessaloniki and the Dean of the Faculty of Sciences for the distinction of the first Greek iGEM team and for inspiring multidisciplinary collaboration among the faculties of the university.

### **Presentations**

## Conferences

Oral presentation	Mechanisms of Ageing, Cold Spring Harbor, USA	2024
Poster presentation	10 <sup>th</sup> Aging Research and Drug Discovery Meeting (ARDD), Copenhagen, Denmark	2023
Poster presentation	5 <sup>th</sup> Nothobranchius Symposium, Leuven, Belgium	2023
Poster presentation	4 <sup>th</sup> Nothobranchius Symposium, online	2021
Oral and Poster presentation	iGEM competition final phase called “The Giant Jamboree”, Boston, USA	2017
Poster presentation	11th Panhellenic Scientific Conference in Chemical Engineering, Thessaloniki, Greece	2017
Poster presentation	2nd Bioengineering and Translational Medicine Conference, Minnesota, USA	2017
Poster presentation	4th International Synthetic & Systems Biology Summer School, University of Cambridge, UK	2017

## Workshops

Oral presentation	TEDx NTUA themed “Chaos”, Athens, Greece	2018
Oral presentation	SynBio Workshop – The principles of engineering life, Athens, Greece	2018
Oral presentation	InnovationLab Workshop co-organized by IEEE EMBS Student Chapter AUTH and The Triple Helix Aristotle, Aristotle University of Thessaloniki, Greece	2017

## Publications

R. Laboy, M. Ndoci, M. Vonolfen, **E. Ballhysa**, S. T. Syed, T. Droth, K. Schilling, A. Löhrke, I. Atanassov, A. Antebi (reviewed 2024). Hexokinase regulates Mondo-mediated longevity via the PPP and organellar dynamics. eLife. doi: <https://doi.org/10.1101/2023.06.14.544948>

Ripa, R., **E. Ballhysa**, J. D. Steiner, R. Laboy, A. Annibal, N. Hochhard, C. Latza, L. Dolfi, C. Calabrese, A. M. Meyer, M. C. Polidori, R. U. Muller and A. Antebi (2023). "Refeeding-associated AMPK(gamma1) complex activity is a hallmark of health and longevity." Nat Aging 3(12): 1544-1560.

Ripa, R., A. Mesaros, O. Symmons, **E. Ballhysa**, L. Dolfi and A. Antebi (2023). "Micro-CT Analysis of Fat in the Killifish *Nothobranchius furzeri*." Cold Spring Harb Protoc 2023(8): 107884.



Dolfi, L., R. Ripa, D. Medelbekova, **E. Ballhysa**, O. Symmons and A. Antebi (2023). "Nonlethal Blood Sampling from the Killifish *Nothobranchius furzeri*." *Cold Spring Harb Protoc* 2023(8): 107745.

Annibal, A., R. Ripa, **E. Ballhysa**, C. Latza, N. Hochhard and A. Antebi (2021). "Mass spectrometric characterization of cyclic dinucleotides (CDNs) in vivo." *Anal Bioanal Chem* 413(26): 6457-6468.